



HAL
open science

Modeling of solids

Paolo Vannucci

► **To cite this version:**

| Paolo Vannucci. Modeling of solids. Master. France. 2018. cel-01704993v2

HAL Id: cel-01704993

<https://hal.science/cel-01704993v2>

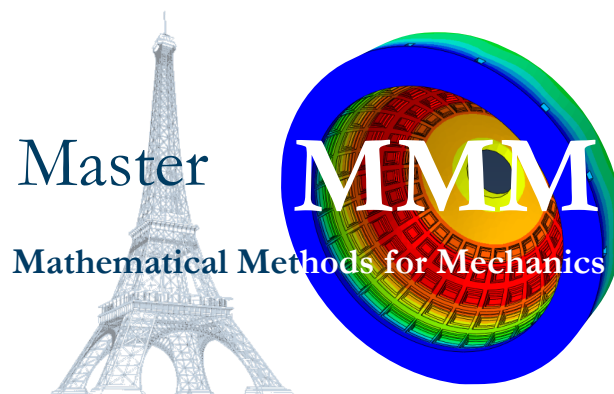
Submitted on 23 Mar 2019 (v2), last revised 31 Jan 2024 (v6)

HAL is a multi-disciplinary open access archive for the deposit and dissemination of scientific research documents, whether they are published or not. The documents may come from teaching and research institutions in France or abroad, or from public or private research centers.

L'archive ouverte pluridisciplinaire **HAL**, est destinée au dépôt et à la diffusion de documents scientifiques de niveau recherche, publiés ou non, émanant des établissements d'enseignement et de recherche français ou étrangers, des laboratoires publics ou privés.

Class notes of the course

Modeling of Solids



Paolo Vannucci

paolo.vannucci@uvsq.fr

Année Universitaire 2015-16

Last update: March 20, 2019

Preface

This text is the support for the course of Modeling of Solids, of the Master of Mechanics of the University Paris-Saclay - Curriculum MMM: Mathematical Methods for Mechanics, held at Versailles.

The course is the continuation of the course Continuum Mechanics - Solids, and as such it is an introduction, for graduate students, to some typical topics of the theory of solid bodies.

The different arguments are dealt with in a simple, succinct way, the objective being to give to students the fundamentals of each argument. Only static problems are considered, being the dynamic of structures dealt with in other courses.

Versailles, December 7, 2015

Contents

Preface	iii
1 Some elements of differential geometry	1
1.1 Curves of points, vectors and tensors	1
1.2 Differentiation of a curve	2
1.3 Integral of a curve of vectors	3
1.4 The Frenet-Serret basis	5
1.5 Curvature of a curve	7
1.6 The Frenet-Serret formulae	9
1.7 The torsion of a curve	10
1.8 Osculating sphere and circle	11
1.9 Exercices	12
2 Cables	15
2.1 Introduction	15
2.2 Mechanical definition of a cable	15
2.3 The intrinsic balance equations	18
2.4 Forces depending upon a potential	18
2.5 Parallel and coplanar forces	19
2.6 Concentrated forces	19
2.7 Cables on surfaces	20
2.8 Applications	21
2.8.1 The catenary	21
2.8.2 The suspension bridge	27
2.8.3 The curve of uniform vertical load	28
2.8.4 The cable coiled on a rough cylinder	29
2.9 Elastic cables	30
2.9.1 The catenary of an elastic cable	31
2.10 Exercices	33
3 Straight rods	35
3.1 Introduction	35
3.2 Balance equations	36
3.3 Compatibility equations	37
3.4 Constitutive equations	38
3.5 The Timoshenko's rod	39
3.6 The Euler-Bernoulli rod	41

3.7	Reduction of the Timoshenko's problem	42
3.8	Isostatic and hyperstatic rods	43
3.9	The torsion equations	45
3.10	The Mohr's theorems	46
3.11	Hyperstatic systems of rods	47
	3.11.1 The Principle of Virtual Displacements for rods	47
	3.11.2 The Müller-Breslau equations	49
	3.11.3 The dummy load method	52
3.12	Effects of a temperature change	52
3.13	Exercises	55
4	Arches	59
4.1	Introduction	59
4.2	Balance equations	60
4.3	Compatibility equations	62
4.4	Constitutive equations	66
4.5	The problem of elastic equilibrium for the arches	67
4.6	Transforming the equations of the arches	67
	4.6.1 Transforming the balance equations	67
	4.6.2 Transforming the elastic equilibrium equations	69
	4.6.3 The Euler-Bernoulli model for arches	69
	4.6.4 Arches of constant section	70
	4.6.5 Circular arches	70
4.7	Examples	71
	4.7.1 Example 1	71
	4.7.2 Example 2	72
	4.7.3 Example 3	72
4.8	Exercices	73
5	Slender rods	77
5.1	Cosserat rods	77
	5.1.1 Reference configuration	78
	5.1.1.1 First approach	78
	5.1.1.2 Second approach	79
	5.1.2 Deformed configuration	79
	5.1.3 Balance equations	82
	5.1.4 Constitutive law	83
5.2	The Kirchhoff's theory for slender rods	83
5.3	The Euler's elastica	84
5.4	The 3D case	88
5.5	The Michell-Prandtl bifurcation	91
5.6	Helicoidal bifurcation	96
5.7	Exercises	98
6	Plates	99
6.1	Problem definition: basic assumptions	99
6.2	The Kirchhoff model for thin plates	101
	6.2.1 The displacement field	101

6.2.2	Strain field	103
6.2.3	Stress field	103
6.2.4	Internal actions	105
6.2.5	Uncoupling bending and extension	107
6.2.6	Balance equations	108
6.2.7	Elastic equilibrium equations	110
6.2.8	Expressions for stresses	111
6.2.9	Transverse shear stresses	112
6.2.10	Plates submitted uniquely to orthogonal loads	113
6.2.11	Evaluation of the transverse normal stress	114
6.2.12	Boundary conditions	115
	6.2.12.1 Simply supported edges	116
	6.2.12.2 Clamped edges	117
	6.2.12.3 Free edges	117
	6.2.12.4 The Kelvin's reduction of the boundary conditions	118
6.2.13	Some exact solutions	120
	6.2.13.1 Elliptic plate	120
	6.2.13.2 Circular plate	120
	6.2.13.3 Equilateral triangular plate	121
	6.2.13.4 Anticlastic bending	121
	6.2.13.5 Navier's method for rectangular plates	124
	6.2.13.6 Levy's method for rectangular plates	124
6.3	The Reissner-Mindlin theory	125
6.4	The Von Karman theory	129
6.5	Exercises	134
7	Membranes	135
7.1	Introduction	135
7.2	Linear theory of prestressed plane membranes	136
7.3	Curved thin membranes	139
	7.3.1 Internal actions	139
	7.3.2 Constitutive equation	140
7.4	Axisymmetric membranes	140
	7.4.1 Equilibrium along a meridian	142
	7.4.2 Equilibrium along a parallel	143
	7.4.3 Equilibrium along the normal to the surface	144
	7.4.4 The system of equilibrium equations	145
	7.4.5 Resolution procedure	145
	7.4.6 Axisymmetric load	148
	7.4.6.1 Global equilibrium	149
	7.4.6.2 Strains and displacements	149
7.5	Exemples of axisymmetric membranes	150
	7.5.1 Spherical domes	151
	7.5.1.1 Conical support	152
	7.5.1.2 Ring beam	153
	7.5.1.3 Deformations and displacements	154
	7.5.1.4 Spherical dome with <i>oculus</i>	156

7.5.1.5	Spherical dome with lantern	157
7.5.1.6	Wind on a spherical dome	158
7.5.2	Elliptical domes	161
7.5.2.1	Elliptical vault under its own weight	162
7.5.2.2	Elliptical pressure tank	163
7.5.3	Conical vaults	164
7.5.3.1	Vertical tip load	166
7.5.3.2	Conical vault under its own weight	166
7.5.3.3	Conical water reservoir	166
7.5.3.4	Wind load on a conical vault	169
7.5.3.5	A concentrated force at the tip	170
7.5.4	Pipes	171
7.5.5	Hyperbolic hyperboloid	171
7.6	Vaults	175
7.6.1	Barrel vaults	175
7.6.2	Cross vaults	178
7.7	Equilibrium of membranes of any shape	182
7.7.1	Hyperbolic paraboloid	185
7.7.2	Paraboloid of revolution	188
7.7.3	Elliptic paraboloid	190

Suggested texts **195**

Chapter 1

Some elements of differential geometry

1.1 Curves of points, vectors and tensors

Be $\mathcal{R} = \{o; \mathbf{e}_1, \mathbf{e}_2, \mathbf{e}_3\}$ a reference frame of the euclidean space \mathcal{E}^1 and let us consider a point $p = (p_1, p_2, p_3)$. If the three coordinates are three continuous functions $p_i(t)$ over the interval $[t_1, t_2] \in \mathbb{R}$, then the mapping $p(t) : [t_1, t_2] \rightarrow \mathcal{E}$ is a *curve* in \mathcal{E} .

The independent variable t is the *parameter* and the equation

$$p(t) = (p_1(t), p_2(t), p_3(t)) \rightarrow \begin{cases} p_1 = p_1(t) \\ p_2 = p_2(t) \\ p_3 = p_3(t) \end{cases} \quad (1.1)$$

is the *parametric point equation of the curve*: to each value of $t \in [t_1, t_2]$ it corresponds a point of the curve in \mathcal{E} , see Fig. 1.1. The curve is *smooth* whenever the functions $p_i(t)$ are of class C^1 .

The vector function $\mathbf{r}(t) = p(t) - o$ is the *position vector* of point p in \mathcal{R} ; the equation

$$\mathbf{r}(t) = r_1(t)\mathbf{e}_1 + r_2(t)\mathbf{e}_2 + r_3(t)\mathbf{e}_3 \rightarrow \begin{cases} r_1 = r_1(t) \\ r_2 = r_2(t) \\ r_3 = r_3(t) \end{cases} \quad (1.2)$$

is the *parametric vector equation* of the curve: to each value of $t \in [t_1, t_2]$ it corresponds a vector of \mathcal{V} that determines a point of the curve in \mathcal{E} through the operation $p(t) = o + \mathbf{r}(t)$.

¹ The Euclidean space \mathcal{E} is the ordinary three-dimensional space, whose elements are geometric points p . A reference frame $\mathcal{R} = \{o; \mathbf{e}_1, \mathbf{e}_2, \mathbf{e}_3\}$ in \mathcal{E} is composed by a point o , called the *origin* of the frame and by a basis $\{\mathbf{e}_1, \mathbf{e}_2, \mathbf{e}_3\}$ of the space vector \mathcal{V} associated to \mathcal{E} , called the *space of translations*: any vector $\mathbf{v} \in \mathcal{V}$ is a function that operates on the points $p \in \mathcal{E} : \forall \mathbf{v} \in \mathcal{V}, \mathbf{v}(p) = q$. Concerning the basis associated to the reference frame \mathcal{R} , we assume it to be *orthonormal*: $\mathbf{e}_i \cdot \mathbf{e}_j = \delta_{ij} \forall i, j = 1, 2, 3$. A *second-rank tensor* is any linear mapping $\mathbf{L} : \mathcal{V} \rightarrow \mathcal{V}$. The space of all the tensors forms a manifold, indicated by $\text{Lin}(\mathcal{V})$. Any tensor can be expressed, in \mathcal{R} , as a sum of dyads: $\mathbf{L} = L_{ij}\mathbf{e}_i \otimes \mathbf{e}_j$. A *dyad* $\mathbf{a} \otimes \mathbf{b}$ is defined as $(\mathbf{a} \otimes \mathbf{b})\mathbf{v} = \mathbf{b} \cdot \mathbf{v} \mathbf{a} \forall \mathbf{v} \in \mathcal{V}$.

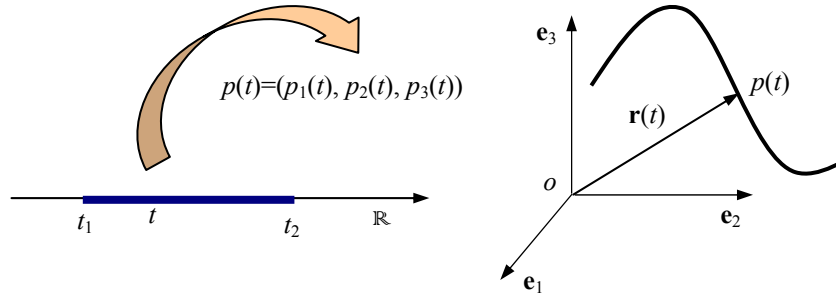


Figure 1.1: Mapping of a curve of points.

The expression $p = p(t)$ is a *curve of points* while $\mathbf{r} = \mathbf{r}(t)$ is a *curve of vectors*. In the same way, we can introduce a *curve of tensors*: if the components $L_{ij}(t)$ are continuous functions of a parameter t , the mapping $\mathbf{L}(t) : [t_1, t_2] \rightarrow \text{Lin}(\mathcal{V})$ defined as

$$\mathbf{L}(t) = L_{ij}(t)\mathbf{e}_i \otimes \mathbf{e}_j, \quad i, j = 1, 2, 3, \quad (1.3)$$

is a *curve of tensors*.

To be noticed that the choice of the parameter is *not unique*: the equation $p = p[\tau(t)]$ still represents the same curve $p = p(t)$, through the *change of parameter* $\tau = \tau(t)$.

1.2 Differentiation of a curve

We define *derivative* of a curve of points $p = p(t)$ in $t = t_0$ the limit

$$\frac{dp(t)}{dt} = \lim_{\varepsilon \rightarrow 0} \frac{p(t_0 + \varepsilon) - p(t_0)}{\varepsilon}; \quad (1.4)$$

being defined as a difference of points, $\frac{dp(t)}{dt}$ is a vector, see Fig. 1.2

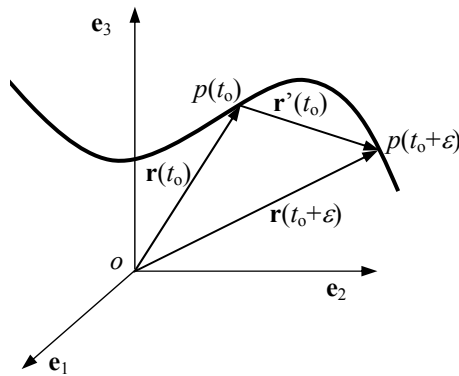


Figure 1.2: Derivative of a curve.

In a similar way we define the derivative of a curve of vectors,

$$\frac{d\mathbf{r}(t)}{dt} = \lim_{\varepsilon \rightarrow 0} \frac{\mathbf{r}(t_0 + \varepsilon) - \mathbf{r}(t_0)}{\varepsilon}; \quad (1.5)$$

and of a curve of tensors

$$\frac{d\mathbf{L}(t)}{dt} = \lim_{\varepsilon \rightarrow 0} \frac{\mathbf{L}(t_0 + \varepsilon) - \mathbf{L}(t_0)}{\varepsilon}, \quad (1.6)$$

being defined as differences of vectors or of tensors, the derivative of a curve of vectors is a vector and that of a curve of tensors is a tensor.

We indicate also $\frac{dp}{dt}$ as p' and, if t is the time, as \dot{p} ; the same will be do also for the derivatives of vector and tensor curves.

The following rules for the differentiation of products or sums of curves can be easily shown using the above definitions:

$$\begin{aligned} (\mathbf{u} + \mathbf{v})' &= \mathbf{u}' + \mathbf{v}', \\ (\alpha\mathbf{v})' &= \alpha'\mathbf{v} + \alpha\mathbf{v}', \quad \alpha(t) : \mathbb{R} \rightarrow \mathbb{R}, \\ (\mathbf{u} \cdot \mathbf{v})' &= \mathbf{u}' \cdot \mathbf{v} + \mathbf{u} \cdot \mathbf{v}', \\ (\mathbf{u} \times \mathbf{v})' &= \mathbf{u}' \times \mathbf{v} + \mathbf{u} \times \mathbf{v}', \\ [\mathbf{v}(\alpha(t))]' &= \mathbf{v}'(\alpha(t)) \alpha'(t), \quad \alpha(t) : \mathbb{R} \rightarrow \mathbb{R}, \\ (\mathbf{u} \otimes \mathbf{v})' &= \mathbf{u}' \otimes \mathbf{v} + \mathbf{u} \otimes \mathbf{v}', \\ (\mathbf{L}\mathbf{u})' &= \mathbf{L}'\mathbf{u} + \mathbf{L}\mathbf{u}', \\ (\mathbf{L}\mathbf{M})' &= \mathbf{L}'\mathbf{M} + \mathbf{L}\mathbf{M}', \\ (\mathbf{L}^{-1})' &= -\mathbf{L}^{-1}\mathbf{L}'\mathbf{L}^{-1}, \\ (\det \mathbf{L})' &= \det \mathbf{L} \mathbf{L}'^{\top} \cdot \mathbf{L}^{-1}. \end{aligned} \quad (1.7)$$

An important case is that of a vector $\mathbf{v}(t)$ whose norm $v(t)$ is constant $\forall t$:

$$(v^2)' = (\mathbf{v} \cdot \mathbf{v})' = \mathbf{v}' \cdot \mathbf{v} + \mathbf{v} \cdot \mathbf{v}' = 2\mathbf{v}' \cdot \mathbf{v} = 0 : \quad (1.8)$$

the derivative of such a vector is orthogonal to it $\forall t$. The contrary is also true, as immediately apparent.

The *second derivative* of a curve is simply defined as the derivative of the derivative of a curve. In such a way, derivatives of any order can be defined and calculated.

Finally, using the above rules and assuming that the reference frame \mathcal{R} is independent from t , we get easily that

$$\begin{aligned} p'(t) &= p'_i(t) \mathbf{e}_i, \\ \mathbf{v}'(t) &= v'_i(t) \mathbf{e}_i, \\ \mathbf{L}'(t) &= L'_{ij}(t) \mathbf{e}_i \otimes \mathbf{e}_j. \end{aligned} \quad (1.9)$$

1.3 Integral of a curve of vectors

We define *integral of a curve of vectors* between a and $b \in [t_1, t_2]$ the curve that is obtained integrating each component of the curve:

$$\int_a^b \mathbf{r}(t) dt = \int_a^b r_i(t) dt \mathbf{e}_i. \quad (1.10)$$

If the curve is regular, we can generalize the second fundamental theorem of the integral calculus

$$\mathbf{r}(t) = \mathbf{r}(a) + \int_a^t \mathbf{r}'(t^*) dt^*. \quad (1.11)$$

Because

$$\mathbf{r}(t) = p(t) - o, \quad \mathbf{r}'(t) = (p(t) - o)' = p'(t), \quad (1.12)$$

we get also

$$p(t) = p(a) + \int_a^t p'(t^*) dt^*. \quad (1.13)$$

The integral of a vector function is the generalization of the vector sum, see Fig. 1.3.

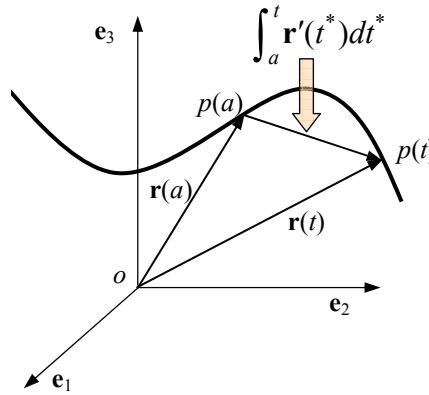


Figure 1.3: Integral of a vector curve.

A simple way to determine a point $p(t)$ on a curve is to fix a point p_0 on the curve and to measure the length $s(t)$ of the arc of curve between $p_0 = p(t = 0)$ and $p(t)$. This length $s(t)$ is called a *curvilinear abscissa* and it can be shown that

$$s(t) = \int_{t_0}^t |(p(t^*) - o)'| dt^* = \int_{t_0}^t |\mathbf{r}'(t^*)| dt^*, \quad (1.14)$$

so that the total length ℓ of a curve is

$$\ell = \int_a^b |\mathbf{r}'(t)| dt. \quad (1.15)$$

From eq. (1.14) we get

$$\frac{ds}{dt} = |\mathbf{r}'(t)| = \sqrt{\left(\frac{dr_1}{dt}\right)^2 + \left(\frac{dr_2}{dt}\right)^2 + \left(\frac{dr_3}{dt}\right)^2} > 0 \quad (1.16)$$

so that $s(t)$ is an increasing function of t and the length of an infinitesimal arc is

$$ds = \sqrt{dr_1^2 + dr_2^2 + dr_3^2} = \sqrt{dx^2 + dy^2 + dz^2}. \quad (1.17)$$

For a plane curve $y = f(x)$, we can always put $t = x$, which gives the parametric equation

$$p(t) = (t, f(t)), \quad (1.18)$$

or in vector form

$$\mathbf{r}(t) = t \mathbf{e}_1 + f(t) \mathbf{e}_2, \quad (1.19)$$

from which we obtain

$$\frac{ds}{dt} = |\mathbf{r}'(t)| = |p'(t)| = \sqrt{1 + f'^2(t)}, \quad (1.20)$$

that gives the length of a plane curve between $t = x_0$ and $t = x$ as a function of the abscissa x :

$$s(x) = \int_{x_0}^x \sqrt{1 + f'^2(t)} dt. \quad (1.21)$$

1.4 The Frenet-Serret basis

We define the *tangent vector* $\boldsymbol{\tau}(t)$ to a regular curve $p = p(t)$ the vector

$$\boldsymbol{\tau}(t) = \frac{p'(t)}{|p'(t)|}. \quad (1.22)$$

By the definition of derivative, this unit vector is always oriented as the increasing values of t ; the straight line tangent to the curve in $p_0 = p(t_0)$ has hence equation

$$q(\bar{t}) = p(t_0) + \bar{t} \boldsymbol{\tau}(t_0). \quad (1.23)$$

If the curvilinear abscissa s is chosen as parameter for the curve, through the change of parameter $s = s(t)$ we get

$$\boldsymbol{\tau}(t) = \frac{p'(t)}{|p'(t)|} = \frac{p'[s(t)]}{|p'[s(t)]|} = \frac{1}{s'(t)} \frac{dp(s)}{ds} \frac{ds(t)}{dt} = \frac{dp(s)}{ds} \rightarrow \boldsymbol{\tau}(s) = p'(s). \quad (1.24)$$

So, if the parameter of the curve is s , the derivative of the curve is $\boldsymbol{\tau}$, i.e. it is automatically a unit vector. The above equation, in addition, shows that the change of parameter does not change the direction of the tangent, because just a scalar, the derivative of the parameter's change, multiplies the vector. Nevertheless, generally speaking, a change of parameter can change the orientation of the curve.

Because the norm of $\boldsymbol{\tau}$ is constant, its derivative is a vector orthogonal to $\boldsymbol{\tau}$, see eq. (1.8). That is why we call *principal normal vector* to a curve the unit vector

$$\boldsymbol{\nu}(t) = \frac{\boldsymbol{\tau}'(t)}{|\boldsymbol{\tau}'(t)|}. \quad (1.25)$$

$\boldsymbol{\nu}$ is defined only on the points of the curve where $\boldsymbol{\tau}' \neq \mathbf{0}$ which implies that $\boldsymbol{\nu}$ is not defined on the points of a straight line. This simply means that there is not, among the

infinite unit normal vectors to a straight line, a normal with special properties, a *principal* one, uniquely linked to $\boldsymbol{\tau}$.

Unlike $\boldsymbol{\tau}$, whose orientation changes with the choice of the parameter, $\boldsymbol{\nu}$ is an *intrinsic* local characteristic of the curve: *it is not affected by the choice of the parameter*. In fact, by its same definition, $\boldsymbol{\nu}$ does not depend upon the reference frame; then, because the direction of $\boldsymbol{\tau}$ is also independent upon the parameter's choice, the only factor that could affect $\boldsymbol{\nu}$ is the orientation of the curve, that depends upon the parameter. But a change of the orientation affects, in (1.25), both $\boldsymbol{\tau}$ and the sign of the increment dt , so that $\boldsymbol{\tau}'(t) = d\boldsymbol{\tau}/dt$ does not change, neither $\boldsymbol{\nu}$, which is hence an intrinsic property of the curve.

The vector

$$\boldsymbol{\beta}(t) = \boldsymbol{\tau}(t) \times \boldsymbol{\nu}(t) \quad (1.26)$$

is called the *binormal vector*; by construction, it is orthogonal to $\boldsymbol{\tau}$ and $\boldsymbol{\nu}$ and it is a unit vector. In addition, it is evident that

$$\boldsymbol{\tau} \times \boldsymbol{\nu} \cdot \boldsymbol{\beta} = 1, \quad (1.27)$$

so the set $\{\boldsymbol{\tau}, \boldsymbol{\nu}, \boldsymbol{\beta}\}$ forms a positively oriented orthonormal basis that can be defined at any regular point of a curve with $\boldsymbol{\tau}' \neq \mathbf{o}$. Such a basis is called the *Frenet-Serret local basis*, local in the sense that it changes with the position along the curve. The plane $\boldsymbol{\tau} - \boldsymbol{\nu}$ is the *osculating plane*, the plane $\boldsymbol{\nu} - \boldsymbol{\beta}$ the *normal plane* and the plane $\boldsymbol{\beta} - \boldsymbol{\tau}$ the *rectifying plane*, see Fig. 1.4. The osculating plane is particularly important: if we

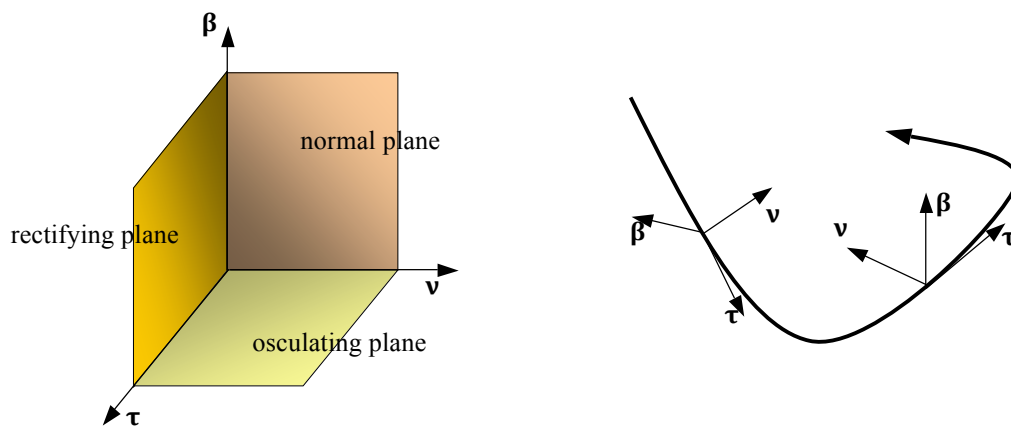


Figure 1.4: The Frenet-Serret basis.

consider a plane passing through three not aligned points of the curve, when these points become closer and closer, still remaining on the curve, the plane tends to the osculating plane: the osculating plane at a point of a curve is the plane that better approaches the curve near the point. A plane curve is entirely contained in the osculating plane, which is fixed.

The principal normal $\boldsymbol{\nu}$ is always oriented towards the part of the space, with respect to the rectifying plane, where the curve is; in particular, for a plane curve, $\boldsymbol{\nu}$ is always directed towards the concavity of the curve. To show it, it is sufficient to prove that the

vector $p(t + \varepsilon) - p(t)$ forms with $\boldsymbol{\nu}$ an angle $\psi \leq \pi/2$, i.e. that $(p(t + \varepsilon) - p(t)) \cdot \boldsymbol{\nu} \geq 0$. In fact,

$$\begin{aligned} p(t + \varepsilon) - p(t) &= \varepsilon p'(t) + \frac{1}{2}\varepsilon^2 p''(t) + o(\varepsilon^2) \rightarrow \\ (p(t + \varepsilon) - p(t)) \cdot \boldsymbol{\nu} &= \frac{1}{2}\varepsilon^2 p''(t) \cdot \boldsymbol{\nu} + o(\varepsilon^2), \end{aligned} \quad (1.28)$$

but

$$p''(t) \cdot \boldsymbol{\nu} = (\boldsymbol{\tau}'|p'| + \boldsymbol{\tau}|p''|) \cdot \boldsymbol{\nu} = (|\boldsymbol{\tau}'||p'| + \boldsymbol{\tau}|p''|) \cdot \boldsymbol{\nu} = |\boldsymbol{\tau}'||p'|, \quad (1.29)$$

so that, to within infinitesimal quantities of order $o(\varepsilon^2)$, we obtain

$$(p(t + \varepsilon) - p(t)) \cdot \boldsymbol{\nu} = \frac{1}{2}\varepsilon^2 |\boldsymbol{\tau}'||p'| \geq 0. \quad (1.30)$$

1.5 Curvature of a curve

It is important, in several situations, to evaluate how much a curve moves away from a straight line, in the neighborhood of a point. To do that, we calculate the angle formed by the tangents at two close points, determined by the curvilinear abscissae s and $s + \varepsilon$, and we measure the angle $\chi(s, \varepsilon)$ that they form, see Fig. 1.5.

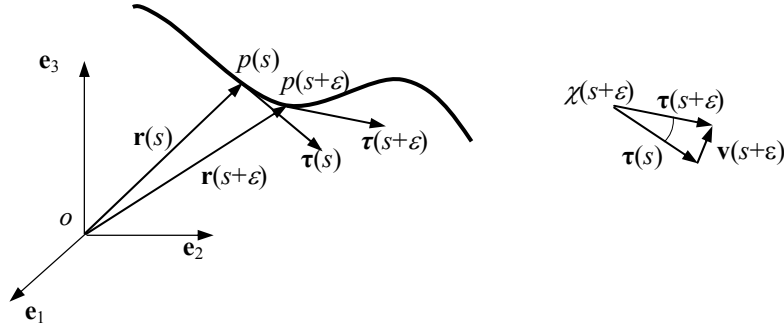


Figure 1.5: Curvature of a curve.

We then define *curvature* of the curve in $p = p(s)$ the limit

$$c(s) = \lim_{\varepsilon \rightarrow 0} \left| \frac{\chi(s, \varepsilon)}{\varepsilon} \right|. \quad (1.31)$$

The curvature is hence a non-negative scalar that measures the rapidity of variation of the direction of the curve per unit length of the curve (that is why $c(s)$ is defined as a function of the curvilinear abscissa); by its same definition, the curvature is an *intrinsic property* of the curve, i.e. independent from the parameter's choice. For a straight line, the curvature is identically null everywhere.

The curvature is linked to the second derivative of the curve:

$$\begin{aligned} c(s) &= \lim_{\varepsilon \rightarrow 0} \left| \frac{\chi(s, \varepsilon)}{\varepsilon} \right| = \lim_{\varepsilon \rightarrow 0} \left| \frac{\sin \chi(s, \varepsilon)}{\varepsilon} \right| = \lim_{\varepsilon \rightarrow 0} \left| \frac{2}{\varepsilon} \sin \frac{\chi(s, \varepsilon)}{2} \right| = \\ &= \lim_{\varepsilon \rightarrow 0} \left| \frac{\mathbf{v}(s, \varepsilon)}{\varepsilon} \right| = \lim_{\varepsilon \rightarrow 0} \left| \frac{\boldsymbol{\tau}(s + \varepsilon) - \boldsymbol{\tau}(s)}{\varepsilon} \right| = |\boldsymbol{\tau}'(s)| = |p''(s)|. \end{aligned} \quad (1.32)$$

Another formula for the calculation of $c(s)$ can be obtained if we consider that

$$\frac{d\boldsymbol{\tau}[s(t)]}{dt} = \frac{d\boldsymbol{\tau}}{ds} \frac{ds}{dt} = \frac{d\boldsymbol{\tau}}{ds} |p'(t)| \rightarrow \frac{d\boldsymbol{\tau}}{ds} = \frac{1}{|p'(t)|} \frac{d\boldsymbol{\tau}}{dt}, \quad (1.33)$$

so that

$$c(s) = |\boldsymbol{\tau}'(s)| = \frac{1}{|p'(t)|} \left| \frac{d\boldsymbol{\tau}}{dt} \right| = \frac{|\boldsymbol{\tau}'(t)|}{|p'(t)|}. \quad (1.34)$$

A better formula can be obtained as follows:

$$\begin{aligned} \frac{d\boldsymbol{\tau}}{ds} &= \frac{1}{|p'(t)|} \frac{d\boldsymbol{\tau}}{dt} = \frac{1}{|p'(t)|} \frac{d}{dt} \frac{p'(t)}{|p'(t)|} = \frac{1}{|p'|} \frac{p''|p'| - p' \frac{p'' \cdot p'}{|p'|}}{|p'|^2} = \\ &= \frac{p'' - \boldsymbol{\tau} p'' \cdot \boldsymbol{\tau}}{|p'|^2} = (\mathbf{I} - \boldsymbol{\tau} \otimes \boldsymbol{\tau}) \frac{p''}{|p'|^2}. \end{aligned} \quad (1.35)$$

By consequence,

$$c(s) = \left| \frac{d\boldsymbol{\tau}(s)}{ds} \right| = \frac{1}{|p'|^2} |(\mathbf{I} - \boldsymbol{\tau} \otimes \boldsymbol{\tau}) p''|. \quad (1.36)$$

Now, we use the following general formula expressing a skew tensor \mathbf{W} :

$$\mathbf{W}\mathbf{W} = -\frac{1}{2} |\mathbf{W}|^2 (\mathbf{I} - \mathbf{w} \otimes \mathbf{w}); \quad (1.37)$$

if we use this formula for $\boldsymbol{\tau}$, so that \mathbf{W} is the axial tensor of $\boldsymbol{\tau}$, we get

$$\mathbf{I} - \boldsymbol{\tau} \otimes \boldsymbol{\tau} = -2 \frac{\mathbf{W}\mathbf{W}}{|\mathbf{W}|^2} = -\mathbf{W}\mathbf{W}, \quad (1.38)$$

because if $\boldsymbol{\tau} = (\tau_1, \tau_2, \tau_3)$, then

$$\begin{aligned} |\mathbf{W}|^2 = \mathbf{W} \cdot \mathbf{W} &= \begin{bmatrix} 0 & -\tau_3 & \tau_2 \\ \tau_3 & 0 & -\tau_1 \\ -\tau_2 & \tau_1 & 0 \end{bmatrix} \cdot \begin{bmatrix} 0 & -\tau_3 & \tau_2 \\ \tau_3 & 0 & -\tau_1 \\ -\tau_2 & \tau_1 & 0 \end{bmatrix} = \\ &= 2(\tau_1^2 + \tau_2^2 + \tau_3^2) = 2. \end{aligned} \quad (1.39)$$

So, recalling that for any skew tensor \mathbf{W} ,

$$\mathbf{W} \mathbf{u} = \mathbf{w} \times \mathbf{u} \quad \forall \mathbf{u} \in \mathcal{V}, \quad (1.40)$$

with \mathbf{w} the axial vector of \mathbf{W} , we get

$$\begin{aligned} |(\mathbf{I} - \boldsymbol{\tau} \otimes \boldsymbol{\tau}) p''| &= |-\mathbf{W}\mathbf{W} p''| = |-\mathbf{W}(\boldsymbol{\tau} \times p'')| = |-\boldsymbol{\tau} \times (\boldsymbol{\tau} \times p'')| = \\ &= |\boldsymbol{\tau} \times (\boldsymbol{\tau} \times p'')| = |\boldsymbol{\tau} \times p''| = \frac{|p' \times p''|}{|p'|}, \end{aligned} \quad (1.41)$$

so that finally

$$c = \frac{|p' \times p''|}{|p'|^3}. \quad (1.42)$$

Applying this last formula to a plane curve $p(t) = (x(t), y(t))$, we get

$$c = \frac{|x'y'' - x''y'|}{(x'^2 + y'^2)^{\frac{3}{2}}} \quad (1.43)$$

and if the curve is given in the form $y = y(x)$, so that the parameter $t = x$, then we obtain

$$c = \frac{|y''|}{(1 + y'^2)^{\frac{3}{2}}}. \quad (1.44)$$

This last formula shows that if $|y'| \ll 1$, like in the infinitesimal theory of strain, then

$$c \simeq |y''|. \quad (1.45)$$

1.6 The Frenet-Serret formulae

From eqs. (1.25) for $t = s$ and (1.34) we get

$$\frac{d\boldsymbol{\tau}}{ds} = c \boldsymbol{\nu} \quad (1.46)$$

which is the *first Frenet-Serret Formula*, giving the variation of $\boldsymbol{\tau}$ per unit length of the curve. Such a variation is a vector whose norm is the curvature and that has as direction that of $\boldsymbol{\nu}$.

Let us now consider the variation of $\boldsymbol{\beta}$ per unit length of the curve; because $\boldsymbol{\beta}$ is a unit vector, we have

$$\frac{d\boldsymbol{\beta}}{ds} \cdot \boldsymbol{\beta} = 0, \quad (1.47)$$

and

$$\boldsymbol{\beta} \cdot \boldsymbol{\tau} = 0 \Rightarrow \frac{d(\boldsymbol{\beta} \cdot \boldsymbol{\tau})}{ds} = \frac{d\boldsymbol{\beta}}{ds} \cdot \boldsymbol{\tau} + \boldsymbol{\beta} \cdot \frac{d\boldsymbol{\tau}}{ds} = 0. \quad (1.48)$$

Through eq. (1.46) and because $\boldsymbol{\beta} \cdot \boldsymbol{\nu} = 0$ we get

$$\frac{d\boldsymbol{\beta}}{ds} \cdot \boldsymbol{\tau} = -c \boldsymbol{\beta} \cdot \boldsymbol{\nu} = 0, \quad (1.49)$$

so that $\frac{d\boldsymbol{\beta}}{ds}$ is necessarily parallel to $\boldsymbol{\nu}$. We then put

$$\frac{d\boldsymbol{\beta}}{ds} = \vartheta \boldsymbol{\nu}, \quad (1.50)$$

which is the *second Frenet-Serret formula*. The scalar $\vartheta(s)$ is called the *torsion of the curve* in $p = p(s)$. So, we see that the variation of $\boldsymbol{\beta}$ per unit length is a vector parallel to $\boldsymbol{\nu}$ and proportional to the torsion of the curve.

We can now find the variation of $\boldsymbol{\nu}$ per unit length of the curve:

$$\frac{d\boldsymbol{\nu}}{ds} = \frac{d(\boldsymbol{\beta} \times \boldsymbol{\tau})}{ds} = \frac{d\boldsymbol{\beta}}{ds} \times \boldsymbol{\tau} + \boldsymbol{\beta} \times \frac{d\boldsymbol{\tau}}{ds} = \vartheta \boldsymbol{\nu} \times \boldsymbol{\tau} + c \boldsymbol{\beta} \times \boldsymbol{\nu}, \quad (1.51)$$

so finally

$$\frac{d\boldsymbol{\nu}}{ds} = -c \boldsymbol{\tau} - \vartheta \boldsymbol{\beta}, \quad (1.52)$$

which is the *third Frenet-Serret formula*: the variation of $\boldsymbol{\nu}$ per unit length of the curve is a vector of the rectifying plane.

The three formulae of Frenet-Serret (discovered independently by J. F. Frenet in 1847 and by J. A. Serret in 1851) can be condensed in the symbolic matrix product

$$\begin{Bmatrix} \boldsymbol{\tau}' \\ \boldsymbol{\nu}' \\ \boldsymbol{\beta}' \end{Bmatrix} = \begin{bmatrix} 0 & c & 0 \\ -c & 0 & -\vartheta \\ 0 & \vartheta & 0 \end{bmatrix} \begin{Bmatrix} \boldsymbol{\tau} \\ \boldsymbol{\nu} \\ \boldsymbol{\beta} \end{Bmatrix}. \quad (1.53)$$

1.7 The torsion of a curve

We have introduced the torsion of a curve in the previous section, with the second formula of Frenet-Serret. The torsion measures the deviation of a curve from flatness: if a curve is planar, it belongs to the osculating plane and $\boldsymbol{\beta}$, which is perpendicular to the osculating plane, is hence a constant vector. So, its derivative is null and by the Frenet-Serret second formula $\vartheta = 0$.

Conversely, if $\vartheta = 0$ everywhere, $\boldsymbol{\beta}$ is a constant vector and hence the osculating plane does not change and the curve is planar. So we have that *a curve is planar if and only if the torsion is null $\forall p(s)$* .

Using the Frenet-Serret formulae in the expression of $p'''(s)$ we get a formula for the torsion:

$$\begin{aligned} p'(t) &= |p'| \boldsymbol{\tau} = \frac{dp}{ds} \frac{ds}{dt} = s' \boldsymbol{\tau} \Rightarrow |p'| = s' \rightarrow \\ p''(t) &= s'' \boldsymbol{\tau} + s' \boldsymbol{\tau}' = s'' \boldsymbol{\tau} + s'^2 \frac{d\boldsymbol{\tau}}{ds} = s'' \boldsymbol{\tau} + c s'^2 \boldsymbol{\nu} \rightarrow \\ p'''(t) &= s''' \boldsymbol{\tau} + s'' \boldsymbol{\tau}' + (c s'^2)' \boldsymbol{\nu} + c s'^2 \boldsymbol{\nu}' = \\ &= s''' \boldsymbol{\tau} + s'' s' \frac{d\boldsymbol{\tau}}{ds} + (c s'^2)' \boldsymbol{\nu} + c s'^3 \frac{d\boldsymbol{\nu}}{ds} = \\ &= s''' \boldsymbol{\tau} + s'' s' c \boldsymbol{\nu} + (c s'^2)' \boldsymbol{\nu} - c s'^3 (c \boldsymbol{\tau} + \vartheta \boldsymbol{\beta}) = \\ &= (s''' - c^2 s'^3) \boldsymbol{\tau} + (s'' s' c + c' s'^2 + 2c s' s'') \boldsymbol{\nu} - c s'^3 \vartheta \boldsymbol{\beta}, \end{aligned} \quad (1.54)$$

so that, through eq. (1.42), we get

$$\begin{aligned} p' \times p'' \cdot p''' &= s' \boldsymbol{\tau} \times (s'' \boldsymbol{\tau} + c s'^2 \boldsymbol{\nu}) \cdot [(s''' - c^2 s'^3) \boldsymbol{\tau} + \\ &+ (s'' s' c + c' s'^2 + 2c s' s'') \boldsymbol{\nu} - c s'^3 \vartheta \boldsymbol{\beta}] = \\ &= -c^2 s'^6 \vartheta = -c^2 |p'|^6 \vartheta = -\frac{|p' \times p''|^2}{|p'|^6} |p'|^6 \vartheta, \end{aligned} \quad (1.55)$$

so that, finally,

$$\vartheta = -\frac{p' \times p'' \cdot p'''}{|p' \times p''|^2}. \quad (1.56)$$

To remark that while the curvature is linked to the second derivative of the curve, the torsion is a function also of the third derivative.

Unlike curvature, which is intrinsically positive, the torsion can be negative. In fact, still using the Frenet-Serret formulae,

$$\begin{aligned}
 p(s + \varepsilon) - p(s) &= \varepsilon p' + \frac{1}{2}\varepsilon^2 p'' + \frac{1}{6}\varepsilon^3 p''' + o(\varepsilon^3) = \\
 &= \varepsilon \boldsymbol{\tau} + \frac{1}{2}\varepsilon^2 c \boldsymbol{\nu} + \frac{1}{6}\varepsilon^3 (c \boldsymbol{\nu})' + o(\varepsilon^3) = \\
 &= \varepsilon \boldsymbol{\tau} + \frac{1}{2}\varepsilon^2 c \boldsymbol{\nu} + \frac{1}{6}\varepsilon^3 (c' \boldsymbol{\nu} - c^2 \boldsymbol{\tau} - c \vartheta \boldsymbol{\beta}) + o(\varepsilon^3) \rightarrow \\
 (p(s + \varepsilon) - p(s)) \cdot \boldsymbol{\beta} &= -\frac{1}{6}\varepsilon^3 c \vartheta + o(\varepsilon^3).
 \end{aligned} \tag{1.57}$$

The above dot product determines if the point $p(s + \varepsilon)$ is located, with respect to the osculating plane, on the side of $\boldsymbol{\beta}$ or on the opposite one, see Fig. 1.6: if following the curve for increasing values of s , $\varepsilon > 0$, the point passes into the semi-space of $\boldsymbol{\beta}$ from the opposite one, because $1/6 c \varepsilon^3 > 0$, it will be $\vartheta < 0$, while in the opposite case it will be $\vartheta > 0$.

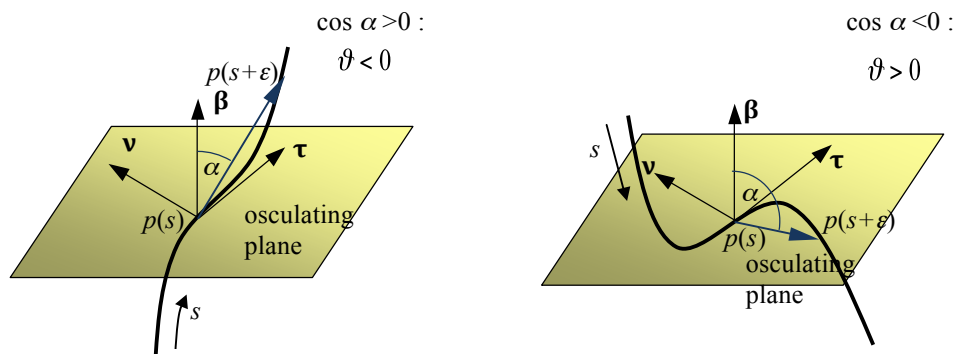


Figure 1.6: Torsion of a curve.

This result is intrinsic, i.e. it does not depend upon the choice of the parameter, hence of the positive orientation of the curve; in fact, $\boldsymbol{\nu}$ is intrinsic, but changing the orientation of the curve, $\boldsymbol{\tau}$, and hence $\boldsymbol{\beta}$, change of orientation.

1.8 Osculating sphere and circle

The *osculating sphere*² to a curve at a point p is a sphere to which the curve tends to adhere in the neighborhood of p . Mathematically speaking, if q_s is the center of the sphere relative to point $p(s)$, then

$$|p(s + \varepsilon) - q_s|^2 = |p(s) - q_s|^2 + o(\varepsilon^3). \tag{1.58}$$

²The word *osculating* comes from the latin word *osculo* that means to kiss; an osculating sphere or circle or plane is a geometric object that is very close to the curve, as close as two lovers are in a kiss.

Using this definition, discarding the terms of order $o(\varepsilon^3)$ and using the Frenet-Serret formulae, we get:

$$\begin{aligned}
|p(s + \varepsilon) - q_s|^2 &= |p(s) - q_s + \varepsilon p' + \frac{1}{2}\varepsilon^2 p'' + \frac{1}{6}\varepsilon^3 p''' + o(\varepsilon^3)|^2 = \\
&= |p(s) - q_s + \varepsilon \boldsymbol{\tau} + \frac{1}{2}\varepsilon^2 c \boldsymbol{\nu} + \frac{1}{6}\varepsilon^3 (c\boldsymbol{\nu})' + o(\varepsilon^3)|^2 = \\
&= |p(s) - q_s|^2 + 2\varepsilon(p(s) - q_s) \cdot \boldsymbol{\tau} + \varepsilon^2 + \varepsilon^2 c(p(s) - q_s) \cdot \boldsymbol{\nu} + \\
&\quad \frac{1}{3}\varepsilon^3(p(s) - q_s) \cdot (c'\boldsymbol{\nu} - c^2\boldsymbol{\tau} - c\vartheta\boldsymbol{\beta}) + o(\varepsilon^3),
\end{aligned} \tag{1.59}$$

which gives

$$\begin{aligned}
(p(s) - q_s) \cdot \boldsymbol{\tau} &= 0, \\
(p(s) - q_s) \cdot \boldsymbol{\nu} &= -\frac{1}{c} = -\rho, \\
(p(s) - q_s) \cdot \boldsymbol{\beta} &= -\frac{c'}{c^2\vartheta} = \frac{\rho'}{\vartheta},
\end{aligned} \tag{1.60}$$

and finally

$$q_s = p + \rho \boldsymbol{\nu} - \frac{\rho'}{\vartheta} \boldsymbol{\beta}, \tag{1.61}$$

so the center of the sphere belongs to the normal plane; the sphere is not defined for a plane curve. ρ is the *radius of curvature* of the curve, defined as

$$\rho = \frac{1}{c}. \tag{1.62}$$

The radius of the osculating sphere is

$$\rho_s = |p - q_s| = \sqrt{\rho^2 + \left(\frac{\rho'}{\vartheta}\right)^2}. \tag{1.63}$$

The intersection between the osculating sphere and the osculating plane at a same point p is the *osculating circle*. This circle has the property to share the same tangent in p with the curve and its radius is the radius of curvature, ρ . From eq. (1.61) we get the position of the osculating circle center q :

$$q = p + \rho \boldsymbol{\nu}. \tag{1.64}$$

The osculating circle is a diametral circle of the osculating sphere only when $q = q_s$, so if and only if

$$\frac{\rho'}{\vartheta} = -\frac{c'}{c^2\vartheta} = 0, \tag{1.65}$$

i.e. when the curvature is constant.

1.9 Exercises

1. The curve whose polar equation is

$$r = a \theta, \quad a \in \mathbb{R},$$

is an *Archimede's spiral*. Find its curvature, its length for $\theta \in [0, 2\pi)$ and prove that any straight line passing by the origin is divided by the spiral in segments of constant length $2\pi a$ (that is why it is used to record disks).

2. The curve whose polar equation is

$$r = a e^{b\theta}, \quad a, b \in \mathbb{R},$$

is the *logarithmic spiral*. Prove that the origin is an asymptotic point of the curve, find its curvature and the length of the segment in which a straight line by the origin is divided by two consecutive intersections with the spiral. Then prove that the curve is plane and its *equiangular property*: $(p(\theta) - o) \cdot \boldsymbol{\tau}(\theta) = \text{const.}$

3. The curve whose parametric equation is

$$p(\theta) = a(\cos \theta + \theta \sin \theta)\mathbf{e}_1 + a(\sin \theta - \theta \cos \theta)\mathbf{e}_2$$

with the parameter θ the angle formed by $p(\theta) - o$ with the x_1 -axis is the *involute of the circle*. Find its curvature and length for $\theta \in [0, 2\pi)$ and prove that the geometrical set of the points $p(\theta) + \rho(\theta)\boldsymbol{\nu}(\theta)$ is exactly the circle of center o and radius a (that is why the involute of the circle is used to profile engrenages).

4. The curve whose parametric equation is

$$p(\theta) = a \cos \omega\theta \mathbf{e}_1 + a \sin \omega\theta \mathbf{e}_2 + b\omega\theta \mathbf{e}_3$$

is a *helix* that winds on a circular cylinder of radius a . Show that the angle formed by the helix and any generatrix of the cylinder is constant (a property that defines a helix in the general case). Then, find its length for $\theta \in [0, 2\pi)$, curvature, torsion and pitch (the distance, on a same generatrix, between two successive intersections with the helix). Prove then the *Bertrand's theorem*: a curve is a cylindrical helix if and only if the ratio $c/\vartheta = \text{const.}$ Finally, prove that for the above circular helix there are two constants A and B such that

$$p' \times p'' = A\mathbf{u}(\theta) + B\mathbf{e}_3,$$

with

$$\mathbf{u} = \sin \omega\theta \mathbf{e}_1 - \cos \omega\theta \mathbf{e}_2;$$

find then A and B .

5. For the curve whose cylindrical equation is

$$\begin{cases} r = 1, \\ z = \sin \theta \end{cases}$$

find the highest curvature and determine whether or not it is planar.

Chapter 2

Cables

2.1 Introduction

We define as a *cable* a special type of continuum body: a curve endowed with a linear mass density. This definition is not sufficient to characterize mechanically a cable (also a curved rod geometrically is a curve): the fundamental relation mechanically defining a cable must be given in terms of internal actions, which is done in the next section.

A cable is called *inextensible* if the distance

$$\Delta s = s_B - s_A \tag{2.1}$$

measured along the cable between two arbitrary points p_A and p_B of the curve, determined on it by two curvilinear abscissae $s_B > s_A$, is constant at any time t . If this does not happen, the cable is *extensible*.

2.2 Mechanical definition of a cable

We use the *Euler Sections Principle*, valid for any continuum body, to define mechanically a cable. This principle states simply that *a body is in equilibrium if and only if any of its parts is in equilibrium*.

For the whole body, this necessitates the equilibrium of all the external forces applied to the body, actions and reactions. But if one isolates, ideally, a part of the body, then only a part of the whole external forces will be directly applied to the isolated portion of the body, so, generally speaking, the equilibrium of the isolated part will be restored only by admitting the existence of some actions, called the *internal actions*, that are transmitted to the isolated part by the remaining parts of the body, throughout the contact zones. Physically speaking, these internal actions are the resultant and resultant moment of the contact forces, i.e. of the stresses that the different parts of the body exchange at any point of it. The Euler's section in the case of a curve reduces of course to a point, called the *separation point*.

This concept is shared by all the continuum bodies, that differ for the definition of the type of internal actions that they can develop at any point of the continuum.

We give then the following mechanical definition:

a cable is a curvilinear unidimensional continuum body whose internal actions that two ideally separated parts of it exchange through the separation point are statically equivalent to a single tension force applied exactly in correspondence of the separation point.

Such a tensile force is currently named *tension in the cable* and will be indicated in the following by $\boldsymbol{\theta}(s)$, and its norm, the intensity of the force, by $\theta(s)$.

This is the physical property that mechanically defines a cable in our model; it is true for extensible or inextensible cables. Let us see now what are the consequences of this definition.

To this purpose, we write the statics balance equations for the part (1) of a cable of length ℓ , from $p_0 = p(s = 0)$, the beginning of the cable, to the point $p(s)$, see Fig. 2.1. For the while, we assume that only distributed loads, whose linear intensity is $\mathbf{f}(s)$, act upon the cable. $\boldsymbol{\theta}(s)$ is the tension that the part (2) of the cable, that between $p(s)$ and $p_1 = p(s = \ell)$ apply to the part (1):

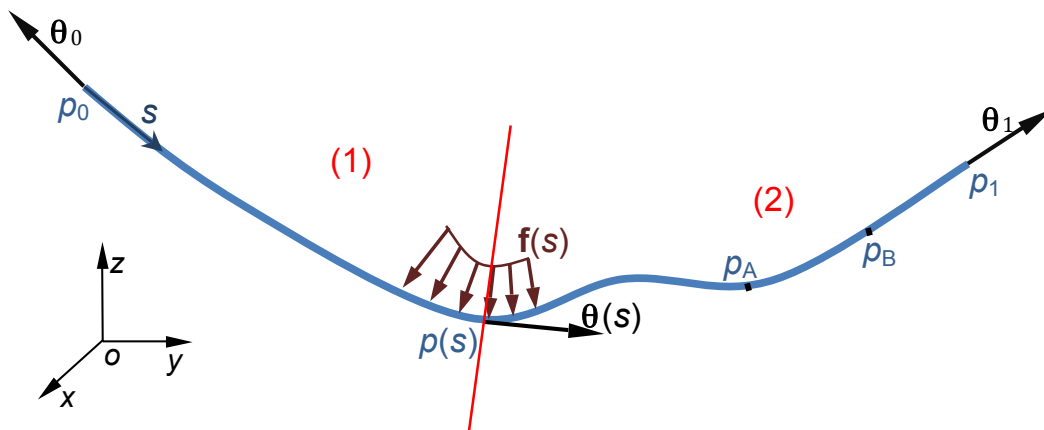


Figure 2.1: General scheme of a cable

- balance of the forces:

$$\boldsymbol{\theta}_0 + \int_0^s \mathbf{f}(s^*) ds^* + \boldsymbol{\theta}(s) = \mathbf{o}, \quad (2.2)$$

- balance of the moments, with respect to a point o :

$$(p_0 - o) \times \boldsymbol{\theta}_0 + \int_0^s (p(s^*) - o) \times \mathbf{f}(s^*) ds^* + (p(s) - o) \times \boldsymbol{\theta}(s) = \mathbf{o}. \quad (2.3)$$

Differentiating these equations, we get the *local balance equations* for the cable:

$$\begin{aligned} \mathbf{f}(s) + \frac{d\boldsymbol{\theta}(s)}{ds} &= \mathbf{o}, \\ (p(s) - o) \times \mathbf{f}(s) + \frac{d}{ds} [(p(s) - o) \times \boldsymbol{\theta}(s)] &= \mathbf{o}. \end{aligned} \quad (2.4)$$

After differentiating the second term in eq. (2.4)₂ we get

$$\begin{aligned} (p(s) - o) \times \mathbf{f}(s) + \boldsymbol{\tau}(s) \times \boldsymbol{\theta}(s) + (p(s) - o) \times \frac{d\boldsymbol{\theta}(s)}{ds} &= \mathbf{o} \rightarrow \\ (p(s) - o) \times \left(\mathbf{f}(s) + \frac{d\boldsymbol{\theta}(s)}{ds} \right) + \boldsymbol{\tau}(s) \times \boldsymbol{\theta}(s) &= \mathbf{o}, \end{aligned} \quad (2.5)$$

which gives, through the (2.4)₁,

$$\boldsymbol{\tau}(s) \times \boldsymbol{\theta}(s) = \mathbf{o} \quad \forall s, \quad (2.6)$$

so that

$$\boldsymbol{\theta}(s) = \theta(s) \boldsymbol{\tau}(s) \quad \forall s. \quad (2.7)$$

Then, at the equilibrium the tension is a force which is constantly tangent to the cable. Because the fundamental assumption is that the tension is a tensile force, it is necessarily

$$\theta(s) \geq 0 \quad \forall s. \quad (2.8)$$

Eqs. (2.7) and (2.8) defines mechanically a cable. To remark that a cable cannot transmit couples; in fact, the moment of $\boldsymbol{\theta}(s)$ with respect to $p(s)$ vanishes identically $\forall s$, as a consequence of the fact that $\boldsymbol{\theta}(s)$ is applied exactly in $p(s)$. Finally, a cable is a unidimensional continuum body without compression, shear and bending stiffness, but with only tension stiffness.

In a dual approach, we could assume eqs. (2.7) and (2.8) as the mathematical conditions defining a cable. Then, the local balance of the moments is always fulfilled because, through eqs. (2.4)₁, (2.7) and (2.8) we get

$$\begin{aligned} (p(s) - o) \times \mathbf{f}(s) + \frac{d}{ds}[(p(s) - o) \times \boldsymbol{\theta}(s)] &= \mathbf{o} \rightarrow \\ - (p(s) - o) \times \frac{d}{ds}[\theta(s)\boldsymbol{\tau}(s)] + \boldsymbol{\tau}(s) \times \theta(s)\boldsymbol{\tau}(s) &+ \\ (p(s) - o) \times \frac{d}{ds}[\theta(s)\boldsymbol{\tau}(s)] &= \mathbf{o} \text{ identically.} \end{aligned} \quad (2.9)$$

Finally, for cables it is the balance of the forces, eq. (2.4)₁, that defines equilibrium. The balance of moments, eq. (2.4)₂, can be used either to define the tension $\boldsymbol{\theta}(s)$, eq. (2.7), or, if this last is assumed *a priori*, it is automatically satisfied $\forall s$.

Intrinsically, eq. (2.4)₁ states that the equilibrium of the cable, no matter if it is extensible or not, is possible only thanks to the configuration of this last: in fact, applying the above vector equation to the infinitesimal interval $[s, s + ds]$, equilibrium can be satisfied, if $\mathbf{f}(s)$, $\boldsymbol{\theta}(s)$ and $\boldsymbol{\theta}(s + ds)$ are not collinear, only thanks to a curvature of the cable: the statics of cables is a *matter of geometry*. So, if the cable is free, it will find a configuration able to ensure the equilibrium under the action of the applied loads, while if it is wrapped on a surface, the configuration of the cable on the surface will develop contact forces equilibrated with the tension of the cable at the ends.

The balance equations of the whole cable are:

$$\begin{aligned} \boldsymbol{\theta}_0 + \int_0^\ell \mathbf{f}(s) ds + \boldsymbol{\theta}_1 &= \mathbf{o}, \\ (p_0 - o) \times \boldsymbol{\theta}_0 + \int_0^\ell (p(s) - o) \times \mathbf{f}(s) ds &+ (p_1 - o) \times \boldsymbol{\theta}_1 = \mathbf{o}. \end{aligned} \quad (2.10)$$

In the previous equations, it is $\boldsymbol{\theta}_0 = \boldsymbol{\theta}(s = 0)$ and $\boldsymbol{\theta}_1 = \boldsymbol{\theta}(s = \ell)$. From eq. (2.10), we get immediately that

$$\boldsymbol{\theta}_0 = -\theta(s = 0)\boldsymbol{\tau}(s = 0), \quad \boldsymbol{\theta}_1 = \theta(s = \ell)\boldsymbol{\tau}(s = \ell). \quad (2.11)$$

2.3 The intrinsic balance equations

The local force balance equation can be projected onto the intrinsic frame of Frenet-Serret. From the first formula of Frenet-Serret (1.46) we get

$$\mathbf{f}(s) + \frac{d}{ds}[\theta(s) \boldsymbol{\tau}(s)] = \mathbf{f}(s) + \frac{d\theta(s)}{ds}\boldsymbol{\tau}(s) + c(s) \theta(s) \boldsymbol{\nu}(s) = \mathbf{o}. \quad (2.12)$$

If we put, in the Frenet-Serret frame, $\mathbf{f} = (f_\tau, f_\nu, f_\beta)$, we obtain the three scalar *intrinsic balance equations* (Jc. Bernoulli, 1698):

$$\begin{aligned} \frac{d\theta}{ds} + f_\tau &= 0, \\ c \theta + f_\nu &= 0, \\ f_\beta &= 0. \end{aligned} \quad (2.13)$$

To remark that $f_\nu < 0$. In several problems, however, the equilibrium configuration is not known and constitutes, together with $\theta(s)$, the unknown of the problem.

The intrinsic equations state that the cable finds always a configuration of equilibrium where, pointwise, the component of the external load on $\boldsymbol{\beta}$ is null; i.e. the loads belong to the osculating plane.

The first of (2.13) gives us a general result: whenever $f_\tau = 0$, $\theta(s) = \text{const}$. The second one also gives us an interesting result: if $f_\nu = 0$, then $c \theta = 0$ and there are two possible cases: the first one is $\theta \neq 0 \forall s \Rightarrow c = 0 \forall s$: the equilibrium configuration is a straight line. So, e.g., all the parts of a cable that are unloaded assume as configuration of equilibrium a straight line. The other possibility is $\theta = 0 \forall s \Rightarrow c$ can take any value, i.e. the equilibrium configuration is undetermined: in the case of null tension, the cable can take any possible configuration, all of them are equilibrated; this is the case, e.g., of a cable simply lying on a horizontal plane, without tension forces applied to its ends.

2.4 Forces depending upon a potential

Be $\mathbf{f}(s) = \nabla U$; then

$$f_\tau = \mathbf{f}(s) \cdot \boldsymbol{\tau}(s) = \nabla U \cdot \boldsymbol{\tau}(s) = \nabla U \cdot \frac{d\mathbf{p}(s)}{ds} = \frac{\partial U}{\partial x} \frac{dx}{ds} + \frac{\partial U}{\partial y} \frac{dy}{ds} + \frac{\partial U}{\partial z} \frac{dz}{ds} = \frac{dU}{ds}. \quad (2.14)$$

So

$$f_\tau + \frac{d\theta}{ds} = 0 \rightarrow \frac{d(\theta + U)}{ds} = 0 \Rightarrow \theta + U = \text{const}. \quad (2.15)$$

This means that θ is maximum where U is minimum; that is why in a cable in equilibrium under the action of its own weight the highest tension is in correspondence of its highest point.

2.5 Parallel and coplanar forces

Be $\mathbf{f}(s) = f(s) \mathbf{e}$, with \mathbf{e} a constant unit vector. The balance of forces between $s = 0$ and s gives then

$$\theta(s)\boldsymbol{\tau}(s) = \theta(0)\boldsymbol{\tau}(0) - \int_0^s f(s^*)ds^* \mathbf{e}. \quad (2.16)$$

By consequence, $\boldsymbol{\theta}(s) = \theta(s)\boldsymbol{\tau}(s)$ is a linear combination of $\boldsymbol{\tau}(0)$ and $\mathbf{e} \forall s$, i.e. the curve lies in the plane passing through $p(0)$ and containing \mathbf{e} .

This result is valid also for the case of coplanar forces, i.e. of forces of the type $\mathbf{f}(s) = f_1\mathbf{e}_1 + f_2\mathbf{e}_2$, with \mathbf{e}_1 and \mathbf{e}_2 two constant unit vectors. In fact:

$$\theta(s)\boldsymbol{\tau}(s) = \theta(0)\boldsymbol{\tau}(0) - \int_0^s f_1(s^*)ds^* \mathbf{e}_1 - \int_0^s f_2(s^*)ds^* \mathbf{e}_2. \quad (2.17)$$

In addition, this is true also for the case of concentrated forces, see below.

2.6 Concentrated forces

The local and intrinsic balance equations are valid uniquely if $\mathbf{f}(s)$ is regular, i.e. if it has not discontinuities, like in the case of concentrated forces.

We can tackle such a problem in the following way: be $\mathbf{f}_p(s)$ a distribution of forces in the interval $(s - \varepsilon, s + \varepsilon)$; we define the concentrated load associated to $\mathbf{f}_p(s)$ as the vector

$$\mathbf{F} = \lim_{\varepsilon \rightarrow 0^+} \int_{s-\varepsilon}^{s+\varepsilon} \mathbf{f}_p(s^*)ds^*. \quad (2.18)$$

In such a way, the concentrated force is treated as a particular distributed load over an interval that tends toward zero. Writing the balance of the forces between $s - \varepsilon$ and $s + \varepsilon$ we get

$$\theta(s + \varepsilon)\boldsymbol{\tau}(s + \varepsilon) - \theta(s - \varepsilon)\boldsymbol{\tau}(s - \varepsilon) + \int_{s-\varepsilon}^{s+\varepsilon} \mathbf{f}(s^*)ds^* + \int_{s-\varepsilon}^{s+\varepsilon} \mathbf{f}_p(s^*)ds^* = \mathbf{o}, \quad (2.19)$$

whose limit for $\varepsilon \rightarrow 0$ gives

$$\mathbf{F} = \theta^- \boldsymbol{\tau}^- - \theta^+ \boldsymbol{\tau}^+, \quad (2.20)$$

where $\theta^- = \lim_{\varepsilon \rightarrow 0} \theta(s - \varepsilon)$ etc. This law let us see that the presence of a concentrated load produces, generally speaking, a discontinuity of both θ , the tension, and $\boldsymbol{\tau}$, the direction of the cable.

The above equation is nothing but the rule of parallelogram of the forces, which implies that the three forces are coplanar, see Fig. 2.2.

The discontinuity on $\theta(s)$ vanishes if and only if \mathbf{F} acts along the bissectrice of the angle formed by $\boldsymbol{\tau}^-$ and $-\boldsymbol{\tau}^+$.

Equation (2.20) must be written in correspondence of each concentrated load, while in all the other parts, the local or intrinsic balance equations govern the problem.

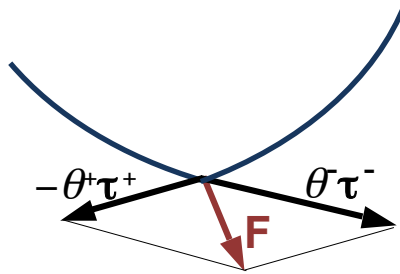


Figure 2.2: Concentrated loads.

2.7 Cables on surfaces

Let us consider the case of a cable wrapped on a surface, which gives the reaction of contact $\boldsymbol{\phi}$; we assume that $\boldsymbol{\phi}$ is much greater than all the other distributed forces, like the weight of the cable, so that all of them are negligible with respect to $\boldsymbol{\phi}$. In such a situation, the intrinsic balance equations become

$$\begin{aligned} \frac{d\theta}{ds} + \phi_\tau &= 0, \\ c\theta + \phi_\nu &= 0, \\ \phi_\beta &= 0. \end{aligned} \tag{2.21}$$

In the case of a frictionless contact between the cable and the surface, if this last is regular and of unit normal \mathbf{N} , it is

$$\begin{aligned} \boldsymbol{\phi}(s) \times \mathbf{N}(s) &= \mathbf{o}, \\ \boldsymbol{\tau}(s) \cdot \mathbf{N}(s) &= 0, \end{aligned} \Rightarrow \phi_\tau = 0 \quad \forall s. \tag{2.22}$$

Hence, by the (2.21)₁, we get

$$\frac{d\theta}{ds} = 0, \tag{2.23}$$

i.e. the tension is constant everywhere in the cable, and in particular it is equal to the tensile loads applied to the ends of the cable. Moreover, because $\phi_\tau = 0$,

$$\boldsymbol{\phi}(s) = \phi(s) \boldsymbol{\nu}(s) = -\phi(s)\mathbf{N}(s) \iff \boldsymbol{\nu}(s) \times \mathbf{N}(s) = \mathbf{o} \quad \forall s. \tag{2.24}$$

Then, by the *Theorem of Bernstein*, the cable wraps the surface along one of its geodetic lines.

Let us now suppose that there is friction in the contact between the cable and the surface, and let assume the Coulomb's non-slipping condition:

$$\sigma |\phi_N(s)| \geq |\phi_\tau(s)| \quad \forall s, \quad (2.25)$$

with σ the *friction coefficient*. If the cable is wrapped on the surface along a geodetic line, then $\boldsymbol{\nu}(s) = \mathbf{N}(s)$, so we get

$$\sigma |\phi_\nu(s)| \geq |\phi_\tau(s)| \quad \forall s, \quad (2.26)$$

and by the intrinsic equations (2.21) we get

$$\sigma c \theta \geq \left| \frac{d\theta}{ds} \right| \rightarrow \sigma c \geq \left| \frac{1}{\theta} \frac{d\theta}{ds} \right| = \left| \frac{d \log \theta}{ds} \right|. \quad (2.27)$$

For the whole cable we get hence the overall non slipping condition

$$\int_0^\ell \sigma c(s) ds \geq \int_0^\ell \left| \frac{d \log \theta(s)}{ds} \right| ds \geq \left| \int_0^\ell \frac{d \log \theta(s)}{ds} ds \right| = \left| \log \frac{\theta(\ell)}{\theta(0)} \right|, \quad (2.28)$$

with ℓ the winding length of the cable on the surface. If now we assume $\theta(\ell) > \theta(0)$, then we obtain the non-slipping condition that links the tension at $s = \ell$ with that at $s = 0$:

$$\theta(\ell) \leq \theta(0) e^{\int_0^\ell \sigma c(s) ds}. \quad (2.29)$$

This condition depends upon the friction coefficient, the winding length and the curvature of the cable.

2.8 Applications

2.8.1 The catenary

The *catenary* is the equilibrium curve of an inextensible, homogeneous cable that is supported at the ends and that is acted upon uniquely by its own weight¹, see Fig. 2.3.

Be ℓ the length of the catenary, which is fixed in $p_0 = (x_0, y_0)$ and $p_1 = (x_1, y_1)$, $|p_0 - p_1| < \ell$. The only force is

$$\mathbf{f}(s) = -\mu g \mathbf{e}_2, \quad (2.30)$$

with μ the mass per unit length of the cable; because \mathbf{e}_2 is a constant vector, the equilibrium curve is contained in a vertical plane, the one passing by p_0 and p_1 . Looking for the

¹The problem of the catenary has been very important in the history of mechanics and mathematics, because it is one of the problems at the origin of both the differential calculus and of the calculus of variations. It was proposed by Jc. Bernoulli to scientists in 1690, and besides his solution, he obtained different methods of solution by his brother, Jh. Bernoulli, Leibniz and Huygens.

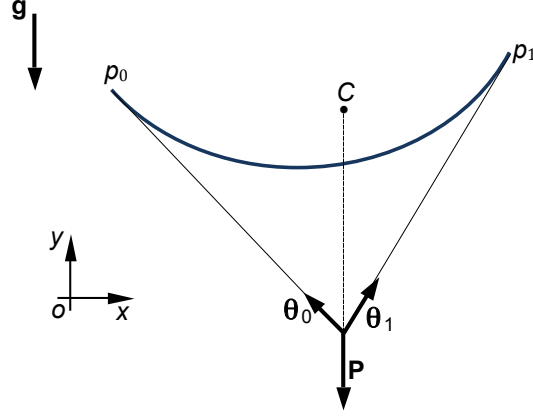


Figure 2.3: The catenary.

equilibrium curve in the form $y = y(x)$ we have

$$\begin{aligned}
 p - o &= x\mathbf{e}_1 + y(x)\mathbf{e}_2, \\
 \boldsymbol{\tau} &= (\mathbf{e}_1 + y'\mathbf{e}_2) \frac{1}{\sqrt{1 + y'^2}}, \\
 \boldsymbol{\nu} &= (-y'\mathbf{e}_1 + \mathbf{e}_2) \frac{1}{\sqrt{1 + y'^2}}, \\
 c &= \frac{y''}{(1 + y'^2)^{\frac{3}{2}}}.
 \end{aligned} \tag{2.31}$$

Then,

$$\begin{aligned}
 f_{\boldsymbol{\tau}} &= \mathbf{f} \cdot \boldsymbol{\tau} = -\mu g \frac{y'}{\sqrt{1 + y'^2}}, \\
 f_{\boldsymbol{\nu}} &= \mathbf{f} \cdot \boldsymbol{\nu} = -\frac{\mu g}{\sqrt{1 + y'^2}},
 \end{aligned} \tag{2.32}$$

so the intrinsic balance equations are

$$\begin{aligned}
 \frac{d\theta}{ds} &= \mu g \frac{y'}{\sqrt{1 + y'^2}}, \\
 \theta \frac{y''}{(1 + y'^2)^{\frac{3}{2}}} &= \frac{\mu g}{\sqrt{1 + y'^2}}.
 \end{aligned} \tag{2.33}$$

To obtain $y(x)$ we project the local balance equation onto \mathbf{e}_1 , and because \mathbf{e}_1 is a constant vector we get

$$\frac{d\theta}{ds} \cdot \mathbf{e}_1 + \mathbf{f} \cdot \mathbf{e}_1 = 0 \rightarrow \frac{d\theta \cdot \mathbf{e}_1}{ds} - \mu g \mathbf{e}_2 \cdot \mathbf{e}_1 = 0 \tag{2.34}$$

which gives the following first integral of the problem:

$$\boldsymbol{\theta} \cdot \mathbf{e}_1 = \text{const} := \theta_0, \tag{2.35}$$

where the scalar θ_0 is the horizontal component of the tension in the cable. θ_0 is hence a constant of the problem; in particular, it is the horizontal component of the reactions in p_0 and p_1 and the tension in the cable in its lowest point. Moreover,

$$\boldsymbol{\theta} \cdot \mathbf{e}_1 = \frac{\theta}{\sqrt{1+y'^2}} = \theta_0 \Rightarrow \theta = \theta_0 \sqrt{1+y'^2}, \quad (2.36)$$

that injected into eq. (2.33)₂ gives the differential equation of the equilibrium curve:

$$\frac{y''}{\sqrt{1+y'^2}} = \frac{\mu g}{\theta_0}. \quad (2.37)$$

To solve the above equation, we put

$$y'' = \frac{dy'}{dx} \quad (2.38)$$

and write it as

$$\frac{dy'}{\sqrt{1+y'^2}} = \frac{\mu g}{\theta_0} dx, \quad (2.39)$$

whose solution is

$$\operatorname{arcsinh} y' = \frac{\mu g}{\theta_0} x + c_1 \rightarrow y' = \sinh \left(\frac{\mu g}{\theta_0} x + c_1 \right), \quad (2.40)$$

and integrating again

$$y = \frac{\theta_0}{\mu g} \cosh \left(\frac{\mu g}{\theta_0} x + c_1 \right) + c_2. \quad (2.41)$$

This is the equation of the catenary. The three constant c_1, c_2 and θ_0 are determined using the two boundary conditions

$$y(x = x_0) = y_0, \quad y(x = x_1) = y_1, \quad (2.42)$$

and the condition that the length of the equilibrium curve is ℓ , because the cable is inextensible:

$$\begin{aligned} \ell &= \int_{p_0}^{p_1} ds = \int_{x_0}^{x_1} \sqrt{1+y'^2} dx = \int_{x_0}^{x_1} \sqrt{1 + \sinh^2 \left(\frac{\mu g}{\theta_0} x + c_1 \right)} dx = \\ &= \int_{x_0}^{x_1} \cosh \left(\frac{\mu g}{\theta_0} x + c_1 \right) dx = \frac{\theta_0}{\mu g} \left[\sinh \left(\frac{\mu g}{\theta_0} x_1 + c_1 \right) - \sinh \left(\frac{\mu g}{\theta_0} x_0 + c_1 \right) \right], \end{aligned} \quad (2.43)$$

We can now find the value of the tension $\theta(y)$: injecting the expression (2.40) of y' into eq. (2.36) we get

$$\theta = \theta_0 \sqrt{1 + \sinh^2 \left(\frac{\mu g}{\theta_0} x + c_1 \right)} = \theta_0 \cosh \left(\frac{\mu g}{\theta_0} x + c_1 \right), \quad (2.44)$$

but for the (2.41), it is

$$\cosh \left(\frac{\mu g}{\theta_0} x + c_1 \right) = \frac{\mu g}{\theta_0} (y - c_2), \quad (2.45)$$

and finally

$$\theta = \mu g(y - c_2). \quad (2.46)$$

The tension in the cable is hence a linear function of the vertical position of the cable, so it is minimum at the lowest point, where it is equal to θ_0 , and maximum for $\max\{y_0, y_1\}$, which could be predicted because \mathbf{f} depends upon a potential.

As a particular case, we consider a cable where $x_0 = 0, x_1 = \alpha\ell, 0 < \alpha < 1, y_0 = y_1 = 0$. If we put $|p_1 - p_0| = x_1 - x_0 = L$, then $\alpha = L/\ell$. In such a situation, the equations that determine c_1 and c_2 become

$$\begin{aligned} c_2 &= -\frac{\theta_0}{\mu g} \cosh c_1, & c_1 &= -\frac{\mu g \alpha \ell}{2\theta_0}, \\ c_2 &= -\frac{\theta_0}{\mu g} \cosh\left(\frac{\mu g}{\theta_0} \alpha \ell + c_1\right), & c_2 &= -\frac{\theta_0}{\mu g} \cosh\left(-\frac{\mu g \alpha \ell}{2\theta_0}\right). \end{aligned} \quad (2.47)$$

To determine θ_0 , we inject these results in eq. (2.43):

$$\begin{aligned} \frac{\theta_0}{\mu g} \left[\sinh\left(\frac{\mu g}{\theta_0} \alpha \ell + c_1\right) - \sinh c_1 \right] &= \ell \rightarrow \\ \sinh\left(\frac{\mu g \alpha \ell}{2\theta_0}\right) - \sinh\left(-\frac{\mu g \alpha \ell}{2\theta_0}\right) &= \frac{\mu g \ell}{\theta_0}. \end{aligned} \quad (2.48)$$

Because \sinh is an odd function, i.e. $\sinh(-x) = -\sinh x \forall x$, we get the equation

$$\sinh \alpha k = k, \quad k = \frac{\mu g \ell}{2\theta_0}. \quad (2.49)$$

The parameter $k > 0$ is half the ratio of the total weight of the cable to the minimal tension θ_0 . Putting

$$\begin{aligned} \xi_1 &= \sinh \alpha k, \\ \xi_2 &= k, \end{aligned} \quad (2.50)$$

the solutions to eq. (2.49) are the intersections of $\xi_1(k)$ and $\xi_2(k)$, see Fig. 2.4.

We observe that k , the abscissa of the intersection point, increases if α decreases, i.e. for a looser cable; because $\mu g \ell / 2 = \text{const.}$, this implies that θ_0 increases with α : the more stretched the cable, the higher θ_0 . In particular, because for $\alpha = 1$

$$\left. \frac{d \sinh k}{dk} \right|_0 = 1, \quad (2.51)$$

the tangent in $k = 0$ to the curve $\xi_1(k)$ is just $\xi_2 = k$; no other intersections between ξ_1 and ξ_2 are possible for $\alpha = 1$, because $\xi_1(k)$ is always increasing, so for $\alpha = 1$, i.e. for a straight equilibrium configuration of the cable, the only possible solution is $k = 0$, which means that $\theta \rightarrow \infty$. Because this is physically impossible, *a cable can never take a rectilinear equilibrium configuration under the only action of its own weight.*

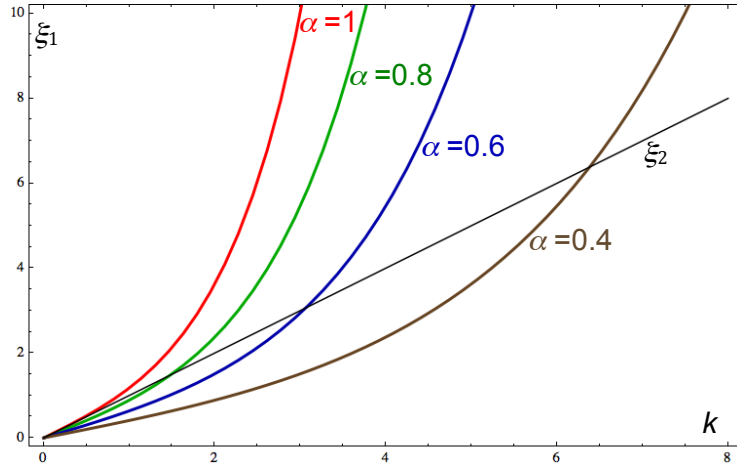


Figure 2.4: The tension in the cable as function of α .

The Taylor's expansion of the catenary's equation (2.41) around a point \bar{x} is

$$y = \frac{\theta_0}{\mu g} \cosh\left(\frac{\mu g}{\theta_0} \bar{x} + c_1\right) + c_2 + \sinh\left(\frac{\mu g}{\theta_0} \bar{x} + c_1\right) (x - \bar{x}) + \frac{1}{2} \frac{\mu g}{\theta_0} \cosh\left(\frac{\mu g}{\theta_0} \bar{x} + c_1\right) (x - \bar{x})^2 + o(|x - \bar{x}|^3). \quad (2.52)$$

The terms of order $o(|x - \bar{x}|^3)$ decrease with the ratio $\mu g/\theta_0$, so, for the same unit mass μ , with the stretch of the cable. Finally, the above equation states that for a stretched cable, the catenary can be well approximated by a parabola.

From the overall balance of the forces on the cable, it is immediate to see that the tangents to the catenary in p_0 and p_1 cross exactly in correspondence of the vertical drawn from the barycenter C of the curve, see Fig. 2.3. The weight \mathbf{P} of the cable is in fact decomposed by the two tensions $-\theta_0$ and θ_1 ; this property was discovered by I. G. Pardies in 1673, well before the finding of the catenary's equation.

If the catenary is put upside down, it becomes the equilibrium curve of a body able to transmit only normal compressive forces: the inverse catenary is hence the equilibrium curve of a masonry or stone or concret arch of constant section submitted uniquely to its own weight. This property was observed by Hooke, that published it under the form of an anagram in 1675², and later confirmed analytically by Jc. Bernoulli in 1704.

In 1740, L. Euler discovered that the catenary is also the *catenoid*, i.e. the curve joining two points at different distances from an axis that, when turned about this axis, produces the surface of revolution of least area.

There is a more elegant way to find the equation of the catenary, that using the calculus of variation. In fact, the equilibrium configuration can be found applying the *Torricelli's principle*: a body acted upon only by its weight is in a stable configuration of equilibrium when its barycenter occupies the lowest position.

²Translated from Latin, the anagram gives the statement: as hangs the flexible line, so but inverted will stand the rigid arch (J. Heyman, *The stone skeleton*, Cambridge University Press, 1995).

The position of the barycenter C is

$$y_C = \frac{\int_{p_0}^{p_1} y ds}{\int_{p_0}^{p_1} ds}, \quad (2.53)$$

and by eq. (1.20) and because the cable is inextensible, so that $\ell = \int_{p_0}^{p_1} ds = \text{const.}$, the problem can be reduced to

$$\min J = \int_{p_0}^{p_1} y \sqrt{1 + y'^2} dx \quad (2.54)$$

with the isoperimetric constraint

$$\int_{p_0}^{p_1} \sqrt{1 + y'^2} dx = \ell. \quad (2.55)$$

Applying the Lagrange multiplier's method, we minimize the functional

$$\min J^* = \int_{p_0}^{p_1} f(y, y'; \psi) dx; \quad (2.56)$$

with

$$f(y, y'; \psi) = (y + \psi) \sqrt{1 + y'^2}. \quad (2.57)$$

The Euler-Lagrange equation with respect to y (the one relative to ψ gives the isoperimetric constraint),

$$\frac{d}{dx} \frac{\partial f}{\partial y'} - \frac{\partial f}{\partial y} = 0, \quad (2.58)$$

because f does not depend explicitly upon x , gives the condition³

$$\frac{d}{dx} \left(f - y' \frac{\partial f}{\partial y'} \right) = 0 \Rightarrow f - y' \frac{\partial f}{\partial y'} = \gamma, \quad \gamma \in \mathbb{R}. \quad (2.59)$$

From eq. (2.57) we obtain

$$\frac{\partial f}{\partial y'} = (y + \psi) \frac{y'}{\sqrt{1 + y'^2}}, \quad (2.60)$$

that injected into eq. (2.59) gives

$$y + \psi = \gamma \sqrt{1 + y'^2} \rightarrow \frac{dy}{\sqrt{(y + \psi)^2 - \gamma^2}} = \frac{dx}{\gamma}. \quad (2.61)$$

³ This is a classical result in analytical mechanics and can be shown introducing the expression of $\frac{\partial f}{\partial y}$ obtained by the Euler-Lagrange equation into $\frac{df(y, y')}{dx}$:

$$\frac{\partial f}{\partial y} = \frac{d}{dx} \frac{\partial f}{\partial y'} \rightarrow \frac{df}{dx} = \frac{\partial f}{\partial y} \frac{dy}{dx} + \frac{\partial f}{\partial y'} \frac{dy'}{dx} = \frac{d}{dx} \frac{\partial f}{\partial y'} \frac{dy}{dx} + \frac{\partial f}{\partial y'} \frac{dy'}{dx} = \frac{d}{dx} \left(y' \frac{\partial f}{\partial y'} \right) \rightarrow \frac{d}{dx} \left(f - y' \frac{\partial f}{\partial y'} \right) = 0.$$

The quantity in the brackets of the last expression is $-H$, the opposite of the integral of Jacobi of the problem. In the end, the constant γ is the opposite of H .

Putting

$$y + \psi = \gamma \cosh z \rightarrow dy = \gamma \sinh z dz \quad (2.62)$$

we get

$$\frac{\gamma \sinh z}{\gamma \sqrt{\cosh^2 z - 1}} dz = \frac{dx}{\gamma} \rightarrow dz = \frac{dx}{\gamma} \rightarrow z = \frac{x}{\gamma} + \beta, \beta \in \mathbb{R}. \quad (2.63)$$

Because

$$z = \operatorname{arccosh} \frac{y + \psi}{\gamma}, \quad (2.64)$$

we obtain finally

$$y = \gamma \cosh \left(\frac{x}{\gamma} + \beta \right) - \psi. \quad (2.65)$$

This equation coincides with the equation (2.41) of the catenary, with $\gamma = \frac{\theta_0}{\mu g}$, $\beta = c_1$ and $\psi = -c_2$.

2.8.2 The suspension bridge

The problem of the suspended bridge (solved by Beeckman en 1615) is similar to that of the catenary, the difference is that the load is uniformly distributed not along the cable, but along its horizontal projection⁴:

$$\mathbf{q}(x) = -q\mathbf{e}_2, \quad q > 0. \quad (2.66)$$

So, now the load to be used into the intrinsic equations

$$\mathbf{f}(s) = -f(s)\mathbf{e}_2, \quad f(s) > 0 \quad \forall s, \quad (2.67)$$

is unknown. It can be deduced as follows:

$$\begin{aligned} \int_{s_1}^{s_2} f(s) ds &= \int_{x_1}^{x_2} f(s) \sqrt{1 + y'^2} dx = \\ \int_{x_1}^{x_2} q dx &= q(x_2 - x_1) \rightarrow f(s) = \frac{q}{\sqrt{1 + y'^2}}. \end{aligned} \quad (2.68)$$

Now, we can proceed just like for the catenary: the intrinsic balance equations are

$$\begin{aligned} \frac{d\theta}{ds} &= q \frac{y'}{1 + y'^2}, \\ \theta \frac{y''}{(1 + y'^2)^{\frac{3}{2}}} &= \frac{q}{1 + y'^2}. \end{aligned} \quad (2.69)$$

From the first equation, we obtain once more the same first integral (2.35), having exactly the same mechanical meaning, and by consequence also eq. (2.36), that injected into eq. (2.69)₂ gives

$$y'' = \frac{q}{\theta_0} \rightarrow y = \frac{q}{2\theta_0} x^2 + c_1 x + c_2. \quad (2.70)$$

⁴This is justified by the fact that the deck of a suspended bridge normally has a weight per unit length q which is far greater than that of the cable, λ , so that to a first approximation this last can be neglected.

The equilibrium curve is hence a parabola; once more, the constants c_1, c_2 and θ_0 are determined using the conditions

$$\begin{aligned} y(x = x_0) &= y_0, \\ y(x = x_1) &= y_1, \\ \ell &= \int_{p_0}^{p_1} ds = \int_{x_0}^{x_1} \sqrt{1 + y'^2} dx. \end{aligned} \tag{2.71}$$

This last, once solved, gives the explicit condition

$$\begin{aligned} \frac{\theta_0}{2q} \left[\left(\frac{q}{\theta_0} x_1 + c_1 \right) \sqrt{1 + \left(\frac{q}{\theta_0} x_1 + c_1 \right)^2} - \left(\frac{q}{\theta_0} x_0 + c_1 \right) \sqrt{1 + \left(\frac{q}{\theta_0} x_0 + c_1 \right)^2} + \right. \\ \left. \log \frac{\frac{q}{\theta_0} x_1 + \sqrt{1 + \left(\frac{q}{\theta_0} x_1 + c_1 \right)^2}}{\frac{q}{\theta_0} x_0 + \sqrt{1 + \left(\frac{q}{\theta_0} x_0 + c_1 \right)^2}} \right] = \ell. \end{aligned} \tag{2.72}$$

The tension can still be recovered using eq. (2.36), that in this case gives

$$\theta(x) = \theta_0 \sqrt{1 + \left(\frac{q}{\theta_0} x + c_1 \right)^2}. \tag{2.73}$$

If, like in the case of the catenary, we consider a cable where $x_0 = 0, x_1 = \alpha\ell, 0 < \alpha < 1, y_0 = y_1 = 0$, then it is easy to check that now

$$\begin{aligned} c_1 &= -\alpha \zeta, \\ c_2 &= 0, \\ 2\alpha \zeta \sqrt{1 + \alpha^2 \zeta^2} + \log \left(\frac{2\alpha \zeta}{\sqrt{1 + \alpha^2 \zeta^2}} + 1 \right) &= 4\zeta, \end{aligned} \tag{2.74}$$

where

$$\zeta = \frac{q\ell}{2\theta_0}. \tag{2.75}$$

2.8.3 The curve of uniform vertical load

We consider a cable wrapped on a rigid plane profile described by the function $y(x)$; the cable is stretched by a tension θ applied at its ends, so that the cable is everywhere in contact with the profile. The weight of the cable is negligible and the contact between the cable and the profile is frictionless. We want to determine $y(x)$ so that the vertical component of the contact force between the cable and the profile is constant everywhere.

Because there is no friction, the reaction on the cable is of the type

$$\boldsymbol{\varphi} = -\varphi \boldsymbol{\nu}, \quad \varphi > 0; \tag{2.76}$$

so, $f_\tau = 0$, $f_\nu = -\varphi$ and by the first intrinsic balance equation (2.13) we get $\theta = \text{const.}$ and of course equal to the tension applied at the ends of the cable. Hence, this problem cannot be equal to the previous one of the suspension bridge, though at a first sight it could seem to be.

The second intrinsic equation gives now

$$\varphi = c \theta, \quad (2.77)$$

while ν has components

$$\nu = \frac{1}{\sqrt{1+y'^2}}(-y', 1). \quad (2.78)$$

The condition that determines the shape $y(x)$ of the curve is

$$-\varphi \cdot \mathbf{e}_2 = p, \quad p > 0, \quad (2.79)$$

so by eq. (2.76)

$$\varphi \nu \cdot \mathbf{e}_2 = p \rightarrow \frac{\varphi}{\sqrt{1+y'^2}} = p, \quad (2.80)$$

that inserted into eq. (2.77) gives the differential equation

$$\frac{y''}{(1+y'^2)^2} = \frac{p}{\theta}. \quad (2.81)$$

This differential equation has not a solution in closed form, and it should be resolved numerically; nevertheless, if the curve is slowly changing, i.e. if $|y'| \ll 1$, then

$$y'' = \frac{p}{\theta} \rightarrow y = \frac{p}{2\theta}x^2 + c_1x + c_2. \quad (2.82)$$

So, in such an approximation, the solution is a parabola. The two constants c_1 and c_2 can be determined using the boundary conditions: $y(x_0) = y_0$, $y(x_1) = y_1$. The value of the vertical load p can be obtained easily: for a parabola whose equation is $y = a x^2 + c_1x + c_2$, because in the above approximation $c \simeq y'' = 2a$, we get comparing with eq. (2.82),

$$p = 2a\theta, \quad (2.83)$$

so it depends linearly upon the tension that stretches the cable.

2.8.4 The cable coiled on a rough cylinder

We consider the case of a cable coiled on a rough cylinder, whose radius is R ; the friction coefficient is σ and we assume that the cable is coiled on a helix of pitch $2\pi b$, the helix being a geodesic of the cylinder. The cable is pulled by a tension θ_0 at the end $s = 0$; we want to know what is the highest tension θ_1 that can be applied to the other end before slipping of the cable on the cylinder.

The equation of the helix is

$$p(\alpha) - o = R \cos \alpha \mathbf{e}_1 + R \sin \alpha \mathbf{e}_2 + b\alpha \mathbf{e}_3, \quad (2.84)$$

α being the winding angle of the cable on the cylinder. The curvature of the helix is constant and equal to

$$c = \frac{R}{R^2 + b^2}, \quad (2.85)$$

so that the non-slipping condition (2.29) becomes

$$\theta_1 \leq \theta_0 e^{\sigma \int_0^\ell \frac{R}{R^2 + b^2} ds} = \theta_0 e^{\sigma \frac{R}{R^2 + b^2} \ell}, \quad (2.86)$$

ℓ being the length of the cable in contact with the cylinder. For a circular helix,

$$s = \sqrt{R^2 + b^2} \alpha, \quad (2.87)$$

so we get the non-slipping condition

$$\theta_1 \leq \theta_0 e^{\sigma \frac{R}{\sqrt{R^2 + b^2}} \alpha \ell}, \quad (2.88)$$

with

$$\alpha_\ell = \frac{\ell}{\sqrt{R^2 + b^2}} \quad (2.89)$$

the winding angle. The friction force that the cable can exert depends hence upon the exponential of α_ℓ . For the case of $b \ll R$, we get

$$\theta_1 < \sim \theta_0 e^{\sigma \alpha_\ell}. \quad (2.90)$$

Just as an exemple, if $\sigma = 1/2$ and $\alpha_\ell = 2\pi$, we get $\theta_1 < \sim 23.14\theta_0$: winding a cable on a rough cylinder is a very effective way to anchor it!

2.9 Elastic cables

The results in the previous sections concern inextensible cables; we consider now what happens if the cable is elastic. To fix the ideas, we consider the equation of an elastic cable whose unstretched length is ℓ and whose points are determined by the vector function

$$\mathbf{r}(s) = p(s) - o, \quad s \in [0, \ell], \quad (2.91)$$

and with end points

$$p_0 = p(s = 0) = (0, 0), \quad p_1 = p(s = \ell) = (x_1, y_1). \quad (2.92)$$

Once more the tangent vector is still defined by eq. (1.22), but now, because the cable is extensible, $|p'(s)| \neq 1$:

$$\boldsymbol{\tau}(s) = \frac{p'(s)}{\lambda(s)}, \quad (2.93)$$

with

$$\lambda(s) = |p'(s)| \quad (2.94)$$

the *stretch* or *elongation* of the elastic cable. If the cable is inextensible, $\lambda(s) = 1$, while generally speaking,

$$\lambda(s) = \sqrt{\left(\frac{dx}{ds}\right)^2 + \left(\frac{dy}{ds}\right)^2}. \quad (2.95)$$

The unique balance equation for an elastic cable is still eq. (2.4)₁, as it can be easily recognized:

$$\boldsymbol{\theta}'(s) + \mathbf{f}(s) = \mathbf{o}. \quad (2.96)$$

About the constitutive law, we restrict our attention to the case of *linearly elastic cables*. In such a case, the constitutive law, generalizing to elastic cables the classical Hooke's law, is

$$\theta(s) = \kappa(\lambda(s) - 1) \quad (2.97)$$

The parameter

$$\kappa = EA \quad (2.98)$$

is the *stiffness* of the cable, E being the Young's modulus of the material and A the area of the cross section of the cable.

2.9.1 The catenary of an elastic cable

As an application, we search for the catenary of an elastic cable (problem solved by Routh in 1891); in this case, we can have also $\ell < \sqrt{x_1^2 + y_1^2}$, because the cable can be stretched to join two points whose distance is $> \ell$ ⁵. The unique load is still given by eq. (2.30). Projecting eq. (2.96) onto the two axes and taking into account that the directions of the axes are fixed, gives

$$\begin{aligned} (\boldsymbol{\theta}'(s) + \mathbf{f}(s)) \cdot \mathbf{e}_1 = 0 &\rightarrow \boldsymbol{\theta}'(s) \cdot \mathbf{e}_1 = 0 \rightarrow \frac{d}{ds}(\boldsymbol{\theta}(s) \cdot \mathbf{e}_1) = 0 \\ (\boldsymbol{\theta}'(s) + \mathbf{f}(s)) \cdot \mathbf{e}_2 = 0 &\rightarrow \boldsymbol{\theta}'(s) \cdot \mathbf{e}_2 = \mu g \rightarrow \frac{d}{ds}(\boldsymbol{\theta}(s) \cdot \mathbf{e}_2) = \mu g \end{aligned} \quad (2.99)$$

The first of the above equations gives once more the first integral of the problem of the catenary, eq. (2.35): the horizontal component of the tension is still a constant, also for an elastic cable. We can transform eq. (2.99)₁ as follows:

$$\begin{aligned} \frac{d}{ds}(\boldsymbol{\theta} \cdot \mathbf{e}_1) &= \frac{d}{ds}(\theta \boldsymbol{\tau} \cdot \mathbf{e}_1) = \frac{d}{ds} \left(\theta \frac{dx}{ds} \right) = \frac{d}{ds} \left(\frac{\theta dx}{\sqrt{dx^2 + dy^2}} \right) = \\ &= \frac{d}{ds} \left(\frac{\theta \frac{dx}{ds}}{\sqrt{\left(\frac{dx}{ds}\right)^2 + \left(\frac{dy}{ds}\right)^2}} \right) = \frac{d}{ds} \left(\frac{\theta \frac{dx}{ds}}{\lambda} \right) = 0. \end{aligned} \quad (2.100)$$

In the same way, eq. (2.99)₂ can be transformed to

$$\frac{d}{ds} \left(\frac{\theta \frac{dy}{ds}}{\lambda} \right) = \mu g. \quad (2.101)$$

⁵However, ℓ cannot be much less than $\sqrt{x_1^2 + y_1^2}$ for applying the Hooke's law.

The first integrals of eqs. (2.100) and (2.101) are

$$\begin{aligned}\frac{dx}{ds} &= \lambda \frac{\theta_0}{\theta}, \\ \frac{dy}{ds} &= \frac{V + \mu g s}{\theta} \lambda,\end{aligned}\tag{2.102}$$

with θ_0 still the horizontal component of the tension and V the vertical component of the tension at the end $s = 0$. To find a solution, we square and add the two equations above, to obtain

$$\theta^2 \left[\left(\frac{dx}{ds} \right)^2 + \left(\frac{dy}{ds} \right)^2 \right] = \lambda^2 [\theta_0^2 + (V + \mu g s)^2],\tag{2.103}$$

and through eq. (2.95) finally

$$\theta = \sqrt{\theta_0^2 + (V + \mu g s)^2}.\tag{2.104}$$

Inverting the constitutive law (2.97) we get

$$\lambda = \frac{\theta}{\kappa} + 1,\tag{2.105}$$

that injected into eq. (2.102) gives, through eq. (2.104),

$$\begin{aligned}\frac{dx}{ds} &= \theta_0 \left(\frac{1}{\kappa} + \frac{1}{\theta} \right) = \theta_0 \left(\frac{1}{\kappa} + \frac{1}{\sqrt{\theta_0^2 + (V + \mu g s)^2}} \right), \\ \frac{dy}{ds} &= (V + \mu g s) \left(\frac{1}{\kappa} + \frac{1}{\theta} \right) = (V + \mu g s) \left(\frac{1}{\kappa} + \frac{1}{\sqrt{\theta_0^2 + (V + \mu g s)^2}} \right),\end{aligned}\tag{2.106}$$

These are the differential equations that describe the equilibrium curve; once integrated, they give

$$\begin{aligned}x &= \frac{\theta_0 s}{\kappa} + \frac{\theta_0}{\mu g} \left(\operatorname{arcsinh} \frac{V + \mu g s}{\theta_0} - \operatorname{arcsinh} \frac{V}{\theta_0} \right), \\ y &= \frac{\mu g s}{\kappa} \left(\frac{V}{\mu g} + \frac{s}{2} \right) + \frac{\theta_0}{\mu g} \left(\sqrt{1 + \left(\frac{V + \mu g s}{\theta_0} \right)^2} - \sqrt{1 + \left(\frac{V}{\theta_0} \right)^2} \right).\end{aligned}\tag{2.107}$$

The two still unknown constants θ_0 and V can be determined imposing the boundary conditions for $s = \ell$: $x(s = \ell) = x_1$, $y(s = \ell) = y_1$, which gives the two conditions

$$\begin{aligned}x_1 &= \frac{\theta_0 \ell}{\kappa} + \frac{\theta_0}{\mu g} \left(\operatorname{arcsinh} \frac{V + \mu g \ell}{\theta_0} - \operatorname{arcsinh} \frac{V}{\theta_0} \right), \\ y_1 &= \frac{\mu g \ell}{\kappa} \left(\frac{V}{\mu g} + \frac{\ell}{2} \right) + \frac{\theta_0}{\mu g} \left(\sqrt{1 + \left(\frac{V + \mu g \ell}{\theta_0} \right)^2} - \sqrt{1 + \left(\frac{V}{\theta_0} \right)^2} \right).\end{aligned}\tag{2.108}$$

These two conditions must usually be solved numerically; in the case of $y_1 = 0$, i.e. with the two end supports at the same level, we get, from eq. (2.108)₂, the expected condition

$$V = -\frac{1}{2} \mu g \ell,\tag{2.109}$$

while eq. (2.108)₁ becomes

$$\frac{\mu g \ell}{2\theta_0} = \sinh \left(\frac{\mu g x_1}{2\theta_0} - \frac{\mu g \ell}{2\kappa} \right), \quad (2.110)$$

equation that for $\kappa \rightarrow \infty$ coincides with eq. (2.49), being $x_1 = \alpha \ell$.

In Fig. 2.5 we show the catenaries of different cables: all the cables are hung between the points $(0,0)$ and $(0,1)$, and the unstretched length of the cables is always $\ell = 1.2$, while $\mu g = 1$ (all the dimensions are in appropriate units), while the cables differ for the value of κ . As expected, the more the κ , the less the depth of the cable; the black curve corresponds to the catenary of an inextensible cable.

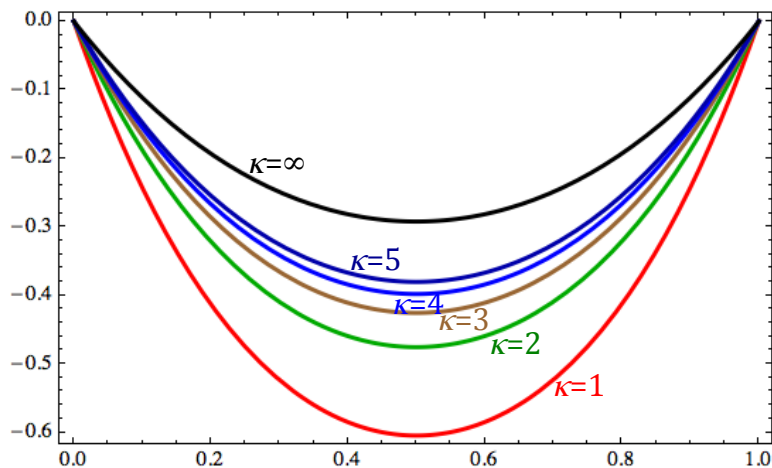


Figure 2.5: Elastic catenaries.

2.10 Exercises

1. An inextensible cable of length 2ℓ is fixed at two points, e.g. two pitons, at the same height and at a distance $2d < 2\ell$. The cable is taut by a concentrated force $\mathbf{f} = f(\cos \alpha, \sin \alpha)$ at mid distance from the ends, see Fig. 2.6. Determine, as a function of α , the equilibrium configuration and the tension in each one of the two parts of the cable. Such a system is currently used by alpinists to realize a relais during a climbing; could you say which is the minimum length of the rope of the relais to make it safer than a relais using a single piton (consider a vertical force)?
2. Make the same exercise but this time the cable is linearly elastic with elastic constant κ . Trace the curve describing the dependence of the force upon the displacement of its point (consider a vertical force).
3. The *velaria* is the equilibrium configuration of a cable acted upon uniquely by wind; if the action of the wind can be represented by a uniform load p acting orthogonally to the cable (a characteristic of all the actions of inviscid fluids), show that the *velaria* is an arc of circle (this problem was solved by Jh. Bernoulli).
4. A variant of the above problem is that of a parallel stream; in such a case, show that the equilibrium configuration of the *velaria* is actually the catenary.

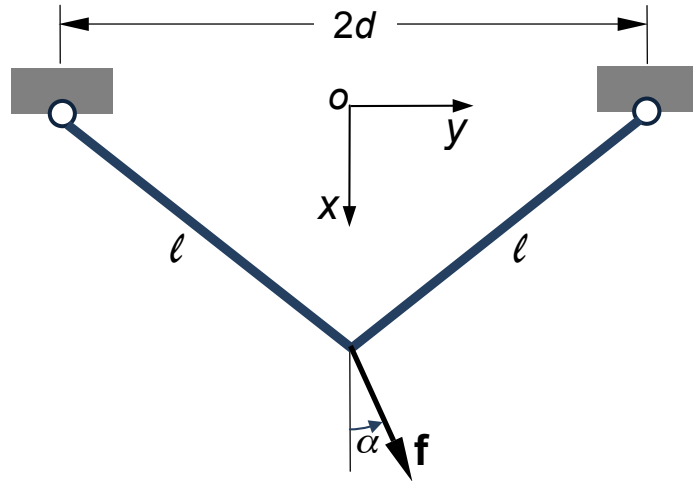


Figure 2.6: Scheme of exercise 1.

5. A cable is coiled on a rough cylinder and the friction coefficient is σ . The cylinder is restrained to rotation by an angular spring whose elastic constant is μ and the cable must bear, at the free end, a mass m , while at the other end it is fixed to the cylinder by a device whose resistance to tension is φ . If the radius of the cylinder is R and the cable is coiled three times on the cylinder along a helix whose pitch is $2\pi b \ll R$, which is the greatest mass that the cable can support?

Chapter 3

Straight rods

3.1 Introduction

The results of the Saint-Venant Problem greatly simplify the study of beams. In fact, the whole stress state at any point of the beam can be found if the internal actions, N, T_1, T_2, M_1, M_2 and M_3 are known.

The problem of the study of structures composed by beams is hence reduced to the study of the internal actions. These ones depend only upon the position along the beam axis, say the axis z . So the equations concerning N, T_1 etc. can be only ordinary differential equations (ODEs), not partial differential equations (PDEs), which simplifies considerably the problem and motivates for the study of beams reduced, ideally, to their axis.

Such theories, idealizing a beam as a one-dimensional element, are called *rod theories* (a rod is considered here to be a beam reduced to its only axis). The objective of the rod theories is hence to provide balance, compatibility and constitutive equations for rods, i.e. for this special type of continuum.

In many practical cases, rods belong to a plane that contains one of their principal axes of inertia of the cross section and are acted upon by loads that belong to such a plane. This is the case of *plane rods*: the rods belong, also after the deformation, to their original plane, where the loads act.

The case of plane rods is much simpler than the general one, because the only possible internal actions reduce to only N, T_2 and M_1 (that we will indicate, in the following, simply by N, T and M , because there is no possibility of ambiguity in the plane case).

In the remainder of this Chapter, we will focus on a particularly important case of plane rods, that of *straight rods*; nevertheless, it is not difficult to generalize the results to the more general cases of plane or also of three-dimensional rods, following the same approach illustrated below.

The objective is to write the balance, compatibility and constitutive equations for straight rods, to arrive to a mechanical model for such elements. We will, namely, introduce two classical models of rods, the more general Timoshenko's one and the very classical Euler-Bernoulli rod model.

A last remark: we remain, in this Chapter, in the framework of classical, linear elasticity. We will generalize the linear theory of rods to arches, i.e. plane curved rods, in Chapter 4, while general rods undergoing large displacements are studied in Chapter 5.

3.2 Balance equations

Let us begin the study of straight rods with the balance equations. The general situation is sketched in Fig. 3.1; loads $p(z)$ and $q(z)$ are the data of the problem. The balance equations can be obtained applying the principle of the sections of Euler to a piece of rod between the positions z and $z + dz$. The assumed positive internal actions are those depicted in the figure. The equilibrium of the rod implies that of the segment under scrutiny, submitted to the external loads and to the internal actions transmitted to the segment by the rest of the rod through the end sections. The balance gives hence:

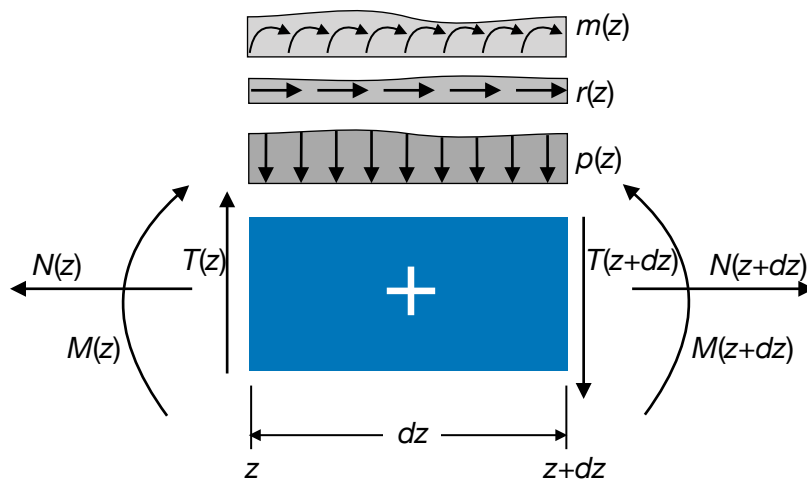


Figure 3.1: General sketch for the rod's balance equations.

- equilibrium to axial force:

$$N(z + dz) - N(z) + r(z)dz = 0; \quad (3.1)$$

- equilibrium to shear force:

$$T(z + dz) - T(z) + p(z)dz = 0; \quad (3.2)$$

- equilibrium to bending moment (e. g. around the point of abscissa z):

$$M(z + dz) - M(z) - T(z + dz)dz - p(z)\frac{dz^2}{2} - m(z)dz = 0. \quad (3.3)$$

Developing the above expressions gives

$$\begin{aligned}
N(z) + \frac{dN(z)}{dz}dz - N(z) + r(z)dz &= 0, \\
T(z) + \frac{dT(z)}{dz}dz - T(z) + p(z)dz &= 0, \\
M(z) + \frac{dM(z)}{dz}dz - M(z) - T(z)dz - \frac{dT(z)}{dz}dz^2 - p(z)\frac{dz^2}{2} - m(z)dz &= 0,
\end{aligned} \tag{3.4}$$

and neglecting the terms of order greater than the first we finally obtain the *balance equations for straight rods*:

$$\begin{aligned}
\frac{dN}{dz} &= -r, \\
\frac{dT}{dz} &= -p, \\
\frac{dM}{dz} &= T + m.
\end{aligned} \tag{3.5}$$

In the special and very common case of $m = 0$, we remark that T is the derivative of M . From the two last relations, we get also, by differentiation,

$$\frac{d^2M}{dz^2} = -p + \frac{dm}{dz}, \tag{3.6}$$

a second-order differential equilibrium equation relating directly the bending moment to the loads.

3.3 Compatibility equations

Let us now turn the attention on geometric considerations. In fact, we need a link, the *compatibility equations of the rods*, between the displacements of the rod and some internal kinematical quantities defining the deformation of the rod. The general situation is that sketched in Fig. 3.2, where w is the axial displacement, v the *deflexion*, i.e. the displacement along y , β is the local rotation of the axis z and φ that of the normal to the undeformed axis z .

We introduce first the *extension* ε , the internal kinematical descriptor of the stretching of the axis z :

$$\varepsilon = \frac{dw}{dz}. \tag{3.7}$$

Then, we define the *curvature* κ of the rod

$$\kappa = -\frac{d\varphi}{dz}; \tag{3.8}$$

the sign $-$ is due to the fact that in the Saint-Venant Problem the positive bending moments are opposite to the positive concavity, see below.

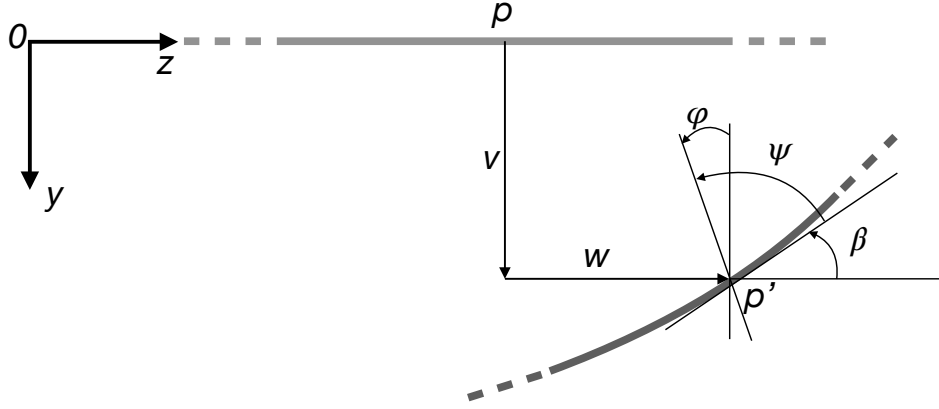


Figure 3.2: General scheme of the kinematics of a rod.

Finally, we introduce the *angular sliding* or *shear* γ of the rod axis, describing how a segment initially parallel to the rod axis changes in the deformation:

$$\gamma = \beta - \varphi. \quad (3.9)$$

From fig. 3.2 we see that

$$\psi = \frac{\pi}{2} + \varphi - \beta \rightarrow \gamma = \beta - \varphi = \frac{\pi}{2} - \psi : \quad (3.10)$$

γ measures the variation of the angle existing between the axis and a segment orthogonal to it, from its initial value of $\pi/2$ to the final one of ψ . For small perturbations,

$$\tan \beta = \frac{dv}{dz} \simeq \beta, \quad (3.11)$$

so we have

$$\gamma = \frac{dv}{dz} - \varphi. \quad (3.12)$$

We remark that there is a substantial difference between a rod and a classical continuum: in the rod theories, derivatives of angular quantities appear: a rod is a *polar continuum*, i.e., unlike classical continuum bodies, it can transmit couples.

3.4 Constitutive equations

We have for the whole only six equations, the balance, eq. (3.5), and the compatibility ones, eqs. (3.7), (3.8) and (3.12), for a set of 9 unknowns on the whole: $N, T, M, v, w, \varphi, \varepsilon, \kappa$ and γ . We need hence three *constitutive equations for the rods*; they can be derived using the results of the Saint-Venant Problem. The approach is energetic: we write first the

strain energy for a beam, U_b , between the two sections 1 and 2:

$$\begin{aligned}
U_b &= \frac{1}{2} \int_{\Omega} \boldsymbol{\sigma} \cdot \boldsymbol{\varepsilon} \, dv = \frac{1}{2} \int_{\Omega} \frac{\sigma_{33}^2}{E} + \frac{1}{\mu} (\sigma_{13}^2 + \sigma_{23}^2) \, dv \\
&= \frac{1}{2} \int_1^2 \int_S \left(\frac{N}{A} + \frac{M y}{J} \right)^2 \frac{1}{E} + \frac{1}{\mu} \left(\frac{T S}{b J_1} \right)^2 \left(1 + \frac{4 \tan^2 \alpha x^2}{b^2} \right) ds \, dz \\
&= \frac{1}{2} \int_1^2 \frac{N^2}{EA} + \frac{\chi T^2}{\mu A} + \frac{M^2}{EJ} \, dz.
\end{aligned} \tag{3.13}$$

Now, thinking at the beam as a rod, we write the energy U_r :

$$U_r = \frac{1}{2} \int_1^2 (N\varepsilon + T\gamma + M\kappa) \, dz. \tag{3.14}$$

This result can be obtained applying the Clapeyron's theorem at the segment dx of the rod, considered as charged uniquely by the internal actions. Of course, the solid being the same, it must be

$$U_b = U_r \quad \forall N, T, M, \tag{3.15}$$

which gives the conditions

$$N\varepsilon = \frac{N^2}{EA}, \quad T\gamma = \frac{\chi T^2}{\mu A}, \quad M\kappa = \frac{M^2}{EJ}, \tag{3.16}$$

and finally the three constitutive equations for the rods:

$$\begin{aligned}
N &= EA\varepsilon, \\
T &= \frac{\mu A}{\chi} \gamma, \\
M &= EJ\kappa.
\end{aligned} \tag{3.17}$$

We remark that, because of the linearity of the problem, the internal actions are proportional to their corresponding kinematical parameter. We dispose now of all the equations for the rod theories.

3.5 The Timoshenko's rod

The compatibility equations can be injected into the constitutive equations to get (from now on, for the sake of shortness, we denote by a prime the derivative with respect to z):

$$\begin{aligned}
N &= EA w', \\
T &= \frac{\mu A}{\chi} (v' - \varphi), \\
M &= -EJ \varphi'.
\end{aligned} \tag{3.18}$$

If now we inject these equations into the balance equations, we get

$$\begin{aligned}
(EAw')' &= -r, \\
\left[\frac{\mu A}{\chi}(v' - \varphi) \right]' &= -p, \\
(-EJ\varphi')' &= T + m = \frac{\mu A}{\chi}(v' - \varphi) + m.
\end{aligned} \tag{3.19}$$

Injecting eq. (3.19)₂ into the differentiated eq. (3.19)₃ gives an equation for φ only:

$$(EJ\varphi'')' = p - m'. \tag{3.20}$$

The above equations are the *elastic equilibrium equations* of a straight rod; in fact, they include in the equilibrium equations the constitutive law and the compatibility equations, so they describe the equilibrium of an elastically deformable rod.

Equations (3.18) and (3.19) define the so-called *Timoshenko's rod model*. In this model, any straight segment originally orthogonal to the rod axis remains straight after the deformation, but *not* necessarily orthogonal to the tangent of the deformed axis, because $\gamma \neq 0$, generally speaking, which implies that $v' \simeq \beta \neq \varphi$.

N and w are uncoupled from T , M , v and φ , but these last are coupled, which complicates the resolution. Anyway, from eq. (3.18)₂ one gets

$$\varphi = v' - \frac{\chi T}{\mu A} \rightarrow \varphi' = v'' - \left(\frac{\chi T}{\mu A} \right)', \tag{3.21}$$

that inserted into eq. (3.18)₃ gives

$$v'' = -\frac{M}{EJ} + \left(\frac{\chi T}{\mu A} \right)'. \tag{3.22}$$

In the particular, and very frequent, case of a homogeneous rod of uniform section, EJ and $\mu A/\chi$ are independent from z ; then, from eq. (3.19)₂ we get

$$\varphi' = v'' + \frac{\chi P}{\mu A}, \tag{3.23}$$

that inserted into eq. (3.18)₃ gives

$$v'' = -\frac{M}{EJ} - \frac{\chi}{\mu A} p. \tag{3.24}$$

The above expressions of v'' can be used to find the deflection of the rod, v , whenever the functions $M(z)$ and $T(z)$ are known, namely from equilibrium equations, e.g. integrating eq. (3.6). In this procedure, we need two *geometric* boundary conditions, fixing the value of v or of φ at the rod's ends, plus two *natural* boundary conditions, i.e. on M or T , if the equilibrium problem is solved integrating eq. (3.6). The rotation φ can be obtained from eq. (3.21) or directly upon integration of eq. (3.18)₃, which needs just one boundary condition, specifying the value of φ at a point of the rod (not necessarily at the edges).

If, on the contrary, the functions $M(z)$ and $T(z)$ cannot be determined upon simple equilibrium considerations, then integrating three times eq. (3.20) gives an expression for φ , to be injected into eq. (3.19)₃ to obtain an equation for v' :

$$v' = \varphi - \frac{\chi}{\mu A} ((EJ\varphi')' + m), \quad (3.25)$$

that integrated gives the deflection v . Because we have integrated four times, four boundary conditions are needed to determine the four integration constants. These can be of two types: geometric, fixing the value of v or φ at the rod's ends, or natural, imposing a value for M or T at the boundaries. The natural boundary conditions concern φ or φ' ; in fact, if at a boundary $z = z_b$ it is $M(z_b) = M_b$, then from eq. (3.20) we get

$$\varphi'(z_b) = -\frac{M_b}{EJ}, \quad (3.26)$$

while if it is $T(z_b) = T_b$ then eq. (3.19)₃ gives the condition

$$(EJ\varphi')'|_{z_b} = -T_b - m(z_b). \quad (3.27)$$

3.6 The Euler-Bernoulli rod

Since the XVIIIth century a simplified model has been proposed by L. Euler and Jacob Bernoulli for the bending case: the basic assumption of the Euler-Bernoulli rod theory is that

$$\beta = \varphi \Rightarrow \gamma = 0. \quad (3.28)$$

Geometrically, this corresponds to the vanishing of the angular sliding, i.e., finally, of the shear deformation: unlike in the Timoshenko's model, *a segment originally orthogonal to the axis remains orthogonal to the deformed axis*. This is the so-called *hypothesis of conservation of the normals*.

For small perturbations, this assumption gives

$$\varphi = \beta \simeq v' \rightarrow \kappa = -\varphi' = -v''. \quad (3.29)$$

The equations for N and ε are not affected by this assumption, while for M and v we get

$$\begin{aligned} M &= -EJv'', \\ (EJv'')'' &= p - m'. \end{aligned} \quad (3.30)$$

These are the celebrated equations of the *Euler-Bernoulli rod model*. The problems for N, T and M are uncoupled and the bending problem is reduced to a fourth-order differential equation for v . For what concerns T , the constitutive equation cannot be used, because this should give $T = 0$ identically, which would imply $M = \text{constant}$, which is

false¹. The shear distribution can however be get through the equilibrium equation (3.5)₃ and using eq. (3.30)₁:

$$T = M' - m = (-EJv'')' - m. \quad (3.31)$$

The above equations are valid for straight rods of any cross section, also variable with z . For the very common case of constant cross section and material, they simplify to

$$\begin{aligned} M &= -EJv'', \\ T &= -EJv''' - m, \\ EJv^{iv} &= p - m'. \end{aligned} \quad (3.32)$$

Also in this case, if the function M can be obtained by equilibrium considerations, then the deflection v is obtained by eq. (3.30)₁,

$$v'' = -\frac{M}{EJ}, \quad (3.33)$$

otherwise eq. (3.30)₂ must be integrated four times. The geometric or natural boundary conditions now concern always v and its derivatives. In fact, the geometric conditions fix the value of v or of v' at one rod's end, while the natural boundary conditions on M and T , through eq. (3.30)₂ and (3.31), fix the value of v'' or of v''' respectively.

The solution of eqs. (3.30) or (3.32), or in the general case of the Timoshenko's model, provides the displacement of the rod, determining hence its deformed shape, the so-called *elastica*.

3.7 Reduction of the Timoshenko's problem

It is possible to reduce eq. (3.20) of the Timoshenko's rod theory to an equation of the fourth order similar to that of the Euler-Bernoulli model, eq. (3.30)₂. This can be done introducing the *auxiliary function* $\eta(z)$ such that

$$\varphi = \eta', \quad (3.34)$$

which inserted into eq. (3.20) gives immediately

$$(EJ\eta'')'' = p - m', \quad (3.35)$$

formally identical to eq. (3.30)₂, provided that v is replaced by η . If eq. (3.34) is injected into eq. (3.18)₃, then we get

$$M = -EJ\eta'', \quad (3.36)$$

¹The assumption (3.29) renders eqs. (3.18)₂ and (3.19)₂ impossible to be satisfied, and hence meaningless, unless $T = 0$ and $p = 0$ everywhere. Hence, in principle the Euler-Bernoulli model is correct only for rods submitted to a pure bending state. However, the model is used also when $T \neq 0$; in such a case, T can be retrieved only through equilibrium, once M determined, eq. (3.31). Practically, the use of the Euler-Bernoulli rod model should be restricted to cases where the shear deformation is negligible with respect to the bending one: this happens for *slender rods*, i.e. for rods where the *slenderness ratio* $\rho/\ell \rightarrow 0$, with $\rho = \sqrt{J/A}$ the radius of gyration of the rod's cross-section, see Ex. 8.

analogous to eq. (3.30)₁. Moreover, if eq. (3.34) is inserted into eq. (3.25) we obtain the link between v and η :

$$v' = \eta' - \frac{\chi}{\mu A}((EJ\eta'')' + m). \quad (3.37)$$

Putting this expression of v' into eq. (3.18)₂ gives

$$T = (-EJ\eta'')' - m = M' - m, \quad (3.38)$$

i.e. the equilibrium equation (3.5)₃ is automatically satisfied.

For the very common case of a rod of constant stiffness, i.e. such that EJ and $\mu A/\chi$ are constant $\forall z$, and without distributed couples, $m = 0$, the above equation gives (the integration constant is inessential, as it can be easily recognized considering that the link imposed by equation (3.37) concerns v')

$$v = \eta - \frac{\chi EJ}{\mu A}\eta''. \quad (3.39)$$

Along with eqs. (3.34), (3.36) and (3.38), this gives the boundary conditions to be satisfied at the rod's ends:

- clamped edge:

$$v = 0, \quad \varphi = 0 \quad \rightarrow \quad \eta - \frac{\chi EJ}{\mu A}\eta'' = 0, \quad \eta' = 0; \quad (3.40)$$

- simply supported edge:

$$v = 0, \quad M = 0 \quad \rightarrow \quad \eta'' = 0, \quad \eta = 0; \quad (3.41)$$

- slide edge:

$$\varphi = 0, \quad T = 0 \quad \rightarrow \quad \eta' = 0, \quad \eta''' = 0; \quad (3.42)$$

- free edge:

$$M = 0, \quad T = 0 \quad \rightarrow \quad \eta'' = 0, \quad \eta''' = 0. \quad (3.43)$$

3.8 Isostatic and hyperstatic rods

The general problem for a rod is: knowing the applied actions p, q, m and the boundary conditions, determine N, T, M, v, w and φ . Three cases are possible: the rod is *hypostatic*, *isostatic* or *hyperstatic*.

Generally speaking, a structure is said to be *isostatic* if the equilibrium equations can be solved uniquely, i.e. if they are sufficient to determine the distribution of the internal actions and of the reaction forces. In the case of a rod, the equilibrium equations are

$$\begin{aligned} N' &= -r, \\ M'' &= -p + m'. \end{aligned} \quad (3.44)$$

T can be obtained through eq. (3.5)₃:

$$T = M' - m, \quad (3.45)$$

once solved the bending equation. Such equations concern internal forces and need, on the whole, three boundary conditions, one for eq. (3.44)₁ and two for eq. (3.44)₂. These conditions are necessarily of the *natural* type, i.e. they concern the value taken by N, T or M at the rod's ends. So, a rod will be isostatic if and only if it is possible to specify the right number of natural boundary conditions for eqs. (3.44), in particular if it is possible to write:

- one and only one boundary condition specifying the value of N at one of the rod's ends;
- two and no more than two boundary conditions specifying the value of M or T at the rod's ends, but at least one of them must concern M .

In fact, only in such a case it is possible to determine a unique solution to the equilibrium equations and hence to determine uniquely the distribution of the internal actions N, T and M everywhere in the rod.

If the number of natural boundary conditions that can be written is greater than three, then eqs. (3.44) cannot satisfy all of them, generally speaking. Equilibrium is *impossible* and the rod is said to be *hypostatic*: the constraint conditions are not sufficient to guarantee equilibrium for every possible external loading.

If, on the contrary, the number of natural boundary conditions that can be written is less than three, then the number of independent constraint conditions is too high to allow writing natural boundary conditions. The rod is said to be *hyperstatic*, in the sense that it is *statically undetermined*: the equations of statics, that is, the equilibrium equations, are not sufficient to determine the distribution of the internal actions and of the reaction forces.

In such a case, the compatibility equations and the constitutive law must enter the problem, i.e., the elastic equilibrium equations (3.19) or (3.30)₂ should be used. In particular:

- for extension, eq. (3.19)₁ is to be used, which needs two boundary conditions, of the geometric or natural type, specifying respectively the value of w or of w' at the rod's ends; at least one of the two boundary conditions must be concern w i.e. it must be of the *geometric* type;
- for bending, eqs. (3.20) and (3.25) are to be used for the Timoshenko's rod, while eq. (3.30)₂ for the Euler-Bernoulli one. In both the cases, four boundary conditions must be specified; they can be of the natural or geometric type, they have been discussed in Sects. 3.5 and 3.6, but at least one of them must concern v , i.e. it must be of the *geometric* type.

For isostatic rods, once the distribution of M determined, the deflection can be calculated through eq. (3.33) for the Euler-Bernoulli rod, or through eq. (3.22) for the Timoshenko's one; in this case, the rotation φ is then determined through eq. (3.21), see Sect. 3.5.

We remark that an imposed displacement of a rod's edge *stresses an hyperstatic rod, but not an isostatic one*. In fact, an imposed displacement corresponds to a geometric boundary condition, that concerns only hyperstatic rods. In the case of an isostatic one, only natural boundary conditions, i.e. concerning N, T or M , are needed to determine the distribution of the internal actions; as a consequence, these last are insensitive to any imposed displacement of rod's edge.

For ending this Section, we remark that the difference in the resolution of isostatic or hyperstatic rods is in the number and types of boundary conditions to be specified, besides the differential equations, of the first or second order in the first case, of the second or fourth order for the second one.

It is important to notice that, because equilibrium equations are sufficient to determine the distribution of the internal actions for isostatic rods, such distributions are not affected by the stiffness characteristics of the rod, i.e. N, T and M are independent from the distributions $EA, \mu A/\chi$ and EJ , also in the case where these last are not constant throughout the rod. This is not the case for hyperstatic rods (and in general for hyperstatic structures): the distribution of the internal actions, and hence the reaction forces, depend upon the distribution of the stiffnesses. However, for the Euler-Bernoulli model, if the rod has constant properties, M and T are still independent from the stiffnesses, as it can be easily checked; this is true also for the extension behavior.

3.9 The torsion equations

The results found for straight rods can be easily generalized to include an out-of-plane effect, that of torsion M_T . The general scheme is sketched in Fig. 3.3:

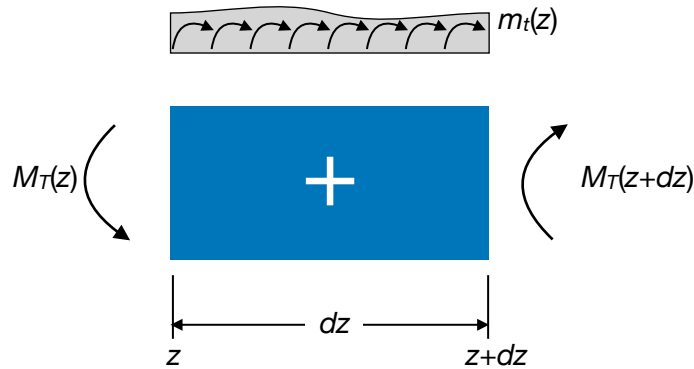


Figure 3.3: Scheme for the torsion of a rod.

- balance of the torsion:

$$\begin{aligned}
 M_T(z+dz) - M_T(z) + m_t(z)dz &= 0 \rightarrow \\
 M_T(z) + \frac{dM_T(z)}{dz}dz - M_T(z) + m_t(z)dz &= 0 \rightarrow \\
 \frac{dM_T}{dz} &= -m_t;
 \end{aligned} \tag{3.46}$$

- compatibility equations: the kinematical descriptor of torsion is the *twist angle* θ ; it is linked to the internal descriptor α , giving the relative rotation of two sections separated by a distance dz by the relation

$$\alpha = \frac{d\theta}{dz}; \quad (3.47)$$

- constitutive law: the strain energy of torsion for a beam is (see Ex. 8 Chapt. 4)

$$U_b = \frac{1}{2} \int_1^2 \frac{q}{\mu J_0} M_T^2 dz, \quad (3.48)$$

and as a rod

$$U_r = \frac{1}{2} \int_1^2 M_T \alpha dz, \quad (3.49)$$

so we get

$$M_T = \frac{\mu J_0}{q} \alpha, \quad (3.50)$$

a result already known from the Sant-Venant theory.

Finally we have

$$\begin{aligned} M_T &= \frac{\mu J_0}{q} \theta', \\ \left(\frac{\mu J_0}{q} \theta' \right)' &= -m_t, \end{aligned} \quad (3.51)$$

These equations for torsion are formally identical to those for extension, eqs. (3.18)₁ and (3.19)₁.

3.10 The Mohr's theorems

Let us now consider the case of a bent rod of constant stiffness EJ and without distributed couples; then, in the framework of the Euler-Bernoulli model,

$$M' = T, \quad T' = -p \rightarrow M'' = -p, \quad v'' = -\frac{M}{EJ}. \quad (3.52)$$

These two differential equations are formally identical; so, the *elastica* of a rod coincides with the diagram of the bending moment M^* generated by a fictitious load

$$p^* = \frac{M}{EJ} \rightarrow v = M^*. \quad (3.53)$$

This is the *Theorem of Mohr* (1868); to remark that p^* is the curvature. Deriving eq. (3.53)₂ gives

$$v' = (M^*)' = T^*, \quad (3.54)$$

i.e. the inclination φ of the *elastica* is given by the fictitious shear T^* ($\beta \simeq \tan \beta = v'$ for small perturbations). This is the *corollary of Mohr*.

The fictitious load p^* is to be applied to a fictitious rod, having the same dimensions of the real rod but whose boundary conditions must in general be changed:

- for a simply supported rod, the *elastica* has $v = 0$ and $v' \neq 0$ at the edges; the corresponding edges of the fictitious rod can be found considering that in the correspondence it must be $M^* = 0$ and $T^* \neq 0$; hence the fictitious rod must be simply supported, like the real rod;
- for a cantilever: at the clamped edge, $v = 0$ and $v' = 0$: the corresponding edge in the fictitious rod must be a free edge, because in such a way $M^* = 0$ and $T^* = 0$; at the free edge of the cantilever, $v \neq 0$ and $v' \neq 0$: in the corresponding edge of the fictitious rod it must be $M^* \neq 0$ and $T^* \neq 0$, so this edge must be clamped: a cantilever rod is transformed into a fictitious cantilever where the edges are swapped.

Other situations can be studied in a similar way. The use of the Mohr's theorem, and corollary, is normally bounded to isostatic rods. In fact, in such a case the use of the Mohr's technique allows for finding deflections and rotations using exclusively equilibrium considerations, so without the need of solving differential equations.

In the case of hyperstatic rods, as we have seen above, the solution of the static problem passes through the determination of the displacements and rotations, so in this case the Mohr's theorem and corollary become useless in this context. Nevertheless, the corollary of Mohr can be used in some methods for the static resolution of hyperstatic systems of rods.

3.11 Hyperstatic systems of rods

The equations of rods allow, in principle, for studying any problem of rod structures, regardless of the degree of hyperstaticity. However, in practice they can be used only in simple cases, e.g. for single rods, because very quickly their use becomes too much complicate.

Actually, this approach is complete: it provides any type of information (v, w, M etc.) everywhere in a rod. So, the question is to know whether or not it can exist an approach which, paying the price of a lower information, can be nevertheless used effectively for more complicated rod structures.

The answer is yes, and the approach is based upon the Principle of Virtual Displacements (PVD); such a method is sometimes called the *force method for solving hyperstatic rod structures*, because the unknown of the method are generalized forces (forces or couples). We introduce it in the following Section, specifying since now that the method, though based upon the PVD, valid for any type of material behavior, is *valid only for a linear structural behavior*. This assumption implies actually two distinct and equally important hypotheses: the material is linearly elastic, on one hand, and the perturbations are small, on the other hand.

3.11.1 The Principle of Virtual Displacements for rods

The PVD can be adapted to rods; first of all, we define a *state of virtual displacements-deformations for a rod* a state for which v, w, φ are

- i. regular (continuous and with piecewise continuous derivatives);
- ii. infinitesimal;
- iii. independent from time.

Be N, T, M, p, r a field of equilibrated actions, i. e.

$$\begin{aligned}\frac{dN}{dz} &= -r, \\ \frac{dT}{dz} &= -p, \quad + \text{ b. c.} \\ \frac{dM}{dz} &= T,\end{aligned}\tag{3.55}$$

We can then prove the following

Theorem. (*Principle of Virtual Displacements for rods*): be $\{v^*, w^*, \varphi^*\}$ a field of virtual displacements for a rod of length ℓ in equilibrium under the action of external and internal actions; then

$$\int_0^\ell (N\varepsilon^* + T\gamma^* + M\kappa^*) dz = \int_0^\ell (p v^* + r w^*) dz.\tag{3.56}$$

Proof. We remark first that the the left-hand side of the above equation is the internal virtual work, produced by the internal actions for the deformations corresponding to the considered virtual displacements field, while to the right-hand side we have the external virtual work, i.e. that produced by the external applied loads. Hence, once more, the PVD states the equality of the internal and external virtual works.

Because, by hypothesis, v^*, w^* and φ^* are sufficiently regular, we can calculate the internal virtual deformations for the rod

$$\varepsilon^* = \frac{dw^*}{dz}, \quad \gamma^* = \frac{dv^*}{dz} - \varphi^*, \quad \kappa^* = -\frac{d\varphi^*}{dz}.\tag{3.57}$$

Then, the internal virtual work becomes

$$\int_0^\ell \left[N \frac{dw^*}{dz} + T \left(\frac{dv^*}{dz} - \varphi^* \right) - M \frac{d\varphi^*}{dz} \right] dz,\tag{3.58}$$

and integrating by parts we get

$$[N w^* + T v^* - M \varphi^*]_0^\ell + \int_0^\ell \left[\varphi^* \left(\frac{dM}{dz} - T \right) - w^* \frac{dN}{dz} - v^* \frac{dT}{dz} \right] dz.\tag{3.59}$$

The boundary term, the first one in the above equation, vanishes because at the edges it is either an internal action either its dual kinematical descriptor to vanish. Because the actions are equilibrated, eqs. (3.55) are satisfied, so that the term in brackets under the sign of integral vanishes and finally we get

$$\int_0^\ell (N\varepsilon^* + T\gamma^* + M\kappa^*) dz = \int_0^\ell (p v^* + r w^*) dz.\tag{3.60}$$

□

We remark that constitutive equations have not been used in the proof of the PVD, so it is valid for any type of material behavior, not only for the elastic rods.

3.11.2 The Müller-Breslau equations

We introduce the method through an example, shown in Fig. 3.4; the structure in object is twice hyperstatic and, thanks to the assumption of linear behavior, using the principle of superposition of the effects, we can think to the structure as the sum of three isostatic structures. This is a key point of the method: *the original hyperstatic structures is transformed into the sum of isostatic structures, that can be solved separately using nothing but equilibrium conditions*. In particular, the original structure is decomposed into:

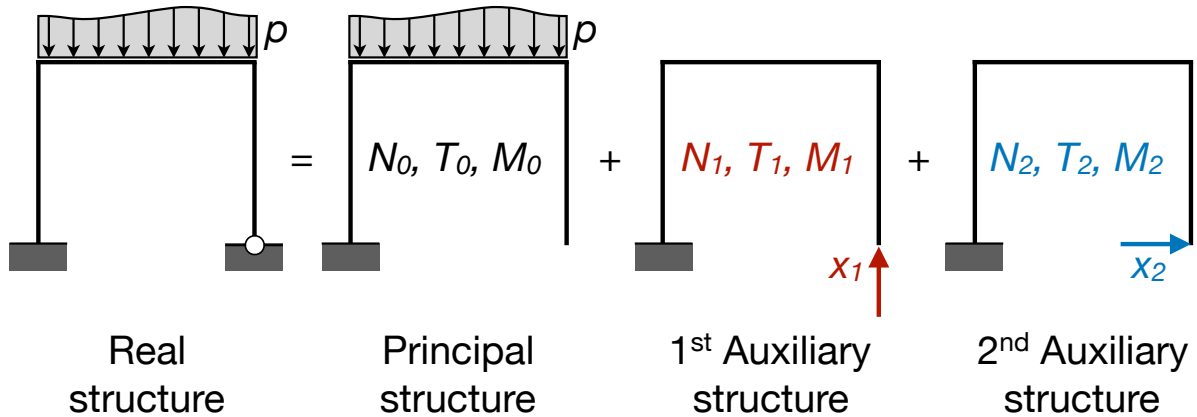


Figure 3.4: Scheme for the analysis of hyperstatic rod structures.

- a *principal structure*: the hyperstatic constraints have been removed (their choice is not unique and anyway arbitrary) and the isostatic structure so obtained is acted upon only by the given, known loads;
- a number of *auxiliary structures* equal to the number of hyperstatic constraints removed (in the example, two); each one of the auxiliary structures is like the principal one, hence isostatic, but it is *loaded uniquely by an unknown generalized force*, a reaction, statically dual of the corresponding removed hyperstatic constraint.

Hence, there is an unknown generalized force for each degree of hyperstaticity, and each one of them is applied to an auxiliary structure; in our example, we have hence two unknowns, x_1 and x_2 , indicated in Fig. 3.4. These unknowns are determined imposing the *geometrical condition that their corresponding displacement is equal to the one prescribed in the real structure (usually, it is null)*. We remark hence that in this method the unknowns are forces and the equations, compatibility conditions on the displacements.

Because each one of the structures decomposing the original hyperstatic one is isostatic, it is possible to determine everywhere the internal actions merely using balance equations. We indicate with

- N_0, T_0, M_0 the internal actions in the principal structure;
- N_i, T_i, M_i those in the i^{th} auxiliary structure *loaded with* $x_i = 1$.

Thanks to the assumption of linearity, the actual internal actions in the real, hyperstatic structure, are given by the superposition of the effects:

$$\begin{aligned} N &= N_0 + \sum_{i=1}^n x_i N_i, \\ T &= T_0 + \sum_{i=1}^n x_i T_i, \\ M &= M_0 + \sum_{i=1}^n x_i M_i, \end{aligned} \tag{3.61}$$

with n the degree of hyperstaticity.

To determine the unknowns x_i we use the PVD; to this purpose, we consider as virtual displacements those of the real structure, that are of course surely admissible. As forces, we consider those in each one of the auxiliary structures; because these structures are isostatic, the internal actions, calculated using balance equations, are surely equilibrated with the external loads. As a consequence, we are authorized to use the PVD with such a system of forces and field of virtual (actually, in this case real) displacements. We apply the PVD as much times as the auxiliary structures, i.e. as the degree of hyperstaticity:

- 1st auxiliary structure:

- virtual work of the external forces ($x_1 = 1$): if, in the real structure, the point of application of x_1 undergoes an imposed displacement $\boldsymbol{\delta}_1$, then such virtual work will be equal to

$$\delta_1 = \mathbf{e}_1 \cdot \boldsymbol{\delta}, \tag{3.62}$$

where \mathbf{e}_1 is the unit vector oriented like x_1 ; usually, $\boldsymbol{\delta} = \mathbf{o}$, so $\delta_1 = 0$;

- virtual work of the internal forces (we indicate with Ω the whole structure and with ℓ a generic curvilinear abscissa along the rods composing the structure):

$$\int_{\Omega} (N_1 \varepsilon + T_1 \gamma + M_1 \kappa) d\ell; \tag{3.63}$$

the first equation is hence

$$\int_{\Omega} (N_1 \varepsilon + T_1 \gamma + M_1 \kappa) d\ell = \delta_1; \tag{3.64}$$

- 2nd auxiliary structure: proceeding in the same way we obtain

$$\int_{\Omega} (N_2 \varepsilon + T_2 \gamma + M_2 \kappa) d\ell = \delta_2. \tag{3.65}$$

In the above equations, the internal kinematical descriptors ε, γ and κ are those in the real structure. So, using the constitutive equations of elastic rods and the superposition

of the effects we get

$$\begin{aligned}
\varepsilon &= \frac{N}{EA} = \frac{N_0 + x_1 N_1 + x_2 N_2}{EA}, \\
\gamma &= \chi \frac{T}{\mu A} = \chi \frac{T_0 + x_1 T_1 + x_2 T_2}{\mu A}, \\
\kappa &= \frac{M}{EJ} = \frac{M_0 + x_1 M_1 + x_2 M_2}{EJ}.
\end{aligned} \tag{3.66}$$

Replacing the relations above in the two PVD equations, after regrouping the terms we get

$$\begin{aligned}
&x_1 \int_{\Omega} \left(\frac{N_1^2}{EA} + \chi \frac{T_1^2}{\mu A} + \frac{M_1^2}{EJ} \right) d\ell + x_2 \int_{\Omega} \left(\frac{N_1 N_2}{EA} + \chi \frac{T_1 T_2}{\mu A} + \frac{M_1 M_2}{EJ} \right) d\ell \\
&+ \int_{\Omega} \left(\frac{N_1 N_0}{EA} + \chi \frac{T_1 T_0}{\mu A} + \frac{M_1 M_0}{EJ} \right) d\ell = \delta_1, \\
&x_1 \int_{\Omega} \left(\frac{N_1 N_2}{EA} + \chi \frac{T_1 T_2}{\mu A} + \frac{M_1 M_2}{EJ} \right) d\ell + x_2 \int_{\Omega} \left(\frac{N_2^2}{EA} + \chi \frac{T_2^2}{\mu A} + \frac{M_2^2}{EJ} \right) d\ell \\
&+ \int_{\Omega} \left(\frac{N_2 N_0}{EA} + \chi \frac{T_2 T_0}{\mu A} + \frac{M_2 M_0}{EJ} \right) d\ell = \delta_2.
\end{aligned} \tag{3.67}$$

These equations have the form of a symmetric system of linear algebraic equations; in the general case of n degrees of hyperstaticity, we have a system of n equations with n unknowns x_i that can be synthetically written in the form

$$\eta_{ij} x_j = \eta_{i0} + \delta_i, \tag{3.68}$$

with

$$\begin{aligned}
\eta_{ij} &= \eta_{ji} = \int_{\Omega} \left(\frac{N_i N_j}{EA} + \chi \frac{T_i T_j}{\mu A} + \frac{M_i M_j}{EJ} \right) d\ell, \\
\eta_{i0} &= - \int_{\Omega} \left(\frac{N_i N_0}{EA} + \chi \frac{T_i T_0}{\mu A} + \frac{M_i M_0}{EJ} \right) d\ell.
\end{aligned} \tag{3.69}$$

The terms on the diagonal, η_{ii} are necessarily positive, as it is apparent from the above equations. Equations (3.68) are the *Müller-Breslau equations* (1886), with the coefficients of the unknowns given by eq. (3.69). They provide the classical method for the resolution of hyperstatic systems of elastic rods. In the very frequent case of slender rods, the extension and shear deformations are much smaller than the bending one, so they can be neglected and the calculation of the coefficients is greatly simplified, as it is reduced to the only bending terms.

It is worth notice that imposed displacements to a constrained point, like those produced by ground settlements in a bridge or a building foundation structure, stress an hyperstatic structure. This is not the case for an isostatic one, because in that case the distribution of the internal actions is uniquely determined by the equilibrium equations. As imposed displacements are kinematical conditions, they do not enter the equilibrium equations and, by consequence, do not stress an isostatic structure.

As a last point we remark that once determined the unknowns x_i , the real distribution of the internal actions in the structure can be easily calculated using eq. (3.61).

3.11.3 The dummy load method

The method of the forces does not allow to retrieve all the information about the rod, e.g. it does not give the displacements. Anyway, we can calculate the displacement v in a point still using the PVD, by the so-called *dummy load method*. To this purpose, we apply the PVD using as displacement field the real one and as forces those in any equilibrated isostatic system acted upon uniquely by a unit force, the *dummy load*, dual of the displacement v to be found.

The virtual work of the external forces is hence equal to v , while that of the internal forces is

$$\int_{\Omega} \left(\frac{N N_d}{EA} + \chi \frac{T T_d}{\mu A} + \frac{M M_d}{EJ} \right) dl, \quad (3.70)$$

where N, T, M are the real internal actions; they are already known by a previous calculation, for instance a merely static one if the structure is isostatic or having solved the Müller-Breslau equations if it is hyperstatic. N_d, T_d, M_d are the internal actions produced on the isostatic structure by the dummy load; being the structure isostatic, they can be calculated by simple static conditions, hence they are equilibrated.

Finally, the PVD gives

$$v = \int_{\Omega} \left(\frac{N N_d}{EA} + \chi \frac{T T_d}{\mu A} + \frac{M M_d}{EJ} \right) dl. \quad (3.71)$$

3.12 Effects of a temperature change

A final question concerns the effects of the temperature changes. We still use the Hooke-Duhamel model (see Ex. 12, Chapt. 3):

$$\boldsymbol{\varepsilon} = \boldsymbol{\varepsilon}_m + \boldsymbol{\varepsilon}_t, \quad (3.72)$$

where $\boldsymbol{\varepsilon}_m$ is the mechanical deformation, given by the Lamé's inverse equations (??), while the thermal deformation $\boldsymbol{\varepsilon}_t$ is given by

$$\boldsymbol{\varepsilon}_t = \Delta t \alpha \mathbf{I}, \quad (3.73)$$

where Δt is the temperature variation with respect to a state where, conventionally, $\boldsymbol{\varepsilon}_t = \mathbf{0}$, and α is the *coefficient of thermal expansion*.

For what concerns Δt , the usual assumption in the rod theory is that it has a linear variation through the thickness of the rod, see Fig. 3.5, which is rigorously true in a stationary heat flow; if h is the thickness of the section,

$$t(y) = t_0 + \frac{\delta t}{h} y, \quad t_0 = \frac{t^+ + t^-}{2}, \quad \delta t = t^+ - t^-. \quad (3.74)$$

The global temperature change is hence decomposed into a uniform, t_0 , and an anti-symmetric one, δt . Now, we need to link $\boldsymbol{\varepsilon}_t$ to the descriptors $\varepsilon_t, \gamma_t, \kappa_t$ of the *thermal deformation*. To this end, we consider a length of rod between the sections 1 and 2 and

we write the strain energy of the beam and of the rod, that must be equal. Because for a Saint-Venant beam it is $\sigma_{11} = \sigma_{22} = \sigma_{12} = 0$, we have

$$\frac{1}{2} \int_1^2 (\sigma_{33}\varepsilon_{33t} + 2\sigma_{13}\varepsilon_{13t} + 2\sigma_{23}\varepsilon_{23t}) dv = \frac{1}{2} \int_1^2 (N\varepsilon_t + T\gamma_t + M\kappa_t) dz. \quad (3.75)$$

But $\varepsilon_{13t} = \varepsilon_{23t} = 0$, because of eq. (3.73); then, using the Saint-Venant Problem results and the linear variation of t through the rod thickness we get, for the left-hand term,

$$\frac{1}{2} \int_1^2 \left[\int_S \alpha \left(\frac{N}{A} + \frac{M y}{J} \right) \left(t_0 + \frac{\delta t}{h} y \right) ds \right] dz = \frac{1}{2} \int_1^2 \alpha \left(N t_0 + M \frac{\delta t}{h} \right) dz, \quad (3.76)$$

the other terms are null because the frame axes have their origin in the centroid of the cross section S . So, because this equation must be true for all the possible choices of the sections 1 and 2, the two integrands must be equal, which gives

$$\begin{aligned} \varepsilon_t &= \alpha t_0, \\ \gamma_t &= 0, \\ \kappa_t &= \alpha \frac{\delta t}{h}. \end{aligned} \quad (3.77)$$

Shear deformation is not affected by temperature changes; extension is influenced only by uniform and bending only by antisymmetric changes of temperature. According to eq. (3.72), the deformations of the rod are hence given by

$$\begin{aligned} \varepsilon &= \varepsilon_m + \varepsilon_t, \\ \gamma &= \gamma_m, \\ \kappa &= \kappa_m + \kappa_t, \end{aligned} \quad (3.78)$$

where the subscript m indicates the *mechanical* part of the deformation, linked to the internal actions by the constitutive equations (3.17):

$$N = EA \varepsilon_m, \quad T = \frac{\mu A}{\chi} \gamma_m, \quad M = EJ \kappa_m, \quad (3.79)$$

while the total deformation is still linked to the displacement components by the compatibility equations (3.7), (3.8) and (3.12)

$$\varepsilon = -w', \quad \gamma = v' - \varphi, \quad \kappa = -\varphi'. \quad (3.80)$$

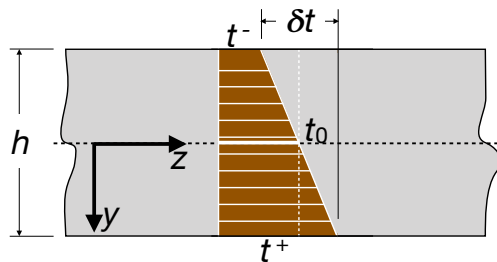


Figure 3.5: Decomposition of a linear temperature change on a rod.

From the previous equations we get hence

$$\begin{aligned}
N &= EA(\varepsilon - \varepsilon_t) = EA(w' - \alpha t_0), \\
T &= \frac{\mu A}{\chi}(v' - \varphi), \\
M &= EJ(\kappa - \kappa_t) = -EJ\left(\varphi' + \alpha \frac{\delta t}{h}\right),
\end{aligned} \tag{3.81}$$

that inserted into the equilibrium equations (3.5) give finally the *thermo-elastic equilibrium equations* for the Timoshenko's rod model:

$$\begin{aligned}
(EA(w' - \alpha t_0))' &= -r, \\
\left(\frac{\mu A}{\chi}(v' - \varphi)\right)' &= -p, \\
\left(EJ\left(\varphi' + \alpha \frac{\delta t}{h}\right)\right)' &= -\left(\frac{\mu A}{\chi}(v' - \varphi)\right) - m.
\end{aligned} \tag{3.82}$$

For the Euler-Bernoulli rod, the first equation above does not change, the second one is, as usual, meaningless, while eq. (3.81)₃ becomes ($\varphi = v'$),

$$M = EJ(\kappa - \kappa_t) = -EJ\left(v'' + \alpha \frac{\delta t}{h}\right), \tag{3.83}$$

that inserted into the equilibrium equation (3.6) finally gives

$$\left(EJ\left(v'' + \alpha \frac{\delta t}{h}\right)\right)'' = p - m'. \tag{3.84}$$

In the Müller-Breslau equations, the presence of a temperature field can be accounted for inserting eqs. (3.77) and (3.78) in the expressions of ε and κ in eqs. (3.66):

$$\begin{aligned}
\varepsilon &= \varepsilon_m + \varepsilon_t = \frac{N}{EA} + \alpha t_0 = \frac{N_0 + x_1 N_1 + x_2 N_2}{EA} + \alpha t_0, \\
\gamma &= \gamma_m = \chi \frac{T}{\mu A} = \chi \frac{T_0 + x_1 T_1 + x_2 T_2}{\mu A}, \\
\kappa &= \kappa_m + \kappa_t = \frac{M}{EJ} + \alpha \frac{\delta t}{h} = \frac{M_0 + x_1 M_1 + x_2 M_2}{EJ} + \alpha \frac{\delta t}{h}.
\end{aligned} \tag{3.85}$$

Once these expressions inserted into the PVD equations, e.g. eqs. (3.64) and (3.65), we get the final form of the Müller-Breslau equations for the thermo-elastic case:

$$\eta_{ij} x_j = \eta_{i0} + \eta_{it} + \delta_i, \tag{3.86}$$

where

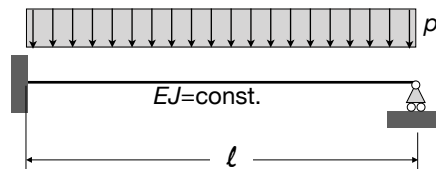
$$\eta_{it} = - \int_{\Omega} \alpha \left(t_0 N_i + \frac{\delta t}{h} M_i \right) dl. \tag{3.87}$$

To end this Section, we recall that for an isostatic equation the distribution of the internal actions N, T and M is uniquely determined by the equilibrium equations (3.5)₁ and (3.6), see Sect. 3.8. Because in such equations the effects of temperature changes, that are deformation effects, do not enter, *temperature changes do not produce any internal action in isostatic structures, but only deformations*. This is not the case of hyperstatic structures, like eqs. (3.81) to (3.84) clearly show. Hence, unlike isostatic rods, *hyperstatic rods are stressed by temperature changes*.

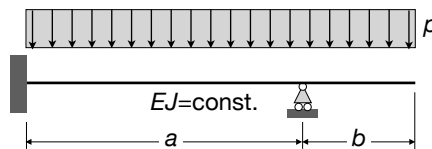
3.13 Exercises

Nota bene: *unless otherwise specified, the exercises below are to be solved using the Euler-Bernoulli rod model.*

1. Determine the elastica of a cantilever beam with $EJ = \text{const.}$, loaded:
 - i. by a uniform load p ;
 - ii. by a concentrated force F at the free edge (this is the *Galileo's problem*);
 - iii. by a couple M at the free edge.
2. Determine the function $J(z)$ that a homogeneous uniformly loaded cantilever must have to bend along a circular arch of radius R .
3. Determine the axial force N and displacement w of a vertical rod with $EA = \text{const.}$ clamped at its ends and submitted to its own weight.
4. Determine the variation $h(z)$ of the height of a rectangular cross section of a cantilever loaded by a concentrated force at its free edge in order to have everywhere the same highest stress σ_{33} (*Galileo's problem of the rod of uniform strength*).
5. What does it change in the previous problem if it is the highest Von Mises equivalent stress to be constant throughout the rod length?
6. Determine the displacement v of the center of a clamped-clamped rod loaded at mid-span by a concentrated force F .
7. Study the structure in the figure and determine the maximum deflection.



8. Study the same problem but now using the Timoshenko's rod model. Show that in this case the solution tends to that of the Euler-Bernoulli model when the slenderness ratio $\rho/\ell \rightarrow 0$; how to interpret this result?
9. Find the displacement of the free edge of the rod in the figure using the results of the previous exercises.

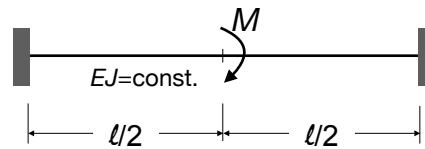


10. Find the deflexion and rotation of the beam of exercise 1 using the Mohr's theorem and corollary.
11. A rod clamped at the ends is thermally loaded by:
 - i. a uniform temperature t_0 ;

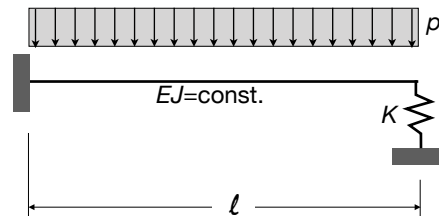
ii. a through the thickness linear variation of the type $t^- = -t$, $t^+ = +t$.

Study the structure in both the cases, finding the reactions, internal actions and displacements.

12. Consider again the two cases of the previous exercise, but now the rod is simply supported; what changes for the rod?
13. Study the structure in the figure, finding also the rotation of the central point.

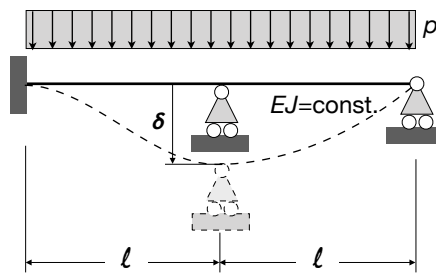


14. Study the structure in the figure.

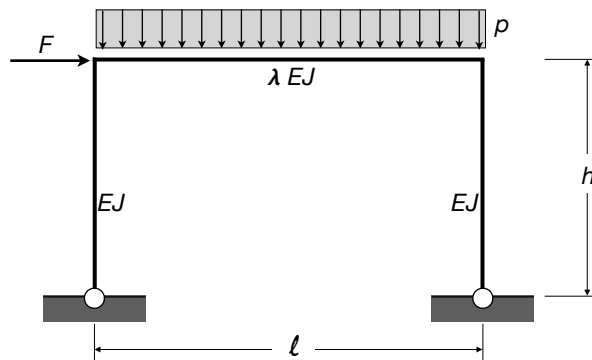


15. Make the same, loading now the rod uniquely by a thermal load of the type $t^- = -t$, $t^+ = +t$.
16. Determine the support reactions and internal actions of an elastic simply supported rod of length l and constant bending stiffness EJ when a point at the abscissa $z = a$ is submitted to an imposed deflection δ . Why the problem cannot be solved using uniquely equilibrium equations, i.e., why contrarily to what seems at a first sight, this problem is not isostatic?
17. An infinitely long pipe, whose weight per unit length is p and whose constant bending stiffness is EJ , lays on a horizontal plane, that can be considered as infinitely rigid. The pipe must be lifted at a certain point, by a crane, of a height equal to h . Which is the lifting force that the crane must produce?
18. A rod whose length is l , weight per unit length p and constant bending stiffness EJ , lays on a horizontal plane, that can be considered as infinitely rigid. At the left end, the rod is acted upon by a vertical force F . For what conditions the equilibrium is ensured? How much the left end of the rod will be lifted up by F ?
19. A rod whose length is l , weight per unit length p , thickness h and constant bending stiffness EJ , lays on a horizontal plane, that can be considered as infinitely rigid. The rod is heated on its upper surface to a temperature t , while the lower part is at the temperature $-t$. Determine the vertical displacement of the mid point of the rod. Which is the minimum value of t to lift up the rod?
20. Study the case of an elastic rod of length $l \rightarrow \infty$ that is submitted to a concentrated load F and that lays on an elastic substrate whose elastic constant is k (this is the case of a rod on a Winkler's soil).

21. Study now the case of a rod on an elastic soil, with finite length ℓ and submitted to a uniform load p . Can you predict the result?
22. Study the case of a pile of length ℓ driven into an elastic soil of elastic constant k and submitted, at its top, to an horizontal force F .
23. Solve exercise 8 using the Müller-Breslau equations.
24. Solve exercise 9 using the dummy load method.
25. Solve exercise 11 using the Müller-Breslau equations and the dummy load method.
26. Solve exercise 13 using the Müller-Breslau equations and the dummy load method
27. Solve exercise 14 using the Müller-Breslau equations.
28. Solve the structure in the figure using the Müller-Breslau equations.



29. Make the same, loading now the rod uniquely by a thermal load of the type $t^- = -t$, $t^+ = +t$.
30. Solve the structure in the following figure using the Müller-Breslau equations (neglect the axial and shear deformations). What happens when $\lambda \rightarrow \infty$?



Chapter 4

Arches

4.1 Introduction

Arches are plane curved rods. They are currently used in a lot of situations; in civil engineering, the most impressive realizations are some bridges, see Fig. 4.1. Arches are used



Figure 4.1: Some examples of arch bridges.

since long time (probably the most ancient arches in the world are two arches in Italy, at Velia and Volterra, both from the IVth century b.C.), though in the form of arches composed of carved stone voussoirs or masonry bricks. Arches, in fact, have a great advantage with respect to rectilinear rods: while rods are mainly subjected to bending, internal axial forces are dominating in arches: strain energy is stored in the form of bending energy in rods, while mainly, though not exclusively, in the form of extension energy in arches. This is rather advantageous, because axial stiffness and strength are normally much greater than the bending ones: arches bear greater loads than rectilinear loads. A simple scheme gives account of this: let us consider a rectilinear, simply supported rod of span ℓ submitted to a uniform weight p . The highest bending moment, at mid-span, is $M_{max} = \frac{p\ell^2}{8}$. For equilibrium, such a couple must be balanced by an internal couple given by internal stresses. This internal couple has a small lever arm, less than the thickness of the cross section. As a consequence, the cross section must have a rather great thickness, in order

on one side to increase the internal lever arm, on the other side to decrease stresses and bring them under the admissible value.

If now we consider an arch hinged at the ends and submitted to the same load, the horizontal reactions give a couple at mid-span that balances the couple given by p ; in the limit, the bending moment at mid-span can be null, and the section is submitted exclusively to an axial force equal to the horizontal reactions. This is a much more favorable structural situation, that allows to the structure, for the same cross section and material, to carry more important loads or to cover much longer spans.

This simple case allows also for understating a basic fact: in a simply supported or clamped arch vertical loads produce also horizontal reactions. If the arch is simply supported at one of the two ends, then these horizontal reactions do not exist and the arch is actually just a curved beam, it works almost exclusively in bending: it is the presence of the horizontal reactions that makes a curved rod an effective arch.

In the following, we study the statics of elastic curved rods and then we apply the theory to the statics of arches.

4.2 Balance equations

We consider a curvilinear plane rod like in Fig. 4.2; s is a curvilinear abscissa, that we will put, conventionally, equal to zero at the left end of the rod. We then consider a part of the rod between two sections at the abscissae s and $s+ds$ infinitesimally close together, Fig. 4.3, so that we can consider as constant the curvature of the rod in the part ds , and be $d\theta$ the infinitesimal angle subtended by the two normals to the rod at s and ds , that meet together in o , the centre of the local osculating circle.

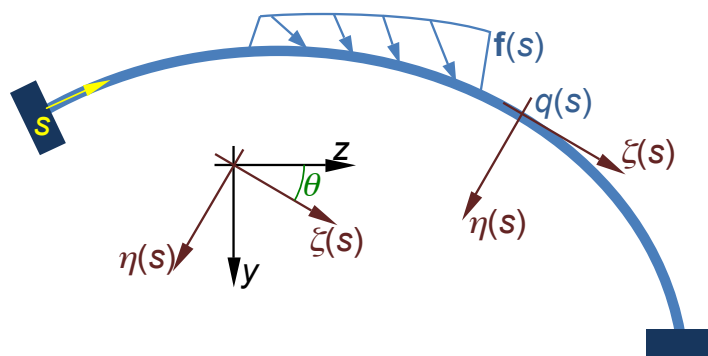


Figure 4.2: General scheme of an arch.

We remain in the framework of small strain and displacements and write the balance equations in the undeformed configuration. Then, referring to Fig. 4.3, it is easy to write the balance equations:

- horizontal equilibrium:

$$T \sin \frac{d\theta}{2} + N \cos \frac{d\theta}{2} - r ds + (T + dT) \sin \frac{d\theta}{2} - (N + dN) \cos \frac{d\theta}{2} = 0; \quad (4.1)$$

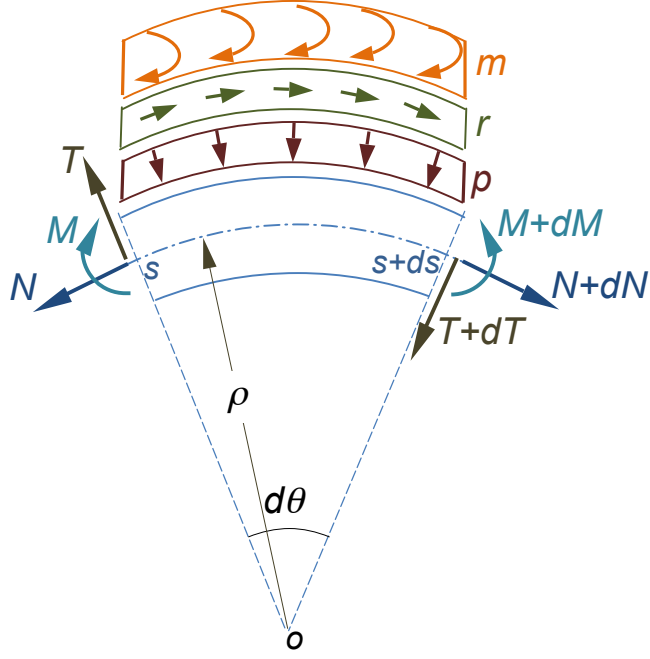


Figure 4.3: General scheme for the balance equations.

- vertical equilibrium:

$$T \cos \frac{d\theta}{2} - N \sin \frac{d\theta}{2} - p ds - (T + dT) \cos \frac{d\theta}{2} - (N + dN) \sin \frac{d\theta}{2} = 0; \quad (4.2)$$

- rotation equilibrium (written here with respect to o):

$$M + m ds + (N + dN)\rho + r\rho ds - N\rho - (M + dM) = 0, \quad (4.3)$$

with ρ the radius of curvature. Because ds is infinitesimal, $d\theta \rightarrow 0$ so that $\cos \frac{d\theta}{2} \simeq 1$ while $\sin \frac{d\theta}{2} \simeq \frac{d\theta}{2}$. By consequence, once simplified the balance equations transform to

$$\begin{aligned} dN &= T d\theta - r ds, \\ dT &= -N d\theta - p ds, \\ dM &= \rho dN + \rho r ds + m ds. \end{aligned} \quad (4.4)$$

Injecting eq. (4.4)₁ into eq. (4.4)₃ and considering that $ds = \rho d\theta$, we finally get

$$\begin{aligned} \frac{dN}{ds} &= \frac{T}{\rho} - r, \\ \frac{dT}{ds} &= -\frac{N}{\rho} - p, \\ \frac{dM}{ds} &= T + m. \end{aligned} \quad (4.5)$$

Unlike the case of rectilinear rods, now all the balance equations are coupled; to remark that for $\rho \rightarrow \infty$, i.e. for a curvilinear rod that tends to become rectilinear, the above equations tend to those of the straight rods.

Introducing now the symbolic matrix

$$\mathbf{D}_1 = \begin{bmatrix} \frac{d}{ds} & -\frac{1}{\rho} & 0 \\ \frac{1}{\rho} & \frac{d}{ds} & 0 \\ 0 & -1 & \frac{d}{ds} \end{bmatrix} \quad (4.6)$$

along with the vectors of the internal actions, \mathbf{S} , and of the applied loads, \mathbf{f} ,

$$\mathbf{S} = \begin{Bmatrix} N \\ T \\ M \end{Bmatrix}, \quad \mathbf{f} = \begin{Bmatrix} r \\ p \\ m \end{Bmatrix}, \quad (4.7)$$

eq. (4.5) can be given in matrix form:

$$\mathbf{D}_1 \mathbf{S} + \mathbf{f} = \mathbf{o}. \quad (4.8)$$

Implicitly, the above equations have been written in the local frame $\{\zeta(s), \eta(s)\}$, see Fig. 4.2. They can be written in a fixed frame $\{z, y\}$ simply writing that:

$$\mathbf{f} = \mathbf{Q} \mathbf{f}^* : = \begin{Bmatrix} r \\ p \\ m \end{Bmatrix} \begin{bmatrix} \cos \theta & \sin \theta & 0 \\ -\sin \theta & \cos \theta & 0 \\ 0 & 0 & 1 \end{bmatrix} \begin{Bmatrix} r^* \\ p^* \\ m^* \end{Bmatrix}, \quad (4.9)$$

where the symbol $*$ denotes a vector written in the fixed frame $\{z, y\}$ and \mathbf{Q} the rotation tensor operating the change of frame from $\{z, y\}$ to $\{\zeta(s), \eta(s)\}$. Of course, $\mathbf{Q} = \mathbf{Q}(s)$, because $\theta = \theta(s)$.

So, finally, the matrix equation (4.8) written in the fixed frame $\{z, y\}$ is simply

$$\mathbf{D}_1 \mathbf{S} + \mathbf{Q} \mathbf{f}^* = \mathbf{o}. \quad (4.10)$$

4.3 Compatibility equations

Just as for straight rods, we need to link the displacement of the arch to the kinematical quantities defining its deformation. We write such relations in the local frame $\{\zeta(s), \eta(s)\}$, see Fig. 4.4.

A point $q(s)$ of the arch centerline becomes, after deformation, the point $q'(s)$, so the displacement vector is

$$\mathbf{u}(s) = q'(s) - q(s) = u_\tau(s) \boldsymbol{\tau}(s) + u_\nu(s) \boldsymbol{\nu}(s). \quad (4.11)$$

We want express the link between the internal kinematical quantities defining the deformation of the arch and the following geometrical quantities, defining the transformation of the cross section of the arch in correspondence of $q(s)$:

- $v(s)$, the displacement along $\eta(s)$, i.e. parallel to the principal normal $\boldsymbol{\nu}(s)$;

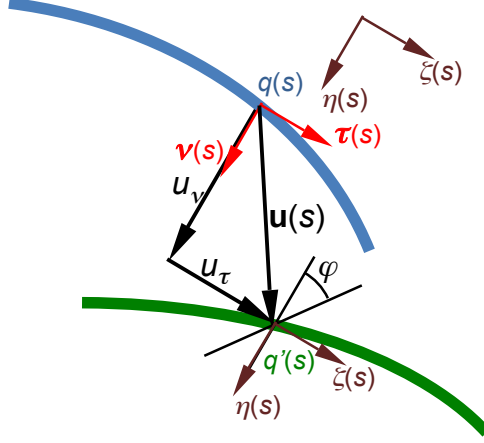


Figure 4.4: General scheme for the compatibility equations.

- $w(s)$, the displacement along $\zeta(s)$, i.e. parallel to the tangent $\boldsymbol{\tau}(s)$;
- $\varphi(s)$, the rotation of the normal $\boldsymbol{\nu}(s)$.

We introduce the following kinematical quantities for describing the deformation of the arch:

- ε : the extension of the arch mid-line;
- κ : the bending curvature of the arch centerline (not to be confused with the *geometric* curvature c of the arch centerline, i.e. the curvature of the undeformed arch);
- γ : the shear of the cross section.

To define and determine these quantities we need to analyze how a generic point of the cross section is transformed. Remembering that the arch is a plane curve and that the problem is planar, i.e. the arch bends in its plane, it is sufficient to study the transformation of a generic point $\hat{q}(s, \eta)$ of the cross section at the distance η from the centerline (so, actually, $q(s) = \hat{q}(s, 0)$).

We then introduce the displacement of $\hat{q}(s, \eta)$:

$$\hat{\mathbf{u}}(s, \eta) = \hat{u}_\tau(s, \eta)\boldsymbol{\tau}(s) + \hat{u}_\nu(s, \eta)\boldsymbol{\nu}(s), \quad (4.12)$$

and considering the scheme of Fig. 4.4 we recognize immediately that, thanks to the assumptions of small deformations and displacements (namely, $\varphi \rightarrow 0 \Rightarrow \sin \varphi \simeq \varphi$, $\cos \varphi \simeq 1$), we can write

$$\begin{aligned} \hat{u}_\tau(s, \eta) &= w(s) - \eta \sin \varphi \simeq w(s) - \eta \varphi, \\ \hat{u}_\nu(s, \eta) &= v(s) - \eta(1 - \cos \varphi) \simeq v(s). \end{aligned} \quad (4.13)$$

We calculate now the derivatives of $\hat{\mathbf{u}}(s, \eta)$ with respect to η and to the curvilinear abscissa of $\hat{q}(s, \eta)$; this is $\hat{s} \neq s$, due to the geometrical curvature of the arch. Nevertheless, see

Fig. 4.5, it is easy to find the relation between s and \hat{s} :

$$d\theta = \frac{ds}{\rho} = \frac{d\hat{s}}{\rho - \eta} \rightarrow \frac{ds}{d\hat{s}} = \frac{\rho}{\rho - \eta}, \quad (4.14)$$

relation that gives also

$$\frac{\partial \cdot}{\partial \hat{s}} = \frac{\partial \cdot}{\partial s} \frac{ds}{d\hat{s}} = \frac{\partial \cdot}{\partial s} \frac{\rho}{\rho - \eta}. \quad (4.15)$$

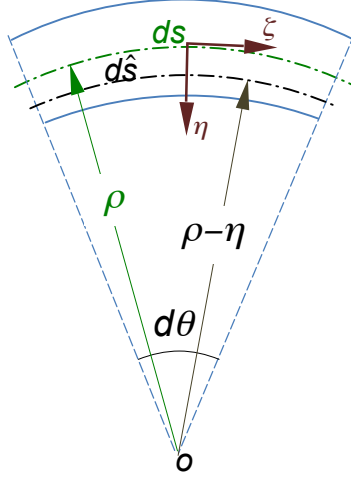


Figure 4.5: Scheme for the relation between ds and $d\hat{s}$.

The derivatives are hence:

$$\begin{aligned} \frac{\partial \hat{\mathbf{u}}}{\partial \hat{s}} &= \frac{\partial v(s)}{\partial \hat{s}} \boldsymbol{\nu}(s) + v(s) \frac{\partial \boldsymbol{\nu}(s)}{\partial \hat{s}} + \frac{\partial (w(s) - \eta \varphi(s))}{\partial \hat{s}} \boldsymbol{\tau}(s) + \\ &\quad (w(s) - \eta \varphi(s)) \frac{\partial \boldsymbol{\tau}(s)}{\partial \hat{s}}, \quad (4.16) \\ \frac{\partial \hat{\mathbf{u}}}{\partial \eta} &= -\varphi(s) \boldsymbol{\tau}(s). \end{aligned}$$

Applying eq. (4.15) to $\frac{\partial \boldsymbol{\tau}(s)}{\partial \hat{s}}$ and $\frac{\partial \boldsymbol{\nu}(s)}{\partial \hat{s}}$, using the Frenet-Serret formulae and remembering that $\vartheta(s) = 0 \forall s$ because the arch is a plane curve, gives finally (we do not write explicitly the dependence on s for the sake of conciseness)

$$\frac{\partial \hat{\mathbf{u}}}{\partial \hat{s}} = \frac{\rho}{\rho - \eta} \left(w' - \frac{v}{\rho} - \eta \varphi' \right) \boldsymbol{\tau} + \frac{\rho}{\rho - \eta} \left(v' + \frac{w}{\rho} - \eta \frac{\varphi}{\rho} \right) \boldsymbol{\nu}, \quad (4.17)$$

where the prime denotes differentiation with respect to s : $w' = \frac{\partial w}{\partial s}$ etc.

We define now mathematically the kinematical quantities introduced above to describe

the deformation of the arch:

$$\begin{aligned}
\varepsilon_\eta(s, \eta) &:= \left(\frac{\partial \hat{\mathbf{u}}}{\partial \hat{s}} \right)_\tau = \frac{\rho}{\rho - \eta} \left(w' - \frac{v}{\rho} - \eta \varphi' \right), \\
\kappa(s) &:= -\varphi', \\
\gamma_\eta(s, \eta) &:= \left(\frac{\partial \hat{\mathbf{u}}}{\partial \hat{s}} \right)_\nu + \left(\frac{\partial \hat{\mathbf{u}}}{\partial \eta} \right)_\tau = \frac{\rho}{\rho - \eta} \left(v' + \frac{w}{\rho} - \eta \frac{\varphi}{\rho} \right) - \varphi,
\end{aligned} \tag{4.18}$$

that can be rearranged to give finally

$$\begin{aligned}
\varepsilon_\eta(s, \eta) &= \frac{\rho}{\rho - \eta} \left(w' - \frac{v}{\rho} + \eta \kappa \right), \\
\kappa(s) &= -\varphi', \\
\gamma_\eta(s, \eta) &= \frac{\rho}{\rho - \eta} \left(v' + \frac{w}{\rho} - \varphi \right).
\end{aligned} \tag{4.19}$$

For *small curvature arches*, i.e. when the radius of curvature ρ is far greater than the thickness of the cross section: $\frac{\rho}{\max \eta} \gg 1 \forall s \Rightarrow \frac{\rho}{\rho - \eta} \rightarrow 1$, the above equations become

$$\begin{aligned}
\varepsilon_\eta(s, \eta) &= w' - \frac{v}{\rho} + \eta \kappa, \\
\kappa(s) &= -\varphi', \\
\gamma(s) &= v' + \frac{w}{\rho} - \varphi.
\end{aligned} \tag{4.20}$$

The term $\varepsilon_\eta(s, \eta)$ is the extension of the fibers at a distance η from the centerline; we can write it as

$$\varepsilon_\eta(s, \eta) = \varepsilon(s) + \eta \kappa, \tag{4.21}$$

where

$$\varepsilon(s) = \varepsilon_\eta(s, \eta = 0) = w' - \frac{v}{\rho}. \tag{4.22}$$

Finally, for small curvature arches, the case which is by far the most interesting in applications and that we will consider in the following, the kinematical quantities describing its deformation can be reduced to quantities referring to the deformation of the centerline, and are

$$\begin{aligned}
\varepsilon(s) &= w' - \frac{v}{\rho}, \\
\gamma(s) &= v' + \frac{w}{\rho} - \varphi, \\
\kappa(s) &= -\varphi'.
\end{aligned} \tag{4.23}$$

These are the compatibility equations for small curvature arches. We remark that in the limit case of $\rho \rightarrow \infty$ the above quantities become

$$\begin{aligned}
\varepsilon(s) &= w', \\
\gamma(s) &= v' - \varphi, \\
\kappa(s) &= -\varphi',
\end{aligned} \tag{4.24}$$

i.e. they coincide, as it must be, with those of the straight rods.

If now we introduce the symbolic matrix

$$\mathbf{D}_2 = \begin{bmatrix} \frac{d}{ds} & -\frac{1}{\rho} & 0 \\ \frac{1}{\rho} & \frac{d}{ds} & -1 \\ 0 & 0 & -\frac{d}{ds} \end{bmatrix} \quad (4.25)$$

along with the vectors of the displacement, $\boldsymbol{\xi}$, and of the deformation, $\boldsymbol{\delta}$,

$$\boldsymbol{\xi} = \begin{Bmatrix} w \\ v \\ \varphi \end{Bmatrix}, \quad \boldsymbol{\delta} = \begin{Bmatrix} \varepsilon \\ \gamma \\ \kappa \end{Bmatrix}, \quad (4.26)$$

eq. (4.23) can be written in matrix form:

$$\mathbf{D}_2 \boldsymbol{\xi} = \boldsymbol{\delta}. \quad (4.27)$$

The same equation can be written in the fixed frame $\{z, y\}$:

$$\mathbf{D}_2 \mathbf{Q} \boldsymbol{\xi}^* = \boldsymbol{\delta}, \quad (4.28)$$

where $\boldsymbol{\xi}^*$ is the displacement vector written in the frame $\{z, y\}$ and \mathbf{Q} is the rotation matrix (4.9).

4.4 Constitutive equations

In the framework of linear elasticity, we assume as constitutive equations for plane arches the same of the straight rods:

$$\begin{aligned} N &= EA\varepsilon, \\ T &= \frac{\mu A}{\chi} \gamma, \\ M &= EJ\kappa, \end{aligned} \quad (4.29)$$

with E the Young's modulus and μ the shear modulus of the material, A the area of the cross section, j the moment of inertia of the cross section about an horizontal axis passing by the barycenter and χ the shear factor of the cross section.

Introducing the matrix

$$\mathbf{C} = \begin{bmatrix} EA & 0 & 0 \\ 0 & \frac{\mu A}{\chi} & 0 \\ 0 & 0 & EJ \end{bmatrix}, \quad (4.30)$$

we can write eq. (4.29) in matrix form:

$$\mathbf{C} \boldsymbol{\delta} = \mathbf{S}. \quad (4.31)$$

4.5 The problem of elastic equilibrium for the arches

We can now put together the constitutive, compatibility and equilibrium equations found above to write the equations of the elastic equilibrium for plane arches. Some simple calculations give

$$\begin{aligned} \left[EA \left(w' - \frac{v}{\rho} \right) \right]' &= \frac{\mu A}{\rho \chi} \left(v' + \frac{w}{\rho} - \varphi \right) - r, \\ \left[\frac{\mu A}{\chi} \left(v' + \frac{w}{\rho} - \varphi \right) \right]' &= -\frac{EA}{\rho} \left(w' - \frac{v}{\rho} \right) - p, \\ (-EJ\varphi')' &= \frac{\mu A}{\chi} \left(v' + \frac{w}{\rho} - \varphi \right) + m. \end{aligned} \quad (4.32)$$

The above equations show that all the equations are coupled; in particular, unlike the case of straight rods, as an effect of the geometry extension and bending are coupled.

We can put the above equations in a matrix form; to this purpose, we inject successively eqs. (4.31) and (4.27) into eq. (4.8) to get easily

$$\mathbf{D}_1 \mathbf{C} \mathbf{D}_2 \boldsymbol{\xi} + \mathbf{f} = \mathbf{o}. \quad (4.33)$$

To write the same equation in the fixed frame $\{z, y\}$, it is sufficient to do the same but with eqs. (4.10), (4.28) and (4.31), and left-multiply by \mathbf{Q}^\top :

$$\mathbf{Q}^\top \mathbf{D}_1 \mathbf{C} \mathbf{D}_2 \mathbf{Q} \boldsymbol{\xi}^* + \mathbf{f}^* = \mathbf{o}. \quad (4.34)$$

No matter of the form given to the above equations, they remain a system of three second-order coupled linear differential equations, that need 6 boundary conditions, three for each end of the arch. Their solution is, normally, impossible analytically and numerical methods must be used.

4.6 Transforming the equations of the arches

The equations found in the previous Sections can be transformed, so as to obtain equations that can be more easily solved; some assumptions on the geometry or the kinematics of the arch can also be introduced, with the same purpose. We consider first the case of the balance equations (4.5), then that of the elastic equilibrium equations (4.32).

4.6.1 Transforming the balance equations

For an isostatic arch the balance equations are sufficient to determine the internal actions N, T and $M \forall s$. A typical example, very used in the applications, especially in bridge constructions, is that of a three-hinged arch, see Fig. 4.6.

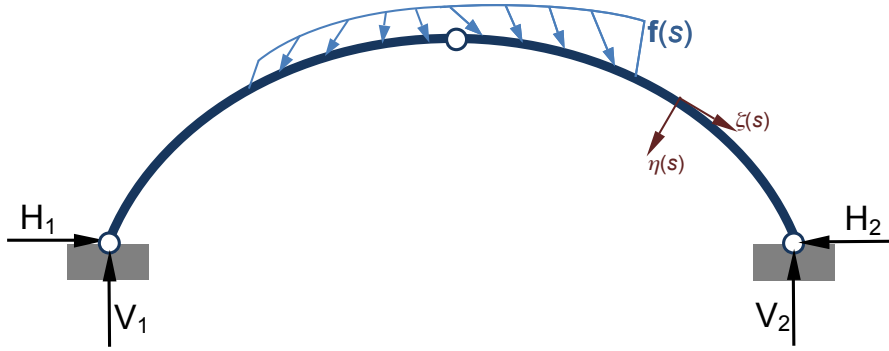


Figure 4.6: Scheme of a three-hinged arch.

We can rearrange the balance equations (4.5) in order to eliminate the shear from eqs. (4.5)_{1,3} so as to obtain a system of two linear differential equations. This can be done as follows: from eq. (4.5)₃ we get

$$T = \frac{dM}{ds} - m, \quad (4.35)$$

that injected into eq. (4.5)₁ gives

$$\frac{dN}{ds} = \frac{1}{\rho} \frac{dM}{ds} - \frac{m}{\rho} - r. \quad (4.36)$$

Then, we differentiate eq. (4.5)₃ to obtain

$$\frac{d^2 M}{ds^2} = \frac{dT}{ds} + \frac{dm}{ds} \quad (4.37)$$

and using eq. (4.5)₂ we get

$$\frac{d^2 M}{ds^2} = -\frac{N}{\rho} - p + \frac{dm}{ds}. \quad (4.38)$$

Equations (4.36) and (4.38) constitute a system of two coupled differential equations where the unknowns are the functions $N(s)$ and $M(s)$. The shear force $T(s)$ can be calculated by eq. (4.35) once $M(s)$ is known.

In the end, we need 3 boundary conditions for the solution of the equilibrium problem of isostatic arches. Once eqs. (4.36) and (4.38) are solved, $T(s)$ can be recovered using eq. (4.5)₃.

Of course, no information about the deformation of the arch is given by the solution of the balance equations; once the problem is solved, one can introduce N , T and M into the constitutive laws, eqs. (4.29), to obtain ε , γ and κ , that introduced in the compatibility equations (4.23), once integrated, give the components of displacement w , v and φ . Nevertheless, it is normally preferable, at least to find the components of displacement at a specific point, to employ other methods, like the dummy load method.

4.6.2 Transforming the elastic equilibrium equations

First of all, for the sake of conciseness, we call

$$\alpha := EA, \quad \beta := \frac{\mu A}{\chi}, \quad \lambda := EJ. \quad (4.39)$$

Then, eqs. (4.32) become

$$\begin{aligned} \left[\alpha \left(w' - \frac{v}{\rho} \right) \right]' &= \frac{\beta}{\rho} \left(v' + \frac{w}{\rho} - \varphi \right) - r, \\ \left[\beta \left(v' + \frac{w}{\rho} - \varphi \right) \right]' &= -\frac{\alpha}{\rho} \left(w' - \frac{v}{\rho} \right) - p, \\ (-\lambda \varphi')' &= \beta \left(v' + \frac{w}{\rho} - \varphi \right) + m. \end{aligned} \quad (4.40)$$

We remark that in the limit case of an arch that tends to be a straight rod, i.e. for $\rho \rightarrow \infty$, the above equations become

$$\begin{aligned} (\alpha w')' &= -r, \\ [\beta (v' - \varphi)]' &= -p, \\ (-\lambda \varphi')' &= \beta (v' - \varphi) + m, \end{aligned} \quad (4.41)$$

that are just the equations of the Timoshenko's rod model.

We can obtain an equivalent expression of eqs. (4.40), where p appears directly into the third equation and where the first and third equations contain exclusively the extension and bending stiffnesses, α and λ . To this purpose, it is sufficient to replace successively eqs. (4.29) and (4.23) into eqs. (4.36) and (4.38) to obtain

$$\begin{aligned} \left[\alpha \left(w' - \frac{v}{\rho} \right) \right]' &= -\frac{1}{\rho} (\lambda \varphi')' - r - \frac{m}{\rho}, \\ \left[\beta \left(v' + \frac{w}{\rho} - \varphi \right) \right]' &= -\frac{\alpha}{\rho} \left(w' - \frac{v}{\rho} \right) - p, \\ (\lambda \varphi')'' &= \frac{\alpha}{\rho} \left(w' - \frac{v}{\rho} \right) + p - m'. \end{aligned} \quad (4.42)$$

Unlike the case of the balance equations, it is not possible to uncouple the elastic equilibrium equations. Six boundary conditions complete eqs. (4.42), they specify either the values of v , w and φ or of their derivatives, at the ends of the arch.

4.6.3 The Euler-Bernoulli model for arches

Let us now generalize the Euler-Bernoulli rod model to arches, assuming that the cross section remains plane and orthogonal to the deformed centerline of the arch, i.e.

$$\varphi = v'. \quad (4.43)$$

Then, eqs. (4.42) become

$$\begin{aligned} \left[\alpha \left(w' - \frac{v}{\rho} \right) \right]' &= -\frac{1}{\rho} (\lambda v'')' - r - \frac{m}{\rho}, \\ (\lambda v'')'' &= \frac{\alpha}{\rho} \left(w' - \frac{v}{\rho} \right) + p - m'. \end{aligned} \quad (4.44)$$

The third equation, where the shear stiffness β appears, is now meaningless; the shear T can be recovered, once solved the above equations, which still needs six boundary conditions, using eq. (4.35).

It is easily checked that for $\rho \rightarrow \infty$ we get the Euler-Bernoulli rod equations.

4.6.4 Arches of constant section

A particular case is that of an arch with a constant section; in such a case $\alpha' = \beta' = \lambda' = 0$, so eqs. (4.42) become

$$\begin{aligned} \alpha \left(w' - \frac{v}{\rho} \right)' &= -\frac{1}{\rho} \lambda \varphi'' - r - \frac{m}{\rho}, \\ \beta \left(v' + \frac{w}{\rho} - \varphi \right)' &= -\frac{\alpha}{\rho} \left(w' - \frac{v}{\rho} \right) - p, \\ \lambda \varphi''' &= \frac{\alpha}{\rho} \left(w' - \frac{v}{\rho} \right) + p - m'. \end{aligned} \quad (4.45)$$

and eqs. (4.44)

$$\begin{aligned} \alpha \left(w' - \frac{v}{\rho} \right)' &= -\frac{1}{\rho} \lambda v''' - r - \frac{m}{\rho}, \\ \lambda v^{iv} &= \frac{\alpha}{\rho} \left(w' - \frac{v}{\rho} \right) + p - m'. \end{aligned} \quad (4.46)$$

4.6.5 Circular arches

A particularly important case of arches is that of circular arches; in such a case, $\rho = \text{const.} \Rightarrow \rho' = 0$, and actually ρ is just the radius of the circle of which the arch is only a circular segment.

It is interesting to see what happens to the equations for the case of constant section: eqs. (4.45) become

$$\begin{aligned} \alpha \left(w'' - \frac{v'}{\rho} \right) &= -\frac{1}{\rho} \lambda \varphi'' - r - \frac{m}{\rho}, \\ \beta \left(v'' + \frac{w'}{\rho} - \varphi' \right) &= -\frac{\alpha}{\rho} \left(w' - \frac{v}{\rho} \right) - p, \\ \lambda \varphi''' &= \frac{\alpha}{\rho} \left(w' - \frac{v}{\rho} \right) + p - m', \end{aligned} \quad (4.47)$$

while eqs. (4.46) become

$$\begin{aligned}\alpha \left(w'' - \frac{v'}{\rho} \right) &= -\frac{1}{\rho} \lambda v''' - r - \frac{m}{\rho}, \\ \lambda v^{iv} &= \frac{\alpha}{\rho} \left(w' - \frac{v}{\rho} \right) + p - m'.\end{aligned}\tag{4.48}$$

4.7 Examples

We give here some examples of the use of the theory developed in this Chapter. All the cases concern circular arches with a constant section. The first two examples have been treated using eqs. (4.47), i.e. the general theory. Then, they have been also treated using eqs. (4.48) of the Euler-Bernoulli model; the results coincide almost perfectly with those reported below, that is why they have not been reported here. The third example concerns an isostatic case, hence the balance equations are sufficient. All the results have been found numerically, using a standard commercial code (Mathematica). All the diagrams in the figures have been normalized, and the deformed shape exaggerated, hence the scale of the diagrams is not real.

4.7.1 Example 1

As a first example, we consider the case of a circular arch of constant section loaded by a uniform load $q = 10$ t/m, with $\rho = 10$ m, spanning a chord $\ell = 17.1$ m, see Fig. 4.7. The cross section is rectangular, with the base $b = 1$ m and the thickness $h = 2$ m; the Young's modulus is $E = 200$ MPa, the Poisson's ration $\nu = 0.2$, the shear factor $\chi = 1.2$. Hence, we get $\alpha = 4 \times 10^7$ kN, $\beta = \alpha/2.88 = 1.39 \times 10^8$ kN and $\lambda = \alpha/3 = 1.33 \times 10^8$ kN m^2 . The ends of the arch are clamped. Hence, the appropriate boundary conditions are $w = v = \varphi = 0$ at both the ends.

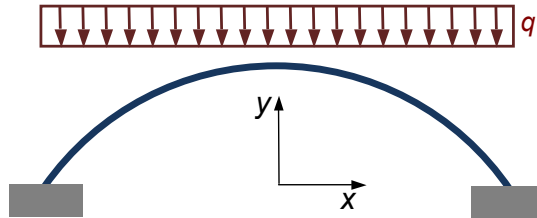


Figure 4.7: Example 1: a uniformly loaded circular arch.

In the following Figures, we report the diagrams, referred to an horizontal axis or to the arch axis, in grey, of w , v , φ , N , T , M and finally of the deformed shape. N is negative everywhere, i.e. the arch is compressed all along s , as it must be, while M changes of sign, as a consequence of the clamped edges.

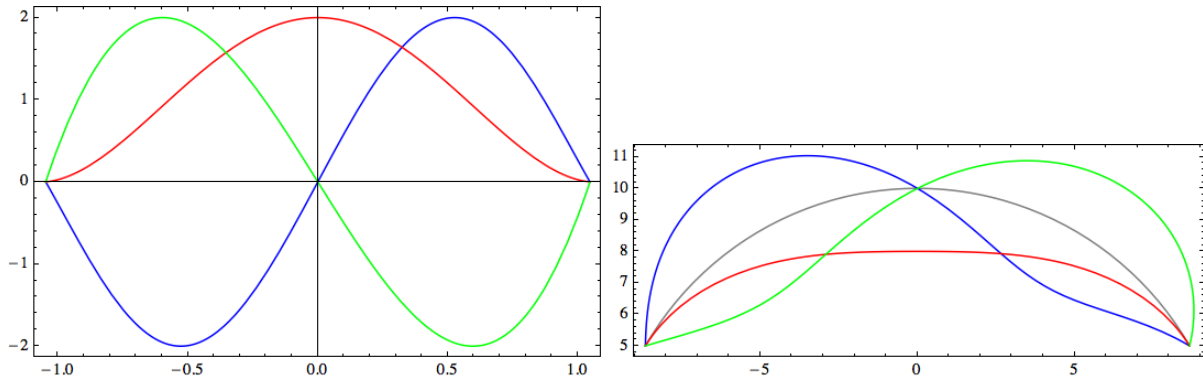


Figure 4.8: Diagrams of w , blue, v , red, and φ , green, example 1.

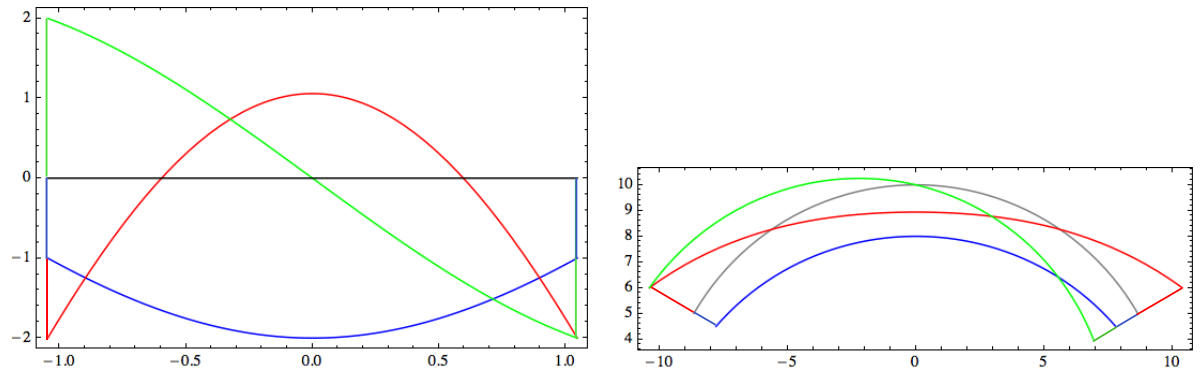


Figure 4.9: Diagrams of N , blue, M , red, and T , green, example 1.

4.7.2 Example 2

A second example is that of a semicircular arch, with constant section, acted upon by a vertical force $F = 5$ kN on the top, see Fig. 4.11. In this case, $\rho = 0.865$ m, $\alpha = 1.5 \times 10^7$ MPa, $\beta = \alpha/2.88$ and $\lambda = \alpha/12 \times 10^4$.

Thanks to the symmetry of the problem, we can study just one half of the structure, acted upon by a force equal to $F/2$ and with a slide as a constraint on the top of the arch. The appropriate boundary conditions are hence: at the left end, $w = \varphi = 0$, $T = -F/2 \Rightarrow \beta(v' + w/\rho - \varphi) = -F/2$, while at the right end it is $w = v = \varphi = 0$. The following diagrams, referring to only half of the arch, show the results for this example.

4.7.3 Example 3

This last example concerns a three-hinge arch, hence an isostatic case. For this reason, we can simply consider the equilibrium equations, either in the form (4.5) or in the form of eqs. (4.36) and (4.38).

The problem is analogous at those of Example 2 and in particular the data are the same, but now the arch has an hinge also at the top, in correspondence of the force F . Again, we can study just one half of the structure, see Fig. 4.15. The boundary conditions now concern exclusively T and M . In fact, no information is given about the value of N at

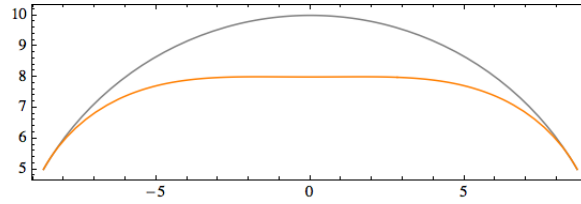


Figure 4.10: Deformed shape of the arch, example 1.

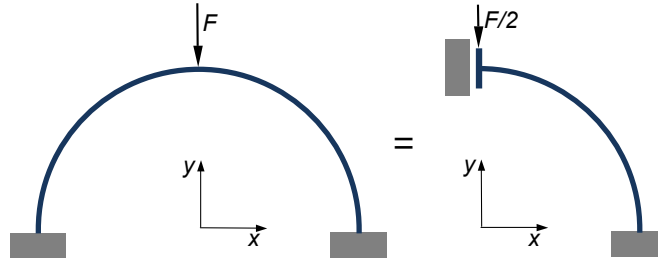


Figure 4.11: Example 2: a circular arch with a concentrated vertical load.

the edges of the arch. In particular, the boundary conditions are: at the left edge, $M = 0$ and $T = -F/2$, while at the right edge $M = 0$. If the system of the two differential equations (4.36) and (4.38) is used, then the condition of the shear force must be written in terms of the derivative of M , eq. (4.5)₃: $T = -F/2 \Rightarrow M' - m = -F/2$. In this case, we have just solved numerically eqs. (4.36) and (4.38), and then obtained T from (4.5)₃. The displacement components w , v and φ have been obtained by the procedure described in Sect. 4.6.1; in particular, the three boundary conditions for integrating the compatibility equations (4.23) are $w = 0$ at the left end and $w = v = 0$ at the right one. The results are presented in Figs. 4.16 to 4.18. To remark that the rotation φ is almost constant.

We remark that in this particular case the balance equations have an analytical solution, that can be easily found using either eqs. (4.5) or eqs. (4.36) and (4.38):

$$\begin{aligned}
 N &= -\frac{F}{2}(\sin \theta + \cos \theta), \\
 T &= \frac{F}{2}(\sin \theta - \cos \theta), \\
 M &= \frac{F}{2}\rho(1 - \sin \theta - \cos \theta).
 \end{aligned}
 \tag{4.49}$$

4.8 Exercises

1. Write the equations of the elastic equilibrium of arches using as variable the angle θ of a polar frame instead of s .
2. Write and solve analytically the balance equations for the circular arch of constant section in Fig. 4.19. Try also to find the functions N , T and M using basic equilibrium considerations.

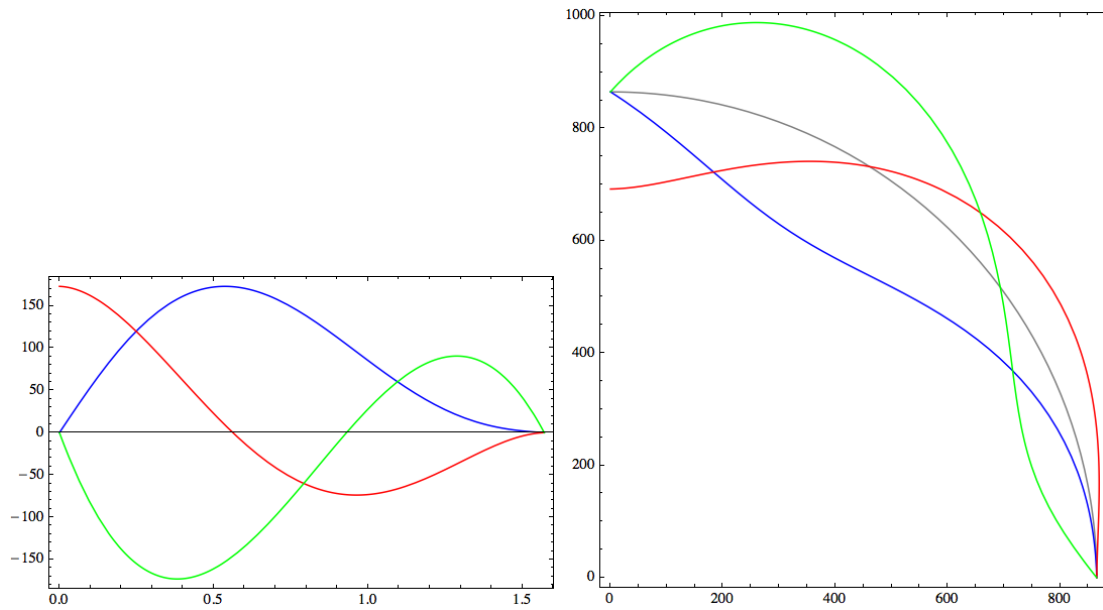


Figure 4.12: Diagrams of w , blue, v , red, and φ , example 2.

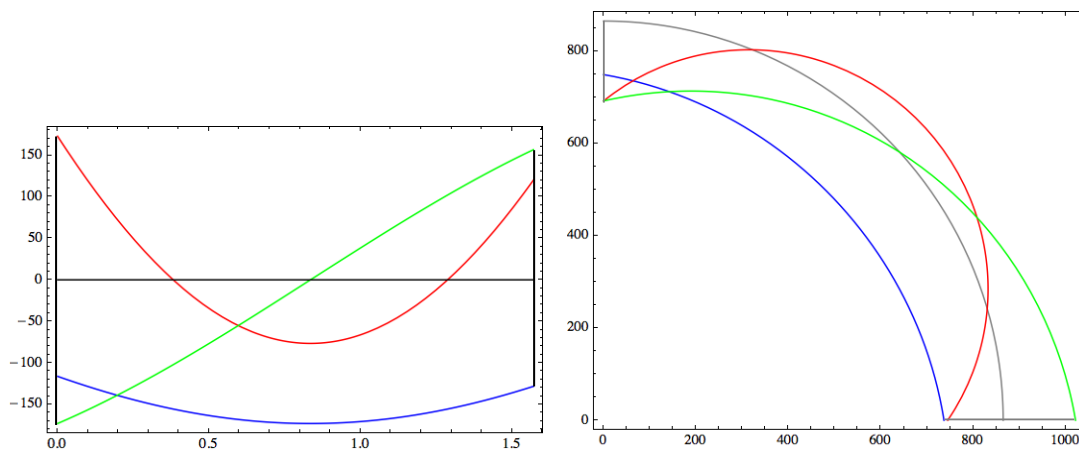


Figure 4.13: Diagrams of N , blue, M , red, and T , green, example 2.

3. For the previous exercise, find the horizontal displacement of the loaded node using the dummy load method (A, J, E, ν and χ are given).
4. Consider again the Example 1, Sect. 4.7.1; in place of the clamped edges, consider a hinge at the left end and a simple horizontal support at the right one. Using the dummy load method find the displacement of the right edge (neglect the effects of N and T).
5. Still for the Example 1 of Sect. 4.7.1, be $A = A_0 \cos \theta$, $J = J_0 \cos \theta$ the variation of the cross section area and moment of inertia, respectively, with the angle θ , the angle of the polar coordinates in a frame centered in the center of the arch. A_0 and J_0 are the values for $\theta = 0$ and they coincide with those specified in the Example 1. Using θ as independent variable, write the equations of the elastic equilibrium for the two cases of the general theory and of the Euler-Bernoulli model.

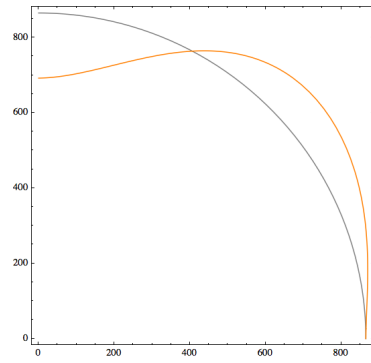


Figure 4.14: Deformed shape of the arch, example 2.

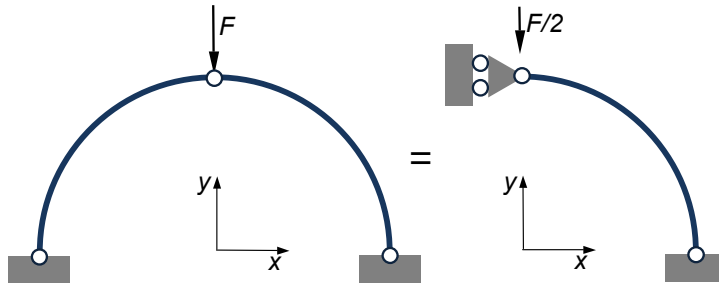


Figure 4.15: Example 3: three-hinged arch.

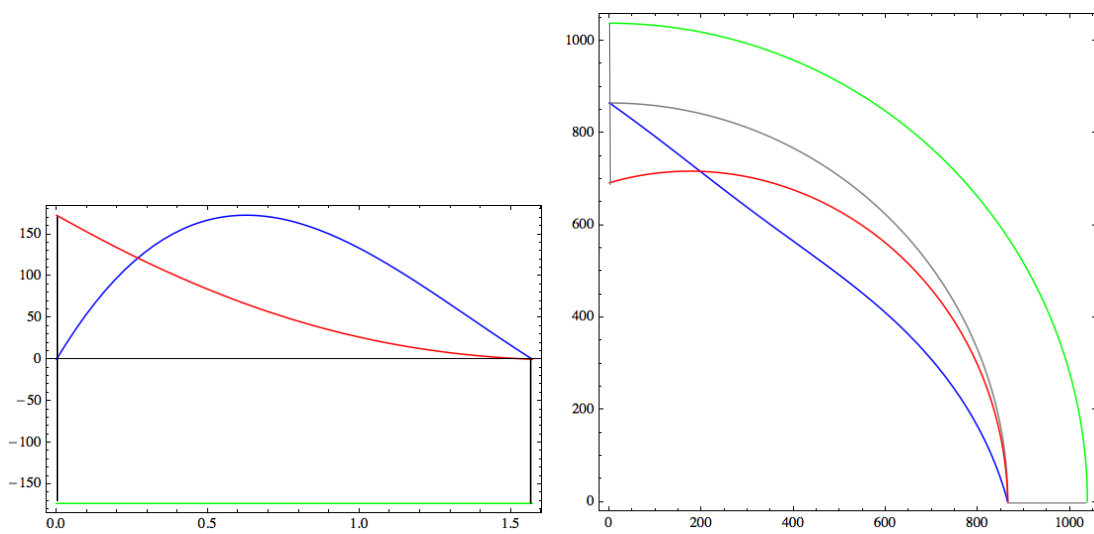


Figure 4.16: Diagrams of w , blue, v , red, and φ , example 3.

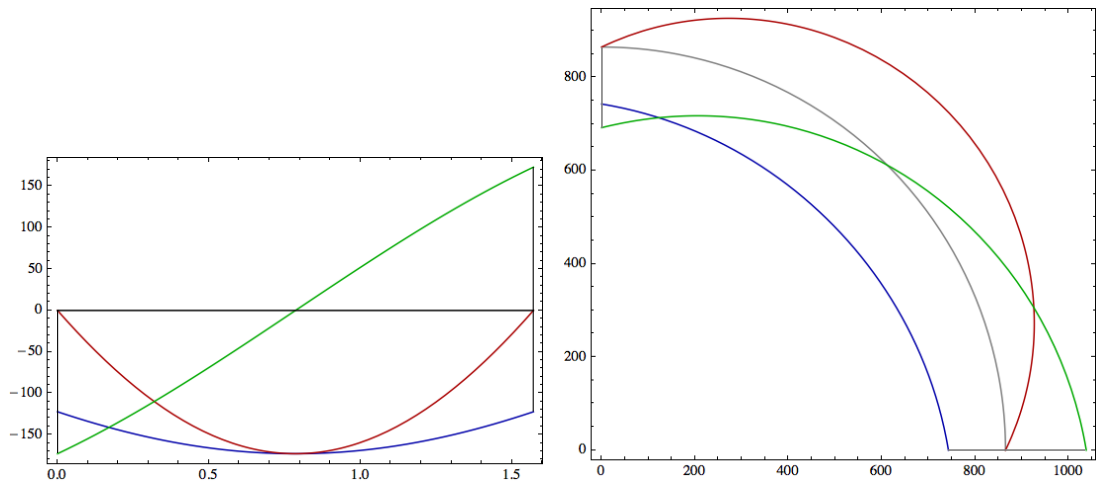


Figure 4.17: Diagrams of N , blue, M , red, and T , green, example 3.

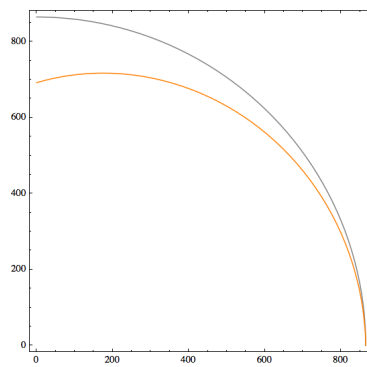


Figure 4.18: Deformed shape of the arch, example 3.

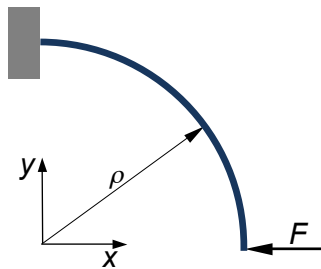


Figure 4.19: Arch of exercise 2.

Chapter 5

Slender rods

5.1 Cosserat rods

We consider a continuum body in the form of a *slender rod*, i.e. a body where one dimension, the length, is much greater than the largest chord of the cross-section, that it is assumed to be constant throughout the rod's length. The rod is not necessarily straight in its undeformed configuration.

We look for a theory particularly adapted to such a continuum body, i.e. taking into account for the geometrical characteristics. In particular, this theory must be able to take into account for the two principal deformation modes: bending and twisting of the rod.

This can be done in the following way: the rod is represented by a line, physically the centerline of the cross-sections, endowed with some directions, i.e. vectors, that may transform independently of the deformation of the line they are attached to.

Such directions attached to the centerline are called *directors* and we call a *Cosserat rod*¹ a material curve that is able to deform independently of the collection of directors assigned to each one of its particles.

The actual configuration of a Cosserat rod is specified by a vector function $\mathbf{r} = p(s, t) - o$, that gives $\forall s \in [s_1, s_2]$, the curvilinear abscissa, the position of a point p of the curve at the instant t with respect to a fixed frame $\mathcal{R} = \{o; \mathbf{e}_1, \mathbf{e}_2, \mathbf{e}_3\}$, and by the set of *directors*

$$\mathbf{d}_k(s, t), \quad k = 1, \dots, n_d. \quad (5.1)$$

We require that, under the change of frame $\mathbf{r} \rightarrow c(t) + \mathbf{Q}(t)\mathbf{r}(s, t)$, with $c(t)$ a translation and $\mathbf{Q}(t)$ a proper rotation $\forall t$, the directors transform as $\mathbf{d}_k \Rightarrow \mathbf{Q}(t)\mathbf{d}_k$, i.e. directors are insensitive to translations. In addition, we require the following *continuity condition*:

$$\mathbf{d}_1 \times \mathbf{d}_2 \cdot p' > 0 \quad \forall s, t. \quad (5.2)$$

¹From the brothers Cosserat, who gave the first general theory for bodies able to transmit also stress couples, 1907.

The physical meaning of this condition will be explained in Sect. 5.1.2; the symbol of prime denotes differentiation with respect to s . The continuity condition imposes the vectors \mathbf{d}_1 , \mathbf{d}_2 and p' to be independent. To remark that $p'(s) = \boldsymbol{\tau}(s) \forall s$.

The most important case is $n_d = 2$; it gives the simplest theory able to account for bending, twisting, extension and also for shear and transverse extensions, i.e. for the deformation of the cross section.

5.1.1 Reference configuration

Conventionally, we take the configuration of the rod at $t = 0$ as the reference configuration and will indicate any quantity attached to it by the superscript 0. So, the reference configuration is determined by

$$\begin{aligned} \mathbf{r}^0 &= p^0(s) - o, \\ \mathbf{d}_k^0(s), \quad k &= 1, \dots, n_d. \end{aligned} \tag{5.3}$$

So, for the case $n_d = 2$, the initial configuration is determined by the three vectors \mathbf{r}^0 , \mathbf{d}_1^0 , \mathbf{d}_2^0 , along with the continuity condition

$$\mathbf{d}_1^0 \times \mathbf{d}_2^0 \cdot p'^0 > 0 \quad \forall s, t. \tag{5.4}$$

Knowing \mathbf{r}^0 , \mathbf{d}_1^0 , \mathbf{d}_2^0 , it is important to dispose of a differential description of the undeformed rod. There is not a unique way to do that, let us see two classical approaches.

5.1.1.1 First approach

We put $\mathbf{d}_1^0 = \boldsymbol{\nu}$, the principal normal (if this is not defined, like for straight rods, it can be fixed arbitrarily, e.g. as coincident with one of the principal axes of inertia of the cross section) and $\mathbf{d}_2^0 = \boldsymbol{\beta}$, the binormal. If we call $p'^0 = \boldsymbol{\tau} := \mathbf{d}_3^0$, then the triad $\{\mathbf{d}_1^0, \mathbf{d}_2^0, \mathbf{d}_3^0\}$ forms a positively oriented frame that coincides with the Frenet-Serret frame (without loss of generality, we take the directors as unit vectors).

Hence, the variation of the the directors along s , in the reference configuration, is given by the Frenet-Serret formulae:

$$\begin{aligned} \mathbf{d}_1'^0 &= \boldsymbol{\nu}' = -c^0 \mathbf{d}_3^0 - \vartheta^0 \mathbf{d}_2^0, \\ \mathbf{d}_2'^0 &= \boldsymbol{\beta}' = \vartheta^0 \mathbf{d}_1^0, \\ \mathbf{d}_3'^0 &= \boldsymbol{\tau}' = c^0 \mathbf{d}_1^0. \end{aligned} \tag{5.5}$$

Of course, such a result is correct only upon the assumption that the directors remain coincident with $\boldsymbol{\nu}$, $\boldsymbol{\beta}$, $\boldsymbol{\tau}$ to the curve as s varies. This is not necessary: we can choose also a set of directors attached to the curve but turning independently of it.

5.1.1.2 Second approach

We use a unique director \mathbf{d}_1^0 orthogonal to the curve:

$$p'^0 \cdot \mathbf{d}_1^0 = 0, \quad (5.6)$$

subtending the angle φ with $\boldsymbol{\nu}$:

$$\mathbf{d}_1^0 = \boldsymbol{\nu} \cos \varphi + \boldsymbol{\beta} \sin \varphi. \quad (5.7)$$

The quantity $\varphi'(s)$ is the twist of \mathbf{d}_1^0 with respect to the axis. Because

$$\mathbf{d}_1^0 \cdot \boldsymbol{\nu} = \cos \varphi, \quad (5.8)$$

it is

$$(\mathbf{d}_1^0 \cdot \boldsymbol{\nu})' = \mathbf{d}_1^{0'} \cdot \boldsymbol{\nu} + \mathbf{d}_1^0 \cdot \boldsymbol{\nu}' = -\varphi' \sin \varphi, \quad (5.9)$$

and using the Frenet-Serret formula for $\boldsymbol{\nu}$ and the expression of \mathbf{d}_1^0 , we get

$$(\mathbf{d}_1^0 \cdot \boldsymbol{\nu})' - \vartheta_0 \sin \varphi = -\varphi' \sin \varphi. \quad (5.10)$$

This equation, for $\varphi \neq 0$, allows for determining the twist of the rod in terms of the torsion and the derivative of \mathbf{d}_1^0 .

5.1.2 Deformed configuration

The deformed configuration is defined by

$$\mathbf{r} = p(s, t) - o, \quad (5.11)$$

together with a relation linking the new directors to the old ones:

$$\mathbf{d}_k = \mathbf{d}_k(\mathbf{d}_k^0; s, t). \quad (5.12)$$

Generally speaking, the \mathbf{d}_k s are no more unit vectors nor mutually orthogonal. However, the following assumptions are usually done:

- \mathbf{d}_1 and \mathbf{d}_2 preserve their initial length and remain orthogonal: $\mathbf{d}_1 \cdot \mathbf{d}_2 = 0$;
- the plane whose normal is

$$\mathbf{d}_3 = \mathbf{d}_1 \times \mathbf{d}_2 \quad (5.13)$$

determines the section of the rod at s . So defined, \mathbf{d}_3 is a unit vector orthogonal to \mathbf{d}_1 and \mathbf{d}_2 ; the set $\{\mathbf{d}_1, \mathbf{d}_2, \mathbf{d}_3\}$ forms hence a positively oriented orthonormal basis;

- \mathbf{d}_3 , unlike \mathbf{d}_3^0 , is not necessarily tangent to the deformed rod: generally speaking

$$\mathbf{d}_3 \times \mathbf{r}' \neq \mathbf{o}; \quad (5.14)$$

- the following *continuity condition* holds:

$$\mathbf{r}' \cdot \mathbf{d}_3 > 0 \quad \forall s; \quad (5.15)$$

this condition is, for rods, the corresponding of the general 3D condition $\det \mathbf{F} > 0$, with \mathbf{F} the *deformation gradient*: it excludes that the section may be so severely sheared so as to contain the tangent to the axis.

To remark, hence, that generally speaking the section not necessarily coincides with the cross section, this last being contained by the plane orthogonal to the tangent p' to the deformed rod.

For the kinematical description of the rod's deformed configuration, we determine the triad $\{\mathbf{d}_1, \mathbf{d}_2, \mathbf{d}_3\}$ with respect to a fixed one, e.g. $\{\mathbf{e}_1, \mathbf{e}_2, \mathbf{e}_3\}$, the triad of \mathcal{R} . Because both these triads are orthonormal and positively oriented, they are related by a proper rotation tensor $\mathbf{Q}(s)$, i.e. $\forall s \exists \mathbf{Q}(s), \mathbf{Q}^{-1} = \mathbf{Q}^\top, \det \mathbf{Q} = 1$

$$\mathbf{d}_k(s) = \mathbf{Q}(s)\mathbf{e}_k, \quad k = 1, 2, 3. \quad (5.16)$$

The tensor $\mathbf{Q}(s)$ depends upon three parameters; a classical choice is that of the *Euler's angles*: the *precession* $\psi \in [0, 2\pi)$, the *nutation* $\theta \in [0, \pi]$ and the *proper rotation* $\varphi \in [0, 2\pi)$, see Fig. 5.1. In such a case, it can be shown that

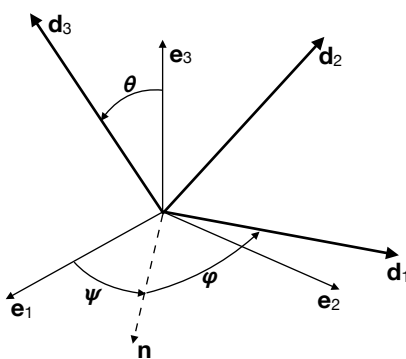


Figure 5.1: Euler's angles.

$$\mathbf{Q} = \begin{bmatrix} \cos \psi \cos \varphi - \sin \psi \sin \varphi \cos \theta & -\cos \psi \sin \varphi - \sin \psi \cos \varphi \cos \theta & \sin \psi \sin \theta \\ \sin \psi \cos \varphi + \cos \psi \sin \varphi \cos \theta & -\sin \psi \sin \varphi + \cos \psi \cos \varphi \cos \theta & -\cos \psi \sin \theta \\ \sin \varphi \sin \theta & \cos \varphi \sin \theta & \cos \theta \end{bmatrix}. \quad (5.17)$$

Let, in the fixed frame,

$$\mathbf{r}(s) = x_k(s)\mathbf{e}_k \rightarrow \mathbf{r}_{,s}(s) = x_{k,s}(s)\mathbf{e}_k = y_k(s)\mathbf{d}_k(s), \quad (5.18)$$

with x_k the components of \mathbf{r} in the fixed frame $\mathcal{R} = \{o; \mathbf{e}_1, \mathbf{e}_2, \mathbf{e}_3\}$ and y_k those of $\mathbf{r}_{,s}$ in the local basis $\{\mathbf{d}_1, \mathbf{d}_2, \mathbf{d}_3\}$. So, we get

$$x_{k,s}(s)\mathbf{e}_k = y_k(s)\mathbf{Q}(s)\mathbf{e}_k = \mathbf{Q}(s)(y_k(s)\mathbf{e}_k), \quad (5.19)$$

which gives

$$\begin{aligned} x_{1,s} &= y_1(\cos \psi \cos \varphi - \sin \psi \sin \varphi \cos \theta) - y_2(\cos \psi \sin \varphi + \sin \psi \cos \varphi \cos \theta) + \\ &\quad y_3 \sin \psi \sin \theta, \\ x_{2,s} &= y_1(\sin \psi \cos \varphi + \cos \psi \sin \varphi \cos \theta) - y_2(\sin \psi \sin \varphi - \cos \psi \cos \varphi \cos \theta) - \\ &\quad y_3 \cos \psi \sin \theta, \\ x_{3,s} &= y_1 \sin \varphi \sin \theta + y_2 \cos \varphi \sin \theta + y_3 \cos \theta. \end{aligned} \quad (5.20)$$

We introduce now the following *local kinematical descriptors* of the rod's deformation:

$$\begin{aligned}\kappa_1 &:= \mathbf{d}_{2,s} \cdot \mathbf{d}_3, \\ \kappa_2 &:= \mathbf{d}_{3,s} \cdot \mathbf{d}_1, \\ \tau &:= \mathbf{d}_{1,s} \cdot \mathbf{d}_2.\end{aligned}\tag{5.21}$$

Geometrically, these quantities represent the local variation of the directors, i.e. of their direction, when passing from a point of the rod to another one infinitely close to it. In particular, see Fig. 5.2,

- κ_1 is a *material curvature* associated with \mathbf{d}_1 ;
- κ_2 is a *material curvature* associated with \mathbf{d}_2 ;
- τ , the *twist*, is a *material curvature* associated with \mathbf{d}_3 .

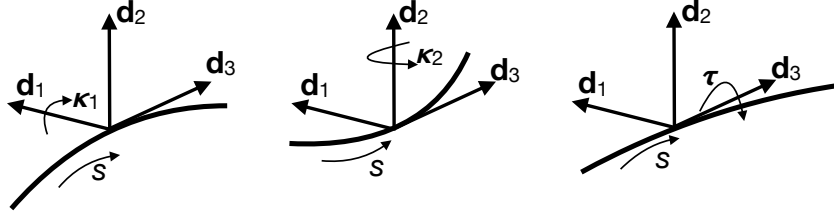


Figure 5.2: Material curvatures.

Using eq. (5.16) and after differentiation, we get

$$\begin{aligned}\kappa_1 &= \theta_{,s} \cos \varphi + \psi_{,s} \sin \theta \sin \varphi, \\ \kappa_2 &= -\theta_{,s} \sin \varphi + \psi_{,s} \sin \theta \cos \varphi, \\ \tau &= \varphi_{,s} + \psi_{,s} \cos \theta.\end{aligned}\tag{5.22}$$

The functions y_k, κ_1, κ_2 and τ constitute the *strains*, i.e. the rod's deformation descriptors in the directors theory. They are almost universally used as measures of strain in a rod, e.g. Clebsch (1862) and Love (1927). Some authors, e.g. Saint Venant, preferred other approaches, namely the second definition of twist given above.

We can also express the variations $\mathbf{d}_{k,s}$ of the directors as functions of the curvatures and of the twist. This can be done if one considers that, being the \mathbf{d}_k s unit orthogonal vectors, it is (no summation on the dummy indexes)

$$\begin{aligned}\mathbf{d}_k \cdot \mathbf{d}_{k,s} &= 0, \\ \mathbf{d}_k \cdot \mathbf{d}_j &= 0 \Rightarrow \\ (\mathbf{d}_k \cdot \mathbf{d}_j)_{,s} &= 0 \rightarrow \mathbf{d}_{k,s} \cdot \mathbf{d}_j = -\mathbf{d}_k \cdot \mathbf{d}_{j,s}.\end{aligned}\tag{5.23}$$

So, because

$$\begin{aligned}\kappa_1 &= \mathbf{d}'_2 \cdot \mathbf{d}_3 = -\mathbf{d}_2 \cdot \mathbf{d}'_3, \\ \kappa_2 &= \mathbf{d}'_3 \cdot \mathbf{d}_1 = -\mathbf{d}_3 \cdot \mathbf{d}'_1, \\ \tau &= \mathbf{d}'_1 \cdot \mathbf{d}_2 = -\mathbf{d}_1 \cdot \mathbf{d}'_2,\end{aligned}\tag{5.24}$$

then we get

$$\begin{aligned}\mathbf{d}'_1 &= \tau \mathbf{d}_2 - \kappa_2 \mathbf{d}_3, \\ \mathbf{d}'_2 &= -\tau \mathbf{d}_1 + \kappa_1 \mathbf{d}_3, \\ \mathbf{d}'_3 &= \kappa_2 \mathbf{d}_1 - \kappa_1 \mathbf{d}_2,\end{aligned}\tag{5.25}$$

or in a succinct form

$$\mathbf{d}'_j = \boldsymbol{\omega} \times \mathbf{d}_j, \quad j = 1, 2, 3,\tag{5.26}$$

with $\boldsymbol{\omega}$ the *Darboux vector*:

$$\boldsymbol{\omega} = \kappa_1 \mathbf{d}_1 + \kappa_2 \mathbf{d}_2 + \tau \mathbf{d}_3.\tag{5.27}$$

The Darboux vector $\boldsymbol{\omega}$ can be interpreted as the rotation velocity of the material local basis $\{\mathbf{d}_1, \mathbf{d}_2, \mathbf{d}_3\}$ when the rod is followed at unit speed. So, κ_1, κ_2 and τ can be seen as the velocity of rotation (or equivalently, the rotation per unit length of s) around $\mathbf{d}_1, \mathbf{d}_2$ and \mathbf{d}_3 respectively. To remark that κ_1 and κ_2 are different from c , and τ from ϑ , as defined in Chapter 1.

5.1.3 Balance equations

We assume the following fundamental stress principle for rods: across any section ideally dividing the rod into two parts, the action of one part onto the other one is equivalent to a resultant force \mathbf{F} and a resultant couple \mathbf{M} . Hence, contrarily to classical elastic 3D bodies, a rod is a continuum able to transmit couples, not only forces. Let $\mathbf{q}(s)$ the vector function of the forces distributed along the rod's axis and $\mathbf{m}(s)$ those representing distributed couples. The balance equations for a portion $[a, b] \subset [s_1, s_2]$ of the rod are:

$$\begin{aligned}\mathbf{F}_b - \mathbf{F}_a + \int_a^b \mathbf{q} \, ds &= \mathbf{o}, \\ \mathbf{M}_b - \mathbf{M}_a + \mathbf{r}_a \times \mathbf{F}_a - \mathbf{r}_b \times \mathbf{F}_b + \int_a^b \mathbf{m} + \mathbf{r} \times \mathbf{q} \, ds &= \mathbf{o}.\end{aligned}\tag{5.28}$$

when $a \rightarrow b$, the above equations take their local form:

$$\begin{aligned}\mathbf{F}' + \mathbf{q} &= \mathbf{o}, \\ \mathbf{M}' + \mathbf{r}' \times \mathbf{F} + \mathbf{m} + \mathbf{r} \times \mathbf{q} &= \mathbf{o}.\end{aligned}\tag{5.29}$$

The boundary conditions to be associated to eqs. (5.29) prescribe the value of $\mathbf{F}, \mathbf{M}, \mathbf{r}$ and/or \mathbf{r}' at s_1 and s_2 , the rod's ends. If

$$\begin{aligned}\mathbf{F} &= F_k \mathbf{d}_k, \\ \mathbf{M} &= M_k \mathbf{d}_k,\end{aligned}\tag{5.30}$$

so that

$$\begin{aligned}\mathbf{F}' &= F'_k \mathbf{d}_k + F_k \mathbf{d}'_k, \\ \mathbf{M}' &= M'_k \mathbf{d}_k + M_k \mathbf{d}'_k,\end{aligned}\tag{5.31}$$

and using eqs. (5.25) we get the following form of the local balance equations:

$$\begin{aligned}
F'_1 + \kappa_2 F_3 - \tau F_2 + q_1 &= 0, \\
F'_2 + \tau F_1 - \kappa_1 F_3 + q_2 &= 0, \\
F'_3 + \kappa_1 F_2 - \kappa_2 F_1 + q_3 &= 0,
\end{aligned}
\tag{5.32}$$

and

$$\begin{aligned}
M'_1 - \tau M_2 + \kappa_2 M_3 + m_1 + y_2 F_3 - y_3 F_2 + x_2 q_3 - x_3 q_2 &= 0, \\
M'_2 + \tau M_1 - \kappa_1 M_3 + m_2 + y_3 F_1 - y_1 F_3 + x_3 q_1 - x_1 q_3 &= 0, \\
M'_3 - \kappa_2 M_1 + \kappa_1 M_2 + m_3 + y_1 F_2 - y_2 F_1 + x_1 q_2 - x_2 q_1 &= 0.
\end{aligned}
\tag{5.33}$$

5.1.4 Constitutive law

We assume an elastic behavior for the rod and we put, generally speaking,

$$\begin{aligned}
\mathbf{F} &= \mathbf{F}(y_k, \kappa_1, \kappa_2, \tau, s), \\
\mathbf{M} &= \mathbf{M}(y_k, \kappa_1, \kappa_2, \tau, s);
\end{aligned}
\tag{5.34}$$

we also assume that such functions are at least of class C^1 with respect to all the variables. Concerning these last, they can get any value, except s that belongs to the interval $[s_1, s_2]$, and the continuity condition (5.15). Once the constitutive law injected into the balance equations, we obtain a system of six nonlinear differential equations in six unknowns. The problem is hence posed correctly, but the equations can be solved analytically only in a few simple cases.

5.2 The Kirchhoff's theory for slender rods

Kirchhoff (1859) has extended a previous result of Euler (1744) in formulating a theory for slender rods undergoing large displacements but small strains. The consequence of the large displacements assumption is that the elastic equilibrium problem is, in general, nonlinear because the balance equations cannot be written in the undeformed, known, configuration, but in the deformed, unknown, one.

The assumptions of the Kirchhoff's theory are:

- i. the axis of the rod is inextensible;
- ii. the stress couple \mathbf{M} depends linearly on the curvatures and on the twist;
- iii. there is no shear between the cross-section and the axis;
- iv. the cross-section is nondeformable in its plane.

We remark that assumptions iii and iv are the classical assumptions of the Euler-Bernoulli theory of rods. As a consequence, regardless of the deformation,

$$\mathbf{d}_3 \times \mathbf{r}' = \mathbf{o},
\tag{5.35}$$

i.e. \mathbf{d}_3 remains tangent to the deformed rod's axis. Hence,

$$\mathbf{r}' = y_j \mathbf{d}_j = y_3 \mathbf{d}_3 \Rightarrow y_1 = y_2 = 0 \quad \forall s. \quad (5.36)$$

and

$$y_3 = |\mathbf{r}'| \quad \forall s. \quad (5.37)$$

The assumption of inextensibility gives

$$|\mathbf{r}'| = 1 \Rightarrow y_3 = 1 \rightarrow \mathbf{r}' = \mathbf{d}_3 \quad \forall s. \quad (5.38)$$

The assumption on the constitutive law implies not only that the components of \mathbf{M} are linear functions of the dual curvature/twist, but also that they are uncoupled:

$$M_1 = A \kappa_1, \quad M_2 = B \kappa_2, \quad M_3 = C \tau, \quad (5.39)$$

with A, B, C constants depending upon the elastic properties of the material and on the geometry of the cross-section. The assumption of non-deformability of the cross-section implies that the directors \mathbf{D}_1 and \mathbf{D}_2 of the undeformed shape remain orthogonal and of unit length.

Several interesting solutions have been given for Kirchhoff's rods in the case of initially straight rods; in this case

$$y_1 = y_2 = 0, \quad y_3 = 1, \quad \kappa_1^0 = \kappa_2^0 = \tau^0 = 0. \quad (5.40)$$

The most famous application is that of the *elastica of Euler*.

5.3 The Euler's elastica

The problem of the so-called *elastica* (Euler, 1744) is that of determining the forms in which an initially straight rod can be held by forces and couples applied to its ends only, when the rod is bent in a principal inertia plane, so that the deformed axis is a plane curve and there is no twist. Hence:

- $\mathbf{m} = \mathbf{q} = \mathbf{o}$, for the assumption on the loads;
- $\kappa_1 = \tau = 0$, for the assumption on the deformation;
- $y_1 = y_2 = 0$, for the assumption on the undeformability of the cross-section;
- $y_3 = 1$, for the assumption of inextensibility;
- $M_1 = M_3 = 0$, for the assumption on the deformation.

Hence eqs. (5.32) and (5.33) become

$$\begin{aligned} F'_1 + \kappa_2 F_3 &= 0, & F'_2 &= 0, & F'_3 - \kappa_2 F_1 &= 0, \\ F_2 &= 0, & M'_2 + F_1 &= 0, \end{aligned} \quad (5.41)$$

while the last of (5.33) is now an identity.

We consider, for the load, a unique force

$$\mathbf{R} = R \mathbf{e}_1 \quad (5.42)$$

applied at $s = s_2$. This gives, see Fig. 5.3,

$$F_1(s) = R \sin \theta(s), \quad F_3(s) = R \cos \theta(s). \quad (5.43)$$

Injecting these relations into eqs. (5.41)_{1,3} gives the same result:

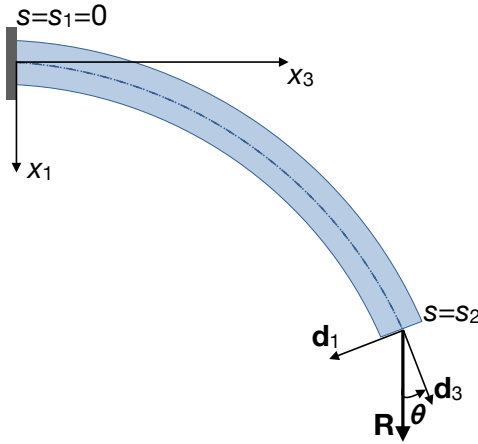


Figure 5.3: Scheme of the Euler's elastica.

$$\theta' R \cos \theta + k_2 R \cos \theta = 0 \rightarrow k_2 = -\theta', \quad (5.44)$$

while eqs. (5.41)₅ and (5.39) give

$$B k_2' + R \sin \theta = 0 \rightarrow k_2' = -\frac{R}{B} \sin \theta, \quad (5.45)$$

and finally we obtain the second order differential equation

$$\theta'' = \frac{R}{B} \sin \theta. \quad (5.46)$$

The resolution of this equation is not easy; to this purpose, we first integrate once to get

$$\frac{1}{2}(\theta')^2 - \frac{R}{B}(\cos \theta_0 - \cos \theta) = 0, \quad (5.47)$$

with θ_0 the value of θ at $s = s_2$. We can rewrite the above equation as

$$\frac{d\theta}{ds} = \pm \sqrt{\frac{2R}{B}(\cos \theta_0 - \cos \theta)}; \quad (5.48)$$

for the case in Fig. 5.3 the sign minus is to be taken; we then get

$$\frac{d\theta}{\sqrt{\cos \theta_0 - \cos \theta}} = -\sqrt{\frac{2R}{B}} ds, \quad (5.49)$$

and finally

$$\int_0^{\theta_0} \frac{d\theta}{\sqrt{\cos \theta_0 - \cos \theta}} = -\sqrt{\frac{2R}{B}} \int_0^L ds = -L\sqrt{\frac{2R}{B}}. \quad (5.50)$$

The integral above is an elliptic integral that can be rewritten as

$$\int_0^{\frac{\pi}{2}} \frac{d\phi}{\sqrt{1 - k^2 \sin^2 \phi}} = L\sqrt{\frac{R}{B}}, \quad k = \sin \frac{\theta_0}{2}, \quad k \sin \phi = \sin \frac{\theta}{2}. \quad (5.51)$$

This equation can be rewritten as

$$L = \sqrt{\frac{B}{R}} \mathcal{E}(k), \quad (5.52)$$

with

$$\mathcal{E}(k) = \int_0^{\frac{\pi}{2}} \frac{d\phi}{\sqrt{1 - k^2 \sin^2 \phi}} \quad (5.53)$$

a complete elliptic normal integral of modulus k ; this modulus is fixed once θ_0 fixed. Hence, $\forall \theta_0$ we can obtain the value of R necessary to get θ_0 :

$$R = \frac{B}{L} \mathcal{E}^2(k). \quad (5.54)$$

For any point of the rod it is

$$\frac{dx_1}{ds} = \cos \theta, \quad \frac{dx_3}{ds} = \sin \theta; \quad (5.55)$$

hence, with the boundary conditions $x_1 = x_3 = 0$ for $s = 0$, we get

$$x_1 = \int \cos \theta(s) ds, \quad x_3 = \int \sin \theta(s) ds, \quad (5.56)$$

which in the end gives, after integration, the parametric equation of the elastic in parametric form, $(x_1(s), x_3(s))$.

We consider now the case of a compressive force $\mathbf{R} = -R \mathbf{e}_3$, $R > 0$. we repeat *verbatim* the procedure, but now we change the definition of the angle θ , indicated in Fig. 5.4, so that

$$F_1 = R \sin \theta, \quad F_3 = -R \cos \theta, \quad (5.57)$$

which gives $k_2 = \theta'$ and

$$B \theta'' + R \sin \theta = 0. \quad (5.58)$$

The solution does not change, as it can be checked easily, but now it is

$$\frac{dx_1}{ds} = \sin \theta, \quad \frac{dx_3}{ds} = \cos \theta, \quad (5.59)$$

so

$$x_1 = \int \sin \theta(s) ds, \quad x_3 = \int \cos \theta(s) ds. \quad (5.60)$$

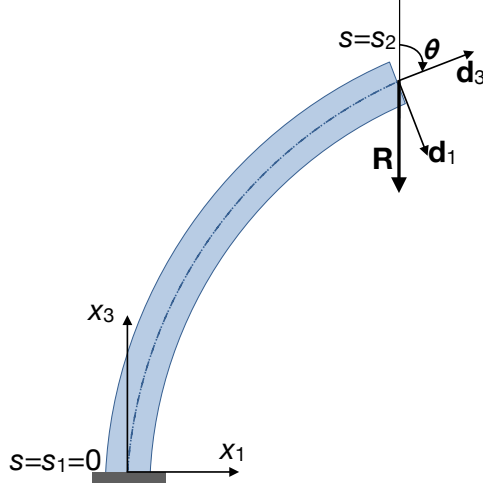


Figure 5.4: Buckling of a rod.

We can study the stability of the rod: when the straight configuration becomes unstable because R increases, a bent state can exist close to the straight one, i.e. $\sin \theta \simeq \theta$. We can hence linearize the equilibrium equation:

$$B \theta'' + R \theta = 0, \quad (5.61)$$

whose solution is

$$\theta = c_1 \cos \left(\sqrt{\frac{R}{B}} s \right) + c_2 \sin \left(\sqrt{\frac{R}{B}} s \right). \quad (5.62)$$

The constants c_1 and c_2 can be determined through the boundary conditions

$$\theta(0) = 0, \quad \theta'(L) = 0; \quad (5.63)$$

with such boundary conditions, the only solution is the trivial one, $\theta(s) = 0 \quad \forall s$ (fundamental configuration), unless

$$R = R_b = \frac{\pi^2 B}{4L^2}; \quad (5.64)$$

this is the *Euler buckling load*: when $R \geq R_b$, the rod can buckle. To determine the deflection of point $s = s_2 = L$ in the buckled state, we go back to the first integral of the equilibrium equations, that in this case is

$$\frac{1}{2} \left(\frac{d\theta}{ds} \right)^2 + \frac{R}{B} (\cos \theta_0 - \cos \theta) = 0. \quad (5.65)$$

Because now $dx_1 = ds \sin \theta$, we get

$$x_1(L) = 2k \sqrt{\frac{B}{R}} \int_0^{\frac{\pi}{2}} \sin \phi d\phi = 2k \sqrt{\frac{B}{R}} = 2k \sin \frac{\theta_0}{2} \sqrt{\frac{B}{R}}. \quad (5.66)$$

It is possible to remove the assumption of axial inextensibility; in this case, the length of the rod just before buckling becomes $L \left(1 - \frac{R}{EA}\right)$ and the buckling load changes to

$$R_b = \frac{\pi^2 B}{4L^2 \left(1 - \frac{R}{EA}\right)^2}; \quad (5.67)$$

practically, this correction has no importance.

5.4 The 3D case

Let us now consider a more general case, where the rod is acted upon by a force \mathbf{R} and couple \mathbf{M} at one end, balanced by another force and couple at the other end. No distributed loads nor couples are present. So, eqs. (5.32) and (5.33) become

$$\begin{aligned} F'_1 + \kappa_2 F_3 - \tau F_2 &= 0, \\ F'_2 + \tau F_1 - \kappa_1 F_3 &= 0, \\ F'_3 + \kappa_1 F_2 - \kappa_2 F_1 &= 0, \end{aligned} \tag{5.68}$$

and

$$\begin{aligned} M'_1 - \tau M_2 + \kappa_2 M_3 + y_2 F_3 - y_3 F_2 &= 0, \\ M'_2 + \tau M_1 - \kappa_1 M_3 + y_3 F_1 - y_1 F_3 &= 0, \\ M'_3 - \kappa_2 M_1 + \kappa_1 M_2 + y_1 F_2 - y_2 F_1 &= 0. \end{aligned} \tag{5.69}$$

Using the Kirchhoff's theory, i.e. putting $y_1 = y_2 = 0$, $y_3 = 1$, we get

$$\begin{aligned} M'_1 - \tau M_2 + \kappa_2 M_3 &= F_2, \\ M'_2 + \tau M_1 - \kappa_1 M_3 &= -F_1, \\ M'_3 - \kappa_2 M_1 + \kappa_1 M_2 &= 0, \end{aligned} \tag{5.70}$$

and introducing the constitutive laws (5.39) we obtain

$$\begin{aligned} A \kappa'_1 - (B - C) \kappa_2 \tau &= F_2, \\ B \kappa'_2 - (C - A) \kappa_1 \tau &= -F_1, \\ C \tau' - (A - B) \kappa_1 \kappa_2 &= 0. \end{aligned} \tag{5.71}$$

These equations are formally identical to the Euler's rigid body motion equations:

$$\begin{aligned} A \dot{p} - (B - C) q r &= M_1, \\ B \dot{q} - (C - A) r p &= M_2, \\ C \dot{r} - (A - B) p q &= M_3, \end{aligned} \tag{5.72}$$

where $\boldsymbol{\omega} = (p, q, r)$ is the angular velocity and A, B, C are the principal moments of inertia. There is hence a mechanical analogy between the problem of the elastic rod and that of a spinning top.

From eq. (5.71) we can obtain a first integral of the rod problem: injecting the expression of F_1 and F_2 given by eqs. (5.71)_{1,2} into eq. (5.68)₃ we get

$$F'_3 + A \kappa_1 \kappa'_2 + B \kappa_2 \kappa'_1 + (A - B) \kappa_1 \kappa_2 \tau = 0, \tag{5.73}$$

and from eq. (5.71)₃ we have

$$(A - B) \kappa_1 \kappa_2 \tau = C \tau \tau', \tag{5.74}$$

that injected into eq. (5.73) gives

$$\begin{aligned} \frac{d}{ds} \left[F_3 + \frac{1}{2} (A \kappa_1^2 + B \kappa_2^2 + C \tau^2) \right] &= 0 \rightarrow \\ F_3 + \frac{1}{2} (A \kappa_1^2 + B \kappa_2^2 + C \tau^2) &= \text{const.} \end{aligned} \quad (5.75)$$

Injecting relations (5.22) into the previous equation gives an equation for the Euler's angles:

$$\begin{aligned} F_3 + \frac{1}{2} [A (\theta_{,s} \cos \varphi + \psi_{,s} \sin \theta \sin \varphi)^2 + \\ B (-\theta_{,s} \sin \varphi + \psi_{,s} \sin \theta \cos \varphi)^2 + \\ C (\varphi_{,s} + \psi_{,s} \cos \theta)^2] &= \text{const.} \end{aligned} \quad (5.76)$$

Another first integral can be obtained observing that $\forall s$ the projection of $\mathbf{M}(s)$ onto the fixed vector \mathbf{e}_3 is a constant; introducing the Euler's angles,

$$\begin{aligned} \mathbf{d}_1 \cdot \mathbf{e}_3 &= \sin \varphi \sin \theta, \\ \mathbf{d}_2 \cdot \mathbf{e}_3 &= \cos \varphi \sin \theta, \\ \mathbf{d}_3 \cdot \mathbf{e}_3 &= \cos \theta, \end{aligned} \quad (5.77)$$

we get

$$\mathbf{M} \cdot \mathbf{e}_3 = A \kappa_1 \sin \varphi \sin \theta + B \kappa_2 \cos \varphi \sin \theta + C \tau \cos \theta = \text{const.} \quad (5.78)$$

It should be worth to obtain a third first integral, for having then three relations for φ, θ and ψ . Generally speaking, this third relation is not known. So, let us assume that $A = B$; this is the case, e.g., of circular or square cross-sections. Then, from eq. (5.71)₃ we get immediately

$$C \tau' = 0 \Rightarrow \tau = \text{const.} \quad (5.79)$$

The twist of the rod is necessarily constant; the system (5.71) can now be integrated in closed form:

$$\begin{aligned} \kappa_1' &= \alpha \kappa_2 + \varphi_2, \\ \kappa_2' &= \beta \kappa_1 - \varphi_1, \end{aligned} \quad (5.80)$$

with

$$\alpha = \frac{B - C}{A} \tau = \text{const.}, \quad \beta = \frac{C - A}{B} \tau = \text{const.}, \quad \varphi_1 = \frac{F_1}{B}, \quad \varphi_2 = \frac{F_2}{A}. \quad (5.81)$$

If $F_1 = F_2 = 0$, i.e. for the case of a rod acted upon only by couples, we get the system of two differential equations

$$\begin{aligned} \kappa_1' &= \alpha \kappa_2, \\ \kappa_2' &= \beta \kappa_1, \end{aligned} \quad (5.82)$$

with, because $A = B$,

$$\alpha = -\beta = \left(1 - \frac{C}{A} \right) \tau. \quad (5.83)$$

The integral of the above system is

$$\begin{aligned}\kappa_1 &= c_1 \cos(\tau s) - c_2 \sin(\tau s), \\ \kappa_2 &= c_2 \cos(\tau s) + c_1 \sin(\tau s);\end{aligned}\tag{5.84}$$

c_1 and c_2 can be determined using the boundary conditions

$$\kappa_1(s=0) = \frac{M_1(s=0)}{A}, \quad \kappa_2(s=0) = \frac{M_2(s=0)}{B}.\tag{5.85}$$

An interesting interpretation of these results can be given in the framework of the linear stability theory of dynamical systems². In this framework, the equilibrated configuration is given by $\kappa_1 = \kappa_2 = 0$ and the Jacobian matrix is

$$J = \begin{bmatrix} 0 & (1 - \frac{C}{A}) \tau \\ - (1 - \frac{C}{A}) \tau & 0 \end{bmatrix}\tag{5.86}$$

with two complex conjugate eigenvalues:

$$\lambda_{1,2} = \pm i \left| \tau \left(1 - \frac{C}{A} \right) \right|.\tag{5.87}$$

Hence, this configuration is an *attractor* and in particular it is a *center*: the attractor is stable. Mechanically speaking, this can be interpreted in the following way: starting from an initial perturbed condition $(\kappa_1^0, \kappa_2^0) \neq (0, 0)$, the two curvatures along s , the independent variable for this problem, change so as to follow a circle in the *phase space* (κ_1, κ_2) with center $(0, 0)$ and radius $\sqrt{(\kappa_1^0)^2 + (\kappa_2^0)^2}$. In particular, it is possible that for certain values of s , the two curvatures take again the value (κ_1^0, κ_2^0) , but generally speaking they change continuously with s and both of them can change of sign. This is in accordance with the analytical solution given above. To remark that, because

$$C \simeq \frac{A}{1 + \nu},\tag{5.88}$$

it is impossible, if some couple is applied at the rod's ends, i.e. for not null initial conditions, that the rod preserves the configuration of a straight line.

Another solution of eqs. (5.75) and (5.82) is that of a rod bent in a circular helix. In fact, let the rod be acted upon by a longitudinal force R_3 and a twisting couple M_3 ; because, by the same definition of helix, the inclination of a helix is constant, i.e. $\frac{d\theta}{ds} = 0$, then eq. (5.71) gives

$$\begin{aligned}\kappa_1 &= \psi' \sin \varphi \cos \alpha, \\ \kappa_2 &= \psi' \cos \varphi \cos \alpha, \\ \tau &= \varphi' + \psi' \sin \alpha.\end{aligned}\tag{5.89}$$

Because $\tau = \text{const.}$ and $A = B$, from eq. (5.75) we get

$$\kappa_1^2 + \kappa_2^2 = \psi'^2 \cos^2 \alpha = \text{const.},\tag{5.90}$$

so, being $\alpha = \text{const.}$, $\psi' = \text{const.}$ and as a consequence of eq. (5.89), also $\varphi' = \text{const.}$ Finally, the curve has a constant curvature and torsion: it is then a helix traced on a circular cylinder.

²The reader is addressed to the book of Strogatz given in the suggested literature for an insight in the linear stability theory of dynamical systems. It is nice to notice that eq. (5.82) is a particular case of the so-called Romeo and Juliet model, proposed by Strogatz to model the dynamics of a love affair. Rather unexpectedly, there is some analogy between the equilibrium of slender rods and falling in love!

5.5 The Michell-Prandtl bifurcation

Some peculiar bifurcation phenomena concern slender rods. The *Michell-Prandtl* or *Prandtl-Timoshenko* bifurcation happens when a rod of length ℓ , initially straight when unstrained, is subjected to only bending couples at its ends.

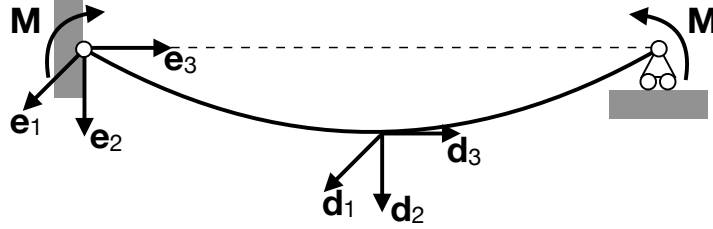


Figure 5.5: Rod acted upon by couples at its ends.

To fix the ideas, we consider the case in Fig. 5.5, where the couple at the ends is $\mathbf{M} = M\mathbf{e}_1$. No other loads are applied to the rod, so that eqs. (5.71) are now

$$\begin{aligned} A \kappa_1' - (B - C)\kappa_2 \tau &= 0, \\ B \kappa_2' - (C - A)\kappa_1 \tau &= 0, \\ C \tau' - (A - B)\kappa_1 \kappa_2 &= 0. \end{aligned} \quad (5.91)$$

These equations are formally identical to those of a *Poinsot's motion*, e.g. the equations ruling the motion of a gyroscope. We take care of choosing \mathbf{d}_1 and \mathbf{d}_2 corresponding with two principal axes of inertia of the cross-section, and initially parallel to the corresponding \mathbf{e}_i , see Fig. 5.5. The linear, fundamental solution of the above equations is, of course,

$$\kappa_1 = \frac{M}{A}, \quad \kappa_2 = 0, \quad \tau = 0, \quad (5.92)$$

i.e., the rod bends in the plane orthogonal to \mathbf{M} .

To investigate the existence of a bifurcated solution, we use the *Euler's method of adjacent equilibria*, i.e. we look for an equilibrated configuration close to the fundamental one. To this end, we write the equilibrium equation near the fundamental configuration, retaining only linear terms. In other words, we linearize the equilibrium equations in the variated configuration. For doing that, we write all the equations as, e.g.,

$$\kappa_1 = \kappa_1^0 + \bar{\kappa}_1, \quad (5.93)$$

where κ_1^0 is the value of κ_1 in correspondence of the fundamental solution, while $\bar{\kappa}_1$ is the variation with respect to such a solution and κ_1 is the value in correspondence of the variated solution. We write hence the equilibrium equations for the variations of the different quantities with respect to the fundamental solution. In particular,

$$\begin{aligned} \kappa_1 &= \kappa_1^0 + \bar{\kappa}_1 = \frac{M}{A} + \kappa_1 \rightarrow \kappa_1' = \bar{\kappa}_1', \\ \kappa_2 &= \kappa_2^0 + \bar{\kappa}_2 = \bar{\kappa}_2 \rightarrow \kappa_2' = \bar{\kappa}_2', \\ \tau &= \tau_0 + \bar{\tau} = \bar{\tau} \rightarrow \tau' = \bar{\tau}'. \end{aligned} \quad (5.94)$$

So, eqs. (5.91) become

$$\begin{aligned}
A \bar{\kappa}'_1 - (B - C) \bar{\kappa}_2 \bar{\tau} &= 0, \\
B \bar{\kappa}'_2 - (C - A) \left(\frac{M}{A} + \bar{\kappa}_1 \right) \bar{\tau} &= 0, \\
C \bar{\tau}' - (A - B) \left(\frac{M}{A} + \bar{\kappa}_1 \right) \bar{\kappa}_2 &= 0,
\end{aligned} \tag{5.95}$$

and after linearization we obtain

$$\begin{aligned}
A \bar{\kappa}'_1 &= 0, \\
B \bar{\kappa}'_2 - (C - A) \frac{M}{A} \bar{\tau} &= 0, \\
C \bar{\tau}' - (A - B) \frac{M}{A} \bar{\kappa}_2 &= 0,
\end{aligned} \tag{5.96}$$

or

$$\begin{aligned}
\bar{\kappa}'_1 &= 0, \\
\bar{\kappa}'_2 &= \mu_1 \bar{\tau}, \\
\bar{\tau}' &= \mu_2 \bar{\kappa}_2,
\end{aligned} \tag{5.97}$$

with

$$\mu_1 = -\frac{A - C}{AB} M, \quad \mu_2 = \frac{A - B}{AC} M. \tag{5.98}$$

We need now to write the boundary conditions, $\mathbf{M} = M \mathbf{e}_1$ at $s = 0, \ell$, in the frame of the directors, $\{\mathbf{d}_1, \mathbf{d}_2, \mathbf{d}_3\}$. Because we are dealing with small variations with respect to the fundamental solution, the rotation transforming the basis $\{\mathbf{e}_1, \mathbf{e}_2, \mathbf{e}_3\}$ into $\{\mathbf{d}_1, \mathbf{d}_2, \mathbf{d}_3\}$ is a small rotation, say γ . As a consequence, the rotation tensor $\mathbf{Q}(\gamma)$ of this transformation, that generally speaking can be represented in the form

$$\mathbf{Q}(\gamma) = \mathbf{I} + \sin \gamma \mathbf{W} + (1 - \cos \gamma) \mathbf{W}^2, \tag{5.99}$$

can be linearized: for small γ , $\sin \gamma \simeq \gamma$, $\cos \gamma \simeq 1$, so that

$$\mathbf{Q}(\gamma) \simeq \mathbf{I} + \gamma \mathbf{W}, \tag{5.100}$$

and finally

$$\mathbf{d}_i = \mathbf{Q}(\gamma) \mathbf{e}_i \simeq (\mathbf{I} + \gamma \mathbf{W}) \mathbf{e}_i, \quad i = 1, 2, 3. \tag{5.101}$$

In the above equations, \mathbf{W} is the axial tensor of the rotation axis, $\mathbf{W} = -\mathbf{W}^\top$. To invert this relation, we write

$$\begin{aligned}
(\mathbf{I} + \gamma \mathbf{W})^\top \mathbf{d}_i &= (\mathbf{I} + \gamma \mathbf{W})^\top (\mathbf{I} + \gamma \mathbf{W}) \mathbf{e}_i \rightarrow \\
(\mathbf{I} - \gamma \mathbf{W}) \mathbf{d}_i &= (\mathbf{I} - \gamma \mathbf{W} + \gamma \mathbf{W} - \gamma^2 \mathbf{W}^2) \mathbf{e}_i,
\end{aligned} \tag{5.102}$$

so finally, neglecting higher order terms,

$$\mathbf{e}_i = \mathbf{d}_i - \gamma \mathbf{W} \mathbf{d}_i = \mathbf{d}_i - \gamma \times \mathbf{d}_i, \tag{5.103}$$

with $\boldsymbol{\gamma} = (\gamma_1, \gamma_2, \gamma_3)$ the axial vector corresponding to tensor $\boldsymbol{\gamma} \mathbf{W}$, representing the infinitesimal rotation of the cross-section. It is then natural to identify the changes in the rotation, per unit s , with curvatures:

$$\kappa_1 = \gamma_1', \quad \kappa_2 = \gamma_2', \quad \tau = \gamma_3'. \quad (5.104)$$

Hence, the boundary conditions become

$$\mathbf{M} = M \mathbf{e}_1 = M(\mathbf{I} - \boldsymbol{\gamma} \mathbf{W})\mathbf{d}_1 = M(\mathbf{d}_1 - \boldsymbol{\gamma} \times \mathbf{d}_1) \quad \text{at } s = 0, \ell. \quad (5.105)$$

Along the three directors we have then

$$\begin{aligned} M_1 &= \mathbf{M} \cdot \mathbf{d}_1 = M, \\ M_2 &= \mathbf{M} \cdot \mathbf{d}_2 = M(\mathbf{d}_1 - \boldsymbol{\gamma} \times \mathbf{d}_1) \cdot \mathbf{d}_2 = -M \gamma_3, \\ M_3 &= \mathbf{M} \cdot \mathbf{d}_3 = M(\mathbf{d}_1 - \boldsymbol{\gamma} \times \mathbf{d}_1) \cdot \mathbf{d}_3 = M \gamma_2, \end{aligned} \quad (5.106)$$

and hence, putting

$$\gamma_i = \gamma_i^0 + \bar{\gamma}_i, \quad M_i = M_i^0 + \bar{M}_i, \quad i = 1, 2, 3, \quad (5.107)$$

we have, because $M_1^0 = M, M_2^0 = M_3^0 = 0$ and $\gamma_2^0 = \gamma_3^0 = 0$,

$$\begin{aligned} M_1^0 + \bar{M}_1 &= M && \rightarrow \bar{M}_1 = 0, \\ M_2^0 + \bar{M}_2 &= -M \gamma_3 && \rightarrow \bar{M}_2 = -M \bar{\gamma}_3, \\ M_3^0 + \bar{M}_3 &= M \gamma_2 && \rightarrow \bar{M}_3 = M \bar{\gamma}_2. \end{aligned} \quad (5.108)$$

Then, because

$$M_1 = A \kappa_1 \rightarrow M_1^0 + \bar{M}_1 = A \kappa_1^0 + A \bar{\kappa}_1 \rightarrow \bar{M}_1 = A \bar{\kappa}_1, \quad (5.109)$$

and similarly for M_2 and M_3 , we have, for $s = 0, \ell$,

$$\begin{aligned} \bar{M}_1 &= A \bar{\kappa}_1 = 0 && \rightarrow \bar{\kappa}_1 = 0, \\ \bar{M}_2 &= B \bar{\kappa}_2 = -M \bar{\gamma}_3 && \rightarrow \bar{\kappa}_2 = -\frac{M}{B} \bar{\gamma}_3, \\ \bar{M}_3 &= C \bar{\tau} && \rightarrow \bar{\tau} = \frac{M}{C} \bar{\gamma}_2. \end{aligned} \quad (5.110)$$

Hence, from eqs. (5.97)₁ and (5.110)₁ we get that the solution for direction \mathbf{d}_1 is

$$\bar{\kappa}_1 = 0 \Rightarrow \kappa_1 = \frac{M}{A} \quad \forall s, \quad (5.111)$$

and, as a consequence,

$$\gamma_1' = \kappa_1 \Rightarrow \gamma_1 = \int \kappa_1 ds = \frac{M}{A} s + \gamma_1(s=0). \quad (5.112)$$

The two remaining equations (5.113)_{2,3} are coupled:

$$\begin{aligned} \bar{\kappa}_2' &= \mu_1 \bar{\tau}, \\ \bar{\tau}' &= \mu_2 \bar{\kappa}_2, \end{aligned} \quad (5.113)$$

Once more, this system of two differential equations is similar to system (5.82) and it can be interpreted in the same way. In particular, if $\mu_1\mu_2 > 0$, the solution $\bar{\kappa}_2 = \bar{\tau} = 0$, i.e. the fundamental solution, is a *saddle point*, i.e. it is unstable: the curvatures $\bar{\kappa}_2$ and $\bar{\tau}$ can change of sign along s . If $\mu_1\mu_2 < 0$, then the fundamental solution is a *center* and $\bar{\kappa}_2$ and $\bar{\tau}$ can change cyclically along s .

We can easily solve eqs. (5.113) differentiating the first one:

$$\bar{\kappa}_2'' = \mu_1 \bar{\tau}' \rightarrow \bar{\kappa}_2'' + \lambda^2 \bar{\kappa}_2 = 0, \quad \text{with } \lambda^2 = -\mu_1\mu_2. \quad (5.114)$$

The solution is

$$\kappa_2 = \bar{\kappa}_2 = c_1 \sin(\lambda s) + c_2 \cos(\lambda s), \quad (5.115)$$

which gives

$$\tau = \bar{\tau} = \frac{\bar{\kappa}_2'}{\mu_1} = \frac{\lambda}{\mu_1} [c_1 \cos(\lambda s) - c_2 \sin(\lambda s)]. \quad (5.116)$$

The two other rotations can be found as well:

$$\begin{aligned} \gamma_2 = \bar{\gamma}_2 = \bar{\kappa}_2' &\rightarrow \gamma_2 = \int \bar{\kappa}_2 ds = \frac{1}{\lambda} [-c_1 \cos(\lambda s) + c_2 \sin(\lambda s) + c_3], \\ \gamma_3 = \bar{\gamma}_3 = \bar{\tau}' &\rightarrow \gamma_3 = \int \bar{\tau} ds = \frac{1}{\mu_1} [c_1 \sin(\lambda s) + c_2 \cos(\lambda s) + c_4]. \end{aligned} \quad (5.117)$$

The constants c_1, c_2, c_3, c_4 can be determined through the boundary conditions

$$\bar{\kappa}_2(s=0, \ell) = -\frac{M}{B} \bar{\gamma}_3(s=0, \ell), \quad \bar{\tau}(s=0, \ell) = \frac{M}{C} \bar{\gamma}_2(s=0, \ell), \quad (5.118)$$

that give the homogeneous system

$$\begin{aligned} \left(1 + \frac{M}{B \mu_1}\right) c_2 + \frac{M}{B \mu_1} c_4 &= 0, \\ \left(1 + \frac{M}{B \mu_1}\right) \sin(\lambda \ell) c_1 + \left(1 + \frac{M}{B \mu_1}\right) \cos(\lambda \ell) c_2 + \frac{M}{B \mu_1} c_4 &= 0, \\ \left(\frac{\lambda}{\mu_1} + \frac{M}{\lambda C}\right) c_1 - \frac{M}{\lambda C} c_3 &= 0, \\ \left(\frac{\lambda}{\mu_1} + \frac{M}{\lambda C}\right) \cos(\lambda \ell) c_1 - \left(\frac{\lambda}{\mu_1} + \frac{M}{\lambda C}\right) \sin(\lambda \ell) c_2 - \frac{M}{\lambda C} c_3 &= 0. \end{aligned} \quad (5.119)$$

This system gives a non-trivial solution (i.e., $c_1 = c_2 = c_3 = c_4 = 0$, corresponding to the fundamental solution for the rod) only if the determinant of its matrix vanishes, which gives the condition

$$\frac{2M^2(M + B \mu_1)(M \mu_1 + \lambda^2 C)}{B^2 C^2 \lambda^2 \mu_1^3} [\cos(\lambda \ell) - 1] = 0. \quad (5.120)$$

Replacing the expressions of μ_1, μ_2 and λ we get

$$\frac{2 A^2 B^2}{(A - C)^3 (A - B)} [\cos(\lambda \ell) - 1] = 0, \quad (5.121)$$

which shows that it must be $A \neq C$ (always true, as shown below) and $A \neq B$: the Michell-Prandtl bifurcation cannot happen for rods with such cross-section, e.g. for square or circular sections.

Hence, it must be

$$\cos(\lambda\ell) = 1 \rightarrow \lambda_n = 2n \frac{\pi}{\ell} \rightarrow -\mu_1\mu_2 = 4n^2 \frac{\pi^2}{\ell^2} \rightarrow \frac{A-C}{A} \frac{A-B}{B} \frac{A-C}{A} M_n^2 = 4n^2 \frac{\pi^2}{\ell^2}, \quad (5.122)$$

so finally

$$M_n = 2n \frac{\pi}{\ell} \sqrt{\frac{A}{A-B} \frac{B}{A-C} \frac{A}{A-C}}. \quad (5.123)$$

The least value, for $n = 1$, is the *critical Michell-Prandtl bifurcation couple*:

$$M_b = \frac{2\pi}{\ell} \sqrt{\frac{A}{A-B} \frac{B}{A-C} \frac{A}{A-C}}. \quad (5.124)$$

It is apparent that a bifurcated solution can exist if and only if

$$(A-B)(A-C) > 0 \rightarrow A > B \text{ and } A > C \text{ or } A < B \text{ and } A < C. \quad (5.125)$$

Let us better consider this condition: because

$$A = E J_1, \quad B = E J_2, \quad C = \frac{G J_0}{q}, \quad (5.126)$$

with J_1 and J_2 principal moments of inertia of the cross-section and J_0 the polar moment of inertia. As it is, for isotropic bodies,

$$G = \frac{E}{2(1+\nu)} \quad (5.127)$$

and

$$J_0 = J_1 + J_2, \quad (5.128)$$

we have that

$$C = \frac{A+B}{2(1+\nu)} \frac{1}{q}. \quad (5.129)$$

Because the torsion factor $q \geq 1$ ($q = 1$ for circular cross-sections, i.e. when $A=B$, a case that is to be excluded for Michell-Prandtl bifurcation, as seen above), we have that, for ordinary materials, i.e. with a positive Poisson's ratio,

- if $A > B$, $C < \frac{A}{(1+\nu)q} \Rightarrow C < A$;
- if $A < B$, $C > \frac{A}{(1+\nu)q} \Rightarrow A < (1+\nu) C q$.

Then, the Michell-Prandtl bifurcation can happen in two possible cases: $A > B$ and $A > C$ or $A < \min\{B; (1+\nu) C q\}$. The first case is the most interesting for practical applications; it shows that the phenomenon exists only if the rod bends in the plane of the highest inertia. In addition, if we put $\beta = B/A$ we see easily that

$$\lim_{\beta \rightarrow 0} M_b = \lim_{\beta \rightarrow 0} \frac{2\pi}{\ell} A \sqrt{\frac{\beta}{1-\beta} \frac{1+\beta}{2(1+\nu)q-1-\beta}} = 0. \quad (5.130)$$

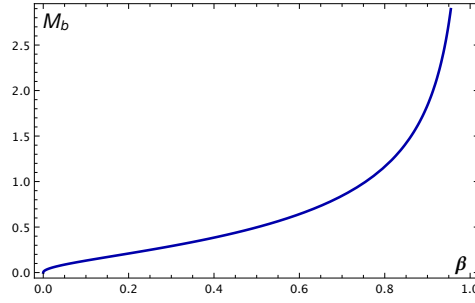


Figure 5.6: The function $M_b(\beta)$, for the case $A = 1, \nu = 0.3, q = 1.5, \ell = 10$.

In other words, M_b decreases for narrow high sections. In Fig. 5.6, the function $M_b(\beta)$ is plotted; it can be noticed that not only $M_b \rightarrow 0$ for $\beta \rightarrow 0$, but also that $M_b \rightarrow \infty$ for $\beta \rightarrow 1$, as seen above ($\beta \rightarrow 1$ when $B \rightarrow A$).

To end this Section, we remark that the bifurcation configuration corresponds to a torsion plus a bending in the plane of B , i.e. the plane $\mathbf{d}_1 - \mathbf{d}_3$, see Fig. 5.7. Such a situation is particularly dangerous for I-shaped steel struts: such slender rods when bent can undergo a similar phenomenon, if not properly constrained.

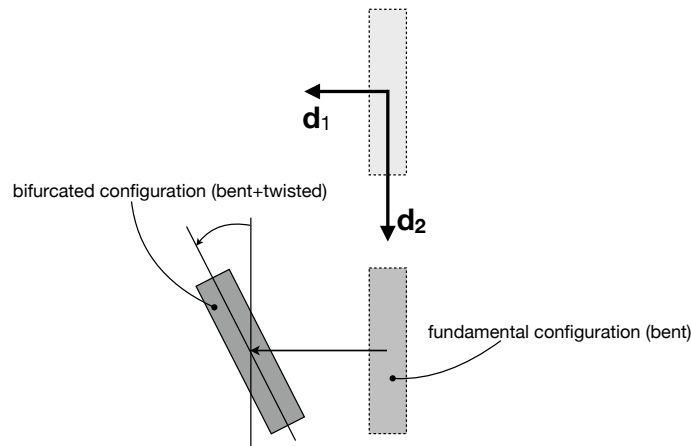


Figure 5.7: Sketch of the deformation in the Michell-Prandtl bifurcation.

5.6 Helicoidal bifurcation

A problem similar to the previous one is that of a straight rod acted upon, at its ends, by a twisting couple $\mathbf{M} = M \mathbf{e}_3$. This problem can be solved following the same approach of the previous Section: the equilibrium equations are still eqs. (5.91) and the same remarks can be done. The fundamental solution now is

$$\kappa_1 = 0, \quad \kappa_2 = 0, \quad \tau = \frac{M}{C}. \quad (5.131)$$

Once linearized, the variated equilibrium equations are

$$\begin{aligned} A \bar{\kappa}'_1 - (B - C) \frac{M}{C} \bar{\kappa}_2 &= 0, \\ B \bar{\kappa}'_2 - (C - A) \frac{M}{C} \bar{\kappa}_1 &= 0, \\ C \bar{\tau}' &= 0, \end{aligned} \quad (5.132)$$

while the boundary conditions for $s = 0, \ell$ become

$$\bar{\kappa}_1 = -\frac{M}{A} \bar{\gamma}_2, \quad \bar{\kappa}_2 = \frac{M}{B} \bar{\gamma}_1, \quad \bar{\tau} = 0. \quad (5.133)$$

This gives, on one hand,

$$\bar{\tau} = 0 \quad \forall s, \quad \bar{\gamma}_3 = \text{const.}, \quad (5.134)$$

and, on the other hand,

$$\begin{aligned} \bar{\kappa}'_1 &= \beta_1 \bar{\kappa}_2, \\ \bar{\kappa}'_2 &= \beta_2 \bar{\kappa}_1, \end{aligned} \quad (5.135)$$

with

$$\beta_1 = -\frac{C - B}{A C} M, \quad \beta_2 = \frac{C - A}{B C} M. \quad (5.136)$$

The resolution of this system of differential equations is quite similar to the problem of the previous Section and at the end we find a critical value of the twisting couple

$$M_t = \frac{2\pi}{\ell} \sqrt{\frac{A C}{C - A} \frac{B C}{C - B}}. \quad (5.137)$$

In this case, the bifurcated solution can exist if and only if

$$(C - A)(C - B) > 0 \rightarrow C > A \text{ and } C > B \text{ or } C < A \text{ and } C < B. \quad (5.138)$$

In particular, for $A < C < B$ or $A > C > B$ this type of bifurcation is not possible. This is the case of a ribbon-like rod, i.e. of a rectangular section with $h \gg b$, where h is the height and b the width of the cross-section. In fact, in this case,

$$A = \frac{b h^3}{12} E, \quad B = \frac{b^3 h}{12} E, \quad C \simeq \frac{b^3 h}{3} G = \frac{2B}{1 + \nu}. \quad (5.139)$$

Hence, because $-1 < \nu \leq 1/2$, it is $A > C > B$: for this type of sections, this kind of bifurcation is not possible. At the opposite side, let us consider cross-sections with an inertia ellipse which is a circle, i.e. $A = B$, like the case of circular or square sections. In this case, it is either $C > A = B$ or $C < A = B$, so bifurcation is possible. In particular,

$$A = B = E J, \quad C = 2 \frac{G J}{q} = \frac{A}{(1 + \nu) q}, \quad (5.140)$$

and if $\nu > 0$, like for ordinary isotropic materials, being $q \geq 1$, it is $C < A$.

The bifurcated configuration is that of a rod with a deflection in both the planes $\mathbf{d}_1 - \mathbf{d}_3$ and $\mathbf{d}_2 - \mathbf{d}_3$, besides a constant twist: such a curve is a helix.

5.7 Exercises

1. A cantilever beam is acted upon by a force R orthogonal to the axis applied at the free end of the rod. The Young's modulus is $E = 20GPa$, the moment of inertia is $J = 10cm^4$ and the length is $L = 5m$. Using the tables for elliptic integrals, calculate the value of R necessary to produce a rotation of $\pi/2$ of the section where the force is applied.
2. A steel bar is acted upon by two identical, opposite couples at the ends, whose value is $M_1 = 100kNm$. The moments of inertia of the cross-section are $J_1 = 150cm^4$ and $J_2 = 15cm^4$, while the torsion factor is $q = 1.5$. Determine the maximal length that the bar can have before bifurcation.

Chapter 6

Plates

6.1 Problem definition: basic assumptions

A plate, see Fig. 6.1, is a solid Ω bounded by two parallel planes, the upper and lower faces S_T and S_B , and by a lateral surface S_L , orthogonal to the two faces, so that, finally, a plate is just a *flat cylinder*. The *mid-plane* is the plane at equal distance from the two faces. We introduce the orthonormal Cartesian frame $\{o; x, y, z\}$, with the axes x and y that belong to the mid-plane. Be h the *thickness* of the plate; for a solid to be really a plate, it must be $h \ll d$, with d the mean chord of the mid-plane. The *contour* of the plate is the line γ intersection of S_L with the mid-plane. Usually, plates are classified as follows:

- thin plates: $\frac{h}{d} \lesssim \frac{1}{10}$;
- moderately thick plates: $\frac{1}{10} \lesssim \frac{h}{d} \lesssim \frac{1}{5}$;
- thick plates: $\frac{h}{d} \gtrsim \frac{1}{5}$.

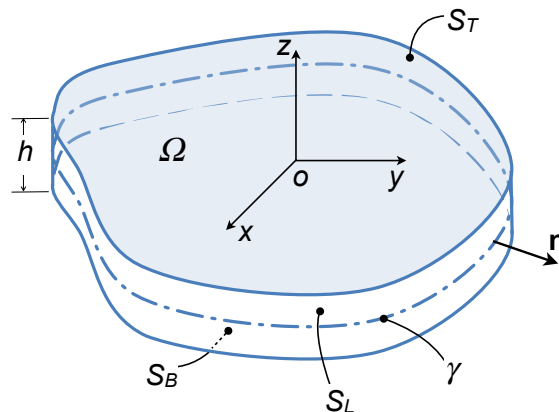


Figure 6.1: General sketch of a plate.

We assume that displacements, rotations and strains are small. As a consequence, the small strain tensor $\boldsymbol{\varepsilon}$ can be taken as an appropriate measure of deformation and the equilibrium equations can be written in the undeformed configuration Ω .

We consider elastic plates, i.e. plates composed by linearly elastic materials whose constitutive law is specified by the Lamé's equations:

$$\boldsymbol{\sigma} = \frac{E}{1+\nu} \left(\boldsymbol{\varepsilon} + \frac{\nu}{1-2\nu} \text{tr} \boldsymbol{\varepsilon} \mathbf{I} \right). \quad (6.1)$$

Finally, the problem so defined is linear.

Concerning the loading, we consider:

- distributed body forces $\mathbf{b}(p)$ on Ω ;
- distributed surface tractions $\boldsymbol{\tau} \left(x, y, \pm \frac{h}{2} \right)$ on S_T and S_B ;
- distributed line forces $\hat{\mathbf{F}}$ and couples $\hat{\mathbf{M}}$ on S_L ;
- distributed couples inside Ω are excluded.

About the body forces $\mathbf{b}(p)$, we consider an *even distribution* with respect to the mid-plane, i.e.

$$\mathbf{b}(x, y, z) = \mathbf{b}(x, y, -z). \quad (6.2)$$

For what concerns the surface tractions¹, let us denote by $\boldsymbol{\tau}^T = (\tau_x^T, \tau_y^T, \tau_z^T)$ the tractions on the surface S_T and by $\boldsymbol{\tau}^B = (\tau_x^B, \tau_y^B, \tau_z^B)$ those on S_B ; generally speaking, we admit that $\boldsymbol{\tau}^T \neq \boldsymbol{\tau}^B$. For the sake of convenience, we decompose the surface tractions into a *symmetric*, $\boldsymbol{\tau}^s$, and *antisymmetric*, $\boldsymbol{\tau}^a$, parts:

$$\boldsymbol{\tau}^s = \frac{\boldsymbol{\tau}^T + \boldsymbol{\tau}^B}{2}, \quad \boldsymbol{\tau}^a = \frac{\boldsymbol{\tau}^T - \boldsymbol{\tau}^B}{2}, \quad (6.3)$$

so that

$$\boldsymbol{\tau}^T = \boldsymbol{\tau}^s + \boldsymbol{\tau}^a, \quad \boldsymbol{\tau}^B = \boldsymbol{\tau}^s - \boldsymbol{\tau}^a. \quad (6.4)$$

The outward unit normals on S_T and S_B are respectively $\mathbf{n}^T = (0, 0, 1)$ and $\mathbf{n}^B = (0, 0, -1)$, so, by the Cauchy's Theorem, on S_T it is²

$$\boldsymbol{\tau}^T = \boldsymbol{\sigma}^T \mathbf{n}^T \rightarrow \sigma_{xz}^T = \tau_x^T = \tau_x^a + \tau_x^s, \quad \sigma_{yz}^T = \tau_y^T = \tau_y^a + \tau_y^s, \quad \sigma_{zz}^T = \tau_z^T = \tau_z^a + \tau_z^s, \quad (6.5)$$

while on S_B

$$\boldsymbol{\tau}^B = \boldsymbol{\sigma}^B \mathbf{n}^B \rightarrow \sigma_{xz}^B = -\tau_x^B = \tau_x^a - \tau_x^s, \quad \sigma_{yz}^B = -\tau_y^B = \tau_y^a - \tau_y^s, \quad \sigma_{zz}^B = -\tau_z^B = \tau_z^a - \tau_z^s. \quad (6.6)$$

¹Often, only lateral forces perpendicular to the plate's surfaces are considered and body forces are neglected; we prefer to develop the theory in the most general case and then consider particular cases; this allows to have a deeper insight in the mechanics of the plates.

²We use the symbol T to denote any quantity evaluated on S_T , i.e. for $z = h/2$, and B for denoting any other quantity evaluated on S_B , i.e. for $z = -h/2$.

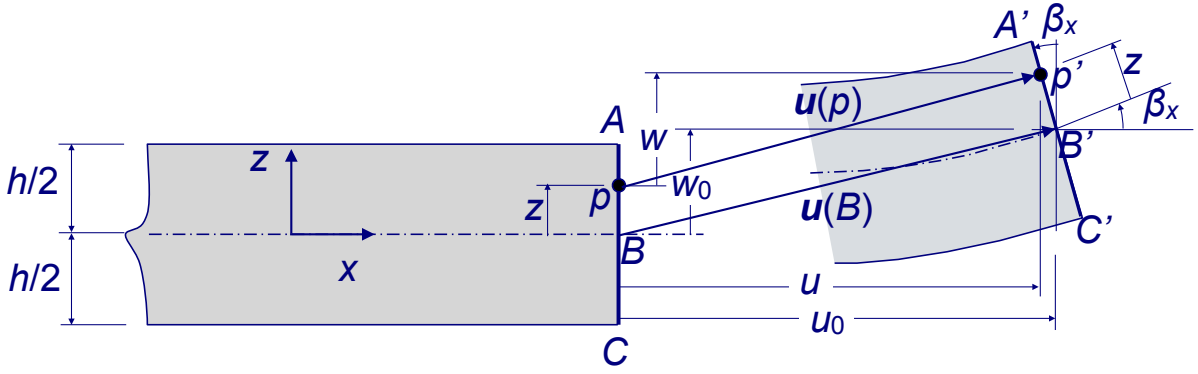


Figure 6.2: Kirchhoff's kinematics in the $\{x, z\}$ plane.

6.2 The Kirchhoff model for thin plates

There are different possible approaches to the construction of a plate theory; we will follow here a classical *axiomatic approach*, i.e. an approach based upon the *a-priori* (i.e. axiomatic) choice of a displacement field. Such choice corresponds to a kinematical model, characterizing the theory.

Putting $\mathbf{u} = (u, v, w)$ the *displacement vector*, we need to specify how the three components $u = u(x, y, z)$, $v = v(x, y, z)$, $w = w(x, y, z)$ of \mathbf{u} vary, and in particular how they change across the thickness, i.e. along z . This choice is suggested, of course, by the particular geometry of the plate. In particular, being h/d a fundamental parameter defining the plate, kinematical models differ from each other as a function of h/d .

6.2.1 The displacement field

In Fig. 6.2 it is schematically represented a cross-section of the plate, along the plane $x - z$, before and after the deformation. Let us consider the segment AC , orthogonal to the mid-plane, with B its intersection with the mid-plane and p a point of AC with the distance z from the mid-plane. After the deformation each material point of the plate moves to a new position indicated by a prime: p goes into p' , B into B' and so on. We can express the displacement $\mathbf{u}(p)$ as

$$\mathbf{u}(p) = p' - p = p' - B' + B' - B + B - p = \mathbf{u}(B) - z\mathbf{e}_3 + p' - B', \quad (6.7)$$

i.e. we can decompose the displacement of any point of Ω as the sum of the displacement of its projection onto the mid-plane plus a position vector, $B - p$, and a local displacement, $p' - B'$, which is the displacement of p' relative to B' . Because $B = (x, y, 0)$, $\mathbf{u}(B) = \mathbf{u}(x, y, 0)$, so we put

$$\mathbf{u}_0 := \mathbf{u}(x, y, 0) = (u_0(x, y), v_0(x, y), w_0(x, y)); \quad (6.8)$$

$\mathbf{u}_0(x, y)$ is a bi-dimensional vector field describing the displacement of the points of the mid-plane. We need now to define the local displacement $p' - B'$. It is exactly at this point that a kinematical model is needed.

The *Kirchhoff model* is based upon three assumptions concerning the deformation of any segment AC . According to the Kirchhoff model, any material segment orthogonal to the mid-plane remains:

- i. a straight segment;
- ii. orthogonal to the deformed mid-surface;
- iii. of the same length.

The third assumption of Kirchhoff states that

$$|p - B| = |p' - B'| = z; \quad (6.9)$$

if β is the angle that the deformed segment $A'C'$ forms with the axis z , then, because of the first Kirchhoff assumption,

$$p' - B' = (-z \sin \beta_x, -z \sin \beta_y, z \cos \beta), \quad (6.10)$$

where β_x and β_y are the angles that z forms with the projections of $A'C'$ onto the planes $x - z$ and $y - z$, respectively. It is an easy task to show that $\beta_x \leq \beta, \beta_y \leq \beta$, Fig. 6.3. The second Kirchhoff assumption lets now affirm that the angle formed by the line

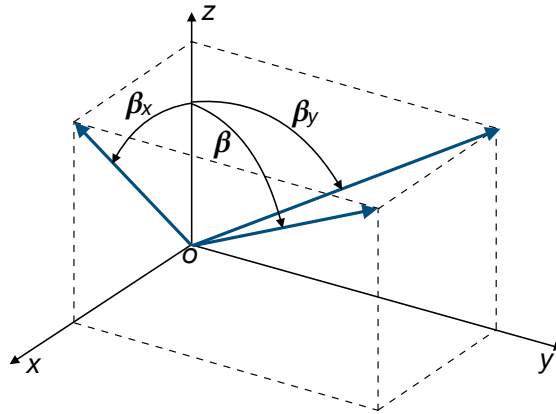


Figure 6.3: Angles scheme.

intersection of the plane containing axis z and $A'C'$ with the tangent plane, in B' , to the bent mid-surface and by the projection of $A'C'$ onto the plane $x - y$ is exactly β ; the same is valid also for the projection angles β_x and β_y . If now we use the assumption of small rotations, then

$$\beta \rightarrow 0 \Rightarrow \beta_x \rightarrow 0, \beta_y \rightarrow 0 \Rightarrow \begin{cases} \beta \simeq \sin \beta \simeq \tan \beta, & \cos \beta \simeq 1, \\ \beta_x \simeq \sin \beta_x \simeq \tan \beta_x = \frac{\partial w_0}{\partial x}, \\ \beta_y \simeq \sin \beta_y \simeq \tan \beta_y = \frac{\partial w_0}{\partial y}. \end{cases} \quad (6.11)$$

Hence,

$$p' - B' \simeq \left(-z \frac{\partial w_0}{\partial x}, -z \frac{\partial w_0}{\partial y}, z \right), \quad (6.12)$$

i.e. within the Kirchhoff model, the local displacement is a linear function of z . Finally

$$\mathbf{u}(p) = \begin{pmatrix} u_0(x, y) - z \frac{\partial w_0(x, y)}{\partial x} \\ v_0(x, y) - z \frac{\partial w_0(x, y)}{\partial y} \\ w_0(x, y) \end{pmatrix}. \quad (6.13)$$

Some remarks about this result:

- $\mathbf{u}(p)$ depends linearly upon z , so all the problem is reduced to find the planar vector field $\mathbf{u}_0(x, y)$ describing the displacement of the points of the mid-plane; the 3D problem has hence been reduced to a 2D one, but this passage, that simplifies remarkably the problem, has heavy consequences, as we will see in the following;
- the kinematics assumptions of the Kirchhoff model are rather heavy; namely, the second one eliminates out-of-plane shear deformations, giving on one hand an increased stiffness to the plate, that cannot deform for shear, and, on the other hand, causing difficulties in the computation of the transversal shear stresses;
- the Kirchhoff assumptions are plausible only for thin plates; when this is not true, they should be removed, especially the first and second ones, passing in this way to higher order theories.

6.2.2 Strain field

The strain field $\boldsymbol{\varepsilon}(p)$ can be easily calculated using the displacement field $\mathbf{u}(p)$:

$$\boldsymbol{\varepsilon}(p) = \frac{\nabla \mathbf{u}(p) + \nabla \mathbf{u}^\top(p)}{2} = \begin{bmatrix} \frac{\partial u_0}{\partial x} - z \frac{\partial^2 w_0}{\partial x^2} & \frac{1}{2} \left(\frac{\partial u_0}{\partial y} + \frac{\partial v_0}{\partial x} \right) - z \frac{\partial^2 w_0}{\partial x \partial y} & 0 \\ \frac{1}{2} \left(\frac{\partial u_0}{\partial y} + \frac{\partial v_0}{\partial x} \right) - z \frac{\partial^2 w_0}{\partial x \partial y} & \frac{\partial v_0}{\partial y} - z \frac{\partial^2 w_0}{\partial y^2} & 0 \\ 0 & 0 & 0 \end{bmatrix}. \quad (6.14)$$

So, $\varepsilon_{xz} = \varepsilon_{yz} = \varepsilon_{zz} = 0$: as a consequence of the Kirchhoff model, $\boldsymbol{\varepsilon}$ is planar. Contrarily to what often said, however, this is *not* a plane strain state, because w is not identically null and \mathbf{u} and $\boldsymbol{\varepsilon}$ depend upon z too. Actually, a plane strain state is typical of long cylinders acted upon by forces that do not vary along the axis of the cylinder; here, the only thing that can be said is that in the Kirchhoff model $\boldsymbol{\varepsilon}$ is planar.

6.2.3 Stress field

About the stress field $\boldsymbol{\sigma}(p)$ a supplementary assumption is made: $\forall p \in \Omega$,

$$\sigma_{zz} = 0. \quad (6.15)$$

This assumption, common also to other plate theories, can be justified as follows:

- from the inverse Lamé's equation,

$$\boldsymbol{\varepsilon} = \frac{1 + \nu}{E} \boldsymbol{\sigma} - \frac{\nu}{E} \text{tr} \boldsymbol{\sigma} \mathbf{I}, \quad (6.16)$$

we get

$$\varepsilon_{zz} = \frac{\sigma_{zz} - \nu(\sigma_{xx} + \sigma_{yy})}{E}, \quad (6.17)$$

and because in the Kirchhoff model $\varepsilon_{zz} = 0$, we get

$$\sigma_{zz} = \nu(\sigma_{xx} + \sigma_{yy}); \quad (6.18)$$

- for common materials, $0 < \nu < 1/2$, so σ_{zz} is at most of the same order of magnitude of σ_{xx} and σ_{yy} ;
- for the assumptions on the loads, σ_{zz} is a smooth function of z ; so, because σ_{zz} is regular and the plate thin, its value cannot increase very much inside the plate with respect to the values that σ_{zz} has on the faces of the plate, S_B and S_T ;
- because the value of σ_{zz} on S_B and S_T is just the value of the contact forces applied to the faces, i.e. τ_z , it has not, in usual situations, a great value compared to the design values of σ_{xx} and σ_{yy} . For this reason, we can neglect σ_{zz} and finally consider that it is null.

These arguments are merely empirical; of course, they are not valid in some situations, i.e. in correspondence of concentrated loads, e.g. impact forces, or of supporting parts. In such cases the stress state is properly a 3D one and in such zones the behavior is, locally, far from that of a plate.

Because $\varepsilon_{xz} = \varepsilon_{yz}$, from eq. (6.1) we get also

$$\sigma_{xz} = \frac{E}{1 + \nu} \varepsilon_{xz} = 0, \quad \sigma_{yz} = \frac{E}{1 + \nu} \varepsilon_{yz} = 0, \quad (6.19)$$

so finally also the stress field is planar:

$$\boldsymbol{\sigma} = \begin{bmatrix} \sigma_{xx} & \sigma_{xy} & 0 \\ \sigma_{xy} & \sigma_{yy} & 0 \\ 0 & 0 & 0 \end{bmatrix}. \quad (6.20)$$

This is a strange situation, because in elasticity, a plane stress state is incompatible with a plane strain one and vice-versa. However, because $\boldsymbol{\varepsilon}(p)$ depends upon x, y and z , this is the same also for the stress field: $\boldsymbol{\sigma}(p)$ is not a plane field.

A dramatic consequence of eq. (6.19) is that the plate cannot be equilibrated under the action of loads that have a component orthogonal to the mid-plane: strictly speaking, the Kirchhoff model concerns plates that are loaded in their plane or by couples on the boundary. This problem will be solved making use directly of the equilibrium equations, cf. Sec. 6.2.9.

We remark also that eq. (6.19) is a consequence not only of the kinematical model, but also of the constitutive law: for generally oriented anisotropic plates, σ_{xz} and σ_{yz} are in general not null, also for the Kirchhoff model.

We can now obtain the constitutive law for a Kirchhoff plate: from eq. (6.16) we get

$$\begin{aligned}\varepsilon_{xx} &= \frac{1}{E}(\sigma_{xx} - \nu\sigma_{yy}), \\ \varepsilon_{yy} &= \frac{1}{E}(\sigma_{yy} - \nu\sigma_{xx}), \\ \varepsilon_{xy} &= \frac{1+\nu}{E}\sigma_{xy},\end{aligned}\tag{6.21}$$

that once inverted give

$$\begin{aligned}\sigma_{xx} &= \frac{E}{1-\nu^2}(\varepsilon_{xx} + \nu\varepsilon_{yy}), \\ \sigma_{yy} &= \frac{E}{1-\nu^2}(\varepsilon_{yy} + \nu\varepsilon_{xx}), \\ \sigma_{xy} &= \frac{E}{1+\nu}\varepsilon_{xy} = 2G\varepsilon_{xy}.\end{aligned}\tag{6.22}$$

We can put the last result in matrix form:

$$\begin{Bmatrix} \sigma_{xx} \\ \sigma_{yy} \\ \sigma_{xy} \end{Bmatrix} = \begin{bmatrix} \frac{E}{1-\nu^2} & \frac{\nu E}{1-\nu^2} & 0 \\ \frac{\nu E}{1-\nu^2} & \frac{E}{1-\nu^2} & 0 \\ 0 & 0 & G \end{bmatrix} \begin{Bmatrix} \varepsilon_{xx} \\ \varepsilon_{yy} \\ 2\varepsilon_{xy} \end{Bmatrix},\tag{6.23}$$

or synthetically

$$\boldsymbol{\sigma} = \mathbb{D} \boldsymbol{\varepsilon},\tag{6.24}$$

with \mathbb{D} the matrix in eq. (6.23). It can be checked that \mathbb{D} corresponds to the so-called *reduced stiffness matrix*, typical of a plane stress state: finally, though the assumptions of the Kirchhoff model do not coincide with those typical of a plane stress state ($\boldsymbol{\sigma}$ is not a plane field), the plate's constitutive law, eq. (6.23) is just like that of a plane stress state.

6.2.4 Internal actions

The internal actions, forces and couples, are obtained integrating through the thickness the stress field. In particular, we introduce:

- the *extension tensor* \mathbf{N} , defined as

$$\mathbf{N} = \int_{-\frac{h}{2}}^{+\frac{h}{2}} \boldsymbol{\sigma} dz,\tag{6.25}$$

whose components

$$\begin{Bmatrix} N_x \\ N_y \\ N_{xy} \end{Bmatrix} = \begin{Bmatrix} \int_{-\frac{h}{2}}^{+\frac{h}{2}} \sigma_{xx} dz \\ \int_{-\frac{h}{2}}^{+\frac{h}{2}} \sigma_{yy} dz \\ \int_{-\frac{h}{2}}^{+\frac{h}{2}} \sigma_{xy} dz \end{Bmatrix} \quad (6.26)$$

are represented in Fig. 6.4;

- the *transverse shear forces*

$$T_x = \int_{-\frac{h}{2}}^{+\frac{h}{2}} \sigma_{xz} dz, \quad T_y = \int_{-\frac{h}{2}}^{+\frac{h}{2}} \sigma_{yz} dz, \quad (6.27)$$

also represented in Fig. 6.4,

- the *bending tensor* \mathbf{M} , defined as

$$\mathbf{M} = \int_{-\frac{h}{2}}^{+\frac{h}{2}} z \boldsymbol{\sigma} dz, \quad (6.28)$$

whose components

$$\begin{Bmatrix} M_x \\ M_y \\ M_{xy} \end{Bmatrix} = \begin{Bmatrix} \int_{-\frac{h}{2}}^{+\frac{h}{2}} z \sigma_{xx} dz \\ \int_{-\frac{h}{2}}^{+\frac{h}{2}} z \sigma_{yy} dz \\ \int_{-\frac{h}{2}}^{+\frac{h}{2}} z \sigma_{xy} dz \end{Bmatrix} \quad (6.29)$$

are still represented in Fig. 6.4.

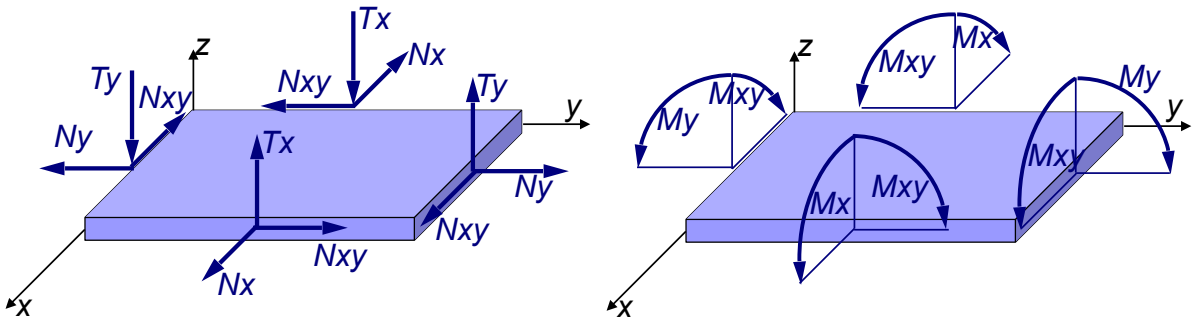


Figure 6.4: Internal actions.

Being integrals of a planar symmetric second-rank tensor, both \mathbf{N} and \mathbf{M} are planar symmetric second-rank tensors too; in addition, they are plane fields too: $\mathbf{N} = \mathbf{N}(x, y)$, $\mathbf{M} = \mathbf{M}(x, y)$. To remark that the units of \mathbf{N} and of the shear forces T_x and T_y are a force per unit length, while those of \mathbf{M} are a force.

6.2.5 Uncoupling bending and extension

The expression of $\boldsymbol{\varepsilon}$ can be written in the form

$$\boldsymbol{\varepsilon} = \boldsymbol{\varepsilon}^0 + z \boldsymbol{\kappa}, \quad (6.30)$$

where

$$\boldsymbol{\varepsilon}^0 = \begin{Bmatrix} \boldsymbol{\varepsilon}_{xx}^0 \\ \boldsymbol{\varepsilon}_{yy}^0 \\ 2\boldsymbol{\varepsilon}_{xy}^0 \end{Bmatrix} = \begin{Bmatrix} \frac{\partial u_0}{\partial x} \\ \frac{\partial v_0}{\partial y} \\ \frac{\partial u_0}{\partial y} + \frac{\partial v_0}{\partial x} \end{Bmatrix} \quad (6.31)$$

is the *in-plane deformation tensor*, describing the strain of the mid-plane, while

$$\boldsymbol{\kappa} = \begin{Bmatrix} \kappa_x \\ \kappa_y \\ 2\kappa_{xy} \end{Bmatrix} = \begin{Bmatrix} -\frac{\partial^2 w_0}{\partial x^2} \\ -\frac{\partial^2 w_0}{\partial y^2} \\ -2\frac{\partial^2 w_0}{\partial x \partial y} \end{Bmatrix} \quad (6.32)$$

is the *curvatures tensor*, describing the bending of the mid-plane. Using this decomposition of $\boldsymbol{\varepsilon}$, we can write

$$\boldsymbol{\sigma} = \mathbb{D}\boldsymbol{\varepsilon} = \mathbb{D}\boldsymbol{\varepsilon}^0 + z\mathbb{D}\boldsymbol{\kappa} \quad (6.33)$$

and because \mathbb{D} , $\boldsymbol{\varepsilon}^0$ and $\boldsymbol{\kappa}$ do not depend upon z , we get

$$\begin{aligned} \mathbf{N} &= \mathbb{D}\boldsymbol{\varepsilon}^0 \int_{-\frac{h}{2}}^{+\frac{h}{2}} dz + \mathbb{D}\boldsymbol{\kappa} \int_{-\frac{h}{2}}^{+\frac{h}{2}} z dz = h \mathbb{D}\boldsymbol{\varepsilon}^0, \\ \mathbf{M} &= \mathbb{D}\boldsymbol{\varepsilon}^0 \int_{-\frac{h}{2}}^{+\frac{h}{2}} z dz + \mathbb{D}\boldsymbol{\kappa} \int_{-\frac{h}{2}}^{+\frac{h}{2}} z^2 dz = \frac{h^3}{12} \mathbb{D}\boldsymbol{\kappa}, \end{aligned} \quad (6.34)$$

i.e. \mathbf{N} depends only upon in-plane strains and \mathbf{M} only upon curvatures: there is no coupling between extension and curvatures nor between bending and in-plane deformation. Actually, the absence of any coupling effect is due to two facts: on one hand, geometry (the flatness of the plate) and on the other hand homogeneity (the plate is composed by a unique layer): generally speaking for shells, i.e. "curved plates", and laminates, i.e. plates obtained superposing layers, coupling effects are present. Finally, extension and bending of the plate can be examined separately, they do not interact.

A plate that is subjected only to in-plane forces, so that $\boldsymbol{\kappa} = \mathbf{0} \Rightarrow \mathbf{M} = \mathbf{0}$, is called a (flat) *membrane* (curved membranes exist too, e.g. an inflated balloon, they are considered in Chapter 7). The membrane regime, however, is compatible only with a distribution of the forces which is point-wise symmetric with respect to the mid-plane, assumption that we have already made.

6.2.6 Balance equations

There are different ways for writing local balance equations. A standard approach is to write the equilibrium to translation and rotation of a small part of the plate, and then discard higher order terms. We prefer here a more concise approach: starting from the 3D equilibrium equations,

$$\operatorname{div}\boldsymbol{\sigma} + \mathbf{b} = \mathbf{o}, \quad (6.35)$$

where $\mathbf{b}(p)$ is the field of body forces (forces per unit volume) on Ω , we obtain, after integration on z ,

$$\begin{aligned} \int_{-\frac{h}{2}}^{\frac{h}{2}} \left(\frac{\partial\sigma_{xx}}{\partial x} + \frac{\partial\sigma_{xy}}{\partial y} + \frac{\partial\sigma_{xz}}{\partial z} + b_x \right) dz &= 0, \\ \int_{-\frac{h}{2}}^{\frac{h}{2}} \left(\frac{\partial\sigma_{xy}}{\partial x} + \frac{\partial\sigma_{yy}}{\partial y} + \frac{\partial\sigma_{yz}}{\partial z} + b_y \right) dz &= 0, \\ \int_{-\frac{h}{2}}^{\frac{h}{2}} \left(\frac{\partial\sigma_{xz}}{\partial x} + \frac{\partial\sigma_{yz}}{\partial y} + \frac{\partial\sigma_{zz}}{\partial z} + b_z \right) dz &= 0. \end{aligned} \quad (6.36)$$

Because the integration bounds are fixed, we can bring the differential operators outside the integration symbol:

$$\begin{aligned} \frac{\partial}{\partial x} \int_{-\frac{h}{2}}^{\frac{h}{2}} \sigma_{xx} dz + \frac{\partial}{\partial y} \int_{-\frac{h}{2}}^{\frac{h}{2}} \sigma_{xy} dz + \int_{-\frac{h}{2}}^{\frac{h}{2}} \left(\frac{\partial\sigma_{xz}}{\partial z} + b_x \right) dz &= 0, \\ \frac{\partial}{\partial x} \int_{-\frac{h}{2}}^{\frac{h}{2}} \sigma_{xy} dz + \frac{\partial}{\partial y} \int_{-\frac{h}{2}}^{\frac{h}{2}} \sigma_{yy} dz + \int_{-\frac{h}{2}}^{\frac{h}{2}} \left(\frac{\partial\sigma_{yz}}{\partial z} + b_y \right) dz &= 0, \\ \frac{\partial}{\partial x} \int_{-\frac{h}{2}}^{\frac{h}{2}} \sigma_{xz} dz + \frac{\partial}{\partial y} \int_{-\frac{h}{2}}^{\frac{h}{2}} \sigma_{yz} dz + \int_{-\frac{h}{2}}^{\frac{h}{2}} \left(\frac{\partial\sigma_{zz}}{\partial z} + b_z \right) dz &= 0, \end{aligned} \quad (6.37)$$

so that, introducing eqs. (6.26) and (6.27), we get

$$\begin{aligned} \frac{\partial N_x}{\partial x} + \frac{\partial N_{xy}}{\partial y} + f_x &= 0, \\ \frac{\partial N_{xy}}{\partial x} + \frac{\partial N_y}{\partial y} + f_y &= 0, \end{aligned} \quad (6.38)$$

and

$$\frac{\partial T_x}{\partial x} + \frac{\partial T_y}{\partial y} + f_z = 0, \quad (6.39)$$

where we have denoted by $\mathbf{f}(x, y) = (f_x, f_y, f_z)$ the vector of the *total applied loads per unit area*:

$$\begin{aligned} f_x(x, y) &= [\sigma_{xz}]_{-\frac{h}{2}}^{\frac{h}{2}} + \int_{-\frac{h}{2}}^{\frac{h}{2}} b_x dz = \sigma_{xz}^T - \sigma_{xz}^B + \beta_x = 2\tau_x^s + \beta_x, \\ f_y(x, y) &= [\sigma_{yz}]_{-\frac{h}{2}}^{\frac{h}{2}} + \int_{-\frac{h}{2}}^{\frac{h}{2}} b_y dz = \sigma_{yz}^T - \sigma_{yz}^B + \beta_y = 2\tau_y^s + \beta_y, \\ f_z(x, y) &= [\sigma_{zz}]_{-\frac{h}{2}}^{\frac{h}{2}} + \int_{-\frac{h}{2}}^{\frac{h}{2}} b_z dz = \sigma_{zz}^T - \sigma_{zz}^B + \beta_z = 2\tau_z^s + \beta_z; \end{aligned} \quad (6.40)$$

in the above equations, $\boldsymbol{\beta}(x, y) = (\beta_x, \beta_y, \beta_z)$ is the vector of *body forces per unit area*:

$$\boldsymbol{\beta} = \int_{-\frac{h}{2}}^{\frac{h}{2}} \mathbf{b} dz. \quad (6.41)$$

Equations (6.38) are the *extension, or membrane, equilibrium equations* of the plate, while eq. (6.39) is the *transverse shear equilibrium equation*.

The bending equilibrium can be obtained in a similar way, now integrating eq. (6.35) once multiplied by z , the distance of each component $\sigma_{ij}(p)$ from the mid-plane:

$$\begin{aligned} \int_{-\frac{h}{2}}^{\frac{h}{2}} z \left(\frac{\partial \sigma_{xx}}{\partial x} + z \frac{\partial \sigma_{xy}}{\partial y} + z \frac{\partial \sigma_{xz}}{\partial z} + z b_x \right) dz &= 0, \\ \int_{-\frac{h}{2}}^{\frac{h}{2}} \left(z \frac{\partial \sigma_{xy}}{\partial x} + z \frac{\partial \sigma_{yy}}{\partial y} + z \frac{\partial \sigma_{yz}}{\partial z} + z b_y \right) dz &= 0, \\ \int_{-\frac{h}{2}}^{\frac{h}{2}} \left(z \frac{\partial \sigma_{xz}}{\partial x} + z \frac{\partial \sigma_{yz}}{\partial y} + z \frac{\partial \sigma_{zz}}{\partial z} + z b_z \right) dz &= 0. \end{aligned} \quad (6.42)$$

Because we are interested in the bending of the plate, the third equation of (6.45) can be discarded, as it concerns the equilibrium to rotation about the axis z . Observing that

$$z \frac{\partial \sigma_{\alpha\beta}}{\partial \alpha} = \frac{\partial (z \sigma_{\alpha\beta})}{\partial \alpha} \quad \alpha, \beta \in \{1, 2\}, \quad (6.43)$$

and that, because $\mathbf{b}(p)$ is an even function, $z\mathbf{b}(p)$ is an odd one so that

$$\int_{-\frac{h}{2}}^{\frac{h}{2}} z b_x dz = \int_{-\frac{h}{2}}^{\frac{h}{2}} z b_y dz = 0, \quad (6.44)$$

we get

$$\begin{aligned} \frac{\partial}{\partial x} \int_{-\frac{h}{2}}^{\frac{h}{2}} z \sigma_{xx} dz + \frac{\partial}{\partial y} \int_{-\frac{h}{2}}^{\frac{h}{2}} z \sigma_{xy} dz + \int_{-\frac{h}{2}}^{\frac{h}{2}} z \frac{\partial \sigma_{xz}}{\partial z} dz &= 0, \\ \frac{\partial}{\partial x} \int_{-\frac{h}{2}}^{\frac{h}{2}} z \sigma_{xy} dz + \frac{\partial}{\partial y} \int_{-\frac{h}{2}}^{\frac{h}{2}} z \sigma_{yy} dz + \int_{-\frac{h}{2}}^{\frac{h}{2}} z \frac{\partial \sigma_{yz}}{\partial z} dz &= 0. \end{aligned} \quad (6.45)$$

Integration by parts gives, cfr. eqs. (6.6), (6.5) and (6.27),

$$\begin{aligned} \int_{-\frac{h}{2}}^{\frac{h}{2}} z \frac{\partial \sigma_{xz}}{\partial z} dz &= [z \sigma_{xz}]_{-\frac{h}{2}}^{\frac{h}{2}} - \int_{-\frac{h}{2}}^{\frac{h}{2}} \sigma_{xz} dz = \\ &= \frac{h}{2} (\sigma_{xz}^T + \sigma_{xz}^B) - T_x = \frac{h}{2} (\tau_x^T - \tau_x^B) - T_x = h \tau_x^a - T_x, \\ \int_{-\frac{h}{2}}^{\frac{h}{2}} z \frac{\partial \sigma_{yz}}{\partial z} dz &= [z \sigma_{yz}]_{-\frac{h}{2}}^{\frac{h}{2}} - \int_{-\frac{h}{2}}^{\frac{h}{2}} \sigma_{yz} dz = \\ &= \frac{h}{2} (\sigma_{yz}^T + \sigma_{yz}^B) - T_y = \frac{h}{2} (\tau_y^T - \tau_y^B) - T_y = h \tau_y^a - T_y. \end{aligned} \quad (6.46)$$

If now we use eq. (6.29) we obtain

$$\begin{aligned}\frac{\partial M_x}{\partial x} + \frac{\partial M_{xy}}{\partial y} &= T_x - h\tau_x^a, \\ \frac{\partial M_{xy}}{\partial x} + \frac{\partial M_y}{\partial y} &= T_y - h\tau_y^a,\end{aligned}\tag{6.47}$$

and injecting this result into eq. (6.39) we get the unique second-order equation including bending and shear equilibrium:

$$\frac{\partial^2 M_x}{\partial x^2} + 2\frac{\partial^2 M_{xy}}{\partial x\partial y} + \frac{\partial^2 M_y}{\partial y^2} + \widehat{f}_z = 0\tag{6.48}$$

where

$$\widehat{f}_z = f_z + h\left(\frac{\partial\tau_x^a}{\partial x} + \frac{\partial\tau_y^a}{\partial y}\right).\tag{6.49}$$

6.2.7 Elastic equilibrium equations

Injecting into eq. (6.34)₁ the expressions of \mathbb{D} and ε^0 we get

$$\begin{aligned}N_x &= \frac{E h}{1 - \nu^2} \left(\frac{\partial u_0}{\partial x} + \nu \frac{\partial v_0}{\partial y} \right), \\ N_y &= \frac{E h}{1 - \nu^2} \left(\nu \frac{\partial u_0}{\partial x} + \frac{\partial v_0}{\partial y} \right), \\ N_{xy} &= G \left(\frac{\partial u_0}{\partial y} + \frac{\partial v_0}{\partial x} \right),\end{aligned}\tag{6.50}$$

which injected into eq. (6.38) gives ($G = E/2(1 + \nu)$)

$$\begin{aligned}\frac{E h}{1 + \nu} \left[\frac{1}{1 - \nu} \left(\frac{\partial^2 u_0}{\partial x^2} + \nu \frac{\partial^2 v_0}{\partial x\partial y} \right) + \frac{1}{2} \left(\frac{\partial^2 u_0}{\partial y^2} + \frac{\partial^2 v_0}{\partial x\partial y} \right) \right] + f_x &= 0, \\ \frac{E h}{1 + \nu} \left[\frac{1}{2} \left(\frac{\partial^2 u_0}{\partial x\partial y} + \frac{\partial^2 v_0}{\partial x^2} \right) + \frac{1}{1 - \nu} \left(\nu \frac{\partial^2 u_0}{\partial x\partial y} + \frac{\partial^2 v_0}{\partial y^2} \right) \right] + f_y &= 0.\end{aligned}\tag{6.51}$$

These are the *elastic membrane equilibrium equations* for isotropic homogeneous plates; they are the 2D equivalent of the rod extension equilibrium equation $EA w'' + p_z = 0$.

Similarly, if now we inject into eq. (6.34)₂ the expressions of \mathbb{D} and κ , we obtain

$$\begin{aligned}M_x &= -\frac{h^3}{12} \frac{E}{1 - \nu^2} \left(\frac{\partial^2 w_0}{\partial x^2} + \nu \frac{\partial^2 w_0}{\partial y^2} \right), \\ M_y &= -\frac{h^3}{12} \frac{E}{1 - \nu^2} \left(\frac{\partial^2 w_0}{\partial y^2} + \nu \frac{\partial^2 w_0}{\partial x^2} \right), \\ M_{xy} &= -\frac{h^3}{12} \frac{E}{1 + \nu} \frac{\partial^2 w_0}{\partial x\partial y},\end{aligned}\tag{6.52}$$

that inserted into eq. (6.48) gives

$$\frac{h^3}{12} \frac{E}{1 - \nu^2} \left(\frac{\partial^4 w_0}{\partial x^4} + 2\frac{\partial^4 w_0}{\partial x^2\partial y^2} + \frac{\partial^4 w_0}{\partial y^4} \right) = \widehat{f}_z.\tag{6.53}$$

Usually, the symbol D is used to denote the bending stiffness of the plate per unit of length:

$$D = \frac{h^3}{12} \frac{E}{1 - \nu^2}, \quad (6.54)$$

so that, once introduced the classical *double laplacian* differential operator,

$$\Delta^2 = \frac{\partial^4 \bullet}{\partial x^4} + 2 \frac{\partial^4 \bullet}{\partial x^2 \partial y^2} + \frac{\partial^4 \bullet}{\partial y^4}, \quad (6.55)$$

eq. (6.53) can be rewritten in the form

$$D\Delta^2 w_0 = \widehat{f}_z. \quad (6.56)$$

This is the celebrated *Germain-Lagrange equation* (1816); it is the 2D corresponding of the elastic bending equilibrium equation $EJ v^{iv} = p_y$ for rods: the Kirchhoff model is, for plates, the equivalent of the Euler-Bernoulli model for the bending of rods. Actually, because $h^3/12$ is the moment of inertia, about axes x or y , of a unit length cross section of the plate, the true difference between the one-dimensional case, rods, and the bi-dimensional one, plates, is in the term $1 - \nu^2$, which is a consequence of the reduced stiffness \mathbb{D} , hence of the fact that $\boldsymbol{\sigma}(p)$ is planar: plates are intrinsically stiffer than rods.

Equations (6.51) and (6.56) are the *elastic equilibrium equations of plates*, respectively for membrane and for bending.

In the same way, from the equilibrium equations for bending, eq. (6.47), we get:

$$\begin{aligned} T_x &= \frac{\partial M_x}{\partial x} + \frac{\partial M_{xy}}{\partial y} + h\tau_x^a = -\frac{h^3}{12} \frac{E}{1 - \nu^2} [w_{0,xxx} + \nu w_{0,xyy} + (1 - \nu)w_{0,xyy}] + h\tau_x^a, \\ T_y &= \frac{\partial M_{xy}}{\partial x} + \frac{\partial M_y}{\partial y} + h\tau_y^a = -\frac{h^3}{12} \frac{E}{1 - \nu^2} [(1 - \nu)w_{0,xyy} + \nu w_{0,xxx} + w_{0,yyy}] + h\tau_y^a, \end{aligned} \quad (6.57)$$

i.e.

$$\begin{aligned} T_x &= -D\Delta w_{0,x} + h\tau_x^a, \\ T_y &= -D\Delta w_{0,y} + h\tau_y^a. \end{aligned} \quad (6.58)$$

6.2.8 Expressions for stresses

Inverting eqs. (6.34) gives

$$\mathbb{D}\boldsymbol{\varepsilon}^0 = \frac{\mathbf{N}}{h}, \quad \mathbb{D}\boldsymbol{\kappa} = \frac{12}{h^3}\mathbf{M}, \quad (6.59)$$

that injected into eq. (6.33) gives

$$\boldsymbol{\sigma} = \frac{1}{h}\mathbf{N} + \frac{12}{h^3}\mathbf{M} z. \quad (6.60)$$

This formula generalizes to plates the *Navier's formula*, giving the normal stress distribution in beams subjected to bending and extension.

6.2.9 Transverse shear stresses

We can now go back to the problem of determining the *transverse shear stresses* σ_{xz} and σ_{yz} , that, as we have seen, are incompatible with the Kirchhoff's assumptions. Actually, we can find them using the equilibrium equations. Let us consider first the component σ_{xz} : from the first component of eq. (6.35) we get

$$\frac{\partial \sigma_{xz}}{\partial z} = -\frac{\partial \sigma_{xx}}{\partial x} - \frac{\partial \sigma_{xy}}{\partial y} - b_x, \quad (6.61)$$

and through the first component of eq. (6.60) we get

$$\frac{\partial \sigma_{xz}}{\partial z} = -\frac{1}{h} \left(\frac{\partial N_x}{\partial x} + \frac{\partial N_{xy}}{\partial y} \right) - \frac{12}{h^3} \left(\frac{\partial M_x}{\partial x} + \frac{\partial M_{xy}}{\partial y} \right) z - b_x, \quad (6.62)$$

If now we use the equilibrium equations, i.e. eqs. (6.38), (6.40) and (6.47), we get

$$\frac{\partial \sigma_{xz}}{\partial z} = \frac{f_x}{h} - b_x - 12 \frac{z}{h^2} \left(\frac{T_x}{h} - \tau_x^a \right), \quad (6.63)$$

and integrating

$$\sigma_{xz} = f_x \frac{z}{h} - \int_0^z b_x dz - 6 \frac{z^2}{h^2} \left(\frac{T_x}{h} - \tau_x^a \right) + \phi_x(x, y). \quad (6.64)$$

The unknown function $\phi_x(x, y)$ can be determined through the boundary conditions; if we put that, see eq. (6.5),

$$\sigma_{xz}^T = \tau_x^T = \tau_x^s + \tau_x^a, \quad (6.65)$$

we get

$$\begin{aligned} \phi_x(x, y) &= \tau_x^s + \tau_x^a - \frac{f_x h}{2} + \int_0^{\frac{h}{2}} b_x dz + \frac{6}{h^2} \frac{h^2}{4} \left(\frac{T_x}{h} - \tau_x^a \right) \\ &= \tau_x^s + \tau_x^a - \frac{\beta_x}{2} - \tau_x^s + \frac{\beta_x}{2} + \frac{3}{2} \left(\frac{T_x}{h} - \tau_x^a \right) \\ &= \frac{3}{2} \frac{T_x}{h} - \frac{\tau_x^a}{2}, \end{aligned} \quad (6.66)$$

so finally,

$$\sigma_{xz} = f_x \frac{z}{h} - \int_0^z b_x dz - 6 \frac{z^2}{h^2} \left(\frac{T_x}{h} - \tau_x^a \right) + \frac{3}{2} \frac{T_x}{h} - \frac{\tau_x^a}{2}. \quad (6.67)$$

or better

$$\sigma_{xz} = \beta_x \frac{z}{h} + 2\tau_x^m \frac{z}{h} - \int_0^z b_x dz + \left(6 \frac{z^2}{h^2} - \frac{1}{2} \right) \tau_x^s + 6 \frac{T_x}{h} \left(\frac{1}{4} - \frac{z^2}{h^2} \right). \quad (6.68)$$

Of course, proceeding in the same way we get a similar expression for σ_{yz} :

$$\sigma_{yz} = \beta_y \frac{z}{h} + 2\tau_y^m \frac{z}{h} - \int_0^z b_y dz + \left(6 \frac{z^2}{h^2} - \frac{1}{2} \right) \tau_y^s + 6 \frac{T_y}{h} \left(\frac{1}{4} - \frac{z^2}{h^2} \right). \quad (6.69)$$

To remark that the two conditions at the surfaces S_T and S_B are matched, see eqs. (6.5) and (6.6):

$$\begin{aligned}\sigma_{xz}^T &= \sigma_{xz} \left(\frac{h}{2} \right) = \tau_x^a + \tau_x^s = \tau_x^T, \\ \sigma_{xz}^B &= \sigma_{xz} \left(-\frac{h}{2} \right) = \tau_x^a - \tau_x^s = -\tau_x^B,\end{aligned}\tag{6.70}$$

and similarly for σ_{yz} .

6.2.10 Plates submitted uniquely to orthogonal loads

The results in the previous Sections have been obtained for the case of a general load, i.e. of a vector of body forces and of surface tractions having all the components different from zero. However, it is interesting to consider the special and very common case of plates loaded by only *orthogonal loads*, i.e. such that

$$b_x = 0, \quad b_y = 0, \quad \tau_x^T = 0, \quad \tau_x^B = 0, \quad \tau_y^T = 0, \quad \tau_y^B = 0.\tag{6.71}$$

In such a case, $f_x(x, y) = f_y(x, y)$ and the equilibrium equations (6.47) simplify to

$$\begin{aligned}\frac{\partial M_x}{\partial x} + \frac{\partial M_{xy}}{\partial y} &= T_x, \\ \frac{\partial M_{xy}}{\partial x} + \frac{\partial M_y}{\partial y} &= T_y,\end{aligned}\tag{6.72}$$

and eq. (6.48) to

$$\frac{\partial^2 M_x}{\partial x^2} + 2 \frac{\partial^2 M_{xy}}{\partial x \partial y} + \frac{\partial^2 M_y}{\partial y^2} + f_z = 0,\tag{6.73}$$

while the elastic equilibrium equations (6.56) and (6.58) respectively to

$$D\Delta^2 w_0 = f_z\tag{6.74}$$

and to

$$\begin{aligned}T_x &= -D\Delta w_{0,x}, \\ T_y &= -D\Delta w_{0,y}.\end{aligned}\tag{6.75}$$

Finally, the expressions of the transverse shear stresses, eqs. (6.68) and (6.69), become

$$\begin{aligned}\sigma_{xz} &= \frac{6}{h} T_x \left(\frac{1}{4} - \frac{z^2}{h^2} \right), \\ \sigma_{yz} &= \frac{6}{h} T_y \left(\frac{1}{4} - \frac{z^2}{h^2} \right).\end{aligned}\tag{6.76}$$

These formulae generalize to plates the classical result of the *Jourawski's formula* for the shear stresses in beams. They state that the variation of the transverse shear stresses σ_{xz} and σ_{yz} through the thickness of the plate is parabolic and that the maximum is get in correspondence of the mid-plane, where they attain 1.5 times their average value:

$$\sigma_{xz}^{max} = \frac{3}{2} \frac{T_x}{h}, \quad \sigma_{yz}^{max} = \frac{3}{2} \frac{T_y}{h}.\tag{6.77}$$

6.2.11 Evaluation of the transverse normal stress

We can assess now the assumption $\sigma_{zz} = 0$ made and empirically justified in Sect. 6.2.3. Let us consider, for the sake of simplicity, the case of $\mathbf{b} = \mathbf{o}$ and of only orthogonal lateral loads, i.e. $\boldsymbol{\tau}^T = (0, 0, \tau_z^T)$, $\boldsymbol{\tau}^B = (0, 0, \tau_z^B)$. From the third component of the equilibrium equation (6.35) and from eqs. (6.39) and (6.76) we get

$$\begin{aligned} \frac{\partial \sigma_{zz}}{\partial z} &= -\frac{\partial \sigma_{zx}}{\partial x} - \frac{\partial \sigma_{zy}}{\partial y} = -\frac{6}{h} \left(\frac{1}{4} - \frac{z^2}{h^2} \right) \left(\frac{\partial T_x}{\partial x} + \frac{\partial T_y}{\partial y} \right) \\ &= \frac{12\tau_z^s}{h} \left(\frac{1}{4} - \frac{z^2}{h^2} \right). \end{aligned} \quad (6.78)$$

Integrating,

$$\sigma_{zz} = \frac{12\tau_z^s}{h} z \left(\frac{1}{4} - \frac{1}{3} \frac{z^2}{h^2} \right) + \phi_z(x, y), \quad (6.79)$$

and from the boundary condition on S_T ,

$$\sigma_{zz}^T = \sigma_{zz} \left(\frac{h}{2} \right) = \tau_z^T = \tau_z^s + \tau_z^a \rightarrow \phi_z(x, y) = \tau_z^a, \quad (6.80)$$

so finally

$$\sigma_{zz} = \tau_z^s \frac{z}{h} \left(3 - 4 \frac{z^2}{h^2} \right) + \tau_z^a. \quad (6.81)$$

The distribution of σ_{zz} so found matches the value of the applied tractions on the two surfaces S_T and S_B :

$$\sigma_{zz}^T = \tau_z^a + \tau_z^s = \tau_z^T, \quad \sigma_{zz}^B = \tau_z^a - \tau_z^s = -\tau_z^B, \quad (6.82)$$

and its variation, cubic, is shown in Fig. 6.5; the maximum value is get either on S_T or S_B and it is equal to the applied traction, which is, usually, far below the value of the in-plane stresses $\sigma_{\alpha\beta}$, $\alpha, \beta \in \{1, 2\}$. This considerations better justify the assumption $\sigma_{zz} = 0$ everywhere in the plate.

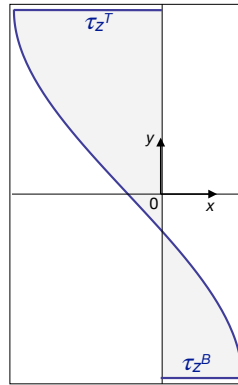


Figure 6.5: Diagram of σ_{zz} .

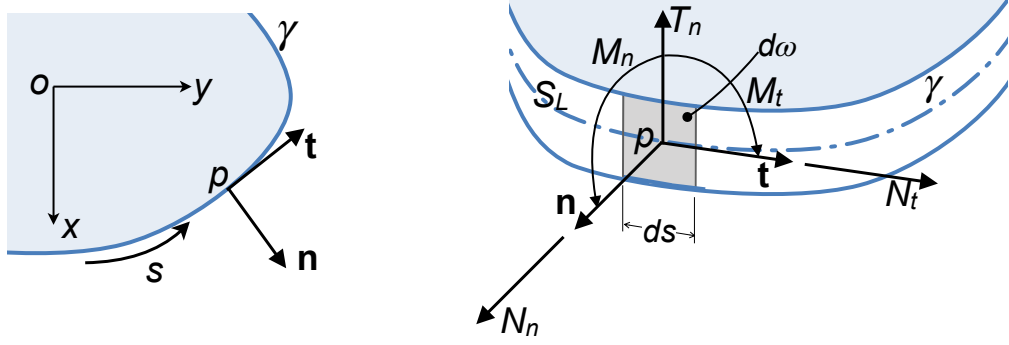


Figure 6.6: Boundary actions.

6.2.12 Boundary conditions

The equilibrium equations (6.38) and (6.48) are not sufficient to determine all the static unknowns: plates are *intrinsically hyperstatic bodies*. We need hence to introduce in the computation not only the balance equations, but also the constitutive law, i.e. we need to make use of the *elastic* equilibrium equations (6.51) and (6.56). These are partial differential equations of the second and fourth order respectively. The question of how many and which boundary conditions are to be associated to eqs. (6.51) and (6.56) has needed a long period to be solved and the arguments that lead to the solution are detailed below. In order to write the boundary conditions, we refer to a generic situation for the boundary of the plate, the lateral surface S_L whose trace in the mid-plane is the curve γ , see Fig. 6.6; at a point $p \in \gamma$, $\mathbf{n} = (n_x, n_y, 0)$ and $\mathbf{t} = (-n_y, n_x, 0)$ are the unit vectors of the mid-plane respectively orthogonal and tangent to γ .

On an infinitesimal surface element $d\omega \in S_L$ of width ds , there are the actions $\mathbf{N}_{\mathbf{n}} = (N_n, N_t)$ for extension, T_n , for shear, and $\mathbf{M}_{\mathbf{n}} = (M_n, M_t)$ for bending, see again Fig. 6.6. Because \mathbf{N} and \mathbf{M} are second-rank tensors, we have that

$$\mathbf{N}_{\mathbf{n}} = \mathbf{N} \mathbf{n} \rightarrow \begin{cases} N_n = (\mathbf{n} \otimes \mathbf{n}) \cdot \mathbf{N} = N_x n_x^2 + 2N_{xy} n_x n_y + N_y n_y^2, \\ N_t = (\mathbf{t} \otimes \mathbf{n}) \cdot \mathbf{N} = N_{xy}(n_x^2 - n_y^2) + n_x n_y (N_y - N_x), \end{cases} \quad (6.83)$$

and in the same way

$$\mathbf{M}_{\mathbf{n}} = \mathbf{M} \mathbf{n} \rightarrow \begin{cases} M_n = (\mathbf{n} \otimes \mathbf{n}) \cdot \mathbf{M} = M_x n_x^2 + 2M_{xy} n_x n_y + M_y n_y^2, \\ M_t = (\mathbf{t} \otimes \mathbf{n}) \cdot \mathbf{M} = M_{xy}(n_x^2 - n_y^2) + n_x n_y (M_y - M_x). \end{cases} \quad (6.84)$$

For what concerns T_n , it is obtained by simple projection on \mathbf{n} of the shear forces vector $\mathbf{T} = (T_x, T_y)$:

$$T_n = \mathbf{T} \cdot \mathbf{n} = T_x n_x + T_y n_y. \quad (6.85)$$

In the same way, we can proceed for the displacement vector of the mid-plane, $\mathbf{u}_0 = (u_0, v_0, w_0)$. In particular, we need to project \mathbf{u}_0 on \mathbf{n} , \mathbf{t} and \mathbf{e}_z , the unit vector of the axis z :

$$\begin{aligned} u_n &= \mathbf{u}_0 \cdot \mathbf{n} = (u_0, v_0, w_0) \cdot (n_x, n_y, 0) = u_0 n_x + v_0 n_y, \\ u_t &= \mathbf{u}_0 \cdot \mathbf{t} = (u_0, v_0, w_0) \cdot (-n_y, n_x, 0) = -u_0 n_y + v_0 n_x, \\ u_z &= \mathbf{u}_0 \cdot \mathbf{e}_z = (u_0, v_0, w_0) \cdot (0, 0, 1) = w_0. \end{aligned} \quad (6.86)$$

We can now write the boundary conditions for any point of the border and let us begin with the boundary conditions for the membrane equations:

- *kinematical* (or *geometrical*) conditions:

$$u_n = \hat{u}_n, \quad u_t = \hat{u}_t; \quad (6.87)$$

- *natural* conditions:

$$N_n = \hat{F}_n, \quad N_t = \hat{F}_t, \quad (6.88)$$

where $\hat{u}_n, \hat{u}_t, \hat{F}_n$ and \hat{F}_t are known values. A list, not exhaustive but comprehending the more important and common cases of boundary conditions for the membrane equations, is given below:

- supported border: $u_n = 0, u_t = 0$;
- supported border free to slide along \mathbf{t} : $u_n = 0, N_t = 0$;
- free unloaded border: $N_n = 0, N_t = 0$;
- free loaded border: $N_n = \hat{F}_n, N_t = \hat{F}_t$.

Let us now consider the boundary conditions for the bending equation; now, a point $p \in \gamma$ can have:

- a displacement along z : w_0 ;
- a rotation about \mathbf{t} : $\frac{\partial w_0}{\partial \mathbf{n}}$;
- a rotation about \mathbf{n} : $\frac{\partial w_0}{\partial \mathbf{t}}$.

Statically, the possible actions are:

- a shear: T_n ;
- a bending moment: M_n ;
- a twisting moment: M_t .

The conditions to be written must be specified for each case, let us see the most important ones.

6.2.12.1 Simply supported edges

In this case the boundary conditions are

$$w_0 = 0, \quad M_n = 0. \quad (6.89)$$

For the case of a border orthogonal to the x -axis, i.e. for $\mathbf{n} = \mathbf{e}_x$,

$$M_n = M_x = -\frac{h^3}{12} \frac{E}{1 - \nu^2} \left(\frac{\partial^2 w_0}{\partial x^2} + \nu \frac{\partial^2 w_0}{\partial y^2} \right), \quad (6.90)$$

so the natural condition becomes

$$\frac{\partial^2 w_0}{\partial x^2} + \nu \frac{\partial^2 w_0}{\partial y^2} = 0. \quad (6.91)$$

Because on such a border $x = \text{const.}$ and $w_0 = 0$,

$$\frac{\partial^2 w_0}{\partial y^2} = 0, \quad (6.92)$$

and finally the natural boundary condition can be written

$$\frac{\partial^2 w_0}{\partial x^2} = 0. \quad (6.93)$$

For this particular case, originally, Navier proposed the boundary conditions

$$w_0 = 0, \quad \Delta w_0 = 0, \quad (6.94)$$

that actually are equivalent to the above ones.

6.2.12.2 Clamped edges

For such a case, the boundary conditions are

$$w_0 = 0, \quad \frac{\partial w_0}{\partial \mathbf{n}} = 0. \quad (6.95)$$

To recall that

$$\frac{\partial w_0}{\partial \mathbf{n}} = \nabla w_0 \cdot \mathbf{n} = \left(\frac{\partial w_0}{\partial x}, \frac{\partial w_0}{\partial y}, \frac{\partial w_0}{\partial x} \right) \cdot (n_x, n_y, 0) = \frac{\partial w_0}{\partial x} n_x + \frac{\partial w_0}{\partial y} n_y. \quad (6.96)$$

6.2.12.3 Free edges

According to the approach of Poisson (1829), there are three boundary conditions to be written for a free edge:

$$T_n = \hat{F}_z, \quad M_n = \hat{M}_n, \quad M_t = \hat{M}_t. \quad (6.97)$$

Actually, this is true also for the two previous cases, where one could write:

- simply supported edge:

$$w_0 = 0 \Rightarrow T_n \neq 0, \quad \frac{\partial w_0}{\partial \mathbf{t}} = 0 \Rightarrow M_t \neq 0, \quad M_n = 0 \Rightarrow \frac{\partial w_0}{\partial \mathbf{n}} \neq 0;$$

- clamped edge:

$$w_0 = 0 \Rightarrow T_n \neq 0, \quad \frac{\partial w_0}{\partial \mathbf{t}} = 0 \Rightarrow M_t \neq 0, \quad \frac{\partial w_0}{\partial \mathbf{n}} = 0 \Rightarrow M_n \neq 0.$$

However, this approach is *false*: in fact, $\frac{\partial w_0}{\partial \mathbf{n}}$ and $\frac{\partial w_0}{\partial \mathbf{t}}$ are not independent, so the number of boundary conditions cannot be three. The reduction of the number of boundary conditions from 3 to 2, and their correct expression, can be illustrated by a classical procedure due to Kelvin, detailed in the next Section³.

³The method proposed by Kelvin (1867) to introduce the correct boundary conditions was first established by Kirchhoff through a variational approach (1850).

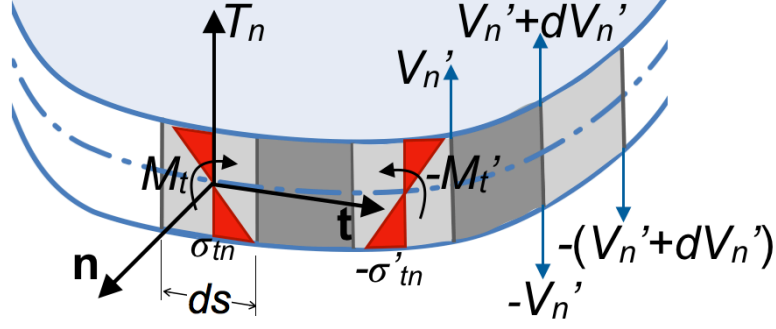


Figure 6.7: Kelvin's reduction of the boundary conditions.

6.2.12.4 The Kelvin's reduction of the boundary conditions

Let us imagine of subdividing the plate's edge into a series of parallel stripes of infinitesimal width ds , see Fig. 6.7. On each stripe acts a shear

$$T_n ds \quad (6.98)$$

and a twisting moment

$$M_t ds. \quad (6.99)$$

We add, ideally, two equal and opposite couples to each stripe: the first one is the fictitious couple

$$-M'_t ds, \quad (6.100)$$

result of the shear stress $-\sigma'_{tn}$ and opposite to the real moment M_t . The second couple is composed by two vertical, and again fictitious, forces $\pm V'_n$ applied on the edges of the stripe, so as that

$$V'_n ds = M'_t ds \Rightarrow V'_n = M'_t. \quad (6.101)$$

On the following stripe, in the sense of \mathbf{t} , we add the couple $-(M'_t + dM'_t)ds$ and the forces $\pm(V'_n + dV'_n)ds$, giving a moment equal and opposite to $-(M'_t + dM'_t)ds$, and so on for all the stripes. On the edge shared by two neighbouring stripes, the forces $-V'_n$ and $(V'_n + dV'_n)$ give the net force, per unit length,

$$\frac{dV'_n}{ds} = \frac{dM'_t}{ds}, \quad (6.102)$$

while the twist moment per unit length is $M_t - M'_t$. For the Saint Venant's Principle, because the moments $-M'_t ds$ and $V'_n ds$ are equilibrated, the static and elastic regime of the plate is not affected sufficiently far from the edge (for a distance, say, of the order of the plate's thickness). If now we chose $|M'_t| = |M_t|$, the twisting moment is null on the boundary and it is substituted by a distribution of vertical forces, per unit length, equal to

$$\frac{dV_n}{ds} = \frac{dM_t}{ds}. \quad (6.103)$$

These forces, called *substitution forces*, are statically equivalent to the twist moment M_t . The vertical reaction of a support is hence not T_n , but

$$T_n^* = T_n + \frac{dM_t}{ds}. \quad (6.104)$$

The force T_n^* is called the *Kirchhoff's shear*. Mechanically, this result shows that in the Kirchhoff's model the action of M_t on an edge does not give rise to a deformation, but only to a reaction, in the form of a vertical force.

Finally, the correct boundary conditions are just two and namely:

- for a free edge:

$$T_n^* = \hat{F}_z, \quad M_n = \hat{M}_n \rightarrow w_0 \neq 0, \quad \frac{\partial w_0}{\partial \mathbf{n}} \neq 0, \quad \frac{\partial w_0}{\partial \mathbf{t}} \neq 0; \quad (6.105)$$

- for a simply supported edge:

$$w_0 = 0, \quad M_n = 0 \rightarrow T_n^* \neq 0, \quad \frac{\partial w_0}{\partial \mathbf{n}} \neq 0, \quad \frac{\partial w_0}{\partial \mathbf{t}} = 0; \quad (6.106)$$

- for a clamped edge:

$$w_0 = 0, \quad \frac{\partial w_0}{\partial \mathbf{n}} = 0 \rightarrow T_n^* \neq 0, \quad M_n \neq 0, \quad \frac{\partial w_0}{\partial \mathbf{t}} = 0. \quad (6.107)$$

We can also obtain an expression of T_n^* as function of w_0 : if, e.g., $\mathbf{n} = \mathbf{e}_x$, then

$$T_n^* = T_x^* = T_x + \frac{\partial M_{xy}}{\partial y} = -\frac{h^3}{12} \frac{E}{1-\nu^2} \left[\frac{\partial^3 w_0}{\partial x^3} + (2-\nu) \frac{\partial^3 w_0}{\partial x \partial y^2} \right]; \quad (6.108)$$

in the same way, if $\mathbf{n} = \mathbf{e}_y$, we get

$$T_n^* = T_y^* = T_y + \frac{\partial M_{xy}}{\partial x} = -\frac{h^3}{12} \frac{E}{1-\nu^2} \left[\frac{\partial^3 w_0}{\partial y^3} + (2-\nu) \frac{\partial^3 w_0}{\partial x^2 \partial y} \right]. \quad (6.109)$$

Then,

$$T_n^* = T_x^* n_x + T_y^* n_y. \quad (6.110)$$

As a last point, we need to consider the case of a discontinuous M_t at some $s = s_0$. In such a case, the substitution force is

$$R = \lim_{\varepsilon \rightarrow 0} \int_{s_0-\varepsilon}^{s_0+\varepsilon} \frac{dM_t}{ds} ds = M_t^+ - M_t^-, \quad (6.111)$$

i.e., R is exactly the difference of the twist moment immediately after and before s_0 . This situation is typical of corners; in particular, for a right angle,

$$M_t^+ = M_t^- \Rightarrow R = -2M_t^-. \quad (6.112)$$

For a corner formed by two orthogonal sides parallel to the axes x and y , we get, see Fig. 6.8

$$R = -2|M_{xy}| = -\frac{h^3}{6} \frac{E}{1+\nu} \left| \frac{\partial^2 w_0}{\partial x \partial y} \right|. \quad (6.113)$$

This is a vertical downward reaction that the supports must give near the corners of a rectangular bent plate.

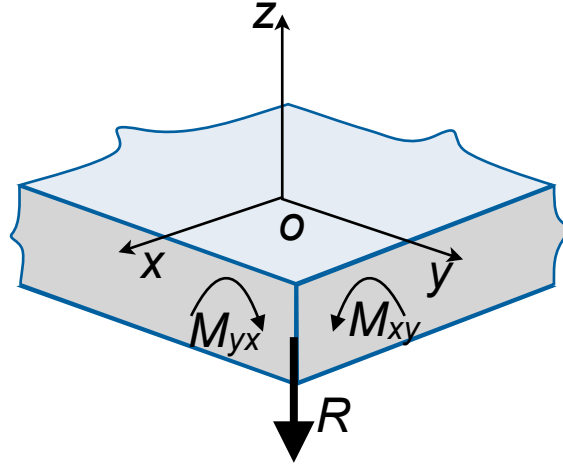


Figure 6.8: The substitution force near a right angle corner.

6.2.13 Some exact solutions

6.2.13.1 Elliptic plate

For an elliptic plate loaded by a uniformly distributed load q and clamped on the edge, the deflection is

$$w_0(x, y) = \frac{q}{D} \frac{\left(\frac{x^2}{a^2} + \frac{y^2}{b^2} - 1\right)^2}{\left(\frac{24}{a^4} + \frac{24}{b^4} + \frac{16}{a^2b^2}\right)}, \quad (6.114)$$

where a and b are the semi axes along x and y , respectively; the maximum deflection is

$$w_0^{max} = w_0(0, 0) = \frac{q}{D} \frac{1}{\left(\frac{24}{a^4} + \frac{24}{b^4} + \frac{16}{a^2b^2}\right)}. \quad (6.115)$$

6.2.13.2 Circular plate

A clamped, uniformly loaded, circular plate of radius R is a particular case of the previous elliptic plate, where $a = b = R$:

$$w_0(x, y) = \frac{q}{64 D} (x^2 + y^2 - R^2)^2, \quad (6.116)$$

with a maximum deflection in the plate's center:

$$w_0^{max} = w(0, 0) = \frac{q R^4}{64 D}. \quad (6.117)$$

In polar coordinates it is

$$w_0(r, \theta) = \frac{q}{64 D} (R^2 - r^2)^2, \quad 0 \leq r \leq R : \quad (6.118)$$

the deflection depends uniquely on the distance r from the plate's center, while it is independent from the angle θ .

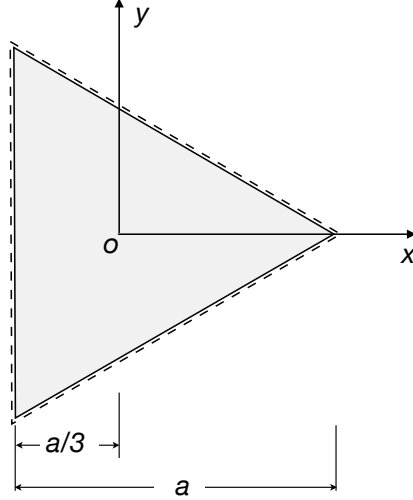


Figure 6.9: Triangular simply supported plate.

6.2.13.3 Equilateral triangular plate

For a plate like that in Fig. 6.9, uniformly loaded by a load q and simply supported on the edges, it is

$$w_0(x, y) = \frac{q}{64 a D} \left[x^3 - 3x^2y - a(x^2 + y^2) + \frac{4}{27}a^3 \right] \left(\frac{4}{9}a^2 - x^2 - y^2 \right). \quad (6.119)$$

6.2.13.4 Anticlastic bending

Let us consider the square plate ABCD in Fig. 6.10; we want to examine to which load and boundary conditions corresponds the solution

$$w_0(x, y) = -\frac{M(x^2 - y^2)}{2D(1 - \nu)}. \quad (6.120)$$

Because

$$\frac{\partial^2 w_0}{\partial x^2} = -\frac{\partial^2 w_0}{\partial y^2} = -\frac{M}{D(1 - \nu)}, \quad (6.121)$$

then

$$\Delta w_0 = 0 \Rightarrow \Delta^2 w_0 = 0 \rightarrow p = 0, \quad (6.122)$$

i.e. there is not a distributed load on the plate. We remark that for $y = \pm x$, i.e. along the square's diagonals, $w_0 = 0$: the diagonals do not move nor deform. Also,

$$\frac{\partial w_0}{\partial \mathbf{e}} = \nabla w_0 \cdot \mathbf{e} = -\frac{M}{D(1 - \nu)}(x, -y) \cdot (e_x, e_y). \quad (6.123)$$

So, if \mathbf{e} is parallel to one of the diagonals, $\mathbf{e} = \frac{1}{\sqrt{2}}(1, \pm 1) \Rightarrow$

$$\frac{\partial w_0}{\partial \mathbf{e}} = \nabla w_0 \cdot \mathbf{e} = -\frac{M}{\sqrt{2}D(1 - \nu)}(x \mp y), \quad (6.124)$$

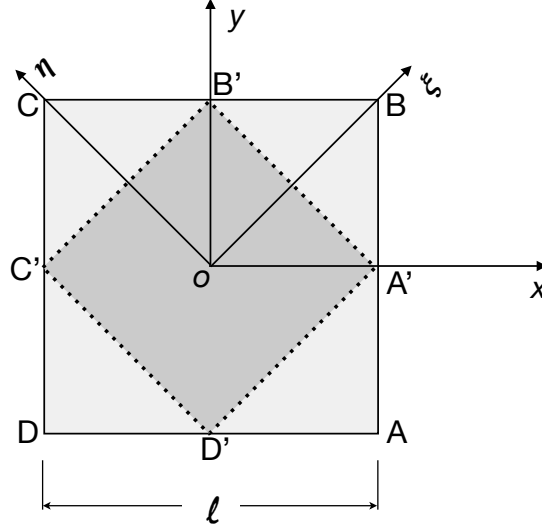


Figure 6.10: Anticlastic bending.

and on a line parallel to \mathbf{e} , $y = \pm x + a$, $a = \text{const}$, we get

$$\frac{\partial w_0}{\partial \mathbf{e}} = \nabla w_0 \cdot \mathbf{e} = \pm \frac{M a}{\sqrt{2D(1-\nu)}} : \quad (6.125)$$

the slope along the segments parallel to the diagonals is constant: such segments remain straight lines and the final bent surface is a ruled surface (i.e. through any point of the plate pass two orthogonal lines entirely belonging to the deformed surface). Then,

$$\begin{aligned} M_x &= -D \left(\frac{\partial^2 w_0}{\partial x^2} + \nu \frac{\partial^2 w_0}{\partial y^2} \right) = M, \\ M_y &= -D \left(\frac{\partial^2 w_0}{\partial y^2} + \nu \frac{\partial^2 w_0}{\partial x^2} \right) = -M, \\ M_{xy} &= -D(1-\nu) \frac{\partial^2 w_0}{\partial x \partial y} = 0, \end{aligned} \quad (6.126)$$

From eq. (6.120) we see that lines parallel to axis x deform into a concave parabola, while those parallel to axis y into a convex one. In addition, the edges of the plate are not fixed, as it is easily checked:

$$\begin{aligned} w_0 \left(\pm \frac{\ell}{2}, y \right) &\neq 0, \quad w_0 \left(x, \pm \frac{\ell}{2} \right) \neq 0, \\ \frac{\partial w_0}{\partial \mathbf{n}} \Big|_{x=\pm \frac{\ell}{2}} &= \pm \frac{\partial w_0}{\partial x} \Big|_{x=\pm \frac{\ell}{2}} \neq 0, \\ \frac{\partial w_0}{\partial \mathbf{n}} \Big|_{y=\pm \frac{\ell}{2}} &= \pm \frac{\partial w_0}{\partial y} \Big|_{y=\pm \frac{\ell}{2}} \neq 0, \end{aligned} \quad (6.127)$$

and

$$\begin{aligned} T_x^* &= T_x + \frac{\partial M_{xy}}{\partial y} = T_x = -D \Delta w_{0,x} = 0, \\ T_y^* &= T_y + \frac{\partial M_{xy}}{\partial x} = T_y = -D \Delta w_{0,y} = 0. \end{aligned} \quad (6.128)$$

So, finally, the only way to deform the plate is to act upon it with distributed bending couples on the edges: M on $x = \pm \frac{\ell}{2}$, $-M$ on $y = \pm \frac{\ell}{2}$, like in Fig. 6.11. Now, let us

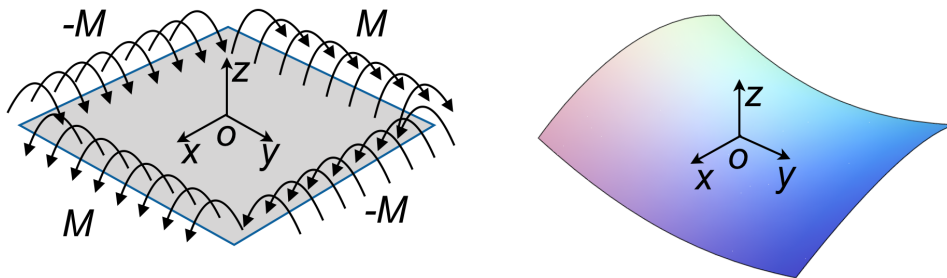


Figure 6.11: Anticlastic bending: actions on the boundary and bent plate.

consider the part $A'B'C'D'$ of the plate shaded in Fig. 6.10; w_0 is still the same, but now the boundary is different. Nevertheless, because the boundary is parallel to the diagonals, we already know that it remains straight. As a consequence, bending moments are null along these lines, but not necessarily the twisting moments. In fact, because the unit normal to the boundary of the shaded part is $\mathbf{n} = \frac{1}{\sqrt{2}}(\pm 1, \pm 1)$, we get

$$\begin{aligned} M_n &= M_x n_x^2 + 2M_{xy} n_x n_y + M_y n_y^2 = M(n_x^2 - n_y^2) = 0, \\ M_t &= M_{xy}(n_x^2 - n_y^2) + n_x n_y (M_y - M_x) = -2M n_x n_y = \pm M, \\ T_n &= T_x n_x + T_y n_y = 0. \end{aligned} \quad (6.129)$$

So, in A' and C' we have a net vertical force $R = -2M$ while in B' and D' $R = 2M$; finally, the plate $A'B'C'D'$ is like in Fig. 6.12. For ending, we remark that the same problem can be studied in the frame $\{\xi, \eta\}$, Fig. 6.10. Because $x = \xi \cos \theta - \eta \sin \theta$, $y = \xi \sin \theta + \eta \cos \theta$, we get

$$w_0(\xi, \eta) = \frac{M \xi \eta}{D(1 - \nu)}. \quad (6.130)$$

This problem is called the *anticlastic bending* of plates. It is currently used in laboratory tests, because, on one hand, it is rather easy to be realized, on the other hand, the stress and strain fields are homogeneous, so allowing reliable measures.

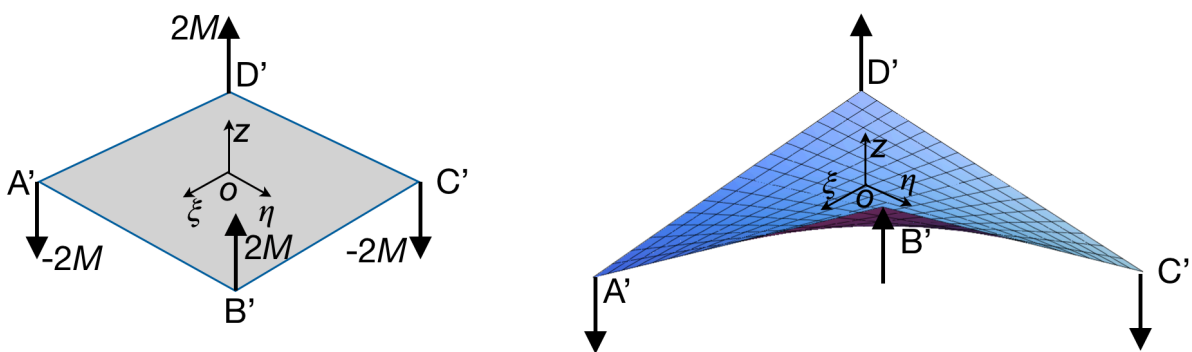


Figure 6.12: Anticlastic bending: actions on the corners and bent plate.

6.2.13.5 Navier's method for rectangular plates

Let us consider a rectangular simply supported plate, $0 \leq x \leq a$, $0 \leq y \leq b$. If the plate is loaded by a distributed load of the type

$$q(x, y) = q_{mn} \sin \frac{m\pi x}{a} \sin \frac{n\pi y}{b}, \quad (6.131)$$

then it is easy to check that the solution $w_0(x, y)$ that satisfies both the field equation (6.56) and the boundary conditions (6.89) is

$$w_0(x, y) = w_{mn} \sin \frac{m\pi x}{a} \sin \frac{n\pi y}{b}. \quad (6.132)$$

Because

$$\Delta^2 w_0 = \pi^4 \left(\frac{m^2}{a^2} + \frac{n^2}{b^2} \right)^2 w_{mn} \sin \frac{m\pi x}{a} \sin \frac{n\pi y}{b}, \quad (6.133)$$

we get that $\forall m, n$ it must be

$$\pi^4 \left(\frac{m^2}{a^2} + \frac{n^2}{b^2} \right)^2 w_{mn} = \frac{q_{mn}}{D} \Rightarrow w_{mn} = \frac{q_{mn}}{\pi^4 \left(\frac{m^2}{a^2} + \frac{n^2}{b^2} \right)^2 D}. \quad (6.134)$$

As any load function can be expressed by a double Fourier series,

$$q(x, y) = \sum_{m=0}^{\infty} \sum_{n=0}^{\infty} q_{mn} \sin \frac{m\pi x}{a} \sin \frac{n\pi y}{b}, \quad (6.135)$$

with

$$q_{mn} = \frac{4}{ab} \int_0^a \int_0^b q(x, y) \sin \frac{m\pi x}{a} \sin \frac{n\pi y}{b} dx dy, \quad (6.136)$$

a solution for a generic load can be obtained superposing the solutions w_{mn} of each harmonic. In particular, for $q(x, y) = q = \text{const}$, we get

$$q_{mn} = \frac{16 q}{\pi^2 mn}, \quad m, n = 1, 3, 5, \dots \quad (6.137)$$

the double series converges quickly for w_0 but slowly for \mathbf{M} .

6.2.13.6 Levy's method for rectangular plates

This method for simply supported plates $0 \leq x \leq a$, $-\frac{b}{2} \leq y \leq \frac{b}{2}$, makes use of simple series: the deflection w_0 is expressed as

$$w_0(x, y) = w_g(x, y) + w_p(x, y), \quad (6.138)$$

where $w_g(x, y)$ is the general integral of the homogeneous equation

$$\Delta^2 w_0 = 0, \quad (6.139)$$

while $w_p(x, y)$ is a particular integral. Generally speaking,

$$w_g(x, y) = \sum_{n=1}^{\infty} Y_n(y) \sin a_n x, \quad a_n = \frac{n\pi}{a}. \quad (6.140)$$

This expression is a solution of (6.139) if and only if

$$Y_n^{iv}(y) - 2a_n^2 Y_n''(y) + a_n^4 Y_n(y) = 0 \quad \forall n. \quad (6.141)$$

The general integral of this equation is

$$Y_n(y) = A_n \sinh a_n y + B_n \cosh a_n y + C_n a_n y \sinh a_n y + D_n a_n y \cosh a_n y. \quad (6.142)$$

The particular integral $w_p(x, y)$ depends on the load; for a uniformly distributed load q ,

$$w_p(x, y) = \frac{q}{24D} (x^4 - 2ax^3 + a^3x) = \frac{4qa^4}{\pi^5 D} \sum_{n=1}^{\infty} \frac{1}{n^5} \sin a_n x, \quad n = 1, 3, 5, \dots \quad (6.143)$$

It can be easily checked that $w_g(x, y)$ and $w_p(x, y)$ satisfy the boundary conditions for $x = 0$ and $x = a$. In addition, for a uniform load only the second and third terms are not null, because for symmetry it must be $Y_n(y) = Y_n(-y)$. In such a case we get

$$w_0(x, y) = \frac{qa^4}{D} \sum_{n=1}^{\infty} \left(\frac{4}{n^5 \pi^5} + \xi_n \cosh a_n y + \eta_n \frac{n\pi y}{a} \sinh a_n y \right) \sin \frac{n\pi x}{a}, \quad n = 1, 3, 5, \dots \quad (6.144)$$

The coefficients ξ_n and η_n are determined by the boundary conditions:

$$w_0(x, \pm \frac{b}{2}) = 0, \quad \frac{\partial^2 w_0}{\partial y^2} \Big|_{y=\pm \frac{b}{2}} = 0, \quad (6.145)$$

that give

$$\xi_n = -\frac{4 + 2\varphi_n \tanh \varphi_n}{n^5 \pi^5 \cosh \varphi_n}, \quad \eta_n = \frac{2}{n^5 \pi^5 \cosh \varphi_n}, \quad \varphi_n = \frac{n\pi b}{2a}. \quad (6.146)$$

This series is very quickly convergent, practically a very good estimation for w_0 is obtained just with the first term; for \mathbf{M} more terms are needed, but the convergence is still rapid.

6.3 The Reissner-Mindlin theory

The main problem with the Kirchhoff's theory is the absence of transverse shear strains, due to the second kinematical assumption of the model, see Sect. 6.2.1, which engenders the vanishing of the transverse shear stresses⁴. It seems hence obvious, in order to let appear transverse stresses σ_{xz} and σ_{yz} , to remove the second kinematical assumption of conservation of the orthogonality of the normal segments. This has been done

⁴We have seen that, with the assumption of symmetric loads distribution, these can be calculated using the equilibrium equations

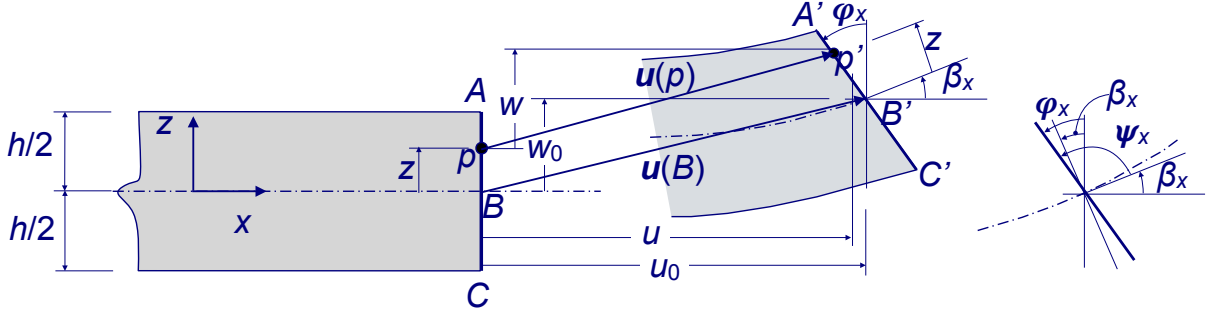


Figure 6.13: Reissner-Mindlin's kinematics in the $\{x, z\}$ plane.

independently, and following two different approaches, by Reissner (1945) and Mindlin (1951).

Removing the second Kirchhoff's kinematical assumption means that a segment originally orthogonal to the mid-plane will be no more orthogonal to the deformed mid-surface. However, we preserve the first and third kinematical assumptions of Kirchhoff: any orthogonal segment remains straight and of the same length.

Geometrically speaking, this means that in the plane $\{x, z\}$, see Fig. 6.13, it will be

$$\psi_x = \frac{\pi}{2} + \varphi_x - \beta_x. \quad (6.147)$$

The shear strain is hence (recall that for the small strain assumption, $\beta_x \simeq \tan \beta_x = \frac{\partial w_0}{\partial x}$)

$$\gamma_x = \frac{\pi}{2} - \psi_x = \beta_x - \varphi_x \simeq \frac{\partial w_0}{\partial x} - \varphi_x. \quad (6.148)$$

Similarly,

$$\gamma_y = \frac{\pi}{2} - \psi_y = \beta_y - \varphi_y \simeq \frac{\partial w_0}{\partial y} - \varphi_y, \quad (6.149)$$

and the displacement field is then (the small strain assumption is still used)

$$\mathbf{u}(x, y, z) = \begin{pmatrix} u_0(x, y) - z\varphi_x(x, y) \\ v_0(x, y) - z\varphi_y(x, y) \\ w_0(x, y) \end{pmatrix} \quad (6.150)$$

so that now the strain tensor becomes

$$\boldsymbol{\varepsilon}(p) = \frac{\nabla \mathbf{u}(p) + \nabla \mathbf{u}^\top(p)}{2} = \begin{bmatrix} \frac{\partial u_0}{\partial x} - z \frac{\partial \varphi_x}{\partial x} & \frac{1}{2} \left(\frac{\partial u_0}{\partial y} + \frac{\partial v_0}{\partial x} \right) - \frac{1}{2} z \left(\frac{\partial \varphi_x}{\partial y} + \frac{\partial \varphi_y}{\partial x} \right) & \frac{1}{2} \left(\frac{\partial w_0}{\partial x} - \varphi_x \right) \\ \frac{1}{2} \left(\frac{\partial u_0}{\partial y} + \frac{\partial v_0}{\partial x} \right) - \frac{1}{2} z \left(\frac{\partial \varphi_x}{\partial y} + \frac{\partial \varphi_y}{\partial x} \right) & \frac{\partial v_0}{\partial y} - z \frac{\partial \varphi_y}{\partial y} & \frac{1}{2} \left(\frac{\partial w_0}{\partial y} - \varphi_y \right) \\ \frac{1}{2} \left(\frac{\partial w_0}{\partial x} - \varphi_x \right) & \frac{1}{2} \left(\frac{\partial w_0}{\partial y} - \varphi_y \right) & 0 \end{bmatrix}. \quad (6.151)$$

Hence, we still can write eq. (6.33), but now the definition of the curvatures changes:

$$\boldsymbol{\kappa} = \left\{ \begin{array}{c} -\frac{\partial\varphi_x}{\partial x} \\ -\frac{\partial\varphi_y}{\partial y} \\ -\left(\frac{\partial\varphi_x}{\partial y} + \frac{\partial\varphi_y}{\partial x}\right) \end{array} \right\}. \quad (6.152)$$

Also, now ε_{xz} and ε_{yz} are different from zero. For the planar part, we still can write eq. (6.33), but now in addition we have also the components of the transverse shear

$$\left\{ \begin{array}{c} \sigma_{xz} \\ \sigma_{yz} \end{array} \right\} = \begin{bmatrix} G & 0 \\ 0 & G \end{bmatrix} \left\{ \begin{array}{c} 2\varepsilon_{xz} \\ 2\varepsilon_{yz} \end{array} \right\}. \quad (6.153)$$

Hence, with the Reissner-Mindlin theory, we can obtain the transverse shear stresses directly from the constitutive law. However, we find here a problem of this theory: σ_{xz} and σ_{yz} are constant through the thickness, because so are ε_{xz} and ε_{yz} , as a consequence of the assumption that any orthogonal segment remains straight also in the bent plate. This result is mechanically inconsistent: on one hand, we obtain tangential stresses $\sigma_{zx} = \sigma_{xz}$ and $\sigma_{zy} = \sigma_{yz}$ different from zero on S_T and S_B , which is correct only if an equal external tangential load is applied. On the other hand, we know, see Sect. 6.2.9, that the correct variation with z of σ_{xz} and σ_{yz} is parabolic.

To solve this inconsistency, one should pass to higher order theories (namely, to the Third Order Shear Deformation Theory of Reddy). In the framework of the Reissner-Mindlin theory, however, a *correction function* $\xi(z)$ is then introduced to have a parabolic variation of σ_{xz} and σ_{yz} through the thickness:

$$\xi(z) = \tau \left[1 - \left(\frac{z}{h/2} \right)^2 \right]. \quad (6.154)$$

The constant τ can be determined in different ways. A first one, is to conserve the value of the shear stress in correspondance of $z = 0$, which results in

$$\tau = \frac{T}{h}, \quad (6.155)$$

i.e. τ corresponds to the mean value of the shear stress produced by the shear force T in the Reissner-Mindlin model without corrections. If, instead, we conserve the shear force T , then

$$\tau = \frac{3T}{2h}. \quad (6.156)$$

Finally, the choice commonly done is to put

$$\tau = \frac{5T}{4h}, \quad (6.157)$$

i.e. a mean value: neither the shear stress nor the shear force are conserved. With such a choice for τ we get

$$\begin{aligned}\sigma_{xz} &= 2G\varepsilon_{xz}(x, y)\xi(z) = \frac{5}{4} \frac{E}{2(1+\nu)} \left[1 - \left(\frac{z}{h/2} \right)^2 \right] \left(\frac{\partial w_0}{\partial x} - \varphi_x \right), \\ \sigma_{yz} &= 2G\varepsilon_{yz}(x, y)\xi(z) = \frac{5}{4} \frac{E}{2(1+\nu)} \left[1 - \left(\frac{z}{h/2} \right)^2 \right] \left(\frac{\partial w_0}{\partial y} - \varphi_y \right),\end{aligned}\tag{6.158}$$

which gives

$$\begin{aligned}T_x &= \int_{-\frac{h}{2}}^{+\frac{h}{2}} \sigma_{xz} dz = \frac{5}{6} \frac{E h}{2(1+\nu)} \left(\frac{\partial w_0}{\partial x} - \varphi_x \right), \\ T_y &= \int_{-\frac{h}{2}}^{+\frac{h}{2}} \sigma_{yz} dz = \frac{5}{6} \frac{E h}{2(1+\nu)} \left(\frac{\partial w_0}{\partial y} - \varphi_y \right).\end{aligned}\tag{6.159}$$

The correction factor is hence $\lambda = \frac{5}{6}$ for the shear forces, while $\lambda = \frac{5}{4}$ for the shear stress.

The expression of \mathbf{N} does not change with respect to the Kirchhoff's theory, while for \mathbf{M} we get

$$\mathbf{M} = \frac{h^3}{12} \mathbb{D}\boldsymbol{\kappa} \Rightarrow \begin{cases} M_x = -\frac{h^3}{12} \frac{E}{1-\nu^2} \left(\frac{\partial \varphi_x}{\partial x} + \nu \frac{\partial \varphi_y}{\partial y} \right), \\ M_y = -\frac{h^3}{12} \frac{E}{1-\nu^2} \left(\frac{\partial \varphi_y}{\partial y} + \nu \frac{\partial \varphi_x}{\partial x} \right), \\ M_{xy} = -\frac{h^3}{12} \frac{E}{1+\nu} \left(\frac{\partial \varphi_x}{\partial y} + \frac{\partial \varphi_y}{\partial x} \right).\end{cases}\tag{6.160}$$

The equilibrium equations (6.38), (6.39) and (6.47) do not change, of course; passing to a unique, higher order equation for bending equilibrium, like eq. (6.48), is now meaningless, because we cannot obtain an equation of elastic equilibrium depending on a unique unknown, $w_0(x, y)$. In fact, the elastic equilibrium equations can be obtained, as usual, injecting the expressions of T_x, T_y, M_x, M_y and M_{xy} into the shear and bending equilibrium equations (the extension equilibrium equations (6.51) do not change), to obtain

$$\begin{aligned}\frac{h^2}{6(1-\nu)} \left[\frac{\partial^2 \varphi_x}{\partial x^2} + (1-\nu) \frac{\partial^2 \varphi_x}{\partial y^2} + \frac{\partial^2 \varphi_y}{\partial x \partial y} \right] + \lambda \left(\frac{\partial w_0}{\partial x} - \varphi_x \right) &= 0, \\ \frac{h^2}{6(1-\nu)} \left[(1-\nu) \frac{\partial^2 \varphi_y}{\partial x^2} + \frac{\partial^2 \varphi_y}{\partial y^2} + \frac{\partial^2 \varphi_x}{\partial x \partial y} \right] + \lambda \left(\frac{\partial w_0}{\partial y} - \varphi_y \right) &= 0, \\ \lambda \frac{E h}{2(1+\nu)} \left(\frac{\partial^2 w_0}{\partial x^2} + \frac{\partial^2 w_0}{\partial y^2} - \frac{\partial \varphi_x}{\partial x} - \frac{\partial \varphi_y}{\partial y} \right) + f_z &= 0.\end{aligned}\tag{6.161}$$

These are three second-order coupled partial differential equations; the unknown functions are $w_0(x, y), \varphi_x(x, y)$ and $\varphi_y(x, y)$. Three boundary conditions are hence needed for each point of the boundary; they must prescribe either

- kinematical conditions: the value of $w_0, \varphi_x, \varphi_y$ (or, more generally, φ_n and φ_t), or:
- natural conditions: the value of T_n, M_n, M_t .

Finally, with the Reissner-Mindlin theory there is no more the problem of the boundary conditions found in the Kirchhoff's theory. Actually, this was a consequence of the kinematical constraint imposed by the second Kirchhoff's assumption so that, once this last removed, the problem disappears.

6.4 The Von Karman theory

The assumption of linear strains, done in the two previous theories, fails to account for the so-called *membrane effect*, by which the tensions in a deflected plate help to react the applied *lateral loads*, i.e. the surface loads orthogonal to the mid-plane.

In order to take into account for such an effect, we introduce a measure of the strain suitable for geometric non-linearities: the *Green-Lagrange strain tensor* \mathbf{L} :

$$\mathbf{L} = \frac{1}{2}(\nabla\mathbf{u} + \nabla\mathbf{u}^\top + \nabla\mathbf{u}^\top\nabla\mathbf{u}); \quad (6.162)$$

if, for the sake of convenience, we still indicate \mathbf{L} by $\boldsymbol{\varepsilon}$, then the components ε_{ij} now are⁵:

$$\begin{aligned} \varepsilon_{xx} &= u_{,x} + \frac{1}{2}(u_{,x}^2 + v_{,x}^2 + w_{,x}^2), \\ \varepsilon_{yy} &= v_{,y} + \frac{1}{2}(u_{,y}^2 + v_{,y}^2 + w_{,y}^2), \\ \varepsilon_{zz} &= w_{,z} + \frac{1}{2}(u_{,z}^2 + v_{,z}^2 + w_{,z}^2), \\ \varepsilon_{xy} &= \frac{1}{2}(u_{,y} + v_{,x} + u_{,x}u_{,y} + v_{,x}v_{,y} + w_{,x}w_{,y}), \\ \varepsilon_{xz} &= \frac{1}{2}(u_{,z} + w_{,x} + u_{,x}u_{,z} + v_{,x}v_{,z} + w_{,x}w_{,z}), \\ \varepsilon_{yz} &= \frac{1}{2}(v_{,z} + w_{,y} + u_{,y}u_{,z} + v_{,y}v_{,z} + w_{,y}w_{,z}). \end{aligned} \quad (6.163)$$

In the theory of plates of Von Karman (1910), only some of the quadratic terms are retained, namely: the quadratic terms in $w_{,x}$, $w_{,y}$ are retained, the other ones, discarded. Von Karman justifies this choice as follows:

- $u_{,x}^2$ is negligible with respect to $u_{,x}$; the same is true for $v_{,y}^2$ and $w_{,z}^2$;
- a similar argument is used also for the terms $v_{,y}v_{,z}$, $w_{,y}w_{,z}$, $u_{,z}u_{,x}$, $w_{,z}w_{,x}$, $u_{,x}u_{,y}$, $v_{,x}v_{,y}$;
- the terms $v_{,x}^2$, $u_{,y}^2$, $w_{,y}^2$, $u_{,z}^2$, $v_{,z}^2$ are of the same order of the dropped terms;
- $w_{,x}$ and $w_{,y}$ are the slopes of cross sections of the deformed mid-plane: they can be large compared to the strain components.

⁵For the sake of shortness, we indicate partial derivatives by a comma followed by the differentiation variable, e.g. $\frac{\partial u}{\partial x} = u_{,x}$ etc.

So, finally:

$$\begin{aligned}
\varepsilon_{xx} &= u_{,x} + \frac{1}{2}w_{,x}^2, \\
\varepsilon_{yy} &= v_{,y} + \frac{1}{2}w_{,y}^2, \\
\varepsilon_{zz} &= w_{,z}, \\
\varepsilon_{xy} &= \frac{1}{2}(u_{,y} + v_{,x} + w_{,x}w_{,y}), \\
\varepsilon_{xz} &= \frac{1}{2}(u_{,z} + w_{,x}), \\
\varepsilon_{yz} &= \frac{1}{2}(v_{,z} + w_{,y}).
\end{aligned} \tag{6.164}$$

We introduce again the vector $\mathbf{u}_0(x, y)$, displacement of the points of the mid-plane and we need to specify how u, v, w vary through the thickness. To this purpose, the Von Karman's theory makes the same kinematical assumptions of the Kirchhoff's theory, so that eq. (6.13) still holds and

$$\begin{aligned}
\varepsilon_{xx} &= e_x - z w_{0,xx}, \\
\varepsilon_{yy} &= e_y - z w_{0,yy}, \\
\gamma_{xy} &= 2\varepsilon_{xy} = e_{xy} - 2z w_{0,xy}, \\
\varepsilon_{xz} &= \varepsilon_{yz} = \varepsilon_{zz} = 0,
\end{aligned} \tag{6.165}$$

where we have put

$$\begin{aligned}
e_x &= u_{0,x} + \frac{1}{2}w_{0,x}^2, \\
e_y &= v_{0,y} + \frac{1}{2}w_{0,y}^2, \\
e_{xy} &= u_{0,y} + v_{0,x} + w_{0,x}w_{0,y}.
\end{aligned} \tag{6.166}$$

Still like in the Kirchhoff's theory, we assume $\sigma_{zz} = 0$, while $\sigma_{xz} = \sigma_{yz} = 0$ as a consequence of the constitutive law and of the kinematical assumptions, that lead, as in the Kirchhoff's theory, to $\varepsilon_{xz} = \varepsilon_{yz} = 0$. Finally, for $\boldsymbol{\sigma}$ we obtain once more the results of the Kirchhoff's theory, eq. (6.22), but now the definition of the strain is different.

Let us now follow a variational approach for finding the equilibrium equations (the same approach can be used also for the classical theory of Kirchhoff⁶).

The strain energy density is

$$\begin{aligned}
U &= \frac{1}{2}\boldsymbol{\sigma} \cdot \boldsymbol{\varepsilon} = \frac{1}{2} \frac{E}{1-\nu^2} \left[(\varepsilon_{xx} + \nu\varepsilon_{yy})\varepsilon_{xx} + (\varepsilon_{yy} + \nu\varepsilon_{xx})\varepsilon_{yy} + \frac{1-\nu}{2}\gamma_{xy}^2 \right] \\
&= \frac{G}{1-\nu} \left(\varepsilon_{xx}^2 + \varepsilon_{yy}^2 + 2\nu\varepsilon_{xx}\varepsilon_{yy} + \frac{1-\nu}{2}\gamma_{xy}^2 \right),
\end{aligned} \tag{6.167}$$

⁶To this purpose, the reader is addressed to the classical text of Langhaar, see the suggested references. In such a text, a presentation of the the variational approach to the boundary conditions is also given.

by consequence, the total strain energy of the plate is

$$U_p = \int_{\Omega} U \, d\omega = \int_S \left(\int_{-\frac{h}{2}}^{\frac{h}{2}} U \, dz \right) dx \, dy, \quad (6.168)$$

where S denotes the mid-surface. Once the integration over z done, we get

$$U_p = U_m + U_b, \quad (6.169)$$

where

- U_m : membrane strain energy, linear in h :

$$\begin{aligned} U_m = \frac{G h}{1 - \nu} \int_S & \left[\left(u_{0,x} + \frac{w_{0,x}^2}{2} \right)^2 + \left(v_{0,y} + \frac{w_{0,y}^2}{2} \right)^2 \right. \\ & + 2\nu \left(u_{0,x} + \frac{w_{0,x}^2}{2} \right) \left(v_{0,y} + \frac{w_{0,y}^2}{2} \right) \\ & \left. + \frac{1 - \nu}{2} (u_{0,x} + v_{0,y} + w_{0,x}w_{0,y})^2 \right] dx; \end{aligned} \quad (6.170)$$

- U_b : bending strain energy, cubic in h :

$$U_b = \frac{G h^3}{12(1 - \nu)} \int_S [w_{0,xx}^2 + w_{0,yy}^2 + 2\nu w_{0,xx}w_{0,yy} + 2(1 - \nu)w_{0,xy}^2] dx \, dy. \quad (6.171)$$

The potential energy of a lateral load $q(x, y)$ acting on the plate is

$$U_q = - \int_S q(x, y) w_0(x, y) dx \, dy, \quad (6.172)$$

so finally the total potential energy is the functional

$$V = U_m + U_b + U_q. \quad (6.173)$$

The principle of the minimum total potential energy is then used: the equilibrium configuration is that giving the least value of V . We need hence to write the conditions giving the minimum of the quadratic functional V of the two independent variables x and y . These conditions are the Euler-Lagrange equations for V : they are the equilibrium equations for the plate. To this purpose, we notice that

$$V = \int_S F(u_0, u_{0,x}, u_{0,y}; v_0, v_{0,x}, v_{0,y}; w_0, w_{0,x}, w_{0,y}, w_{0,xx}, w_{0,xy}, w_{0,yy}; x, y) dx \, dy, \quad (6.174)$$

i.e. F is a functional of three independent functions, u_0, v_0 and w_0 , so we need to write three Euler-Lagrange equations:

$$\frac{\partial F}{\partial \xi} - \frac{\partial}{\partial x} \frac{\partial F}{\partial \xi_x} - \frac{\partial}{\partial y} \frac{\partial F}{\partial \xi_y} + \frac{\partial^2}{\partial x^2} \frac{\partial F}{\partial \xi_{xx}} + \frac{\partial^2}{\partial x \partial y} \frac{\partial F}{\partial \xi_{xy}} + \frac{\partial^2}{\partial y^2} \frac{\partial F}{\partial \xi_{yy}} = 0, \quad (6.175)$$

where ξ can be either u_0, v_0 or w_0 . Because

$$\begin{aligned}
F &= \frac{G h}{1 - \nu} \left[\left(u_{0,x} + \frac{w_{0,x}^2}{2} \right)^2 + \left(v_{0,y} + \frac{w_{0,y}^2}{2} \right)^2 \right. \\
&\quad \left. + 2\nu \left(u_{0,x} + \frac{w_{0,x}^2}{2} \right) \left(v_{0,y} + \frac{w_{0,y}^2}{2} \right) + \frac{1 - \nu}{2} (u_{0,x} + v_{0,y} + w_{0,x}w_{0,y})^2 \right] \\
&\quad + \frac{G h^3}{12(1 - \nu)} [w_{0,xx}^2 + w_{0,yy}^2 + 2\nu w_{0,xx}w_{0,yy} + 2(1 - \nu)w_{0,xy}^2] - q w_0,
\end{aligned} \tag{6.176}$$

we get finally the three equilibrium equations of the plate (the third one is simplified using the first two equations):

$$\begin{aligned}
(e_x + \nu e_y)_{,x} + \frac{1 - \nu}{2} e_{xy,y} &= 0, \\
\frac{1 - \nu}{2} e_{xy,x} + (e_y + \nu e_x)_{,y} &= 0, \\
\Delta^2 w_0 &= \frac{q}{D} + \frac{12}{h^2} [(e_x + \nu e_y)w_{0,xx} + (e_y + \nu e_x)w_{0,yy} + (1 - \nu)e_{xy}w_{0,xy}].
\end{aligned} \tag{6.177}$$

The internal actions as defined in eq. (6.25) become now, through eqs. (6.22) and (6.165),

$$\begin{aligned}
N_x &= \frac{E h}{1 - \nu^2} (e_x + \nu e_y), \\
N_y &= \frac{E h}{1 - \nu^2} (e_y + \nu e_x), \\
N_{xy} &= G h e_{xy} = \frac{E h}{2(1 + \nu)} e_{xy}.
\end{aligned} \tag{6.178}$$

By consequence, eqs. (6.177)_{1,2} can be written in terms of the components of the membrane internal actions; some simple calculations give

$$\begin{aligned}
N_{x,x} + N_{xy,y} &= 0, \\
N_{xy,x} + N_{y,y} &= 0.
\end{aligned} \tag{6.179}$$

We find again eqs. (6.38) for the case $f_x = f_y = 0$, i.e. when the loads parallel to the mid-plane are null (an assumption tacitly done in this case, where the only action is the lateral load q). The above two extension equilibrium equations can be solved using the technique of the *Airy's stress function* $\chi(x, y)$:

$$N_x = \chi_{,yy}, \quad N_y = \chi_{,xx}, \quad N_{xy} = -\chi_{,xy}. \tag{6.180}$$

If \mathbf{N} is related to $\chi(x, y)$ by the previous relations, than eqs. (6.179) are automatically satisfied: the problem of determining \mathbf{N} is reduced to the that of finding a unique scalar function, $\chi(x, y)$. For what concerns eq. (6.177)₃, it becomes

$$D\Delta^2 w_0 = q + N_x w_{0,xx} + N_y w_{0,yy} + 2N_{xy} w_{0,xy}, \tag{6.181}$$

and introducing χ ,

$$D\Delta^2 w_0 = q + \chi_{,yy} w_{0,xx} + \chi_{,xx} w_{0,yy} - 2\chi_{,xy} w_{0,xy}. \tag{6.182}$$

A second relation between $w_0(x, y)$ and $\chi(x, y)$ can be easily obtained: from the equations of N_x, N_y and N_{xy} we get

$$\begin{aligned} h e_x &= \frac{1}{E}(N_x - \nu N_y) = \frac{1}{E}(\chi_{,yy} - \nu\chi_{,xx}), \\ h e_y &= \frac{1}{E}(N_y - \nu N_x) = \frac{1}{E}(\chi_{,xx} - \nu\chi_{,yy}), \\ h e_{xy} &= \frac{N_{xy}}{G} = -\frac{\chi_{,xy}}{G}, \end{aligned} \tag{6.183}$$

while

$$e_{x,yy} + e_{y,xx} - e_{xy,xy} = w_{0,xy}^2 - w_{0,xx}w_{0,yy}. \tag{6.184}$$

Eliminating e_x, e_y and e_{xy} by means of the previous equations gives

$$\Delta^2 \chi = E h (w_{0,xy}^2 - w_{0,xx}w_{0,yy}). \tag{6.185}$$

Equations (6.182) and (6.185) are the fundamental relations in the Von Karman theory of plates. They reduce the problem to the search of two bi-dimensional functions, $w_0(x, y)$ and $\chi(x, y)$. The use of χ automatically ensures the in-plane equilibrium and \mathbf{N} is found by derivation, once χ known.

6.5 Exercises

1. Check that the solution for a circular clamped plate of radius R , loaded by a uniform load q is, in polar coordinates,

$$w(r, \theta) = \frac{q}{64D}(R^2 - r^2)^2.$$

Calculate then the deflection in the center and the couples on the boundary.

2. Using the inverse method, study the case of a rectangular plate, whose sides $2a$ and $2b$ are parallel to the axes x and y respectively, with origin at the plate's center, and whose solution is the field of vertical displacements

$$w = c[(x^2 - a^2)^2 + (y^2 - b^2)^2], \quad c < 0.$$

In particular, find the conditions on the boundary (displacements and forces) and calculate the deflection and the moments in the plate's center.

3. Study a simply supported rectangular plate of sides a and b subjected to the sinusoidal load

$$p(x, y) = p_0 \sin \frac{\pi x}{a} \sin \frac{\pi y}{b}.$$

4. Consider a simply supported square plate of side ℓ , acted upon by a uniform load p ; compare the results for the deflection and moments in the plate's center using first the Navier and then the Levy approach.

Chapter 7

Membranes

7.1 Introduction

We call *membrane* a solid Ω that has the form of a surface (i.e., Ω is delimited by two outer surfaces, parallel to a central *middle surface* having a distance $h/2$ from each one of the outer surfaces, so that the *membrane thickness* h is very small compared to the other dimensions of Ω) and which is able to transmit between its parts *exclusively forces tangential to the middle surface*. Hence, *a membrane cannot transmit couples or forces perpendicular to the middle surface*.

This definition, geometrical and mechanical, states that:

- i. a membrane is a *two-dimensional solid*, i.e. it can be represented by its middle surface, not necessarily flat nor of a precise form: a membrane can be either a solid whose form is determined by the applied loads and constraints, or a solid whose form is perfectly defined;
- ii. when the membrane has not a precise form, e.g. a tissue, a cell membrane etc. (all these bodies have a null bending stiffness and cannot withstand compressive forces), then it is the two-dimensional equivalent of cables and like cables, the equilibrium configuration depends upon the applied loads; the equilibrium problem is in this case *intrinsically nonlinear*, because the equilibrium equations must be written in the deformed, unknown, configuration;
- iii. they can be studied as membranes also two-dimensional bodies having a precise form and a bending stiffness, like plates and shells, when they are submitted to loads that produce deformations only in the tangent plane and with bending strains everywhere null; this is the case, e.g., of plates loaded by in-plane forces, a case already treated in Chap. 6, but also of domes submitted to their own weight, where the membrane regime is, normally, the prevailing one.

In two practical cases the regime of membrane is particularly important:

- for tissues; in such a case the membrane can transmit only tensile forces and the impossibility of compressive forces can produce *wrinkling*, a local instability phenomenon that can be avoided prestressing the membrane;

- for masonry-like structures, e.g. walls, vaults, domes; this is the opposite case of tissues: the structure can practically transmit only compressive forces, because tensile strength is so small and unreliable that often it can be considered as null, and the presence of tensile internal actions produce cracks, the mechanical equivalent of wrinkles in this case.

We consider in the following different problems concerning membranes.

7.2 Linear theory of prestressed plane membranes

We consider the case of a flat membrane Ω that has not flexural stiffness, e.g. a tissue or a drumhead, see Fig. 7.1. The membrane belongs to the plane $x - y$, its boundary is $\partial\Omega$ and $\mathbf{n}(p)$, $\forall p \in \partial\Omega$, is the outward normal to $\partial\Omega$, $\mathbf{n} = (n_x, n_y, 0)$; $\{\mathbf{e}_x, \mathbf{e}_y, \mathbf{e}_z\}$ is the orthonormal basis associated with the frame $\{x, y, z\}$ and $\mathbf{u}(p) = (u, v, w)$, $p \in \Omega$, is the displacement vector. The membrane is acted upon by :

- a distributed load $q(p)\mathbf{e}_z \forall p \in \Omega$;
- a distribution of tensile forces $\mathbf{T}(p)=T_0 \mathbf{n}(p) \forall p \in \partial\Omega$, $T_0 > 0$.

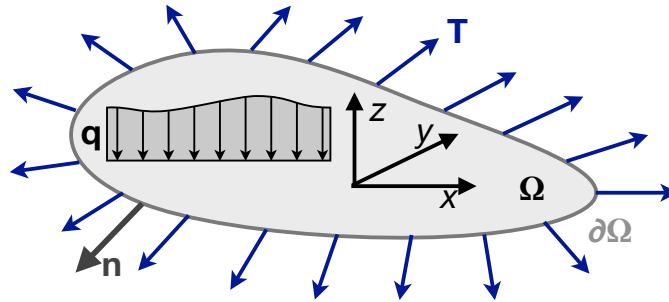


Figure 7.1: General sketch of a prestressed membrane.

We first remark that the membrane cannot find its equilibrium in the undeformed configuration, i.e., it cannot remain plane, whenever the lateral load $q(p) \neq 0$. In fact, because the only internal actions are the so-called *membrane forces*, i.e. forces laying in the tangent plane to the membrane $\forall p \in \Omega$, to equilibrate a lateral load $q(p)\mathbf{e}_z$, the membrane cannot remain in the plane $x - y$ and the equilibrium equations must be written in the deformed configuration: the equilibrium problem is intrinsically nonlinear, as already said.

Nonetheless, a linear theory of prestressed plane membranes can be established if we assume that:

- the vertical displacement w is so small compared to any in-plane dimension of Ω to let us consider $q(p)\mathbf{e}_z$ as unchanged, i.e. independent from the equilibrium configuration $\forall p \in \Omega$ also in the case of following forces;
- the tension T_0 is sufficiently large so as to guarantee a tensile stress state $\forall p \in \Omega$ (i.e., the principal stresses are everywhere positive): wrinkling does not occur;
- T_0 is much larger than any tension stress that can be produced by the lateral load $q(p)$, so that $T(p) \simeq T_0 \forall p \in \Omega$: the stress state is constant everywhere in Ω ;

- *membrane shear forces*, i.e. shear forces in the middle plane of the membrane, are always negligible with respect to T_0 .

With these assumptions, let us write the vertical equilibrium equation of a small portion of membrane. Because of the small displacements assumption and for the absence of wrinkles, the deformed surface is regular and with a small slope in any direction. As a consequence, the angles β_x and β_y that the tangents to the deformed surface form with the axes x and y are small, hence, see Fig. 7.2, we get:

$$\begin{aligned}\beta_x &\simeq \sin \beta_x \simeq \tan \beta_x = \frac{\partial w}{\partial x}, \\ \beta_y &\simeq \sin \beta_y \simeq \tan \beta_y = \frac{\partial w}{\partial y}.\end{aligned}\tag{7.1}$$

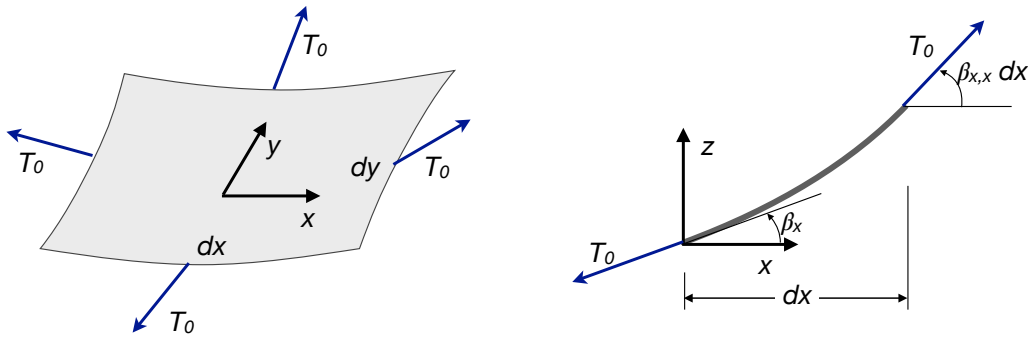


Figure 7.2: Scheme for the equilibrium equation of a prestressed membrane.

So, the equilibrium equation becomes:

$$\left[T_0 \left(\frac{\partial w}{\partial x} + \frac{\partial^2 w}{\partial x^2} dx \right) - T_0 \frac{\partial w}{\partial x} \right] dy + \left[T_0 \left(\frac{\partial w}{\partial y} + \frac{\partial^2 w}{\partial y^2} dy \right) - T_0 \frac{\partial w}{\partial y} \right] dx = -q(x, y) dx dy,\tag{7.2}$$

giving

$$T_0 \left(\frac{\partial^2 w}{\partial x^2} + \frac{\partial^2 w}{\partial y^2} \right) = -q(x, y) \rightarrow \Delta w(x, y) = -\frac{q(x, y)}{T_0}.\tag{7.3}$$

This equation is the two-dimensional corresponding of the equilibrium equation of taut cables, see e.g. eq. (2.70). Depending upon the Laplacian of w , eq. (7.3) is a partial differential equation of the elliptic type.

About the boundary $\partial\Omega$, we need to give some more details: we assume that $\partial\Omega$ is a regular, simple and closed planar curve. So, if $p(t) = (x(t), y(t))$ is a parametric equation of $\partial\Omega$, $0 \leq t \leq \ell$, then we admit that

$$p(t_1) \neq p(t_2) \quad \forall t_1, t_2 \in]0, \ell[, \quad p(0) = p(\ell),\tag{7.4}$$

i.e. the curve is closed and with no intersecting points. In addition, we assume that $\forall p(t) \in \partial\Omega$, exception made for at most a finite number of points, it is

$$\dot{x}^2 + \dot{y}^2 > 0.\tag{7.5}$$

This means that $\partial\Omega$ has the tangent defined everywhere but a finite number of points, i.e. polygonal Ω s are allowed.

Finally, the equilibrium problem of a prestressed membrane is in the form of a Dirichlet problem:

$$\begin{cases} \Delta w = -\frac{q}{T_0} & \text{in } \Omega, \\ w = w_0 & \text{on } \partial\Omega. \end{cases} \quad (7.6)$$

Let us calculate the quantity

$$\mathcal{E} = \frac{1}{2} \int_{\Omega} (\nabla w)^2 dx dy, \quad (7.7)$$

that represents, to within a scalar factor, the strain energy of the membrane; using integration by parts and the Gauss Theorem, we get successively

$$\begin{aligned} \mathcal{E} &= \frac{1}{2} \int_{\Omega} (w_{,x}^2 + w_{,y}^2) dx dy = \frac{1}{2} \int_{\Omega} (w_{,x}w)_{,x} + (w_{,y}w)_{,y} dx dy - \frac{1}{2} \int_{\Omega} w \Delta w dx dy \\ &= \frac{1}{2} \int_{\partial\Omega} w(w_{,x}n_x + w_{,y}n_y) dl - \frac{1}{2} \int_{\Omega} w \Delta w dx dy \\ &= \frac{1}{2} \int_{\partial\Omega} w \frac{\partial w}{\partial \mathbf{n}} dl - \frac{1}{2} \int_{\Omega} w \Delta w dx dy. \end{aligned} \quad (7.8)$$

If we put $w_0 = 0$ on the boundary, because of eq. (7.3) we get

$$\frac{1}{2} \int_{\Omega} (\nabla w)^2 dx dy = \frac{1}{2} \int_{\Omega} \frac{q w}{T_0} dx dy \rightarrow \frac{1}{2} \int_{\Omega} \left[(\nabla w)^2 - \frac{q w}{T_0} \right] dx dy = 0. \quad (7.9)$$

If $q(x, y) = 0$, then the last equation is satisfied $\iff (\nabla w)^2 = 0 \Rightarrow w_{,x} = w_{,y} = 0 \forall p \in \Omega \Rightarrow w = \text{const.}$ everywhere; because $w = 0$ on $\partial\Omega$, then $w = 0 \forall p \in \Omega$.

The Laplacian has a maximum principle: if $\Delta w > 0$ in Ω , then w cannot have internal maxima. In fact, let us suppose that there is a maximum in Ω ; then $w_{,xx} \leq 0$ and $w_{,yy} \leq 0$ in a neighborhood of the maximum. So, therein, $\Delta w = w_{,xx} + w_{,yy} \leq 0$, which contradicts the hypothesis.

In the end,

$$w(x, y) \leq \max_{\partial\Omega} w, \quad (7.10)$$

i.e., $w(x, y)$ is everywhere less than the maximum value that w takes on the boundary: all the deformed surface of the membrane is on one side of the contour plane.

To remark that the principle is not valid for non-quadratic operators, namely for the bi-Laplacian, that holds the bending equilibrium of plates, eq. (6.56): for a plate, due to bending, not all the points are necessarily on the same side of the contour plane.

7.3 Curved thin membranes

7.3.1 Internal actions

The already mentioned *membrane forces* are the internal forces laying in the plane tangent to the middle surface; they are the components of the second-rank tensor \mathbf{N} :

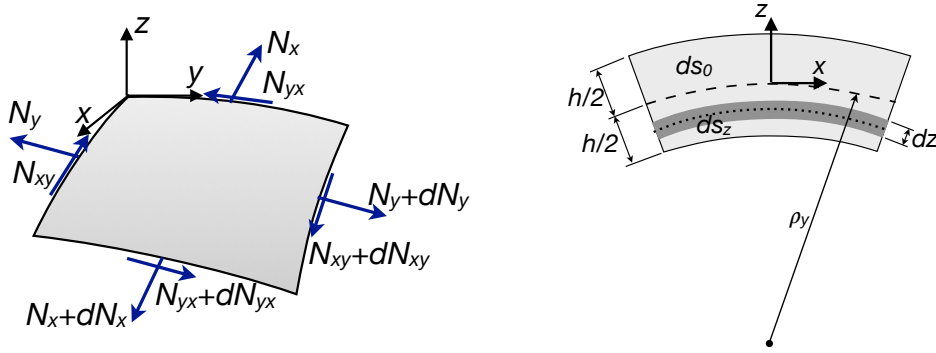


Figure 7.3: Scheme of the internal actions in a curved membrane.

$$\mathbf{N} = \frac{1}{ds_0} \int_{-\frac{h}{2}}^{\frac{h}{2}} \boldsymbol{\sigma} ds_z dz, \quad (7.11)$$

and because

$$ds_z = ds_0 \left(1 + \frac{z}{\rho} \right), \quad (7.12)$$

we get

$$\begin{aligned} N_x &= \int_{-\frac{h}{2}}^{\frac{h}{2}} \sigma_{xx} \left(1 + \frac{z}{\rho_y} \right) dz, & N_y &= \int_{-\frac{h}{2}}^{\frac{h}{2}} \sigma_{yy} \left(1 + \frac{z}{\rho_x} \right) dz, \\ N_{xy} &= \int_{-\frac{h}{2}}^{\frac{h}{2}} \sigma_{xy} \left(1 + \frac{z}{\rho_x} \right) dz, & N_{yx} &= \int_{-\frac{h}{2}}^{\frac{h}{2}} \sigma_{yx} \left(1 + \frac{z}{\rho_y} \right) dz. \end{aligned} \quad (7.13)$$

In the above expressions, ρ_x and ρ_y are the curvature radii of the middle surface along the directions x and y , respectively. It can be noticed that, because in general $\rho_x \neq \rho_y$, $N_{xy} \neq N_{yx}$, though $\sigma_{xy} = \sigma_{yx}$. Nevertheless, if we assume that $h \ll \rho_{min}$, then we obtain, just like for plates,

$$N_x = \int_{-\frac{h}{2}}^{\frac{h}{2}} \sigma_{xx} dz, \quad N_y = \int_{-\frac{h}{2}}^{\frac{h}{2}} \sigma_{yy} dz, \quad N_{xy} = N_{yx} = \int_{-\frac{h}{2}}^{\frac{h}{2}} \sigma_{xy} dz. \quad (7.14)$$

In the following, we will make the above assumption, known as *hypothesis of thin membranes*.

7.3.2 Constitutive equation

Because N_x, N_y and N_{xy} are different from zero, then $\sigma_{xx}, \sigma_{yy}, \sigma_{xy} \neq 0$; actually, $\sigma_{xz} = \sigma_{yz} = 0$ as a consequence of the definition of membrane (absence of transverse shear forces). In addition, we make the assumption that, $\forall p \in \Omega$,

$$|\sigma_{zz}| \ll \max\{|\sigma_{xx}|, |\sigma_{yy}|, |\sigma_{xy}|\}, \quad (7.15)$$

so that we can put

$$\sigma_{zz} = 0. \quad (7.16)$$

This assumption can be justified as done in Sect. 6.2.3 for plates. Finally, like for the case of plates, we obtain again a planar stress field:

$$\boldsymbol{\sigma} = \begin{bmatrix} \sigma_{xx} & \sigma_{xy} & 0 \\ \sigma_{xy} & \sigma_{yy} & 0 \\ 0 & 0 & 0 \end{bmatrix} \quad (7.17)$$

and the constitutive law is still the one find in Sect. 6.2.3:

$$\begin{Bmatrix} \sigma_{xx} \\ \sigma_{yy} \\ \sigma_{xy} \end{Bmatrix} = \begin{bmatrix} \frac{E}{1-\nu^2} & \frac{\nu E}{1-\nu^2} & 0 \\ \frac{\nu E}{1-\nu^2} & \frac{E}{1-\nu^2} & 0 \\ 0 & 0 & G \end{bmatrix} \begin{Bmatrix} \varepsilon_{xx} \\ \varepsilon_{yy} \\ 2\varepsilon_{xy} \end{Bmatrix}, \quad (7.18)$$

or synthetically

$$\boldsymbol{\sigma} = \mathbb{D} \boldsymbol{\varepsilon}, \quad (7.19)$$

with \mathbb{D} the matrix in eq. (7.18). The components $\varepsilon_{xx}, \varepsilon_{yy}, \varepsilon_{xy}$ define the deformation of the middle surface. The constitutive law for the membrane can then be obtained easily:

$$\begin{aligned} N_x &= \int_{-\frac{h}{2}}^{\frac{h}{2}} \sigma_{xx} dz = \frac{E}{1-\nu^2} \int_{-\frac{h}{2}}^{\frac{h}{2}} \varepsilon_{xx} + \nu \varepsilon_{yy} dz = \frac{E h}{1-\nu^2} (\varepsilon_{xx} + \nu \varepsilon_{yy}), \\ N_y &= \int_{-\frac{h}{2}}^{\frac{h}{2}} \sigma_{yy} dz = \frac{E}{1-\nu^2} \int_{-\frac{h}{2}}^{\frac{h}{2}} \varepsilon_{yy} + \nu \varepsilon_{xx} dz = \frac{E h}{1-\nu^2} (\varepsilon_{yy} + \nu \varepsilon_{xx}), \\ N_{xy} &= N_{yx} = \int_{-\frac{h}{2}}^{\frac{h}{2}} \sigma_{xy} dz = 2G \int_{-\frac{h}{2}}^{\frac{h}{2}} \varepsilon_{xy} dz = 2G h \varepsilon_{xy} = \frac{E h}{1+\nu} \varepsilon_{xy}. \end{aligned} \quad (7.20)$$

7.4 Axisymmetric membranes

Let us now consider a special and rather common case, that of axisymmetric membranes, i.e. in the form of a surface of revolution. The general case is sketched in Fig. 7.4.

The elements indicated in Fig. 7.4 are:

- θ : longitude angle, measuring the position of a meridian from an arbitrarily fixed direction;

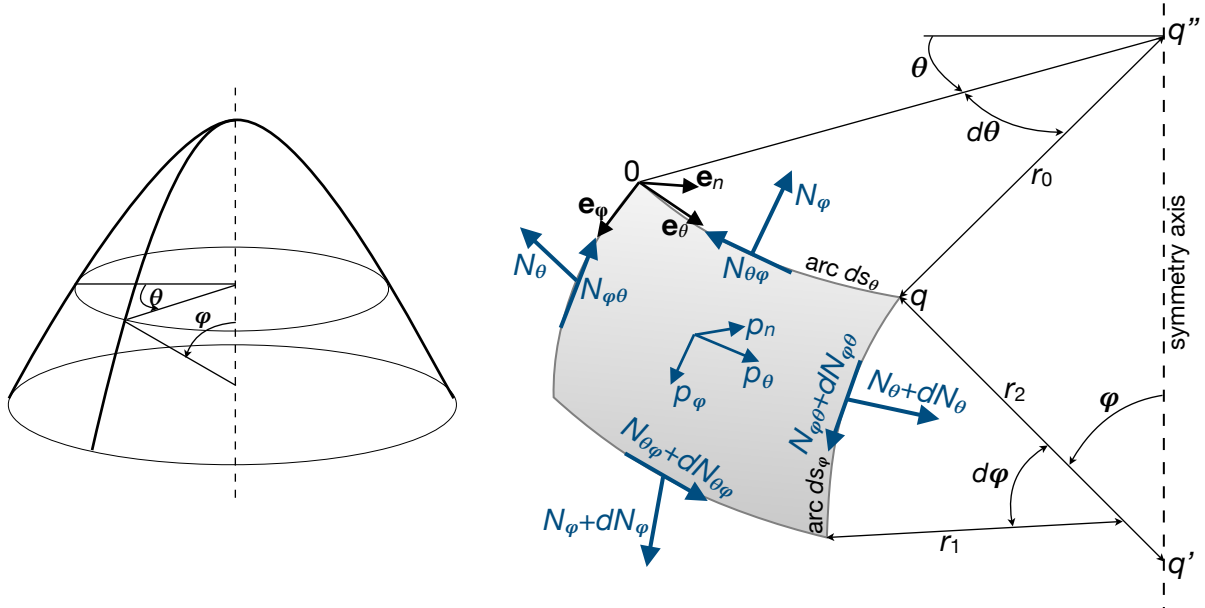


Figure 7.4: Scheme for the equilibrium equations of a membrane of revolution.

- φ : colatitude angle, measuring the angle between the vector $q - q'$ and the symmetry axis;
- $\{\mathbf{e}_\theta, \mathbf{e}_\varphi, \mathbf{e}_n\}$: positively oriented local basis, with \mathbf{e}_θ tangent to the parallel line, \mathbf{e}_φ tangent to the meridian line and \mathbf{e}_n normal to the membrane surface;
- r_1 : curvature radius of the meridian curve;
- $r_2 = |q - q'|$: distance between a point q of the membrane and the symmetry axis, measured along the normal to the membrane at q ;
- $r_0 = r_2 \sin \varphi$: distance between the point q and the symmetry axis, measured in the plane perpendicular to the symmetry axis;
- $ds_\theta = r_0 d\theta = r_2 \sin \varphi d\theta$: length of a small arc of parallel;
- $ds_\varphi = r_1 d\varphi$: length of a small arc of meridian;
- $dA = ds_\theta ds_\varphi = r_1 r_2 \sin \varphi d\varphi d\theta$: area of a small surface of membrane delimited by two couples of infinitesimally close meridians and parallels;
- p_θ : component along \mathbf{e}_θ of the distributed load \mathbf{p} ;
- p_φ : component along \mathbf{e}_φ of the distributed load \mathbf{p} ;
- p_n : component along \mathbf{e}_n of the distributed load \mathbf{p} ;
- N_φ : meridian normal membrane force, per unit length of a parallel arc;
- N_θ : parallel normal membrane force, per unit length of a meridian arc;
- $N_{\varphi\theta}$: shear membrane force, per unit length of a meridian arc;
- $N_{\theta\varphi}$: shear membrane force, per unit length of a parallel arc.

In the hypothesis of thin membrane, $N_{\theta\varphi} = N_{\varphi\theta}$. We write the equilibrium equations for the three directions: \mathbf{e}_φ , i.e. tangent to a meridian, \mathbf{e}_θ , i.e. tangent to a parallel, and \mathbf{e}_n , i.e. normal to the surface. The forces acting upon the element of surface dA are the membrane forces and the applied forces $\mathbf{p}=(p_\theta, p_\varphi, p_n)$.

7.4.1 Equilibrium along a meridian

We need to consider all of the force components acting in the direction \mathbf{e}_φ , tangent to a meridian line. The resultant of the membrane forces N_φ on the upper and lower sides of the surface element dA in Fig. 7.4 is¹

$$\begin{aligned} (N_\varphi + dN_\varphi) \left(r_0 + \frac{dr_0}{d\varphi} d\varphi \right) d\theta - N_\varphi r_0 d\theta &\simeq \left(N_\varphi \frac{dr_0}{d\varphi} d\varphi + dN_\varphi r_0 \right) d\theta = \\ \left(N_\varphi \frac{dr_0}{d\varphi} + \frac{\partial N_\varphi}{\partial \varphi} r_0 \right) d\varphi d\theta &= \frac{\partial}{\partial \varphi} (N_\varphi r_0) d\varphi d\theta. \end{aligned} \quad (7.21)$$

The resultant of the forces N_θ on the lateral sides of dA is

$$\begin{aligned} (N_\theta + N_\theta + \frac{\partial N_\theta}{\partial \theta} d\theta) \sin \frac{d\theta}{2} ds_\varphi &\simeq (2N_\theta + \frac{\partial N_\theta}{\partial \theta} d\theta) \frac{d\theta}{2} ds_\varphi = \\ \left(N_\theta d\theta + \frac{1}{2} \frac{\partial N_\theta}{\partial \theta} d\theta^2 \right) ds_\varphi &\simeq N_\theta ds_\varphi d\theta; \end{aligned} \quad (7.22)$$

this force is horizontal and its component on the tangent to the meridian is

$$N_\theta \cos \varphi ds_\varphi d\theta = N_\theta \cos \varphi r_1 d\varphi d\theta. \quad (7.23)$$

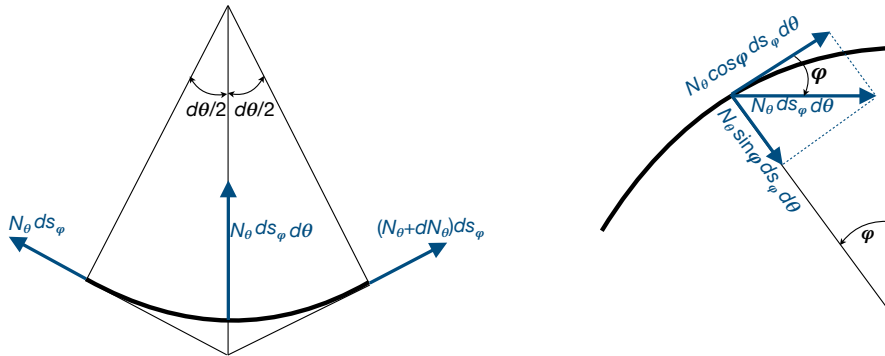


Figure 7.5: Scheme for the forces N_θ .

The resultant of the forces $N_{\varphi\theta}$ is

$$-N_{\varphi\theta} ds_\varphi + \left(N_{\varphi\theta} + \frac{\partial N_{\varphi\theta}}{\partial \theta} d\theta \right) ds_\varphi = \frac{\partial N_{\varphi\theta}}{\partial \theta} r_1 d\varphi d\theta, \quad (7.24)$$

¹In the following, we neglect all the infinitesimal terms $o(d\theta d\varphi)$.

while the forces applied to dA are

$$p_\varphi dA = p_\varphi r_0 r_1 d\varphi d\theta. \quad (7.25)$$

Finally, the equilibrium equations of the forces in the direction of the meridian is

$$\frac{\partial}{\partial \varphi}(N_\varphi r_0) d\varphi d\theta - N_\theta \cos \varphi r_1 d\varphi d\theta + \frac{\partial N_{\varphi\theta}}{\partial \theta} r_1 d\varphi d\theta + p_\varphi r_0 r_1 d\varphi d\theta = 0, \quad (7.26)$$

or, because $r_0 = r_2 \sin \varphi$,

$$\frac{\partial}{\partial \varphi}(r_2 N_\varphi \sin \varphi) - r_1 N_\theta \cos \varphi + r_1 \frac{\partial N_{\varphi\theta}}{\partial \theta} = -p_\varphi r_1 r_2 \sin \varphi. \quad (7.27)$$

7.4.2 Equilibrium along a parallel

In the direction \mathbf{e}_θ , along a parallel line, the resultant of the forces N_θ is, see Fig. 7.5,

$$\left(N_\theta + \frac{\partial N_\theta}{\partial \theta} d\theta - N_\theta \right) \cos \frac{d\theta}{2} ds_\varphi \simeq \frac{\partial N_\theta}{\partial \theta} ds_\varphi d\theta = \frac{\partial N_\theta}{\partial \theta} r_1 d\varphi d\theta, \quad (7.28)$$

while for forces $N_{\theta\varphi}$ it is

$$\begin{aligned} & \left(N_{\theta\varphi} + \frac{\partial N_{\theta\varphi}}{\partial \varphi} d\varphi \right) \left(r_0 + \frac{dr_0}{d\varphi} d\varphi \right) d\theta - N_{\theta\varphi} r_0 d\theta \simeq \\ & \frac{\partial N_{\theta\varphi}}{\partial \varphi} d\varphi r_0 d\theta + N_{\theta\varphi} \frac{dr_0}{d\varphi} d\varphi d\theta = \frac{\partial(r_0 N_{\theta\varphi})}{\partial \varphi} d\varphi d\theta. \end{aligned} \quad (7.29)$$

For the resultant of the forces $N_{\varphi\theta}$ we get, see Fig. 7.6,

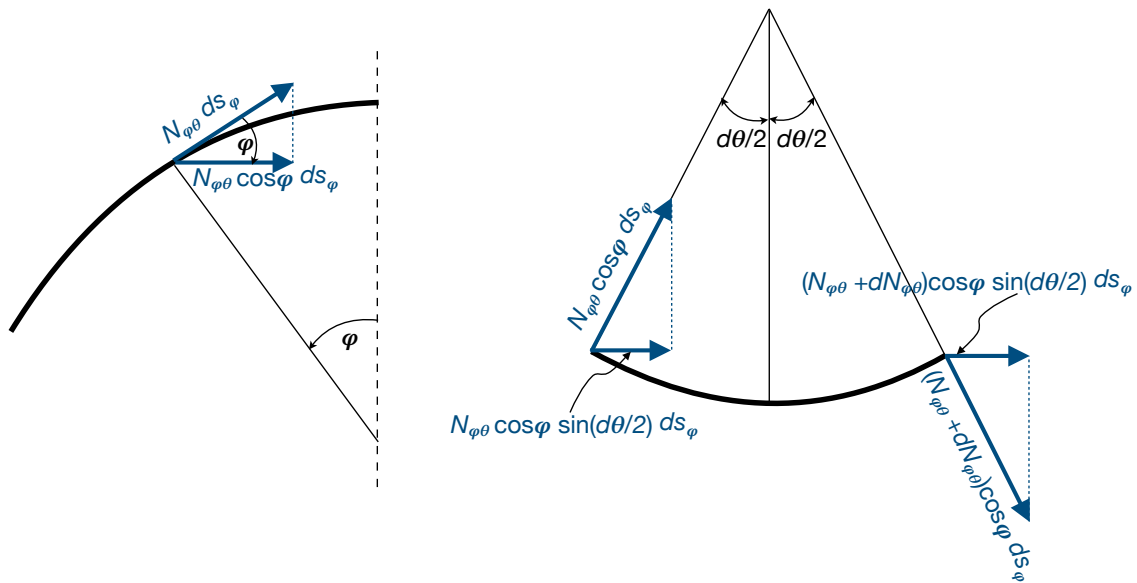


Figure 7.6: Scheme for the forces $N_{\varphi\theta}$.

$$\begin{aligned} \left(N_{\varphi\theta} + N_{\varphi\theta} + \frac{\partial N_{\varphi\theta}}{\partial \theta} d\theta \right) \cos \varphi \sin \frac{d\theta}{2} ds_{\varphi} &\simeq \\ \left(N_{\varphi\theta} + N_{\varphi\theta} + \frac{\partial N_{\varphi\theta}}{\partial \theta} d\theta \right) \cos \varphi \frac{d\theta}{2} ds_{\varphi} &\simeq N_{\varphi\theta} \cos \varphi d\theta ds_{\varphi} = N_{\varphi\theta} r_1 \cos \varphi d\varphi d\theta, \end{aligned} \quad (7.30)$$

while the component of the applied loads along a parallel is

$$p_{\theta} dA = p_{\theta} r_0 r_1 d\varphi d\theta. \quad (7.31)$$

Finally, the equilibrium equation in the direction of a parallel is

$$\frac{\partial N_{\theta}}{\partial \theta} r_1 d\varphi d\theta + \frac{\partial(r_0 N_{\theta\varphi})}{\partial \varphi} d\varphi d\theta + N_{\varphi\theta} r_1 \cos \varphi d\varphi d\theta + p_{\theta} r_0 r_1 d\varphi d\theta = 0, \quad (7.32)$$

i.e., because $r_0 = r_2 \sin \varphi$,

$$r_1 \frac{\partial N_{\theta}}{\partial \theta} + \frac{\partial(r_2 \sin \varphi N_{\theta\varphi})}{\partial \varphi} + N_{\varphi\theta} r_1 \cos \varphi = -p_{\theta} r_1 r_2 \sin \varphi. \quad (7.33)$$

7.4.3 Equilibrium along the normal to the surface

In the direction \mathbf{e}_n , orthogonal to the membrane's surface, the resultant of the forces N_{φ} is, see Fig. 7.7,

$$\begin{aligned} \left[r_0 N_{\varphi} + \left(N_{\varphi} + \frac{\partial N_{\varphi}}{\partial \varphi} d\varphi \right) \left(r_0 + \frac{dr_0}{d\varphi} d\varphi \right) \right] \sin \frac{d\varphi}{2} d\theta &\simeq \\ \left[r_0 N_{\varphi} + \left(N_{\varphi} + \frac{\partial N_{\varphi}}{\partial \varphi} d\varphi \right) \left(r_0 + \frac{dr_0}{d\varphi} d\varphi \right) \right] \frac{d\varphi}{2} d\theta &\simeq N_{\varphi} r_0 d\varphi d\theta. \end{aligned} \quad (7.34)$$

The component of the resultant of the forces N_{θ} along \mathbf{e}_n is, see Fig. 7.5,

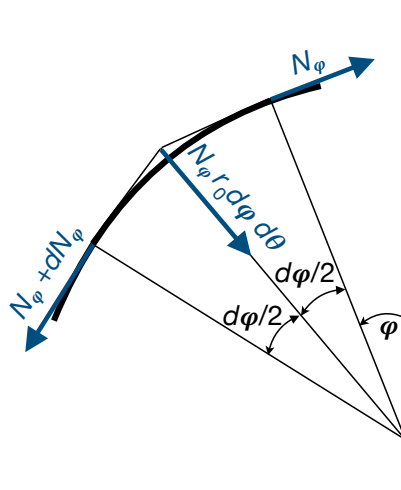


Figure 7.7: Scheme for the forces N_{φ} .

$$N_{\theta} r_1 \sin \varphi d\varphi d\theta, \quad (7.35)$$

while that of the forces $N_{\varphi\theta}$ and $N_{\theta\varphi}$ is null; finally, the component of the applied forces is

$$p_n dA = p_n r_0 r_1 d\varphi d\theta. \quad (7.36)$$

The equilibrium equation in the direction of the normal to the membrane's surface is hence

$$N_\varphi r_0 d\varphi d\theta + N_\theta r_1 \sin \varphi d\varphi d\theta + p_n r_0 r_1 d\varphi d\theta = 0, \quad (7.37)$$

i.e., because $r_0 = r_2 \sin \varphi$,

$$N_\varphi r_2 \sin \varphi + N_\theta r_1 \sin \varphi = -p_n r_0 r_1 \rightarrow \frac{N_\varphi}{r_1} + \frac{N_\theta}{r_2} = -p_n. \quad (7.38)$$

7.4.4 The system of equilibrium equations

The equilibrium equations are three coupled first-order partial differential equations:

$$\begin{aligned} \frac{\partial}{\partial \varphi}(r_2 N_\varphi \sin \varphi) - r_1 \cos \varphi N_\theta + r_1 \frac{\partial N_{\varphi\theta}}{\partial \theta} &= -p_\varphi r_1 r_2 \sin \varphi, \\ r_1 \frac{\partial N_\theta}{\partial \theta} + \frac{\partial(r_2 \sin \varphi N_{\theta\varphi})}{\partial \varphi} + r_1 \cos \varphi N_{\varphi\theta} &= -p_\theta r_1 r_2 \sin \varphi, \\ \frac{N_\varphi}{r_1} + \frac{N_\theta}{r_2} &= -p_n. \end{aligned} \quad (7.39)$$

The four unknown functions are N_φ , N_θ , $N_{\varphi\theta}$ and $N_{\theta\varphi}$; in the hypothesis of thin membrane, they reduce to three ($N_{\varphi\theta} = N_{\theta\varphi}$). Hence, in this framework, the equilibrium equations are sufficient to solve the problem: *a thin membrane is intrinsically isostatic*.

7.4.5 Resolution procedure

From eq. (7.39)₃ we get

$$N_\theta = -p_n r_2 - N_\varphi \frac{r_2}{r_1}, \quad (7.40)$$

that injected in eqs. (7.39)_{1,2} gives

$$\begin{aligned} \frac{\partial}{\partial \varphi}(r_2 \sin \varphi N_\varphi) + r_1 \frac{\partial N_{\varphi\theta}}{\partial \theta} + r_2 \cos \varphi N_\varphi &= -r_1 r_2 (p_\varphi \sin \varphi + p_n \cos \varphi), \\ \frac{\partial}{\partial \varphi}(r_2 \sin \varphi N_{\varphi\theta}) + r_1 \cos \varphi N_{\varphi\theta} - r_2 \frac{\partial N_\varphi}{\partial \theta} &= -r_1 r_2 \left(p_\theta \sin \varphi - \frac{\partial p_n}{\partial \theta} \right). \end{aligned} \quad (7.41)$$

We introduce now the following change of variables:

$$U = r_2 \sin^2 \varphi N_\varphi, \quad V = r_2^2 \sin^2 \varphi N_{\varphi\theta}, \quad (7.42)$$

that used in the previous equations give

$$\begin{aligned} \frac{\partial}{\partial \varphi} \left(\frac{U}{\sin \varphi} \right) + r_1 \frac{\partial}{\partial \theta} \left(\frac{V}{r_2^2 \sin^2 \varphi} \right) + \frac{U}{\sin^2 \varphi} \cos \varphi &= -r_1 r_2 (p_\varphi \sin \varphi + p_n \cos \varphi), \\ \frac{\partial}{\partial \varphi} \left(\frac{V}{r_2 \sin \varphi} \right) + r_1 \cos \varphi \frac{V}{r_2^2 \sin^2 \varphi} - r_2 \frac{\partial}{\partial \theta} \left(\frac{U}{r_2 \sin^2 \varphi} \right) &= -r_1 r_2 \left(p_\theta \sin \varphi - \frac{\partial p_n}{\partial \theta} \right), \end{aligned} \quad (7.43)$$

and once the derivatives done

$$\begin{aligned} \frac{\partial U}{\partial \varphi} \frac{1}{\sin \varphi} - U \frac{\cos \varphi}{\sin^2 \varphi} + \frac{r_1}{r_2^2 \sin^2 \varphi} \frac{\partial V}{\partial \theta} + U \frac{\cos \varphi}{\sin^2 \varphi} &= -r_1 r_2 (p_\varphi \sin \varphi + p_n \cos \varphi), \\ \frac{1}{r_2 \sin \varphi} \frac{\partial V}{\partial \varphi} + V \frac{-\frac{d}{d\varphi}(r_2 \sin \varphi)}{r_2^2 \sin^2 \varphi} + V \frac{r_1 \cos \varphi}{r_2^2 \sin^2 \varphi} - \frac{1}{\sin^2 \varphi} \frac{\partial U}{\partial \theta} &= -r_1 r_2 \left(p_\theta \sin \varphi - \frac{\partial p_n}{\partial \theta} \right). \end{aligned} \quad (7.44)$$

Now, considering that, on the one hand,

$$dr_0 = d(r_2 \sin \varphi) \quad (7.45)$$

and that, on the other hand, see Fig. 7.8,

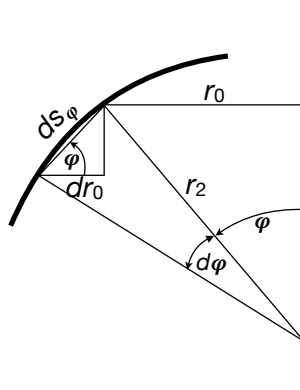


Figure 7.8: Scheme for the geometrical quantities.

$$dr_0 = ds_\varphi \cos \varphi = r_1 \cos \varphi d\varphi, \quad (7.46)$$

we get

$$r_1 \cos \varphi = \frac{d}{d\varphi}(r_2 \sin \varphi); \quad (7.47)$$

injecting this result into eq. (7.44)₂, after reordering we get:

$$\begin{aligned} \frac{\partial V}{\partial \theta} + \frac{r_2^2}{r_1} \sin \varphi \frac{\partial U}{\partial \varphi} &= -r_2^3 \sin^2 \varphi (p_\varphi \sin \varphi + p_n \cos \varphi), \\ \frac{\partial V}{\partial \varphi} - \frac{r_2}{\sin \varphi} \frac{\partial U}{\partial \theta} &= -r_1 r_2^2 \sin \varphi \left(p_\theta \sin \varphi - \frac{\partial p_n}{\partial \theta} \right). \end{aligned} \quad (7.48)$$

Differentiating the first equation with respect to φ , the second one with respect to θ and subtracting we get an equation depending uniquely on U

$$\begin{aligned} \frac{\partial}{\partial \varphi} \left(\frac{r_2^2}{r_1} \sin \varphi \frac{\partial U}{\partial \varphi} \right) + \frac{r_2}{\sin \varphi} \frac{\partial^2 U}{\partial \theta^2} &= \\ \frac{\partial}{\partial \varphi} (r_2^3 \sin^2 \varphi (p_n \cos \varphi - p_\varphi \sin \varphi)) + r_1 r_2^2 \sin \varphi \left(\sin \varphi \frac{\partial p_\theta}{\partial \theta} - \frac{\partial^2 p_n}{\partial \theta^2} \right). \end{aligned} \quad (7.49)$$

After differentiating and reordering the terms we get finally

$$r_2^2 \sin^2 \varphi \frac{\partial^2 U}{\partial \varphi^2} + r_1 r_2 \frac{\partial^2 U}{\partial \theta^2} + \alpha(\varphi, \theta) \frac{\partial U}{\partial \varphi} = p(\varphi, \theta), \quad (7.50)$$

where²

$$\alpha(\varphi, \theta) = r_1 r_2 \sin \varphi \cos \varphi + r_2 \sin^2 \varphi \frac{\partial r_2}{\partial \varphi} - \frac{r_2^2}{r_1} \sin^2 \varphi \frac{\partial r_1}{\partial \varphi},$$

$$p(\varphi, \theta) = r_1 \sin \varphi \left[\frac{\partial}{\partial \varphi} (r_2^3 \sin^2 \varphi (p_n \cos \varphi - p_\varphi \sin \varphi)) + r_1 r_2^2 \sin \varphi \left(\sin \varphi \frac{\partial p_\theta}{\partial \theta} - \frac{\partial^2 p_n}{\partial \theta^2} \right) \right]. \quad (7.51)$$

are two known functions of the geometry and of the loads. Once the function U obtained as solution of eq. (7.50), we obtain N_φ from eq. (7.42)₁ and then N_θ from eq. (7.40). To obtain $N_{\varphi\theta}$, we differentiate eqs. (7.48) with respect to θ and φ respectively and sum up them to obtain

$$\Delta V = r_2 \frac{\partial^2 U}{\partial \varphi \partial \theta} \left(\frac{1}{\sin \varphi} - \frac{r_2}{r_1} \sin \varphi \right) - r_2^3 \sin^2 \varphi \left(\sin \varphi \frac{\partial p_\varphi}{\partial \theta} + \cos \varphi \frac{\partial p_n}{\partial \theta} \right) - r_1 r_2^2 \sin \varphi \left(\sin \varphi \frac{\partial p_\theta}{\partial \theta} - \frac{\partial^2 p_n}{\partial \theta^2} \right). \quad (7.52)$$

Once V obtained as solution of the previous equation, it can be injected into eq. (7.42)₂ to obtain $N_{\varphi\theta}$. It is interesting to notice that, while the partial differential equation (7.52) is of the elliptic type, because the laplacian $\Delta V = \partial^2 V / \partial \varphi^2 + \partial^2 V / \partial \theta^2$ is the typical elliptic operator, eq. (7.50) is elliptic if $r_1 r_2 > 0$, while it is hyperbolic if $r_1 r_2 < 0$. The first case is typical of ellipsoidal-like surfaces, while the second one of the hyperbolic hyperboloid-like ones, Fig. 7.9.

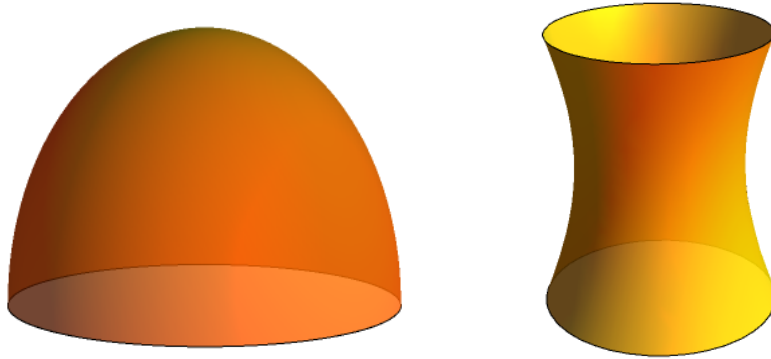


Figure 7.9: Ellipsoidal-like (left) and hyperbolic-like (right) surfaces of revolution.

²To obtain the expression of $\alpha(\varphi, \theta)$ we need to consider that

$$\frac{\partial}{\partial \varphi} \left(\frac{r_2^2}{r_1} \sin \varphi \right) = \frac{1}{r_1^2} \left(r_1 r_2 \frac{\partial (r_2 \sin \varphi)}{\partial \varphi} + r_1 r_2 \sin \varphi \frac{\partial r_2}{\partial \varphi} - \frac{\partial r_1}{\partial \varphi} r_2^2 \sin \varphi \right) = r_2 \cos \varphi + \frac{r_2}{r_1} \sin \varphi \frac{\partial r_2}{\partial \varphi} - \frac{r_2^2}{r_1^2} \sin \varphi \frac{\partial r_1}{\partial \varphi},$$

the last result being obtained thanks to eq. (7.47).

7.4.6 Axisymmetric load

In case of axisymmetric load, eqs. (7.48) can be solved separately, because they are uncoupled: in fact, because nothing depends upon θ , all the derivatives with respect to this variable are null and hence eqs. (7.39) reduce to

$$\begin{aligned} \frac{\partial}{\partial \varphi}(r_2 N_\varphi \sin \varphi) - r_1 N_\theta \cos \varphi &= -p_\varphi r_1 r_2 \sin \varphi, \\ \frac{\partial(r_2 \sin \varphi N_{\theta\varphi})}{\partial \varphi} + r_1 \cos \varphi N_{\varphi\theta} &= -p_\theta r_1 r_2 \sin \varphi, \\ \frac{N_\varphi}{r_1} + \frac{N_\theta}{r_2} &= -p_n, \end{aligned} \quad (7.53)$$

while eqs. (7.48) become

$$\begin{aligned} \frac{\partial U}{\partial \varphi} &= -r_1 r_2 \sin \varphi (p_\varphi \sin \varphi + p_n \cos \varphi), \\ \frac{\partial V}{\partial \varphi} &= -r_1 r_2^2 \sin^2 \varphi p_\theta. \end{aligned} \quad (7.54)$$

Again, after the function U found, i.e. once eq. (7.54)₁ solved, we get from eq. (7.42)₁

$$N_\varphi = \frac{U}{r_2 \sin^2 \varphi}, \quad (7.55)$$

and, from eq. (7.40),

$$N_\theta = -p_n r_2 - \frac{r_2}{r_1} N_\varphi = -p_n r_2 - \frac{U}{r_1 \sin^2 \varphi}. \quad (7.56)$$

For what concerns $N_{\varphi\theta}$, it depends only upon V , eq. (7.42)₂, hence eq. (7.54)₂ describes the tangential internal forces. If $p_\theta = 0$, i.e. if the tangential forces along the parallels are null, then $V = 0 \Rightarrow N_{\varphi\theta} = 0$: the shear forces are everywhere null in the membrane.

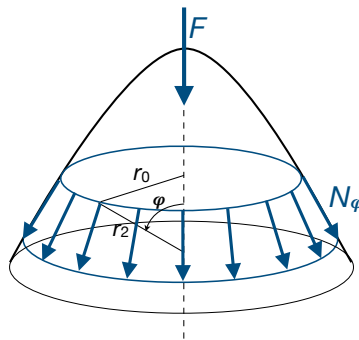


Figure 7.10: Scheme for the equilibrium in case of axisymmetric loads.

7.4.6.1 Global equilibrium

The above results can be found with no need to integrate the equilibrium equations, that can be stated and solved directly. In fact, for the global equilibrium, in the symmetry axis direction, of the part of membrane between $\varphi = 0$ and φ , it must be, see Fig. 7.10,

$$2\pi r_0 \sin \varphi N_\varphi + F = 0 \rightarrow N_\varphi = -\frac{F}{2\pi r_0 \sin \varphi} = -\frac{F}{2\pi r_2 \sin^2 \varphi}, \quad (7.57)$$

where F is the resultant of the loads for the part of membrane under consideration, and then

$$N_\theta = -p_n r_2 - \frac{r_2}{r_1} N_\varphi = -p_n r_2 + \frac{F}{2\pi r_1 \sin^2 \varphi}. \quad (7.58)$$

7.4.6.2 Strains and displacements

The inverse Lamé's equations³

$$\boldsymbol{\varepsilon} = \frac{1+\nu}{E} \boldsymbol{\sigma} - \frac{\nu}{E} \text{tr} \boldsymbol{\sigma} \mathbf{I}, \quad (7.59)$$

can be used to recover the strain field. Considering that

$$\sigma_\theta = \frac{N_\theta}{h}, \quad \sigma_\varphi = \frac{N_\varphi}{h}, \quad \sigma_{\varphi\theta} = \frac{N_{\varphi\theta}}{h}, \quad (7.60)$$

we get

$$\begin{aligned} \varepsilon_\theta &= \frac{1+\nu}{E} \sigma_\theta - \frac{\nu}{E} (\sigma_\varphi + \sigma_\theta) = \frac{1}{E} (\sigma_\theta - \nu \sigma_\varphi) = \frac{1}{h E} (N_\theta - \nu N_\varphi), \\ \varepsilon_\varphi &= \frac{1+\nu}{E} \sigma_\varphi - \frac{\nu}{E} (\sigma_\varphi + \sigma_\theta) = \frac{1}{E} (\sigma_\varphi - \nu \sigma_\theta) = \frac{1}{h E} (N_\varphi - \nu N_\theta), \\ \varepsilon_{\varphi\theta} &= \frac{1+\nu}{E} \sigma_{\varphi\theta} = \frac{1+\nu}{h E} N_{\varphi\theta}. \end{aligned} \quad (7.61)$$

We pass now to determine the displacement field. To this purpose, we need to link the above strain field to the displacement vector $\mathbf{u} = u\mathbf{e}_\theta + v\mathbf{e}_\varphi + w\mathbf{e}_n$; we already know that, for the symmetry of the problem, $u = 0$. Then, let us consider an infinitesimal arc of meridian $dl = r_1 d\varphi$, see Fig. 7.11. The length of dl decreases for the radial displacement w and increases for the tangential displacement v so that the final length will be

$$\begin{aligned} dl' &= dl + (v + dv) - v - (w + w + dw) \sin \frac{d\varphi}{2} \simeq dl + dv - w d\varphi - dw \frac{d\varphi}{2} \\ &= dl + \left(\frac{dv}{d\varphi} - w \right) d\varphi - \frac{1}{2} \frac{dw}{d\varphi} d\varphi^2 \simeq dl + \left(\frac{dv}{d\varphi} - w \right) d\varphi, \end{aligned} \quad (7.62)$$

so that finally

$$\varepsilon_\varphi = \frac{dl' - dl}{dl} = \frac{1}{r_1} \left(\frac{dv}{d\varphi} - w \right). \quad (7.63)$$

³To remark that, because we have a plane stress state, the Lamé's inverse equations are the same of the 3D case.

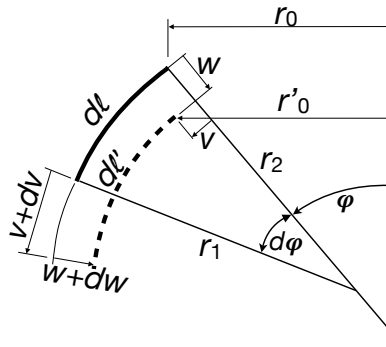


Figure 7.11: Scheme of the deformation of a meridian line.

In the direction of a parallel, the initial radius r_0 becomes

$$r'_0 = r_0 + v \cos \varphi - w \sin \varphi, \quad (7.64)$$

so that

$$\varepsilon_\theta = \frac{2\pi r'_0 - 2\pi r_0}{2\pi r_0} = \frac{1}{r_0}(v \cos \varphi - w \sin \varphi) = \frac{1}{r_2} \left(\frac{v}{\tan \varphi} - w \right). \quad (7.65)$$

From eqs. (7.63) and (7.65) we get

$$\frac{dv}{d\varphi} - \frac{v}{\tan \varphi} = r_1 \varepsilon_\varphi - r_2 \varepsilon_\theta, \quad (7.66)$$

and using eqs. (7.61)

$$\frac{dv}{d\varphi} - \frac{v}{\tan \varphi} = f(\varphi), \quad (7.67)$$

with

$$f(\varphi) = \frac{1}{h E} [N_\varphi(r_1 + \nu r_2) - N_\theta(r_2 + \nu r_1)]. \quad (7.68)$$

The general solution of eq. (7.67) is

$$v = \sin \varphi \left(\int \frac{f(\varphi)}{\sin \varphi} d\varphi + c \right), \quad (7.69)$$

with c a constant to be determined upon the boundary conditions; finally, from eqs. (7.61)₁ and (7.65) we get

$$w = \frac{v}{\tan \varphi} - r_2 \varepsilon_\theta = \frac{v}{\tan \varphi} - \frac{r_2}{h E} (N_\theta - \nu N_\varphi). \quad (7.70)$$

7.5 Examples of axisymmetric membranes

We consider in this Section some cases of axisymmetric membranes that are particularly interesting for applications.

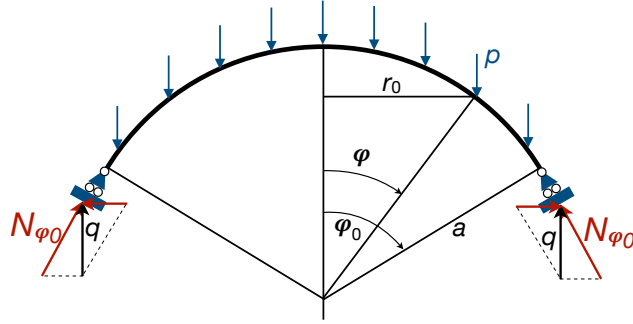


Figure 7.12: Scheme of a spherical dome.

7.5.1 Spherical domes

Let us first consider the case of a spherical dome of radius a submitted to its own weight, whose value per unit area is p , see Fig. 7.12. This problem is historically rather important, because several are the monumental domes all around the world, the most celebrated one being the dome of the Pantheon⁴ in Rome, see Fig. 7.13. In this case, $r_1 = r_2 = a$ while

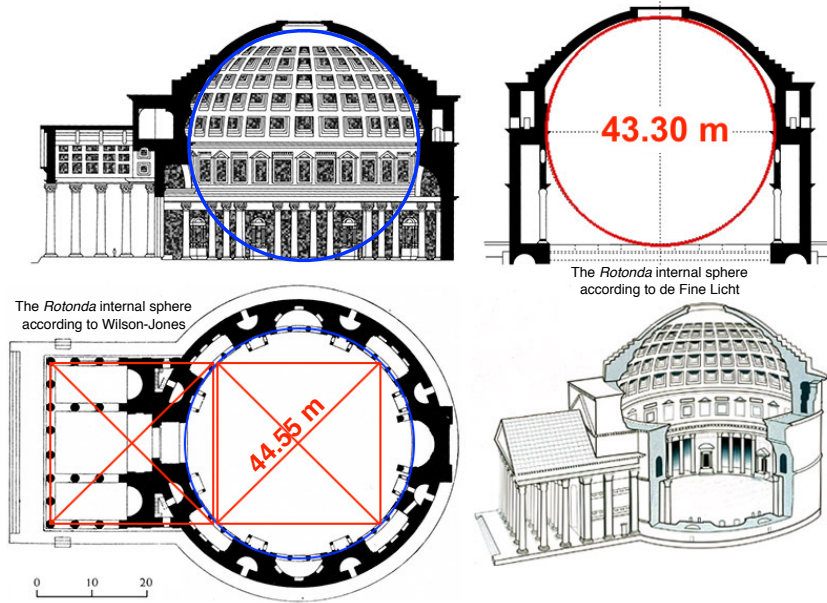


Figure 7.13: Scheme of the Pantheon in Rome.

$\mathbf{p} = (p_\theta, p_\varphi, p_n) = (0, p \sin \varphi, p \cos \varphi)$. Hence, eq. (7.54)₁ becomes

$$\frac{\partial U}{\partial \varphi} = -a^2 p \sin \varphi, \quad (7.71)$$

whose solution is

$$U = a^2 p \cos \varphi + c_1, \quad (7.72)$$

⁴The dome of the Pantheon, whose thickness is not constant, is still today the largest dome in the world in unreinforced concrete. Its inner surface, sculpted by a coffering, is a perfect hemisphere with a radius of 44.55 m (150 Roman feet). The lower part of the sphere, if existing, should exactly touch the floor of the building, Fig. 7.13. The Pantheon was built, probably by the great Nabatean architect Apollodorus of Damascus, under the Emperor Adrian, around 120 a. C.

so that, by eq. (7.55),

$$N_\varphi = \frac{c + a p \cos \varphi}{\sin^2 \varphi}, \quad (7.73)$$

with $c = c_1/a$ to be determined upon the boundary conditions. We consider two different cases.

7.5.1.1 Conical support

This is the case represented in Fig. 7.12: the dome is simply supported at its base and the support has the shape of a conical surface orthogonal to the meridians. In this case, the reaction of the support is tangent to the meridians, i.e. it is directed like, but opposite to, N_φ .

The boundary condition is hence

$$N_\varphi(\varphi_0) = -\frac{q}{\sin \varphi_0}, \quad (7.74)$$

with q the total weight of the dome per unit length:

$$q = \frac{\int_0^{\varphi_0} 2\pi a r_0(\varphi) p d\varphi}{2\pi r_0(\varphi_0)} = \frac{p a \int_0^{\varphi_0} \sin \varphi d\varphi}{\sin \varphi_0} = p a \frac{1 - \cos \varphi_0}{\sin \varphi_0}. \quad (7.75)$$

Replacing this value in eq. (7.74) gives $c = -p a$ and finally

$$N_\varphi = p a \frac{\cos \varphi - 1}{\sin^2 \varphi} = -\frac{p a}{1 + \cos \varphi}, \quad (7.76)$$

which gives also, eq. (7.40),

$$N_\theta = -p a \cos \varphi - N_\varphi = p a \left(\frac{1}{1 + \cos \varphi} - \cos \varphi \right). \quad (7.77)$$

It can be noticed that the same result can be obtained easily also by the approach described in Sect. 7.4.6.1; in fact, the weight of the dome between $\varphi = 0$ and φ is

$$F = \int_0^\varphi 2\pi a r_0(\varphi) p d\varphi = \int_0^\varphi 2\pi p a^2 \sin \varphi d\varphi = 2\pi p a^2 (1 - \cos \varphi), \quad (7.78)$$

so that, using eq. (7.57),

$$N_\varphi = -\frac{p a}{1 + \cos \varphi}, \quad (7.79)$$

as before.

We remark that at the dome's top, $\varphi = 0$, we get $N_\theta = N_\varphi = -p a/2$, while at the dome's base, for a hemispherical dome, i.e. for $\varphi_0 = \pi/2$, it is $N_\varphi = -p a$ and $N_\theta = p a$. It is interesting to note that $N_\varphi < 0 \forall \varphi$, i.e. the meridian lines are completely in compression, while $N_\theta < 0 \iff$

$$\begin{aligned} \frac{1}{1 + \cos \varphi} - \cos \varphi < 0 &\rightarrow \cos^2 \varphi + \cos \varphi - 1 > 0 \rightarrow \\ \cos \varphi < \frac{\sqrt{5} - 1}{2} &\rightarrow \varphi < \sim 51.82^\circ. \end{aligned} \quad (7.80)$$

So, the parallels are in compression only in the upper part of the dome, while they are in tension in the lower one⁵. The polar diagrams of N_φ and N_θ are plotted in Fig. 7.14.

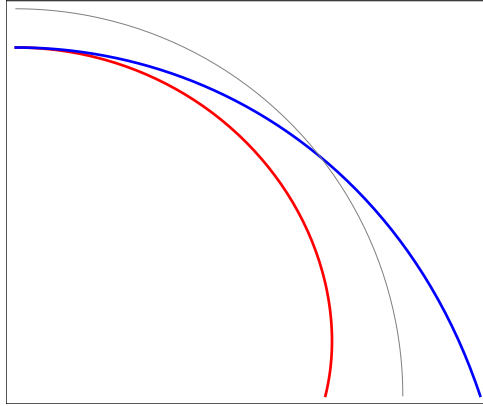


Figure 7.14: Polar diagrams of N_φ , red, and N_θ , blue, for a spherical shell submitted to its own weight (in grey: the profile of the dome; the radial distance between this curve and the curve of a diagram measures the value of the quantity, positive when outward).

7.5.1.2 Ring beam

We consider now the presence of a ring beam, stiffening the border of the dome and simply supported, see Fig. 7.15. In this case, the boundary condition is

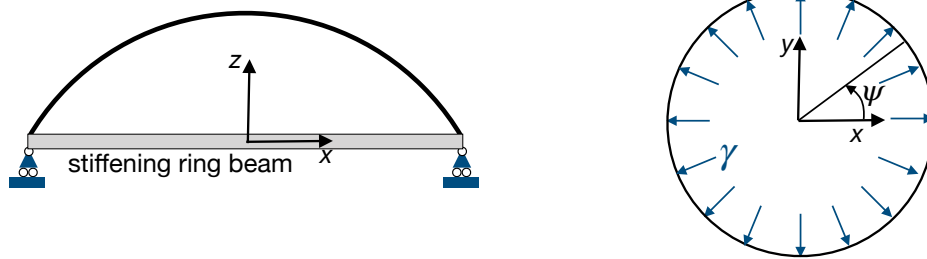


Figure 7.15: Scheme of a spherical dome with a ring beam.

$$N_\varphi(\varphi_0) \sin \varphi_0 = -q, \quad (7.81)$$

so finally we find the same result as in the previous case. However, the traction in the parallel at the springing of the dome, i.e.

$$N_\theta(\varphi_0) = p a \left(\frac{1}{1 + \cos \varphi_0} - \cos \varphi_0 \right), \quad (7.82)$$

⁵In the Pantheon's dome there are, in fact, 14 major cracks in the meridian direction, from the springing of the dome up to about 57° ; they are produced exactly by the tension, in the direction of the parallels, that cannot be absorbed by unreinforced concrete (see F. Masi, I. Stefanou & P. Vannucci: *A study about the origin of the cracks in the Pantheon's dome*. Engineering Failure Analysis, 92, 587-596, 2018). Similar problems exist also in the brick's dome of Saint Peter, in Rome and they gave rise to the famous study of the *three mathematicians* in the XVIIIth century (see E. Benvenuto: *An Introduction to the History of Structural Mechanics - Part II*, Springer, 1991).

is *not* the tension force in the ring itself. In fact, this last is submitted to the radial load

$$\gamma = -N_\varphi(\varphi_0) \cos \varphi_0, \quad (7.83)$$

see Fig. 7.15, that produces the tensile force

$$\begin{aligned} t &= \frac{1}{2} \int_0^\pi \gamma r_0(\varphi_0) \sin \psi \, d\psi = \gamma r_0(\varphi_0) = -N_\varphi(\varphi_0) r_0(\varphi_0) \cos \varphi_0 \\ &= \frac{p a^2}{1 + \cos \varphi_0} \sin \varphi_0 \cos \varphi_0 \neq N_\theta(\varphi_0). \end{aligned} \quad (7.84)$$

The difference in the two tensile forces is absorbed by the membrane through a local bending regime, that cannot be described by a membrane theory⁶.

In fact, for $\varphi = \varphi_0$, the radial displacement of the membrane, here taken as positive if outward, is, see eq. (7.93) in the next Section,

$$w(\varphi_0) = -\frac{p a^2}{h E} \left(\cos \varphi_0 - \frac{1 + \nu}{1 + \cos \varphi_0} \right), \quad (7.85)$$

while that in the ring beam is

$$w_b = \frac{t a}{E_b A_b} = \frac{p a^3 \sin \varphi_0 \cos \varphi_0}{E_b A_b (1 + \cos \varphi_0)}. \quad (7.86)$$

In the above equations, E and ν are the Young's modulus and Poisson's ratio of the material composing the membrane while E_b and A_b are, respectively, the Young's modulus of the ring beam and the area of its cross-section.

When the two displacements are equal, no edge effect is given by the ring beam to the membrane: the regime is everywhere a pure membrane regime. This happens when

$$w_b - w(\varphi_0) = 0 \rightarrow \frac{p a^3 \sin \varphi_0 \cos \varphi_0}{E_b A_b (1 + \cos \varphi_0)} + \frac{p a^2}{h E} \left(\cos \varphi_0 - \frac{1 + \nu}{1 + \cos \varphi_0} \right) = 0. \quad (7.87)$$

For given materials, the solution of this equation depends only upon the geometry of the surface, i.e. upon a and φ_0 . Such a solution describes a curve in the plane $a - \varphi_0$; in particular, it does not depend on the load p . For the points on the curve, $w_b = w(\varphi_0)$ and the regime is of membrane everywhere; for the points above the curve, $w_b < w(\varphi_0)$, so the ring beam applies to the membrane inward radial forces, while the opposite happens for the points below the curve, see Fig. 7.16.

7.5.1.3 Deformations and displacements

From eqs. (7.61), (7.76) and (7.77) we get

$$\begin{aligned} \varepsilon_\varphi &= \frac{p a \nu \cos^2 \varphi + \nu \cos \varphi - \nu - 1}{h E (1 + \cos \varphi)}, \\ \varepsilon_\theta &= -\frac{p a \cos^2 \varphi + \cos \varphi - \nu - 1}{h E (1 + \cos \varphi)}, \end{aligned} \quad (7.88)$$

⁶This is a typical mechanical inconsistency that exists in the equilibrium theory of curved membranes; we will find in the following examples other similar inconsistencies, all of them giving rise to local bending states that extinguish rapidly in a small zone close to the membrane's edge, see the textbooks of Timoshenko and Woinowsky-Krieger or of Novozhilov in the references.

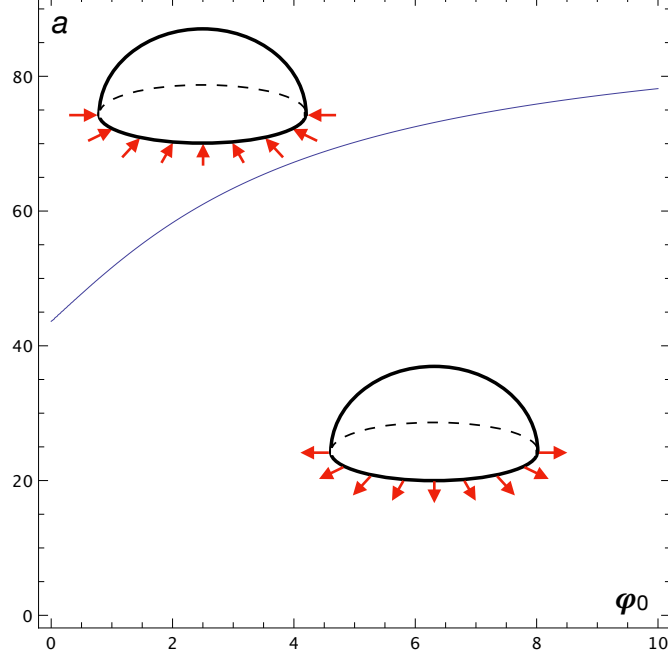


Figure 7.16: Actions of a ring beam on the membrane ($E = E_b$, $A_b = 1$, $h = 0.5$, $\nu = 0.25$).

and from eq. (7.68)

$$f(\varphi) = \frac{p a^2(1 + \nu)}{h E} \frac{\cos^2 \varphi + \cos \varphi - 2}{1 + \cos \varphi}. \quad (7.89)$$

that injected into eq. (7.69) gives

$$\begin{aligned} v &= \frac{p a^2(1 + \nu)}{h E} \sin \varphi \left(\int \frac{\cos^2 \varphi + \cos \varphi - 2}{(1 + \cos \varphi) \sin \varphi} + c \right) \\ &= \frac{p a^2(1 + \nu)}{h E} \sin \varphi \left(\log \frac{1 + \cos \varphi}{2} - \frac{1}{1 + \cos \varphi} + c \right). \end{aligned} \quad (7.90)$$

If we impose a null displacement on the boundary, i.e. $v(\varphi = \varphi_0) = 0$, then we get

$$c = \frac{1}{1 + \cos \varphi_0} - \log \frac{1 + \cos \varphi_0}{2}, \quad (7.91)$$

so finally

$$v = \frac{p a^2(1 + \nu)}{h E} \sin \varphi \left(\log \frac{1 + \cos \varphi}{1 + \cos \varphi_0} + \frac{\cos \varphi - \cos \varphi_0}{(1 + \cos \varphi)(1 + \cos \varphi_0)} \right). \quad (7.92)$$

The displacement w can then be obtained through eq. (7.70):

$$\begin{aligned} w &= \frac{p a^2(1 + \nu)}{h E} \sin \varphi \left[\cos \varphi \left(\log \frac{1 + \cos \varphi}{1 + \cos \varphi_0} + \frac{\cos \varphi - \cos \varphi_0}{(1 + \cos \varphi)(1 + \cos \varphi_0)} \right) \right. \\ &\quad \left. + \frac{\cos \varphi}{1 + \nu} - \frac{1}{1 + \cos \varphi} \right]. \end{aligned} \quad (7.93)$$

The polar diagrams of v and $-w$ are plotted in Fig. 7.17⁷

⁷To remark that the calculation of the radial displacement w has been done according to the basis $\{\mathbf{e}_1, \mathbf{e}_2, \mathbf{e}_3\}$, see Fig. 7.4. Hence, an inward displacement is positive and an outward one is negative.

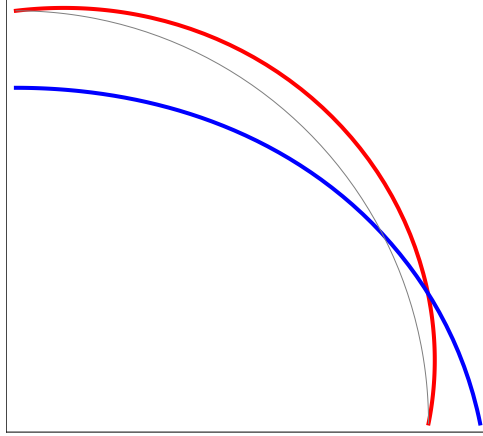


Figure 7.17: Polar diagrams of v , red, and $-w$, blue, for a spherical shell submitted to its own weight (in grey: the profile of the dome; the radial distance between this curve and the curve of a diagram measures the value of the quantity, positive when outward).

7.5.1.4 Spherical dome with *oculus*

Let us now consider the case of a spherical dome with an *oculus*, i.e. a hole, on the top, see Fig. 7.18, of radius r_i . Now, $\varphi_i \leq \varphi \leq \varphi_0$ and $N_\varphi(\varphi_i) = 0$ and using this boundary condition gives $c = -p a \cos \varphi_i$ in eq. (7.73) so that

$$N_\varphi = p a \frac{\cos \varphi - \cos \varphi_i}{\sin^2 \varphi}, \quad (7.94)$$

and

$$N_\theta = p a \left(\frac{\cos \varphi_i - \cos \varphi}{\sin^2 \varphi} - \cos \varphi \right). \quad (7.95)$$

The edge of the oculus is compressed⁸:

$$N_\theta(\varphi_i) = -p a \cos \varphi_i. \quad (7.96)$$

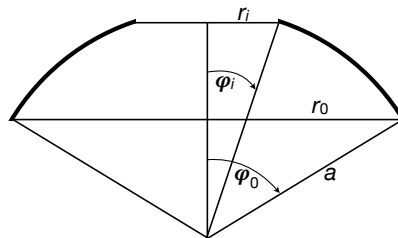


Figure 7.18: Scheme of a spherical dome with an *oculus*.

In order to have a graphical representation of the true displacements of the dome, the opposite of w is plotted in Fig. 7.17.

⁸The Romans already knew this fact: the Pantheon's dome, like others built by the Romans, had an oculus whose edge is reinforced by an arch made by bricks and, probably, by a bronze ring.

7.5.1.5 Spherical dome with lantern

This is the case of the most part of historical domes, see e.g. Fig 7.19. The previous case is modified imposing that now

$$N_\varphi(\varphi_i) = -\frac{q_L}{\sin \varphi_i}, \quad (7.97)$$

where q_L is the weight per unit length of the lantern. This gives now

$$c = -q_L \sin \varphi_i - p a \cos \varphi_i, \quad (7.98)$$

so that



Figure 7.19: Some famous examples of historical domes with lantern.

$$\begin{aligned} N_\varphi &= \frac{p a (\cos \varphi - \cos \varphi_i) - q_L \sin \varphi_i}{\sin^2 \varphi}, \\ N_\theta &= p a \left(\frac{\cos \varphi_i - \cos \varphi}{\sin^2 \varphi} - \cos \varphi \right) + q_L \frac{\sin \varphi_i}{\sin^2 \varphi}. \end{aligned} \quad (7.99)$$

In particular,

$$N_\theta(\varphi_i) = -p a \cos \varphi_i + \frac{q_L}{\sin \varphi_i}, \quad (7.100)$$

that can be positive or negative, i.e. the base of the lantern can be either in compression or in tension.

Because the membrane cannot take on transverse shear forces, a reinforcing ring is necessary at the base of the lantern, see Fig. 7.20; this is submitted to the radial compressive load

$$\gamma = \frac{q_L}{\tan \varphi_i} \quad (7.101)$$

that produces in the ring the traction

$$t = \gamma r_i = q_L a \cos \varphi_i. \quad (7.102)$$

As in the case of the dome supported by a ring beam, also in this case such a force produces in the ring deformations that are not equal to those in the adjacent part of the

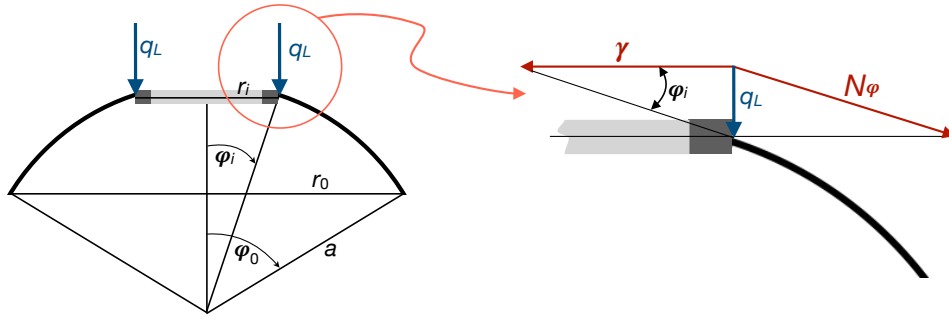


Figure 7.20: Scheme of a spherical dome with lantern.

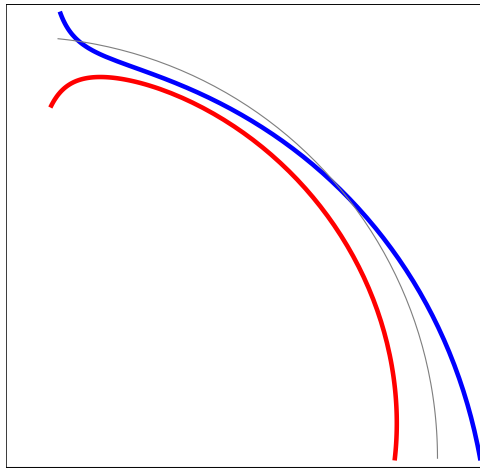


Figure 7.21: Polar diagrams of N_φ , red, and N_θ , blue, for a spherical shell with lantern (in grey: the profile of the dome; the radial distance between this curve and the curve of a diagram measures the value of the quantity, positive when outward).

dome: this produces local bending that is rapidly dissipated in the dome. In Fig. 7.21 we show the polar diagrams of N_φ and N_θ for the case of a spherical dome with a lantern (the diagrams are referred to a case where the total weight of the lantern is equal to $pa^2/10$ and the radius of the lantern is equal to $a/10$).

In Fig. 7.22 we compare the diagrams of N_φ and N_θ for three different cases of spherical domes: entire dome, dome with *oculus* and dome with lantern. The diagrams are referred to a case where the total weight of the lantern is equal to $pa^2/10$ and the radius of the lantern or of the oculus is equal to $a/10$.

7.5.1.6 Wind on a spherical dome

Let us now consider the action of the wind on a spherical dome; if we consider air as a perfect, i.e. inviscid, fluid, the wind's load resume to only a load normal to the dome's surface, i.e. $p_\theta = p_\varphi = 0$, while p_n can be modeled as

$$p_n = p \sin \varphi \cos \theta. \quad (7.103)$$

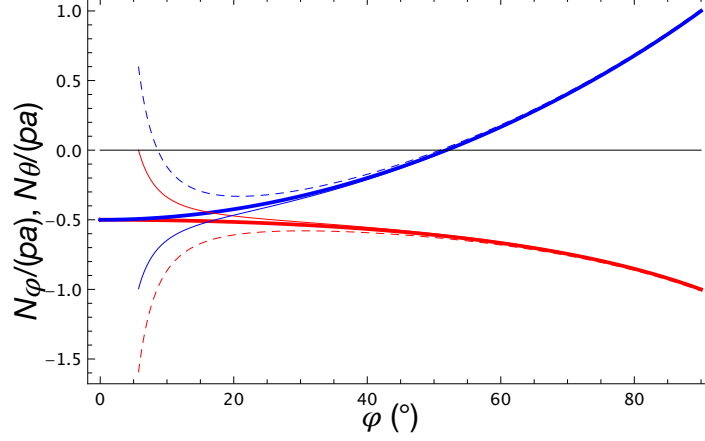


Figure 7.22: Cartesian diagrams of N_φ , red, and N_θ , blue, for an entire spherical shell, thick lines, with an *oculus*, thin lines, and with a lantern, dashed lines.

In such a case, eqs. (7.39) become

$$\begin{aligned} \frac{\partial}{\partial \varphi}(N_\varphi \sin \varphi) - \cos \varphi N_\theta + \frac{\partial N_{\varphi\theta}}{\partial \theta} &= 0, \\ \frac{\partial N_\theta}{\partial \theta} + \frac{\partial(\sin \varphi N_{\theta\varphi})}{\partial \varphi} + \cos \varphi N_{\varphi\theta} &= 0, \\ N_\varphi + N_\theta &= -p a \sin \varphi \cos \theta. \end{aligned} \quad (7.104)$$

If from the third of the above equations we make N_θ explicit and inject its expression into the first two equations, after some standard passages we obtain two equations for N_φ and $N_{\varphi\theta}$:

$$\begin{aligned} \sin \varphi \frac{\partial N_\varphi}{\partial \varphi} + \frac{\partial N_{\varphi\theta}}{\partial \theta} + 2 \cos \varphi N_\varphi + p a \sin \varphi \cos \varphi \cos \theta &= 0, \\ \sin \varphi \frac{\partial N_{\varphi\theta}}{\partial \varphi} - \frac{\partial N_\varphi}{\partial \theta} + 2 \cos \varphi N_{\varphi\theta} + p a \sin \varphi \sin \theta &= 0. \end{aligned} \quad (7.105)$$

To solve the above partial differential equations, we look for a solution of the form⁹

$$N_\varphi = S_\varphi(\varphi) \cos \theta, \quad N_{\varphi\theta} = S_{\varphi\theta}(\varphi) \sin \theta; \quad (7.106)$$

injecting these two expressions into eqs. (7.105) we get a system of two coupled ordinary differential equations:

$$\begin{aligned} \sin \varphi \frac{\partial S_\varphi}{\partial \varphi} + 2 \cos \varphi S_\varphi + S_{\varphi\theta} + p a \sin \varphi \cos \varphi &= 0, \\ \sin \varphi \frac{\partial S_{\varphi\theta}}{\partial \varphi} + 2 \cos \varphi S_{\varphi\theta} + S_\varphi + p a \sin \varphi &= 0. \end{aligned} \quad (7.107)$$

⁹This choice is motivated by the symmetry that the solution should have as a consequence of the symmetrical distribution of the wind load p_n .

To uncouple and solve the above equations, we first add them together and then we subtract the second one from the first one, to obtain

$$\begin{aligned}\sin \varphi \frac{\partial S_1}{\partial \varphi} + (1 + 2 \cos \varphi) S_1 + p a \sin \varphi (1 + \cos \varphi) &= 0, \\ \sin \varphi \frac{\partial S_2}{\partial \varphi} - (1 - 2 \cos \varphi) S_2 - p a \sin \varphi (1 - \cos \varphi) &= 0,\end{aligned}\tag{7.108}$$

where

$$S_1 = S_\varphi + S_{\varphi\theta}, \quad S_2 = S_\varphi - S_{\varphi\theta} \quad \rightarrow \quad S_\varphi = \frac{S_1 + S_2}{2}, \quad S_{\varphi\theta} = \frac{S_1 - S_2}{2}.\tag{7.109}$$

The solution of eqs. (7.108) is

$$\begin{aligned}S_1 &= \frac{1 + \cos \varphi}{\sin^3 \varphi} \left[c_1 + \frac{1}{3} p a \cos \varphi (3 - \cos^2 \varphi) \right], \\ S_2 &= \frac{1 - \cos \varphi}{\sin^3 \varphi} \left[c_2 - \frac{1}{3} p a \cos \varphi (3 - \cos^2 \varphi) \right],\end{aligned}\tag{7.110}$$

that finally gives

$$\begin{aligned}N_\varphi &= \frac{\cos \theta}{\sin^3 \varphi} \left(\frac{c_1 + c_2}{2} + \frac{c_1 - c_2}{2} \cos \varphi + \frac{1}{3} p a \cos^2 \varphi (3 - \cos^2 \varphi) \right), \\ N_{\varphi\theta} &= \frac{\sin \theta}{\sin^3 \varphi} \left(\frac{c_1 - c_2}{2} + \frac{c_1 + c_2}{2} \cos \varphi + \frac{1}{3} p a \cos \varphi (3 - \cos^2 \varphi) \right),\end{aligned}\tag{7.111}$$

and, through eq. (7.104)₃,

$$N_\theta = -\frac{\cos \theta}{\sin^3 \varphi} \left(\frac{c_1 + c_2}{2} + \frac{c_1 - c_2}{2} \cos \varphi + \frac{1}{3} p a (3 \sin^2 \varphi + 2 \cos^4 \varphi) \right).\tag{7.112}$$

The two constants c_1 and c_2 can be determined through the boundary conditions. In the case of a hemispherical dome ($\varphi_0 = \pi/2$), we get that on the border

$$N_\varphi(\varphi_0) = \frac{c_1 + c_2}{2} \cos \theta, \quad N_{\varphi\theta}(\varphi_0) = \frac{c_1 - c_2}{2} \sin \theta,\tag{7.113}$$

We then consider that the moment of the wind load about the line at $\theta = \pi/2$ of the dome's base, i.e. with respect to the diameter of the dome's base orthogonal to the direction of the wind, is null¹⁰. Because such a moment is equal and opposite to the moment of the internal forces at the dome's base, also these internal forces have a null moment:

$$\int_0^{2\pi} N_\varphi(\varphi_0) a^2 \cos \theta \, d\theta = 0.\tag{7.114}$$

The second boundary condition imposes that the component in the direction of the wind of the resultant of the internal forces at the dome's base must be equal and opposite to the total horizontal wind action:

$$\int_0^{2\pi} N_\varphi(\varphi_0) a^2 \sin \theta \, d\theta = - \int_0^{2\pi} \int_0^{\frac{\pi}{2}} p_n a^2 \sin^2 \varphi \cos \theta \, d\theta \, d\varphi.\tag{7.115}$$

¹⁰This is an immediate consequence of the fact that p_s is a radial load.

The two boundary conditions give hence the equations

$$\begin{aligned} \frac{\pi}{2}(c_1 + c_2)a^2 &= 0, \\ \frac{\pi}{2}a(c_1 - c_2) &= -\frac{2}{3}\pi p a^2, \end{aligned} \quad \rightarrow \quad c_1 = -\frac{2}{3}p a, \quad c_2 = \frac{2}{3}p a, \quad (7.116)$$

and finally

$$\begin{aligned} N_\varphi &= -\frac{p a \cos \varphi \cos \theta}{3 \sin^3 \varphi} (2 - 3 \cos \varphi + \cos^3 \varphi), \\ N_\theta &= \frac{p a \cos \theta}{3 \sin^3 \varphi} (2 \cos \varphi - 3 \sin^2 \varphi - 2 \cos^4 \varphi), \\ N_{\varphi\theta} &= -\frac{p a \sin \theta}{3 \sin^3 \varphi} (2 - 3 \cos \varphi + \cos^3 \varphi). \end{aligned} \quad (7.117)$$

The polar diagrams of N_φ , N_θ and $N_{\varphi\theta}$ are plotted in Fig. 7.23.

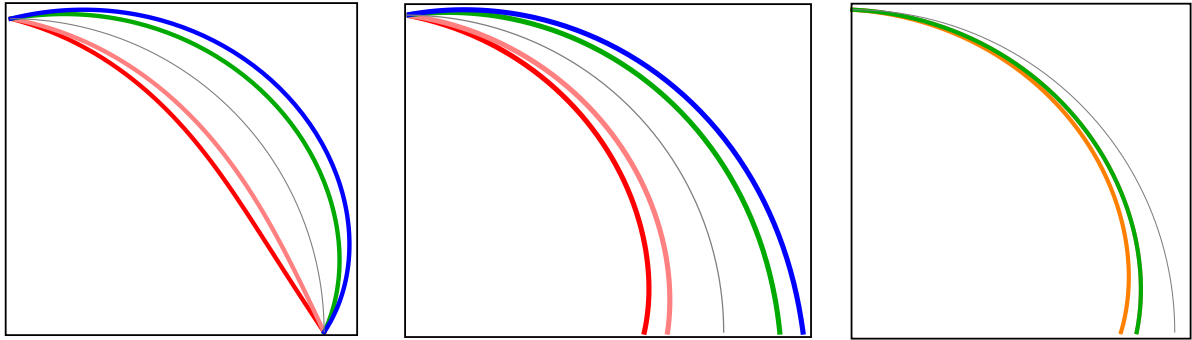


Figure 7.23: Polar diagrams of N_φ , left, $N_\theta/4$, center, $N_{\varphi\theta}/4$, right, plotted for $\theta = 0^\circ$, red, $\theta = 45^\circ$, pink, $\theta = 90^\circ$, orange, $\theta = 135^\circ$, green, and $\theta = 180^\circ$, blue (in grey: the profile of the dome; the radial distance between this curve and the curve of a diagram measures the value of the quantity, positive when outward).

7.5.2 Elliptical domes

We consider the case of an axisymmetric dome whose meridians have the shape of an ellipse of equation

$$\frac{x^2}{a^2} + \frac{y^2}{b^2} = 1, \quad (7.118)$$

like in Fig. 7.24. For such a case,

$$r_1 = \frac{a^2 b^2}{(a^2 \sin^2 \varphi + b^2 \cos^2 \varphi)^{\frac{3}{2}}}, \quad r_2 = \frac{a^2}{(a^2 \sin^2 \varphi + b^2 \cos^2 \varphi)^{\frac{1}{2}}}. \quad (7.119)$$

We consider two load cases: a vault submitted to its own weight and a pressure tank.

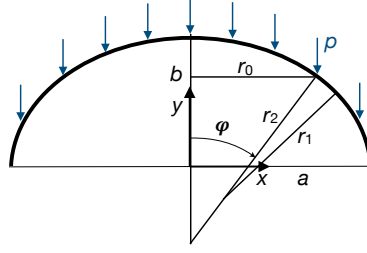


Figure 7.24: Scheme of an elliptical dome submitted to its own weight.

7.5.2.1 Elliptical vault under its own weight

The load vector is $\mathbf{p} = (p_\theta, p_\varphi, p_n) = (0, p \sin \varphi, p \cos \varphi)$, so eq. (7.54)₁ becomes

$$\frac{\partial U}{\partial \varphi} = -\frac{a^4 b^2}{(a^2 \sin^2 \varphi + b^2 \cos^2 \varphi)^2} p \sin \varphi. \quad (7.120)$$

This equation can be solved by a change of variable: we put

$$\cos \psi = \frac{c}{a} \cos \varphi, \quad (7.121)$$

with

$$c^2 = a^2 - b^2. \quad (7.122)$$

Hence,

$$\frac{\partial U}{\partial \varphi} = \frac{\partial U}{\partial \psi} \frac{\partial \psi}{\partial \varphi}, \quad (7.123)$$

and through eqs. (7.120) and (7.121) we get the differential equation

$$\frac{\partial U}{\partial \psi} = -\frac{p a b^2}{c \sin^3 \psi}, \quad (7.124)$$

whose solution is

$$U = -p \frac{a^2 b^2}{2} \left(\frac{1}{2a c} \log \frac{a - c \cos \varphi}{a + c \cos \varphi} - \frac{\cos \varphi}{a^2 \sin^2 \varphi + b^2 \cos^2 \varphi} + c_1 \right). \quad (7.125)$$

To determine the constant c_1 , we consider that, because of eq. (7.55), it must be $U(\varphi = 0) = 0$ (otherwise, N_φ should not be finite at the dome's top). This gives

$$c_1 = \frac{1}{b^2} - \frac{1}{2a c} \log \frac{a - c}{a + c}, \quad (7.126)$$

and finally, from eqs. (7.55) and (7.56) we get

$$\begin{aligned} N_\varphi &= -p \frac{b^2}{2 \sin^2 \varphi} \sqrt{a^2 \sin^2 \varphi + b^2 \cos^2 \varphi} \times \\ &\quad \left[\frac{1}{b^2} - \frac{\cos \varphi}{a^2 \sin^2 \varphi + b^2 \cos^2 \varphi} + \frac{1}{2a c} \log \left(\frac{a - c \cos \varphi}{a + c \cos \varphi} \frac{a + c}{a - c} \right) \right], \\ N_\theta &= -p \frac{a^2 \cos \varphi}{\sqrt{a^2 \sin^2 \varphi + b^2 \cos^2 \varphi}} + \frac{p}{2 \sin^2 \varphi} (a^2 \sin^2 \varphi + b^2 \cos^2 \varphi)^{\frac{3}{2}} \times \\ &\quad \left[\frac{1}{b^2} - \frac{\cos \varphi}{a^2 \sin^2 \varphi + b^2 \cos^2 \varphi} + \frac{1}{2a c} \log \left(\frac{a - c \cos \varphi}{a + c \cos \varphi} \frac{a + c}{a - c} \right) \right]. \end{aligned} \quad (7.127)$$

At the dome's top, $\varphi = 0$, it is

$$N_\varphi = N_\theta = -p \frac{a^2}{2b}. \quad (7.128)$$

To remark that for $a = b$ the above formulae coincide with those already found for the spherical dome, cfr. Sect. 7.5.1.1.

The diagrams of N_φ and N_θ for the case $a = 1.5b$ are plotted in Fig. 7.25.

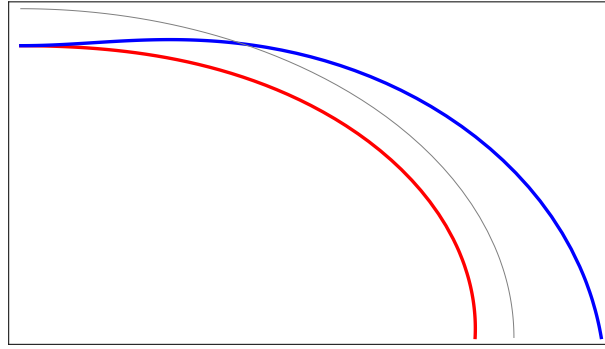


Figure 7.25: Polar diagrams of N_φ , red, and N_θ , blue, for an elliptical shell (in grey: the profile of the dome; the radial distance between this curve and the curve of a diagram measures the value of the quantity, positive when outward).

7.5.2.2 Elliptical pressure tank

Axisymmetric elliptical domes are often used to form the edges of many cylindrical pressure tanks. In this case the load vector is $\mathbf{p} = (p_\theta, p_\varphi, p_n) = (0, 0, -p)$. The procedure followed in the previous case can still be used, but it is easier to follow the procedure of Sect. 7.4.6.1. In fact, the resultant of the pressure load is

$$F = -\pi p r_0^2, \quad (7.129)$$

so from eq. (7.57) we get

$$N_\varphi = \frac{p r_0}{2 \sin \varphi} = \frac{1}{2} \frac{p a^2}{\sqrt{a^2 \sin^2 \varphi + b^2 \cos^2 \varphi}}. \quad (7.130)$$

and from eq. (7.56)

$$N_\theta = \frac{p a^2}{\sqrt{a^2 \sin^2 \varphi + b^2 \cos^2 \varphi}} \left(1 - \frac{a^2 \sin^2 \varphi + b^2 \cos^2 \varphi}{2b^2} \right). \quad (7.131)$$

We see hence that, while $N_\varphi > 0 \forall \varphi$, i.e. the meridians are always in tension, N_θ can change its sign. In particular, at the dome's top

$$N_\varphi(\varphi = 0) = N_\theta(\varphi = 0) = \frac{p a^2}{2b}, \quad (7.132)$$

while at the equator

$$N_\varphi \left(\varphi = \frac{\pi}{2} \right) = \frac{p a}{2}, \quad N_\theta \left(\varphi = \frac{\pi}{2} \right) = p a \left(1 - \frac{a^2}{2b^2} \right), \quad (7.133)$$

so at the equator $N_\theta < 0$ (compression) if $a > b\sqrt{2}$. Finally, a spherical tank corresponds to the special case $a = b$.

The diagrams of N_φ and N_θ for the case $a = 2.5b$ are plotted in Fig. 7.25.

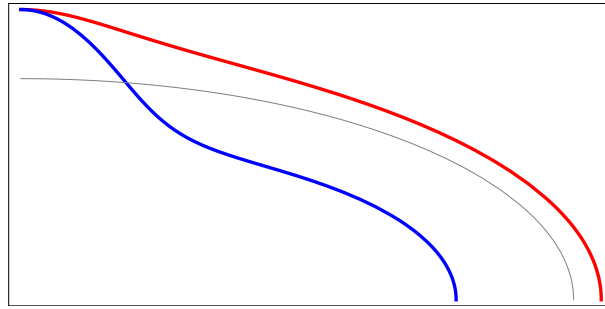


Figure 7.26: Polar diagrams of N_φ , red, and N_θ , blue, for an elliptical pressure tank (in grey: the profile of the dome; the radial distance between this curve and the curve of a diagram measures the value of the quantity, positive when outward).

7.5.3 Conical vaults

We consider a conical vault with the meridians inclined of an angle α on the cone's axis, like in Fig. 7.27; in this case, $r_1 \rightarrow \infty$ and $\varphi = \pi/2 - \alpha$ cannot be used as a variable because it is a constant. Hence, a curvilinear coordinate must be chosen to determine a position on a chosen meridian. This one can be, e.g., the coordinate ξ , measuring along the axis of the cone the distance from the tip, or the distance s , still from the cone's tip but measured directly along a meridian, see Fig. 7.27. Of course,

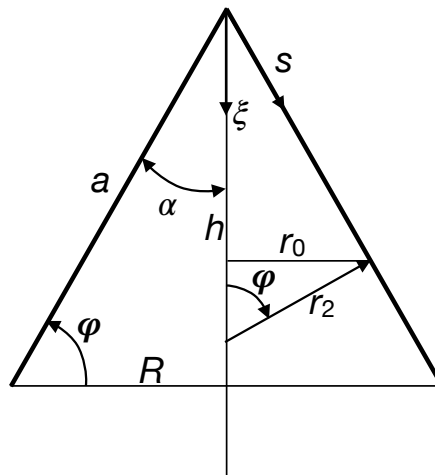


Figure 7.27: Scheme of a conical vault.

$$\xi = s \cos \alpha, \quad (7.134)$$

and

$$r_2 = \xi \frac{\tan \alpha}{\cos \alpha} = s \tan \alpha, \quad r_0 = r_2 \cos \alpha = \xi \tan \alpha = s \sin \alpha. \quad (7.135)$$

R is the radius of the cone's base, h the cone's height and a the length of a meridian:

$$a = \sqrt{R^2 + h^2}. \quad (7.136)$$

If we consider eq. (7.56), we see that, because $r_1 \rightarrow \infty$,

$$N_\theta = -p_n r_2 = -p_n \xi \frac{\tan \alpha}{\cos \alpha} = -p_n s \tan \alpha; \quad (7.137)$$

so, in this case, N_θ and N_s are uncoupled, in particular, N_θ does not depend upon N_s but uniquely upon the load and the distance from the tip.

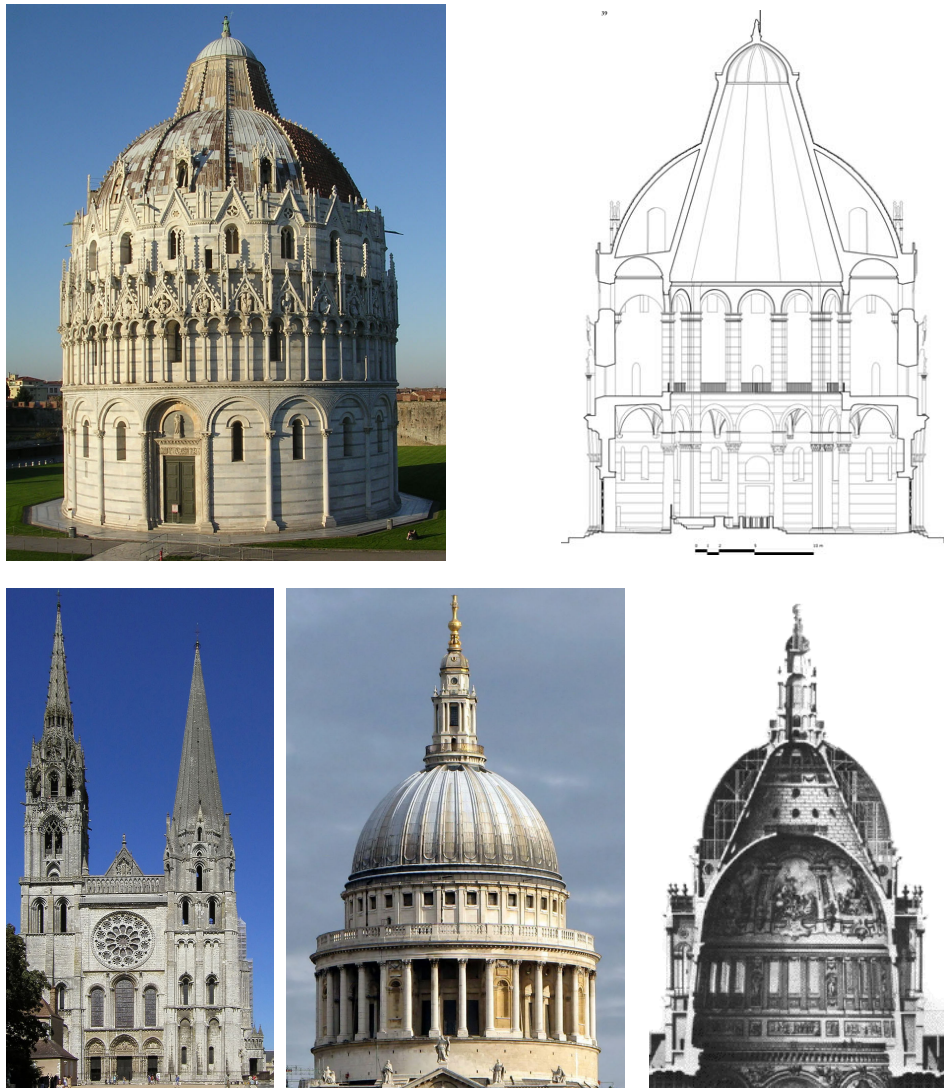


Figure 7.28: Three historical conical vaults; the Baptistery of Pisa (from 1152) and a cross-section of its structure (from the thesis of G. Verdiani, 2003); the Cathedral of Chartres (from 1194), the dome of Saint Paul's Cathedral (from 1675) and a cross-section of its structure.

Historically, some remarkable structures of the Middle Ages have the form of a conical vault, they are shown in Fig. 7.28: the roof of the South Tower of the Chartres Cathedral, the internal supporting structures of the dome of the Baptistery of Pisa and of the dome of Saint Paul's Cathedral, in London.

We consider in the following Sections different load cases for conical vaults.

7.5.3.1 Vertical tip load

We consider the presence of a vertical concentrated force P applied on the tip of the cone. From eq. (7.57) we get (of course, $F = P$)¹¹:

$$N_s = -\frac{P}{2\pi r_0 \sin \varphi} = -\frac{P}{2\pi r_0 \cos \alpha} = -\frac{P}{2\pi \xi \sin \alpha} = -\frac{P}{\pi s \sin 2\alpha}. \quad (7.138)$$

while, because $\mathbf{p} = (p_s, p_\theta, p_n) = (0, 0, 0)$, it is $N_\theta = 0$, see eq. (7.137). This is an interesting result, because, along with the general result $N_{s\theta}=0$ for axisymmetric membranes acted upon by an axisymmetric load, it clearly indicates that the membrane works like if it was constituted by an array of struts, the meridians, working independently. The singularity of N_s at the tip is of course due to the model, that considers a concentrated load.

7.5.3.2 Conical vault under its own weight

In this case, $\mathbf{p} = (p_s, p_\theta, p_n) = (p \cos \alpha, 0, p \sin \alpha)$

$$\begin{aligned} F(\xi) &= \int_0^\xi 2\pi p r_0(\xi^*) \frac{1}{\cos \alpha} d\xi^* = 2\pi p \frac{\tan \alpha}{\cos \alpha} \int_0^\xi \xi^* d\xi^* \\ &= \pi p \xi^2 \frac{\tan \alpha}{\cos \alpha} = \pi p s^2 \tan \alpha \cos \alpha. \end{aligned} \quad (7.139)$$

So, still from eqs. (7.57) and (7.137), we obtain

$$\begin{aligned} N_s &= -\pi p \xi^2 \frac{\tan \alpha}{\cos \alpha} \frac{1}{2\pi \xi \tan \alpha \sin \varphi} = -\frac{p \xi}{2 \cos^2 \alpha} = -\frac{p s}{2 \cos \alpha}, \\ N_\theta &= -p \xi \tan^2 \alpha = -p s \frac{\sin^2 \alpha}{\cos \alpha}. \end{aligned} \quad (7.140)$$

So, both N_s and N_θ are compression forces and their intensities increase linearly with the distance from the tip.

7.5.3.3 Conical water reservoir

We refer to a conical reservoir like in Fig. 7.29, filled with water (or another liquid) of density ρ and we consider it hanged at the upper part. We have now $\varphi = \pi/2\alpha$ and the

¹¹Because φ cannot be used anymore as a variable, we denote by N_s the membrane force along the meridians; in the same way, the index φ is replaced everywhere by s .

load is $\mathbf{p} = (p_s, p_\theta, p_n) = (0, 0, -\rho g(h - \xi))$. The force F for a position determined by a given ξ , or s , is the weight of the mass of water shadowed in Fig. 7.29:

$$\begin{aligned} F &= \int_0^s 2\pi r_0 p_n(s^*) \sin \alpha ds^* = - \int_0^s 2\pi \rho g s^{*2} \sin^2 \alpha ds^* \\ &= -\pi \rho g s^2 \sin^2 \alpha \left(h - \frac{2}{3}s \cos \alpha \right) = -\pi \rho g \xi^2 \tan^2 \alpha \left(h - \frac{2}{3}\xi \right). \end{aligned} \quad (7.141)$$

Hence, again from eqs. (7.57) and (7.137), we obtain

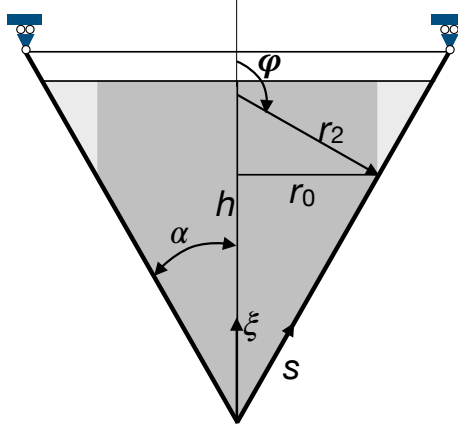


Figure 7.29: Scheme of a conical water reservoir.

$$\begin{aligned} N_s &= \rho g \xi \frac{\tan \alpha}{2 \cos \alpha} \left(h - \frac{2}{3}\xi \right) = \frac{1}{2} \rho g s \tan \alpha \left(h - \frac{2}{3}s \cos \alpha \right), \\ N_\theta &= \rho g \xi \frac{\tan \alpha}{\cos \alpha} (h - \xi) = \rho g s \tan \alpha (h - s \cos \alpha). \end{aligned} \quad (7.142)$$

N_s and N_θ are hence quadratic functions of ξ or s , their variation is plotted in Fig. 7.30 for the case $\alpha = 30^\circ$. It easy to see that

$$\begin{aligned} N_s^{max} &= N_s \left(\xi = \frac{3}{4}h \right) = \frac{3}{16} \rho g h^2 \frac{\tan \alpha}{\cos \alpha}, \\ N_\theta^{max} &= N_\theta \left(\xi = \frac{h}{2} \right) = \frac{1}{4} \rho g h^2 \frac{\tan \alpha}{\cos \alpha}. \end{aligned} \quad (7.143)$$

If a stiffening ring is added to the base of the cone, like in the case of the spherical dome in Sect. 7.5.1.2, this is submitted to the radial load

$$\gamma = -N_s(\xi = h) \sin \alpha = -\frac{1}{6} \rho g h^2 \tan^2 \alpha, \quad (7.144)$$

which gives in the ring the axial compression force

$$t = \gamma R = -\frac{1}{6} \rho g h^3 \tan^3 \alpha. \quad (7.145)$$

Because at the same level $N_\theta = 0$, see Fig. 7.30, the deformation in the ring and the adjacent part of the cone is different; once more, this gives rise to local bending strains and stresses that quickly decrease with the distance from the border.

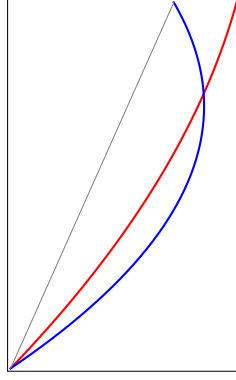


Figure 7.30: Diagrams of N_s , red, and N_θ , blue, for a suspended conical reservoir (in grey: the profile of the reservoir; the horizontal distance between this curve and the curve of a diagram measures the value of the quantity, positive when outward).

The above results can be used easily to study the case where the cone is supported at its base (for instance, in a water tower); in such a case,

$$F = \pi \rho g \tan^2 \alpha \left[\frac{h^3}{3} - \xi^2 \left(h - \frac{2}{3} \xi \right) \right] \quad (7.146)$$

and, by consequence

$$N_s = -\frac{\rho g \tan \alpha}{2\xi \cos \alpha} \left[\frac{h^3}{3} - \xi^2 \left(h - \frac{2}{3} \xi \right) \right]. \quad (7.147)$$

Also in this case, $N_s \rightarrow \infty$ for $s \rightarrow 0$, as a consequence of the assumption of concentrated reaction at the tip. For what concerns N_θ , this does not change with respect to the case of suspended reservoir, because it depends uniquely upon p_n , which is the same in the two cases. In Fig. 7.31 are plotted the diagrams of N_s and N_θ for this case, $\alpha = 30^\circ$ (the curve representing N_s has been cut off near the tip).

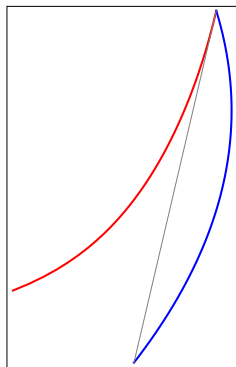


Figure 7.31: Diagrams of N_s , red, and N_θ , blue, for a conical reservoir supported at the tip (in grey: the profile of the reservoir; the horizontal distance between this curve and the curve of a diagram measures the value of the quantity, positive when outward).

7.5.3.4 Wind load on a conical vault

We assume the load to be $\mathbf{p} = (p_s, p_\theta, p_n) = (0, 0, \frac{1}{2}p \cos \alpha \cos \theta)$; because, from the same definition of curvature radius,

$$r_1 = \frac{ds}{d\varphi}, \quad (7.148)$$

eqs. (7.39) become

$$\begin{aligned} \frac{\partial}{\partial s}(r_2 \sin \varphi N_s) - \cos \varphi N_\theta + \frac{\partial N_{s\theta}}{\partial \theta} &= -p_s r_2 \sin \varphi, \\ \frac{\partial N_\theta}{\partial \theta} + \frac{\partial(r_2 \sin \varphi N_{s\theta})}{\partial s} + \cos \varphi N_{s\theta} &= -p_\theta r_2 \sin \varphi, \\ N_\theta &= -p_n r_2, \end{aligned} \quad (7.149)$$

and applied to the present case they give

$$\begin{aligned} \frac{\partial}{\partial s}(s \sin \alpha N_s) - \sin \alpha N_\theta + \frac{\partial N_{s\theta}}{\partial \theta} &= 0, \\ \frac{\partial N_\theta}{\partial \theta} + \frac{\partial(s \sin \alpha N_{s\theta})}{\partial s} + \sin \alpha N_{s\theta} &= 0, \\ N_\theta &= -\frac{1}{2}p s \sin \alpha \cos \theta. \end{aligned} \quad (7.150)$$

Injecting the third equation into the second one gives the equation

$$s \frac{\partial N_{s\theta}}{\partial s} + 2N_{s\theta} = -\frac{1}{2}p s \sin \theta, \quad (7.151)$$

whose solution is

$$N_{s\theta} = -\frac{1}{6}p s \sin \theta + \frac{f_{s\theta}(\theta)}{s^2}. \quad (7.152)$$

To have tip a finite value of $N_{s\theta}$ at the tip, $s = 0$, it must be $f_{s\theta}(\theta) = 0$, so finally

$$N_{s\theta} = -\frac{1}{6}p s \sin \theta. \quad (7.153)$$

Injecting this result and eq. (7.150)₃ into eq. (7.150)₁ gives the equation

$$s \sin \alpha \frac{\partial N_s}{\partial s} + \sin \alpha N_s = \frac{1}{6}p s \cos \theta (1 - 3 \sin^2 \alpha), \quad (7.154)$$

whose solution is

$$N_s = \frac{1}{12}p s \frac{\cos \theta}{\sin \alpha} (1 - 3 \sin^2 \alpha) + \frac{f_s(\theta)}{s}; \quad (7.155)$$

also in this case, to have a finite value of N_s at the tip, it must be $f_s(\theta) = 0$; in the end,

$$N_s = \frac{1}{12}p s \frac{\cos \theta}{\sin \alpha} (1 - 3 \sin^2 \alpha). \quad (7.156)$$

To remark that N_s, N_θ and $N_{s\theta}$ vary linearly with s .

7.5.3.5 A concentrated force at the tip

Let us now consider the case of a (non vertical) concentrated force at the tip $\mathbf{F} = (F_x, F_y, F_z)$. For the equilibrium of the cone, it must be

$$\begin{aligned} F_x &= \int_0^{2\pi} N_s s \sin \alpha \cos \alpha d\theta, \\ F_y &= \int_0^{2\pi} (N_s \sin \alpha \cos \theta - N_{s\theta} \sin \theta) s \sin \alpha d\theta, \\ F_z &= \int_0^{2\pi} (N_s \sin \alpha \sin \theta + N_{s\theta} \cos \theta) s \sin \alpha d\theta. \end{aligned} \quad (7.157)$$

In this case, $\mathbf{p} = (p_s, p_\theta, p_n) = (0, 0, 0)$, so $N_\theta = 0$, like in the case of Sect. 7.5.3.1. Eq. (7.150)₂ becomes

$$\frac{\partial(s \sin \alpha N_{s\theta})}{\partial s} + \sin \alpha N_{s\theta} = 0 \rightarrow s \frac{\partial N_{s\theta}}{\partial s} + 2N_{s\theta} = 0, \quad (7.158)$$

whose solution is

$$N_{s\theta} = \frac{f_1(\theta)}{s^2}. \quad (7.159)$$

Inserting this result into eq. (7.150)₁ gives

$$\frac{\partial}{\partial s}(s \sin \alpha N_s) + \frac{1}{s^2} \frac{df_1(\theta)}{d\theta} = 0 \rightarrow s \frac{\partial N_s}{\partial s} + N_s + \frac{1}{s^2 \sin \alpha} \frac{df_1(\theta)}{d\theta} = 0, \quad (7.160)$$

whose solution is

$$N_s = \frac{1}{s^2 \sin \alpha} \frac{df_1(\theta)}{d\theta} + \frac{f_2(\theta)}{s}. \quad (7.161)$$

We put the two unknown functions

$$f_1(\theta) = A \cos \theta, \quad f_2(\theta) = B \cos \theta, \quad A, B \in \mathbb{R}, \quad (7.162)$$

and we determine the two constants A and B inserting eqs. (7.159) and (7.161) into eqs. (7.157); to be specific, we consider the case $\mathbf{F} = (0, F_y, 0)$, so we get the conditions

$$\begin{aligned} \int_0^{2\pi} \left(-\frac{A \sin \theta}{s \sin \alpha} + B \cos \theta \right) \sin \alpha \cos \alpha d\theta &= 0, \\ \int_0^{2\pi} \left[\left(-\frac{A \sin \theta}{s \sin \alpha} + B \cos \theta \right) \sin \alpha - \frac{1}{s} A \sin \theta \right] \sin \alpha \cos \theta d\theta &= F_y \\ \int_0^{2\pi} \left[\left(-\frac{A \sin \theta}{s \sin \alpha} + B \cos \theta \right) \sin \alpha \sin \theta + \frac{1}{s} A \cos^2 \theta \right] \sin \alpha d\theta &= 0, \end{aligned} \quad (7.163)$$

that give

$$F_y = \pi B \sin^2 \alpha \rightarrow B = \frac{F_y}{\pi \sin^2 \alpha} \rightarrow A = 0. \quad (7.164)$$

Finally, $N_\theta = N_{s\theta} = 0$ while

$$N_s = \frac{F_y}{\pi s \sin^2 \alpha} \cos \theta. \quad (7.165)$$

We have already seen in Sect. 7.5.3.1 that a vertical (upward) force F_x produces the internal action

$$N_s = \frac{F_x}{\pi s \sin 2\alpha}. \quad (7.166)$$

If $F_y = F_x \tan \alpha$, the tip force is aligned with a meridian, i.e. it is tangent to the cone's surface, and, by the superposition of the effects, we get

$$N_s = \frac{F_y}{2\pi s \sin \alpha \cos \alpha} (1 + 2 \cos \theta) = \frac{F_y}{2\pi \xi \sin \alpha} (1 + 2 \cos \theta). \quad (7.167)$$

Once more, the paradox that the membrane forces tend towards infinity when $s \rightarrow 0$ is due to the model of concentrated force.

7.5.4 Pipes

A pipe of radius r is a degenerated conic vault, where $\varphi = \pi/2 \rightarrow \alpha = 0$, $r_1 \rightarrow \infty$ and $r_2 = r$. Eqs. (7.149) become hence

$$\begin{aligned} r \frac{\partial N_s}{\partial s} + \frac{\partial N_{s\theta}}{\partial \theta} &= -p_s r, \\ \frac{\partial N_\theta}{\partial \theta} + r \frac{\partial N_{s\theta}}{\partial s} &= -p_\theta r, \\ N_\theta &= -p_n r. \end{aligned} \quad (7.168)$$

A particularly important case is that of a pipe submitted to an internal pressure $p \rightarrow \mathbf{p} = (p_s, p_\theta, p_n) = (0, 0, -p)$, $p > 0$. Then, eq. (7.168)₃ gives immediately¹²

$$N_\theta = p r. \quad (7.169)$$

Because the load is axisymmetric and $p_\theta = 0$, $N_{s\theta} = 0$, cfr. Sect. 7.4.6. Hence, from eq. (7.168)₁ we get

$$r \frac{\partial N_s}{\partial s} = 0 \rightarrow N_s = f(\theta). \quad (7.170)$$

If we consider an infinitely long pipe, nothing depends upon $s \rightarrow N_{s\theta} = \text{const}$, so N_s has everywhere the value that it takes in a given section (in particular, if it is null somewhere, it is null everywhere).

7.5.5 Hyperbolic hyperboloid

Hyperbolic hyperboloids are quadric ruled surfaces, often used to shape some structures like cooling towers, Fig. 7.32. The Cartesian equation of an axisymmetric hyperbolic hyperboloid of axis z is

$$\frac{x^2}{a^2} + \frac{y^2}{a^2} - \frac{z^2}{b^2} = 1. \quad (7.171)$$

¹²This result is the famous formule of Mariotte, that can be easily found using the global equilibrium approach, cfr. Sect. 7.4.6.1. Mariotte found this result (1686) studying the system of pipes for the fountains of the garden of the *Château de Versailles*.



Figure 7.32: Cooling towers in the form of hyperbolic hyperboloids.

However, for our purposes the best way to tackle the problem is to use a parametric form of the equation of the surface; there are different ways to parameterize the surface of a hyperbolic hyperboloid, the well suited for our study is the following one

$$\begin{cases} x = \alpha \cosh u \cos \theta, \\ y = \alpha \cosh u \sin \theta, & u \in [u_1, u_2]. \\ z = \beta \sinh u + z_0, \end{cases} \quad (7.172)$$

The three constants α, β and z_0 are adjusted to fit the surface to a given case; for a hyperboloid with $0 \leq z \leq h$ and with a minimum radius R_0 , a radius R_1 for $z = 0$ and a radius R_2 for $z = h$, it is

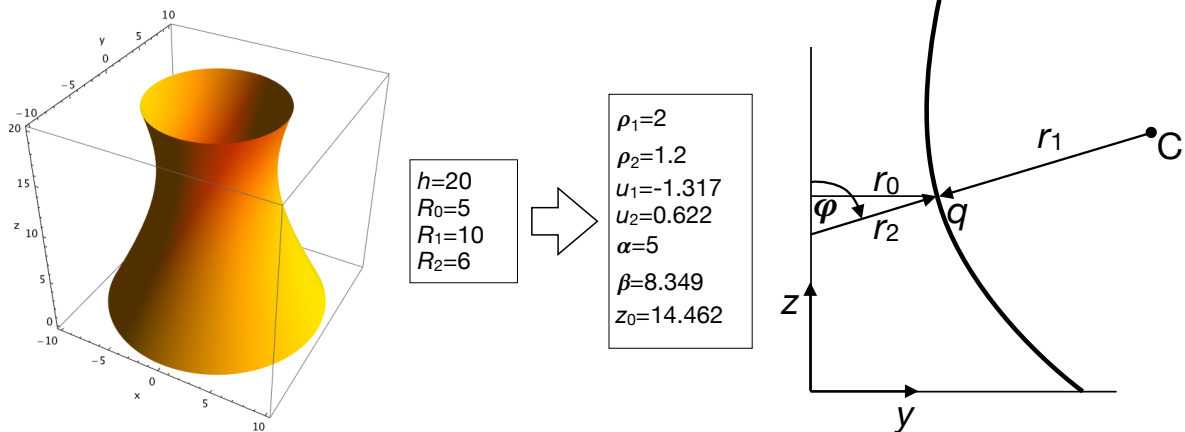


Figure 7.33: Geometry of a hyperboloid; point C denotes the osculating circle center relative to point q .

$$\begin{aligned} \alpha &= R_0, & \beta &= \frac{h}{\sinh u_2 - \sinh u_1}, & z_0 &= -\beta \sinh u_1, \\ u_1 &= \log \left(\rho_1 - \sqrt{\rho_1^2 - 1} \right), & u_2 &= \log \left(\rho_2 + \sqrt{\rho_2^2 - 1} \right). \end{aligned} \quad (7.173)$$

In Fig. 7.33 we show the geometry of a hyperboloid plotted using the above parametric equation. With a little effort, one can calculate

$$\begin{aligned} r_1 &= -\frac{1}{\alpha\beta}(\alpha^2 \sinh^2 u + \beta^2 \cosh^2 u)^{\frac{3}{2}}, \\ r_2 &= \frac{\alpha}{\beta}(\alpha^2 \sinh^2 u + \beta^2 \cosh^2 u)^{\frac{1}{2}}, \end{aligned} \quad (7.174)$$

so¹³

$$r_1 = -\frac{r_2}{\alpha^2}(\alpha^2 \sinh^2 u + \beta^2 \cosh^2 u), \quad (7.175)$$

and

$$\begin{aligned} \sin \varphi &= \frac{\beta \cosh u}{\sqrt{\alpha^2 \sinh^2 u + \beta^2 \cosh^2 u}}, \\ \cos \varphi &= -\frac{\alpha \sinh u}{\sqrt{\alpha^2 \sinh^2 u + \beta^2 \cosh^2 u}}, \\ \tan \varphi &= -\frac{\beta}{\alpha \tanh u}. \end{aligned} \quad (7.176)$$

We consider here the case of a cooling tower submitted uniquely to its own weight. Then,

$$\begin{aligned} \mathbf{p} &= (p_\varphi, p_\theta, p_n) = (p \sin \varphi, 0, p \cos \varphi) \\ &= \frac{p}{\sqrt{\alpha^2 \sinh^2 u + \beta^2 \cosh^2 u}}(\beta \cosh u, 0, \alpha \sinh u). \end{aligned} \quad (7.177)$$

Replacing the above quantities in eq. (7.54)₁ gives the equation

$$\frac{\partial U}{\partial \varphi} = \frac{p}{\beta^2}(\alpha^2 \sinh^2 u + \beta^2 \cosh^2 u)^2. \quad (7.178)$$

Moreover,

$$\frac{\partial U}{\partial u} = \frac{\partial U}{\partial \varphi} \frac{\partial \varphi}{\partial u}, \quad (7.179)$$

and, through eq. (7.176)₃,

$$\frac{\partial \varphi}{\partial u} = \frac{\partial}{\partial u} \arctan \left(-\frac{\beta}{\alpha \tanh u} \right) = \frac{\alpha\beta}{\alpha^2 \sinh^2 u + \beta^2 \cosh^2 u}. \quad (7.180)$$

Hence, we get the equation

$$\frac{\partial U}{\partial u} = p \frac{\alpha}{\beta} (\alpha^2 \sinh^2 u + \beta^2 \cosh^2 u), \quad (7.181)$$

whose solution is

$$U = p \frac{\alpha}{\beta} \left(\frac{\alpha^2 + \beta^2}{4} \sinh 2u + \frac{\beta^2 - \alpha^2}{2} u + c \right), \quad (7.182)$$

¹³To remark the fact that $r_1 < 0$, cfr. Sect. 7.4.5 and Fig. 7.33.

and hence, through eq. (7.55),

$$N_\varphi = p \frac{\beta^2 \cosh^2 u}{(\alpha^2 \sinh^2 u + \beta^2 \cosh^2 u)^{\frac{3}{2}}} \left(\frac{\alpha^2 + \beta^2}{4} \sinh 2u + \frac{\beta^2 - \alpha^2}{2} u + c \right). \quad (7.183)$$

The constant c can be determined imposing that on the upper edge the meridian force is null: $N_\varphi(u = u_2) = 0$; this gives

$$c = - \left(\frac{\alpha^2 + \beta^2}{4} \sinh 2u_2 + \frac{\beta^2 - \alpha^2}{2} u_2 \right), \quad (7.184)$$

and finally

$$N_\varphi = p \frac{\beta^2 \cosh^2 u}{(\alpha^2 \sinh^2 u + \beta^2 \cosh^2 u)^{\frac{3}{2}}} \times \left(\frac{\alpha^2 + \beta^2}{4} (\sinh 2u - \sinh 2u_2) + \frac{\beta^2 - \alpha^2}{2} (u - u_2) \right). \quad (7.185)$$

N_θ can be calculated once more using eq. (7.56):

$$N_\theta = p \alpha^2 \left[\frac{\sinh u}{\beta} \frac{\beta^2 \cosh^2 u}{(\alpha^2 \sinh^2 u + \beta^2 \cosh^2 u)^{\frac{5}{2}}} \times \left(\frac{\alpha^2 + \beta^2}{4} (\sinh 2u - \sinh 2u_2) + \frac{\beta^2 - \alpha^2}{2} (u - u_2) \right) \right]. \quad (7.186)$$

We plot in Fig. 7.34 the diagrams of N_φ and N_θ for the case of the hyperboloid represented in Fig. 7.33.

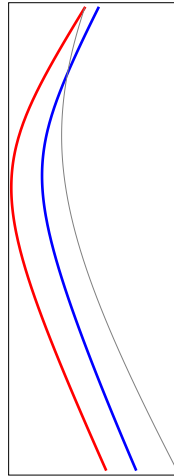


Figure 7.34: Diagrams of N_s , red, and N_θ , blue, for the hyperboloid in Fig. 7.33 (in grey: the profile of the hyperboloid; the horizontal distance between this curve and the curve of a diagram measures the value of the quantity, positive when outward).

We can see that, while $N_\varphi < 0 \forall u$, i.e., the meridians are always in compression, the parallels are in tension in the upper part of the hyperboloid. This solution implicitly implies that the base of the hyperboloid is simply supported in the same way of the spherical dome of Fig. 7.12. This is the reason of the supports that are visible in Fig. 7.32.

7.6 Vaults

Some kinds of vaults can be treated with the theory of axisymmetric membranes; however, there is a substantial difference with respect to the above cases, it concerns the boundary conditions because now the membrane has two supplementary boundaries; we will see that this limits the application of the theory and determines the need to pass to the shell theory, i.e. of structural surfaces having a non null bending stiffness. In order to use the results of the theory of axisymmetric membranes, we limit our study to the vaults having the cross section in the form of an arc of a circle of radius r .

7.6.1 Barrel vaults

A barrel vault is a vault whose cross section is half a circle, see Fig. 7.35. We consider the vault loaded by its own weight: $\mathbf{p} = (p_x, p_\theta, p_n) = (0, p \sin \theta, p \cos \theta)$.

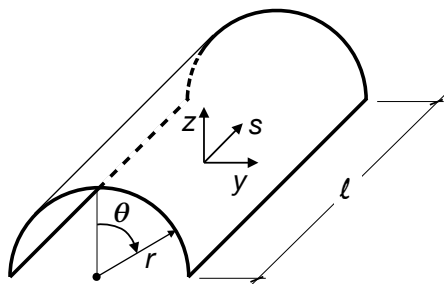


Figure 7.35: Scheme of a barrel vault.

$$\begin{aligned} r \frac{\partial N_s}{\partial s} + \frac{\partial N_{s\theta}}{\partial \theta} &= 0, \\ \frac{\partial N_\theta}{\partial \theta} + r \frac{\partial N_{s\theta}}{\partial s} &= -p r \sin \theta, \\ N_\theta &= -p r \cos \theta. \end{aligned} \tag{7.187}$$

Injecting the third equation in the second one gives

$$\frac{\partial N_{s\theta}}{\partial s} = -2p \sin \theta, \tag{7.188}$$

whose solution is

$$N_{s\theta} = -2p s \sin \theta + f(\theta), \tag{7.189}$$

and replacing this in the first equation above we get

$$r \frac{\partial N_s}{\partial s} - 2p s \cos \theta + f'(\theta) = 0, \tag{7.190}$$

which gives

$$N_s = \frac{p s^2}{r} \cos \theta - \frac{s}{r} f'(\theta) + g(\theta). \tag{7.191}$$

To remark that the effect of the function $g(\theta)$, that account for the boundary conditions, is that of propagating a local effect (that on the boundary) unaltered along a generatrix of the vault. This fact, typical of surfaces where one of the two curvatures is null (this happens also in the conical vaults, see e.g. eq. (7.159), and pipes, eq. (7.170)), is a consequence of the membrane model and it is produced by the equilibrium equations; in an elastic model, where the constitutive law enter the equilibrium equations, this should not happen.

It is also worth noticing that N_θ is unaffected by the boundary conditions and $N_\theta(\pm\pi/2) = 0$: there is no need to have a support for the vault all along the two straight edges. Actually, this solution corresponds to the case of a vault that is supported at the two curved edges and that is bent by its own weight. If we take the reference frame as in Fig. 7.35, then $N_{s\theta}(0) = 0$ by symmetry, which implies that $f(\theta) = 0$, so that

$$N_{s\theta} = -2p s \sin \theta. \quad (7.192)$$

If we impose that at the two curved edges it is $N_s(\pm\ell/2) = 0$, i.e. if we assume that globally the vault corresponds to a simply supported beam, then

$$g(\theta) = -\frac{p \ell^2}{4r} \cos \theta \rightarrow N_s = -\frac{p \cos \theta}{4r} (\ell^2 - 4s^2). \quad (7.193)$$

We remark also that on the two straight edges, $N_s(\pm\pi/2) = N_\theta(\pm\pi/2) = 0$, but the shear force is not null:

$$N_{s\theta} = \mp 2p s. \quad (7.194)$$

This result is inconsistent with the boundary condition of free straight edges. Hence, to make the above solution valid, the shear (7.194) must be applied to the straight edges. This can be done using beams supporting the straight edges, like in Fig. 7.36. Such

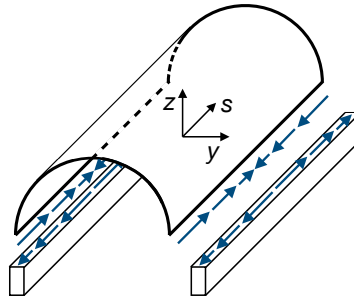


Figure 7.36: Scheme of a barrel vault with supporting beams.

beams are submitted to an axial tension force t

$$t = - \int_s^{\frac{\ell}{2}} N_{s\theta} \left(\theta = \frac{\pi}{2} \right) ds^* = \int_s^{\frac{\ell}{2}} 2p s^* ds^* = \frac{p}{4} (\ell^2 - 4s^2). \quad (7.195)$$

So, from eq. (7.193), we get also that

$$N_s = -\frac{t}{r} \cos \theta, \quad (7.196)$$

from which we see that $N_s \leq 0$ everywhere: the vault is compressed axially and the resultant of N_s is equal to $2t$. In correspondence of a generic cross section, the diagrams of N_s , $N_{s\theta}$ and N_θ are shown in Fig. 7.37. At the two curved edges,

$$N_{s\theta} \left(s = \pm \frac{\ell}{2} \right) = \mp p \ell \sin \theta, \quad (7.197)$$

and also this force must be provided through supporting arches or diaphragms. The solution found in this Section, hence, does *not* correspond to that of a classical barrel vault supported at the two straight edges.

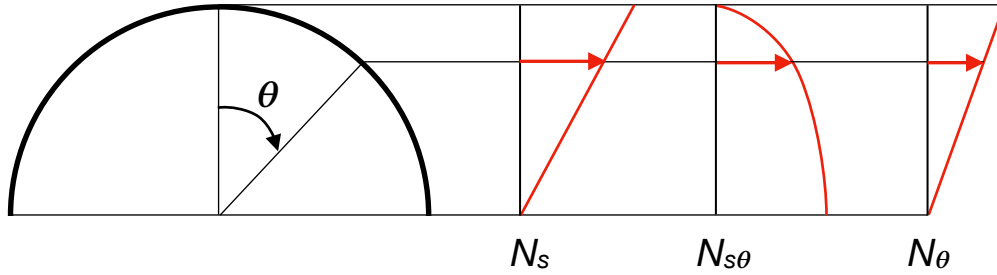


Figure 7.37: Distribution of the membrane forces for a generic cross section of the vault.

In fact, for such a case we should satisfy the boundary conditions

$$N_\theta \left(\theta = \pm \frac{\pi}{2} \right) = -p r, \quad N_s \left(s = \pm \frac{\ell}{2} \right) = N_{s\theta} \left(s = \pm \frac{\ell}{2} \right) = 0, \quad (7.198)$$

that give

$$\begin{aligned} \mp p \ell \sin \theta + f(\theta) &= 0, \\ \frac{p \ell^2}{4r} \cos \theta \mp \frac{\ell}{2r} f'(\theta) + g(\theta) &= 0, \end{aligned} \quad (7.199)$$

and also the conditions

$$N_s \left(\theta = \pm \frac{\pi}{2} \right) = N_{s\theta} \left(\theta = \pm \frac{\pi}{2} \right) = 0, \quad (7.200)$$

that give

$$f(\theta) = \pm p \ell, \quad g(\theta) = 0. \quad (7.201)$$

This result does not coincide with the values found above for $f(\theta)$ and $g(\theta)$, which confirms that the solution found in this Section cannot represent the case of a classical barrel vault supported at the straight edges.

Actually, such a problem is not determined because there are too much boundary conditions to be satisfied: those on the two straight edges. This can be seen also if one considers that it is not possible that N_θ satisfy at $\theta = \pm \pi/2$ boundary conditions other than $N_\theta = 0$. Finally, such a problem is intrinsically hyperstatic and cannot be solved by the membrane theory, based uniquely upon equilibrium equations, i.e. intrinsically isostatic.

7.6.2 Cross vaults

Cross vaults are vaults composed by intersecting vaults; in the simplest scheme, two identical barrel vaults cross at a right angle, so their intersection happens along two diagonal elliptical arches. If these two arches are not reinforced, then the vault is called a *groin vault*. Groin vaults have been widely used, especially for vaults on a square plan; normally, they are realized in bricks and normally used to cover small spans (some exceptions are the vaults of some great Roman *thermae*).

For larger spans to be covered, the diagonal arches are reinforced by ribs and in this case we talk of *rib vaults*; the rib vault is the main architectural element of Gothic architecture and it can take different dimensions and geometries: quadripartite, *barlong*, sexpartite etc. see Fig. 7.38. A cross vault is a typical structure that stands thanks to its geometry;

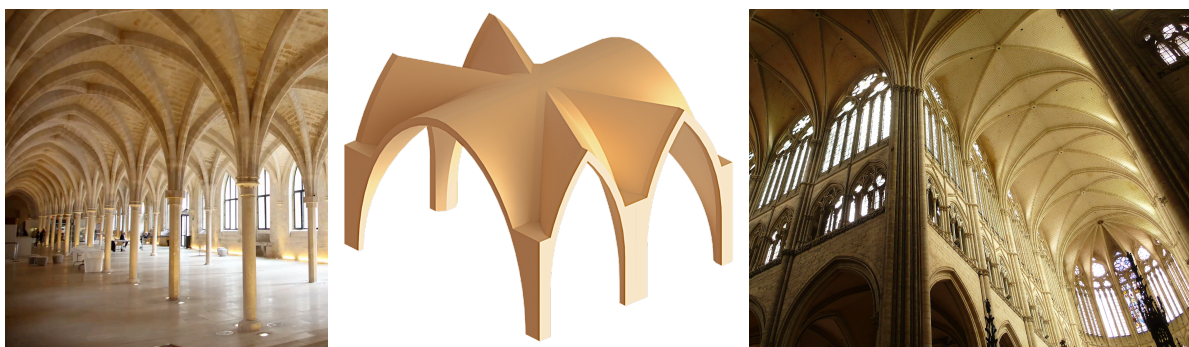


Figure 7.38: Different types of rib vaults. From the left: quadripartite vault of the *Collège des Bernardins*, Paris, scheme of a sexpartite vault, *barlong* vaults of the Cathedral of Amiens.

we study in this Section the equilibrium of a quadripartite rib vault composed by two intersecting identical barrel vaults of radius r , see Fig. 7.39, and submitted to its own weight¹⁴. In such a case, the equilibrium equations for each one of the four parts of the vaults are still eqs. (7.187), whose solution is again the one found in the previous Section:

$$\begin{aligned} N_s &= \frac{p s^2}{r} \cos \theta - \frac{s}{r} f'(\theta) + g(\theta), \\ N_{s\theta} &= -2p s \sin \theta + f(\theta), \\ N_\theta &= -p r \cos \theta. \end{aligned} \tag{7.202}$$

To determine the unknown functions $f(\theta)$ and $g(\theta)$, let us consider one of the eight shells composing the vault in Fig. 7.39, e.g. the shell ABD; we impose

$$N_{s\theta}(s=0) = 0 \quad \forall \theta \quad \rightarrow \quad f(\theta) = 0. \tag{7.203}$$

Then, to determine $g(\theta)$ we assume the solution to be symmetric with respect to the longitudinal and transversal directions: the distribution of the membrane forces in shells

¹⁴This part is essentially inspired by the work of J. Heyman, see references. It is worth noting, however, that in this Section we present just the *membrane solution* for a rib vault while, if the no-tension behavior of the material is considered, the solution is different and cannot be found with the classical membrane theory, cfr. again the book of Heyman

ABD and EFD is the same; this fact implies that $N_{s\theta} = 0$ also on the edge EFD. At the top of the vault, lines AC and EG, $\theta = \pi/2$, it is

$$N_\theta = -p r \cos \theta = -p r, \quad (7.204)$$

i.e. at the top the shells are compressed. If we imagine a horizontal section of the vault like in Fig. 7.40, then the vertical equilibrium can be given only thanks to forces N_θ , because along lines HL and LM the shear forces $N_{s\theta}$ are horizontal. The total vertical component of N_θ on the 8 lines like HL or LM is

$$N_\theta^{vert} = 8N_\theta r \sin \theta (1 - \sin \theta) = -8p r^2 \sin \theta \cos \theta (1 - \sin \theta), \quad (7.205)$$

while the total weight of the vault above the horizontal section (the part shadowed in grey in Fig. 7.40) is

$$Q(\theta) = 8p r^2 \int_0^\theta 1 - \sin \theta^* d\theta^* = 8p r^2 (\theta + \cos \theta - 1). \quad (7.206)$$

Then, if we consider the vertical equilibrium of this part of the vault, we get

$$Q(\theta) + N_\theta^{vert} = 8p r^2 (\theta + \cos \theta - 1 - \sin \theta \cos \theta (1 - \sin \theta)) \neq 0. \quad (7.207)$$

Hence, for the equilibrium to be possible, there is the need of a device that takes on this difference of the vertical forces. Such a device can be only the rib at the intersection of the shells (along the diagonal arches). We then suppose that the rib is compressed by a force P inclined of ψ on the horizontal; hence

$$\tan \theta = \sqrt{2} \tan \psi \rightarrow \sin \psi = \frac{\tan \psi}{\sqrt{1 + \tan^2 \psi}} = \frac{\tan \theta}{\sqrt{2 + \tan^2 \theta}}. \quad (7.208)$$

The vertical equilibrium is satisfied if, see Fig. 7.40,

$$4P \sin \psi = Q(\theta) + N_\theta^{vert} \rightarrow P = \frac{Q(\theta) + N_\theta^{vert}}{4 \sin \psi} \rightarrow \quad (7.209)$$

$$P(\theta) = 2p r^2 (\theta + \cos \theta - 1 - \sin \theta \cos \theta (1 - \sin \theta)) \frac{\sqrt{2 + \tan^2 \theta}}{\tan \theta}.$$

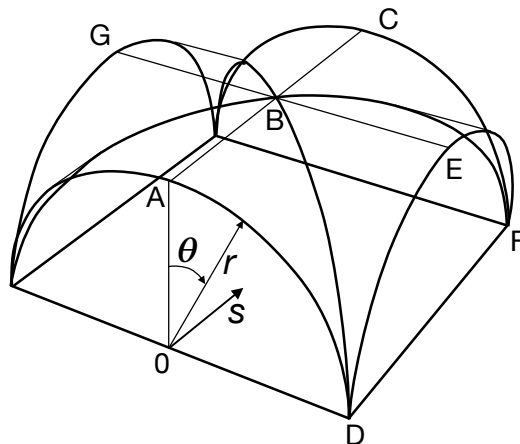


Figure 7.39: Scheme for the calculation of a quadripartite rib vault.

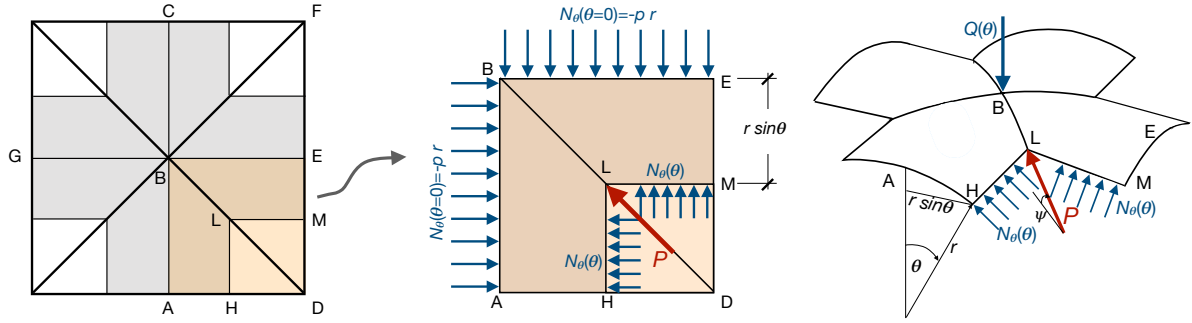


Figure 7.40: Scheme for the calculation of the membrane forces in a quadripartite rib vault.

The diagram of the function $P(\theta)$ is plotted in Fig. 7.41; numerically, one can calculate that

$$P_{max} = P(\theta = 57.61^\circ) = 1.265 p r^2. \quad (7.210)$$

To determine the force N_s^0 along the edges like AD or EF, we make the horizontal

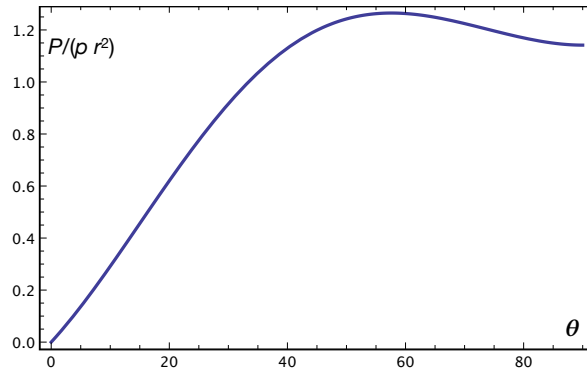


Figure 7.41: Diagram of the function $P(\theta)$.

equilibrium of the rib in the part LMDH, see Fig. 7.42:

$$P \cos \psi + \sqrt{2} \int_0^{r(1-\sin \theta)} N_{s\theta} - N_\theta \cos \theta ds + \sqrt{2} \int_0^{\frac{\pi}{2}} N_s^0 r d\theta = 0. \quad (7.211)$$

Then, on one hand

$$\cos \psi = \frac{1}{\sqrt{1 + \tan^2 \psi}} = \frac{\sqrt{2}}{\sqrt{2 + \tan^2 \theta}}, \quad (7.212)$$

and, on the other hand,

$$\int_0^{r(1-\sin \theta)} N_{s\theta} - N_\theta \cos \theta ds = p \int_0^{r(1-\sin \theta)} r \cos^2 \theta - 2s \sin \theta ds = p r^2 (1 - \sin \theta)^2. \quad (7.213)$$

So, injecting these results into eq. (7.211) we get

$$\frac{P}{\sqrt{2 + \tan^2 \theta}} + p r^2 (1 - \sin \theta)^2 + r \int_0^{\frac{\pi}{2}} N_s^0 d\theta = 0, \quad (7.214)$$

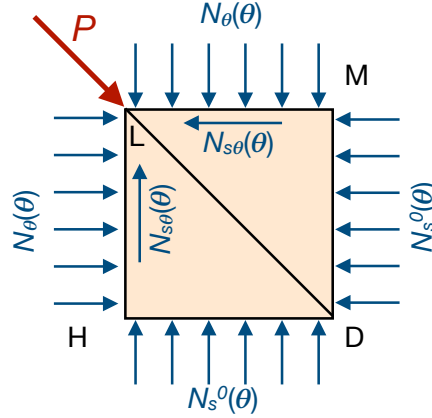


Figure 7.42: Scheme for the calculation of actions N_s^0 (the actions in blue are those applied to the vault, P , in red, is the compression in the rib).

and hence

$$N_s^0(\theta) = \frac{d}{d\theta} \left(\frac{P}{r\sqrt{2 + \tan^2 \theta}} + p r(1 - \sin \theta)^2 \right). \quad (7.215)$$

Injecting now the expression of P , eq. (7.209), and differentiating we obtain finally

$$N_s^0(\theta) = 2p r \left(\frac{(1 - \sin \theta)(1 + 3 \sin^2 \theta)}{\tan \theta} - \frac{\theta + \cos \theta - 1}{\sin^2 \theta} \right). \quad (7.216)$$

Of course, this is actually the expression of function $g(\theta)$ in eq. (7.202)₁. The function $N_s^0(\theta)$ is plotted in Fig. 7.43. As apparent, N_s^0 is a compression and we can remark that

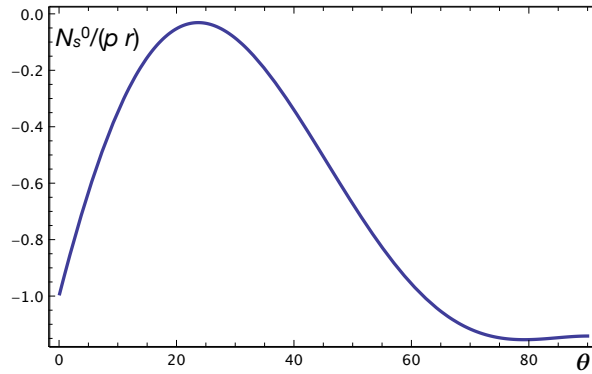


Figure 7.43: Diagram of $N_s^0(\theta)$.

$$-2 \int_0^{\frac{\pi}{2}} r N_s^0 d\theta = 2p r^2, \quad (7.217)$$

just as it must be, in order to equilibrate the forces on AC or GE.

The above results show that on the curved edges like DEF, the cross vault is submitted to horizontal compressions whose resultant is exactly $2p r^2$. Such a force must be equilibrated in some way. The device that was introduced by the *master builders* of the Gothic architecture was the flying buttress. To evaluate where the thrust point is located, i.e. at

which position on the height of the cross-vault to put the flying buttress, we can make the equilibrium to rotation about E of the shell DEFB, see Fig. 7.44:

$$Q_2 d = 2p r^2 h \rightarrow h = \frac{Q_2 d}{2p r^2}, \quad (7.218)$$

where Q_2 is the total weight of half the vault, cfr. eq. (7.206):

$$Q_2 = \frac{1}{2}Q \left(\frac{\pi}{2} \right) = 4p r^2 \left(\frac{\pi}{2} - 1 \right) \simeq 2.283p r^2. \quad (7.219)$$

For what concerns the distance d , this can be calculated with a little effort to be equal to $d \simeq 0.468 r$, so finally $h \simeq 0.534 r$.

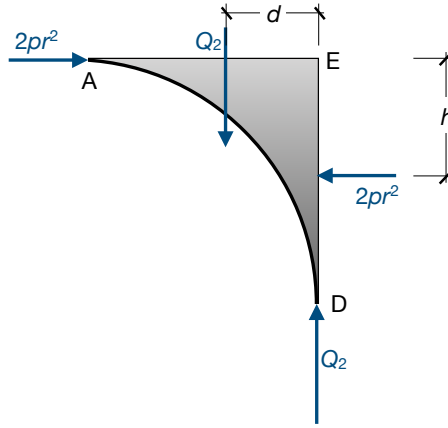


Figure 7.44: Scheme for the calculation of the thrust point.

7.7 Equilibrium of membranes of any shape

We consider in this Section the case of a membrane having a generic form, i.e. not axisymmetric. To this purpose, we refer to the scheme in Fig. 7.45. We consider a small part ABCD of the membrane, whose area is dA and whose projection onto the plane $x-y$ is the rectangle $ABCD$ with sides dx and dy ; in addition:

$$\begin{aligned} \tan \psi &= \frac{\partial z}{\partial x}, & ds_1 \cos \psi &= dx, & \cos \psi &= \frac{1}{\sqrt{1 + \tan^2 \psi}} = \frac{1}{\sqrt{1 + \left(\frac{\partial z}{\partial x} \right)^2}}, \\ \tan \theta &= \frac{\partial z}{\partial y}, & ds_2 \cos \theta &= dy, & \cos \theta &= \frac{1}{\sqrt{1 + \tan^2 \theta}} = \frac{1}{\sqrt{1 + \left(\frac{\partial z}{\partial y} \right)^2}}, \end{aligned} \quad (7.220)$$

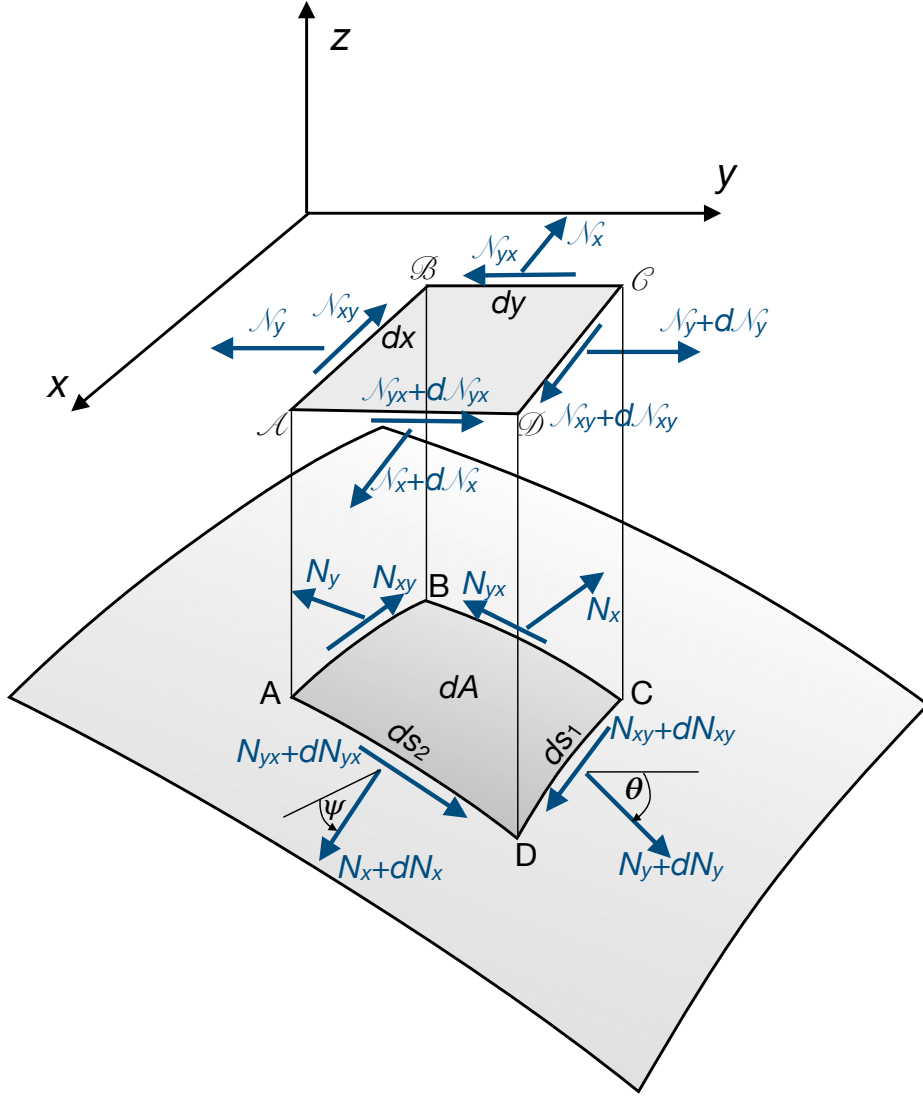


Figure 7.45: Scheme of a generic membrane.

so that

$$\begin{aligned}
 N_x ds_2 \cos \psi &= N_x \frac{\cos \psi}{\cos \theta} dy = \mathcal{N}_x dy, \quad \rightarrow \quad \mathcal{N}_x = N_x \frac{\cos \psi}{\cos \theta}, \\
 N_y ds_1 \cos \theta &= N_y \frac{\cos \theta}{\cos \psi} dx = \mathcal{N}_y dx, \quad \rightarrow \quad \mathcal{N}_y = N_y \frac{\cos \theta}{\cos \psi}, \\
 N_{yx} ds_2 \cos \theta &= \mathcal{N}_{xy} dy, \quad \rightarrow \quad \mathcal{N}_{yx} = N_{yx}, \\
 N_{xy} ds_1 \cos \psi &= \mathcal{N}_{xy} dx, \quad \rightarrow \quad \mathcal{N}_{xy} = N_{xy}, \\
 N_{xy} &= N_{yx} \Rightarrow \mathcal{N}_{xy} = \mathcal{N}_{yx}.
 \end{aligned} \tag{7.221}$$

If $\mathbf{p} = (p_x, p_y, p_z)$ is the load applied to the membrane, then the equivalent $\mathcal{P} = (\mathcal{P}_x, \mathcal{P}_y, \mathcal{P}_z)$ on the projected part $ABCD$ is defined by the equivalence

$$\mathcal{P}_x dx dy = p_x dA, \quad \mathcal{P}_y dx dy = p_y dA, \quad \mathcal{P}_z dx dy = p_z dA. \tag{7.222}$$

We can now write the equilibrium of the projected part $ABCD$; in the direction x

$$-\mathcal{N}_x dy + (\mathcal{N}_x + d\mathcal{N}_x) dy - \mathcal{N}_{xy} dx + (\mathcal{N}_{xy} + d\mathcal{N}_{xy}) dx + \mathcal{P}_x dx dy = 0, \tag{7.223}$$

that gives the partial differential equation

$$\frac{\partial \mathcal{N}_x}{\partial x} + \frac{\partial \mathcal{N}_{xy}}{\partial y} + \mathcal{P}_x = 0. \quad (7.224)$$

In a similar way we obtain, for the direction y ,

$$\frac{\partial \mathcal{N}_{xy}}{\partial x} + \frac{\partial \mathcal{N}_y}{\partial y} + \mathcal{P}_y = 0. \quad (7.225)$$

We introduce now the *Pucher's stress function* (1934), which is the function $\varphi(x, y)$ such that

$$\begin{aligned} \mathcal{N}_x &= \frac{\partial^2 \varphi}{\partial y^2} - \int \mathcal{P}_x dx, \\ \mathcal{N}_y &= \frac{\partial^2 \varphi}{\partial x^2} - \int \mathcal{P}_y dy, \\ \mathcal{N}_{xy} &= -\frac{\partial^2 \varphi}{\partial x \partial y}. \end{aligned} \quad (7.226)$$

It is immediate to check that injecting these expressions into eqs. (7.224) and (7.225) we obtain two identities.

A third equilibrium equation must still be written, the one in the direction of z ; the vertical components of the membrane forces can be obtained as follows

$$\begin{aligned} N_x ds_2 \sin \psi &= \mathcal{N}_x \frac{\cos \theta}{\cos \psi} ds_2 \sin \psi = \mathcal{N}_x \tan \psi dy = \mathcal{N}_x \frac{\partial z}{\partial x} dy, \\ N_y ds_1 \sin \theta &= \mathcal{N}_y \frac{\cos \psi}{\cos \theta} ds_1 \sin \theta = \mathcal{N}_y \tan \theta dx = \mathcal{N}_y \frac{\partial z}{\partial y} dx, \\ N_{xy} ds_1 \sin \psi &= N_{xy} ds_1 \cos \psi \tan \psi = N_{xy} dx \frac{\partial z}{\partial x} = \mathcal{N}_{xy} dx \frac{\partial z}{\partial x}, \\ N_{yx} ds_2 \sin \theta &= N_{yx} ds_2 \cos \theta \tan \theta = N_{yx} dy \frac{\partial z}{\partial y} = \mathcal{N}_{yx} dy \frac{\partial z}{\partial y}. \end{aligned} \quad (7.227)$$

The equilibrium along z is hence

$$\begin{aligned} & -\mathcal{N}_x \frac{\partial z}{\partial x} dy + \left(\mathcal{N}_x \frac{\partial z}{\partial x} + \frac{\partial}{\partial x} \left(\mathcal{N}_x \frac{\partial z}{\partial x} \right) dx \right) dy - \\ & -\mathcal{N}_y \frac{\partial z}{\partial y} dx + \left(\mathcal{N}_y \frac{\partial z}{\partial y} + \frac{\partial}{\partial y} \left(\mathcal{N}_y \frac{\partial z}{\partial y} \right) dy \right) dx - \\ & -\mathcal{N}_{xy} \frac{\partial z}{\partial x} dx + \left(\mathcal{N}_{xy} \frac{\partial z}{\partial x} + \frac{\partial}{\partial y} \left(\mathcal{N}_{xy} \frac{\partial z}{\partial x} \right) dy \right) dx - \\ & -\mathcal{N}_{yx} \frac{\partial z}{\partial y} dy + \left(\mathcal{N}_{yx} \frac{\partial z}{\partial y} + \frac{\partial}{\partial x} \left(\mathcal{N}_{yx} \frac{\partial z}{\partial y} \right) dx \right) dy + \mathcal{P}_z dx dy = 0, \end{aligned} \quad (7.228)$$

and after simplifying we obtain the partial differential equation

$$\frac{\partial}{\partial x} \left(\mathcal{N}_x \frac{\partial z}{\partial x} \right) + \frac{\partial}{\partial y} \left(\mathcal{N}_y \frac{\partial z}{\partial y} \right) + \frac{\partial}{\partial y} \left(\mathcal{N}_{xy} \frac{\partial z}{\partial x} \right) + \frac{\partial}{\partial x} \left(\mathcal{N}_{yx} \frac{\partial z}{\partial y} \right) + \mathcal{P}_z = 0. \quad (7.229)$$

After differentiating and once introduced the values of $\partial\mathcal{N}_x/\partial x$ and of $\partial\mathcal{N}_y/\partial y$ that can be deduced from eqs. (7.224) and (7.225), the last equation becomes

$$\mathcal{N}_x \frac{\partial^2 z}{\partial x^2} + \mathcal{N}_y \frac{\partial^2 z}{\partial y^2} + 2\mathcal{N}_{xy} \frac{\partial^2 z}{\partial x \partial y} = -\mathcal{P}_z + \mathcal{P}_x \frac{\partial z}{\partial x} + \mathcal{P}_y \frac{\partial z}{\partial y}. \quad (7.230)$$

Introducing the Pucher's stress function $\varphi(x, y)$ we get the linear second-order partial differential equation

$$a(x, y) \frac{\partial^2 \varphi}{\partial x^2} - 2b(x, y) \frac{\partial^2 \varphi}{\partial x \partial y} + c(x, y) \frac{\partial^2 \varphi}{\partial y^2} = q(x, y), \quad (7.231)$$

where

$$\begin{aligned} a(x, y) &= \frac{\partial^2 z}{\partial y^2}, \quad b(x, y) = \frac{\partial^2 z}{\partial x \partial y}, \quad c(x, y) = \frac{\partial^2 z}{\partial x^2}, \\ q(x, y) &= -\mathcal{P}_z + \frac{\partial}{\partial x} \left(\frac{\partial z}{\partial x} \int \mathcal{P}_x dx \right) + \frac{\partial}{\partial y} \left(\frac{\partial z}{\partial y} \int \mathcal{P}_y dy \right) \end{aligned} \quad (7.232)$$

are known functions depending upon the membrane's form and load. When $\partial^2 z/\partial y^2$ and $\partial^2 z/\partial x^2$ have the same sign, i.e. if the radiuses of curvature in the two orthogonal directions x and y are on the same side of the membrane's surface, then eq. (7.231) is of the elliptic type, otherwise hyperbolic.

The general problem of the equilibrium of a membrane of any shape is hence reduced to the search for a scalar function of two variables, $\varphi(x, y)$; once this found, the internal actions are recovered by differentiation, through eqs. (7.226). It is worth noticing, on one hand, that the problem is still intrinsically isostatic (the determination of the distribution of the internal actions needs just the equilibrium equations, there is no need to introduce the elastic behavior of the membrane to find them), and, on the other hand, that the use of the stress function automatically ensures that the distribution of the internal actions, once calculated through eqs. (7.226), is equilibrated.

We consider in the next Sections some applications of the above results.

7.7.1 Hyperbolic paraboloid

Let us first consider the case of a membrane in the form of a hyperbolic paraboloid whose Cartesian equation is

$$z = h \frac{x y}{a b}, \quad (7.233)$$

see Fig. 7.46. In such a case,

$$\begin{aligned} \frac{\partial z}{\partial x} &= \frac{h y}{a b}, \quad \frac{\partial z}{\partial y} = \frac{h x}{a b}, \\ a(x, y) &= \frac{\partial^2 z}{\partial y^2} = 0, \quad b(x, y) = \frac{\partial^2 z}{\partial x \partial y} = \frac{h}{a b}, \quad c(x, y) = \frac{\partial^2 z}{\partial x^2} = 0, \\ q(x, y) &= \mathcal{P}_z - \frac{h}{ab} (\mathcal{P}_x y + \mathcal{P}_y x), \end{aligned} \quad (7.234)$$

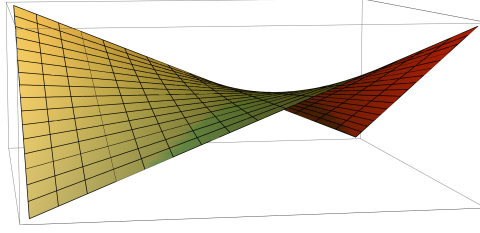


Figure 7.46: Scheme of a hyperbolic paraboloid; the two families of straight lines belonging to the surface are visible in the plot.

i.e. the principal curvatures are null: as well known, this is a ruled surface. Equation (7.231) becomes

$$2 \frac{h}{a b} \frac{\partial^2 \varphi}{\partial x \partial y} = q(x, y). \quad (7.235)$$

For the case, very frequent, of vertical loads, $\mathcal{P}_x = \mathcal{P}_y = 0$, and if, in addition, $\mathcal{P}_z = \mathcal{P} = \text{const.}$, then we have the equation

$$2 \frac{h}{a b} \frac{\partial^2 \varphi}{\partial x \partial y} = \mathcal{P}, \quad (7.236)$$

whose solution is

$$\varphi(x, y) = \frac{a b}{2h} \mathcal{P} x y + f_1(x) + f_2(y). \quad (7.237)$$

Injecting this result into eqs. (7.226) gives

$$\mathcal{N}_x = \frac{\partial^2 f_2}{\partial y^2}, \quad \mathcal{N}_y = \frac{\partial^2 f_1}{\partial x^2}, \quad \mathcal{N}_{xy} = N_{xy} = -\frac{a b \mathcal{P}}{2h}, \quad (7.238)$$

and hence, through eqs. (7.221) and (7.234),

$$\begin{aligned} N_x &= \mathcal{N}_x \frac{\cos \theta}{\cos \psi} = \mathcal{N}_x \sqrt{\frac{1 + \left(\frac{\partial z}{\partial x}\right)^2}{1 + \left(\frac{\partial z}{\partial y}\right)^2}} = \frac{\partial^2 f_2}{\partial y^2} \sqrt{\frac{c^2 + y^2}{c^2 + x^2}}, \\ N_y &= \mathcal{N}_y \frac{\cos \psi}{\cos \theta} = \mathcal{N}_y \sqrt{\frac{1 + \left(\frac{\partial z}{\partial y}\right)^2}{1 + \left(\frac{\partial z}{\partial x}\right)^2}} = \frac{\partial^2 f_1}{\partial x^2} \sqrt{\frac{c^2 + x^2}{c^2 + y^2}}, \end{aligned} \quad (7.239)$$

where for the sake of shortness we have posed

$$c^2 = \frac{a^2 b^2}{h^2}. \quad (7.240)$$

The two unknown functions $f_1(x)$ and $f_2(y)$ are determined upon the boundary conditions; if, e.g., we fix \mathcal{N}_x , i.e. N_x for $x = 0$, this amounts to impose that

$$\frac{\partial^2 f_2}{\partial y^2} = \mathcal{N}_x = N_x \frac{1}{\sqrt{1 + \frac{y^2}{c^2}}}. \quad (7.241)$$

In the same way, fixing \mathcal{N}_y for $y = 0$ implies that

$$\frac{\partial^2 f_1}{\partial x^2} = \mathcal{N}_y = N_y \frac{1}{\sqrt{1 + \frac{x^2}{c^2}}}. \quad (7.242)$$

It is worth noticing that, because f_2 depends uniquely upon y , its value, i.e. that of \mathcal{N}_x , is constant on the lines $x = \text{const.}$; for the same reason, f_1 , and hence \mathcal{N}_y , is constant along the lines $y = \text{const.}$ Such lines are the characteristic straight lines of the ruled surface. As a consequence if, e.g., the edges cannot bear the forces \mathcal{N}_x and \mathcal{N}_y , these are null everywhere.

It is also interesting to notice that the distribution of the forces $\mathcal{N}_{xy} = N_{xy}$ does not depend upon the boundary conditions; in other words, these last can concern uniquely \mathcal{N}_x and \mathcal{N}_y .

A more interesting case is that where not \mathcal{P}_z but the load p_z is constant, $p_z = p$; in that case,

$$\mathcal{P}_z = -p \frac{h}{a b} \sqrt{x^2 + y^2 + c^2}. \quad (7.243)$$

Equation (7.231) becomes

$$\frac{\partial^2 \varphi}{\partial x \partial y} = -\frac{p}{2} \sqrt{x^2 + y^2 + c^2}, \quad (7.244)$$

and hence, through eq. (7.226)₃,

$$\mathcal{N}_{xy} = N_{xy} = \frac{p}{2} \sqrt{x^2 + y^2 + c^2}. \quad (7.245)$$

The expressions for \mathcal{N}_x and \mathcal{N}_y can be obtained integrating and differentiating, still in accordance with eqs. (7.226):

$$\begin{aligned} \mathcal{N}_x &= -\frac{p y}{2} \log \frac{x + \sqrt{x^2 + y^2 + c^2}}{\sqrt{y^2 + c^2}}, \\ \mathcal{N}_y &= -\frac{p x}{2} \log \frac{y + \sqrt{x^2 + y^2 + c^2}}{\sqrt{x^2 + c^2}}. \end{aligned} \quad (7.246)$$

Finally, the expressions of N_x and N_y can be obtained by eqs. (7.239):

$$\begin{aligned} N_x &= -\frac{p y}{2} \sqrt{\frac{c^2 + y^2}{c^2 + x^2}} \log \frac{x + \sqrt{x^2 + y^2 + c^2}}{\sqrt{y^2 + c^2}}, \\ N_y &= -\frac{p x}{2} \sqrt{\frac{c^2 + x^2}{c^2 + y^2}} \log \frac{y + \sqrt{x^2 + y^2 + c^2}}{\sqrt{x^2 + c^2}}. \end{aligned} \quad (7.247)$$

The above result corresponds to the case where $N_x = N_y = 0$ for $x = 0$, $y = 0$. The variation of the actions N_x and N_{xy} are plotted in Fig. 7.47 (the plot of N_y is equal to that of N_x , but turned of $\pi/2$).

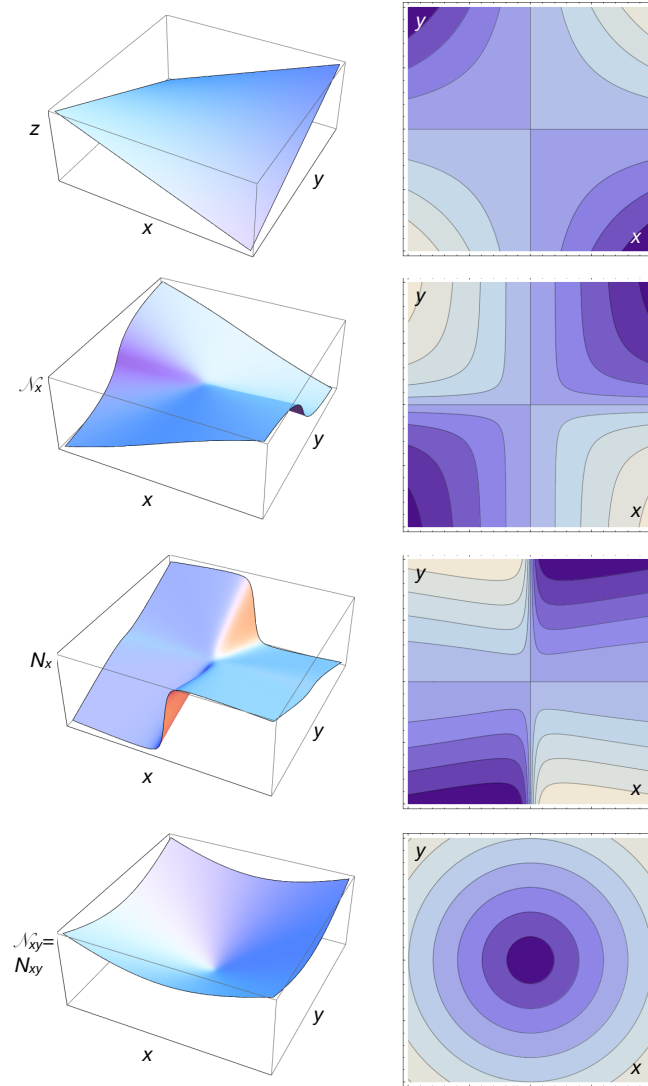


Figure 7.47: Case of a hyperbolic paraboloid with $a = b = 1, h = 10, p_z = 1$, shown at the top of the figure: 3D plots and contourplots of $\mathcal{N}_x, N_x, N_{xy}$.

7.7.2 Paraboloid of revolution

We consider the case of a paraboloid of revolution of equation

$$z = \frac{x^2 + y^2}{h}, \quad (7.248)$$

still submitted to a vertical load $\mathcal{P}_z = \mathcal{P}$ per unit of projected horizontal area. In this case

$$a(x, y) = \frac{\partial^2 z}{\partial y^2} = \frac{2}{h}, \quad b(x, y) = \frac{\partial^2 z}{\partial x \partial y} = 0, \quad c(x, y) = \frac{\partial^2 z}{\partial x^2} = \frac{2}{h}, \quad q(x, y) = \mathcal{P}, \quad (7.249)$$

and eq. (7.231) becomes

$$\Delta \varphi = -\frac{\mathcal{P}h}{2}, \quad (7.250)$$

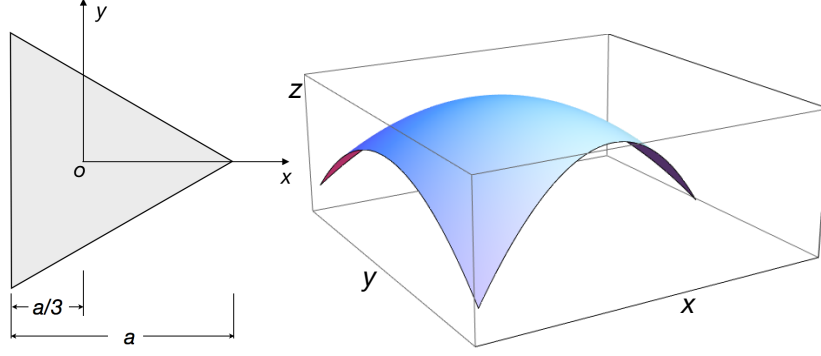


Figure 7.48: Scheme of a paraboloid of revolution on a triangular plan.

a typical elliptical problem. To make an example, let us consider the case of membrane over a triangular plan like in Fig. 7.48. We apply an inverse method: we fix the stress function

$$\varphi = -\frac{1}{8}\mathcal{P}h \left(x^2 + y^2 + \frac{x}{a}(3y^2 - x^2) \right), \quad (7.251)$$

and verify that it satisfies the equations. Actually, it is immediate to check that this function satisfy eq. (7.250) and that on each one of the three sides

$$\varphi = -\frac{1}{54}\mathcal{P}a^2h. \quad (7.252)$$

Hence, the derivatives of φ in the direction of the border are null and by consequence the forces orthogonal to the border are null too, because of eqs. (7.226). Hence,

$$\begin{aligned} \mathcal{N}_x &= \frac{\partial^2 \varphi}{\partial y^2} = -\frac{1}{4}\mathcal{P}h \left(1 + \frac{3x}{a} \right), \\ \mathcal{N}_y &= \frac{\partial^2 \varphi}{\partial x^2} = -\frac{1}{4}\mathcal{P}h \left(1 - \frac{3x}{a} \right), \\ \mathcal{N}_{xy} &= N_{xy} = -\frac{\partial^2 \varphi}{\partial x \partial y} = \frac{3}{4}\mathcal{P}h \frac{y}{a}. \end{aligned} \quad (7.253)$$

By consequence, through eqs. (7.221), we get

$$\begin{aligned} N_x &= \mathcal{N}_x \frac{\cos \theta}{\cos \psi} = \mathcal{N}_x \sqrt{\frac{1 + \left(\frac{\partial z}{\partial x}\right)^2}{1 + \left(\frac{\partial z}{\partial y}\right)^2}} = -\frac{1}{4}\mathcal{P}h \left(1 + \frac{3x}{a} \right) \sqrt{\frac{h^2 + 4x^2}{h^2 + 4y^2}}, \\ N_y &= \mathcal{N}_y \frac{\cos \psi}{\cos \theta} = \mathcal{N}_y \sqrt{\frac{1 + \left(\frac{\partial z}{\partial y}\right)^2}{1 + \left(\frac{\partial z}{\partial x}\right)^2}} = -\frac{1}{4}\mathcal{P}h \left(1 - \frac{3y}{a} \right) \sqrt{\frac{h^2 + 4y^2}{h^2 + 4x^2}}. \end{aligned} \quad (7.254)$$

The variation of the actions N_x , N_y and N_{xy} for a paraboloid with $a = 3$, $h = 1$, $\mathcal{P}_z = 1$ are plotted in Fig. 7.49.

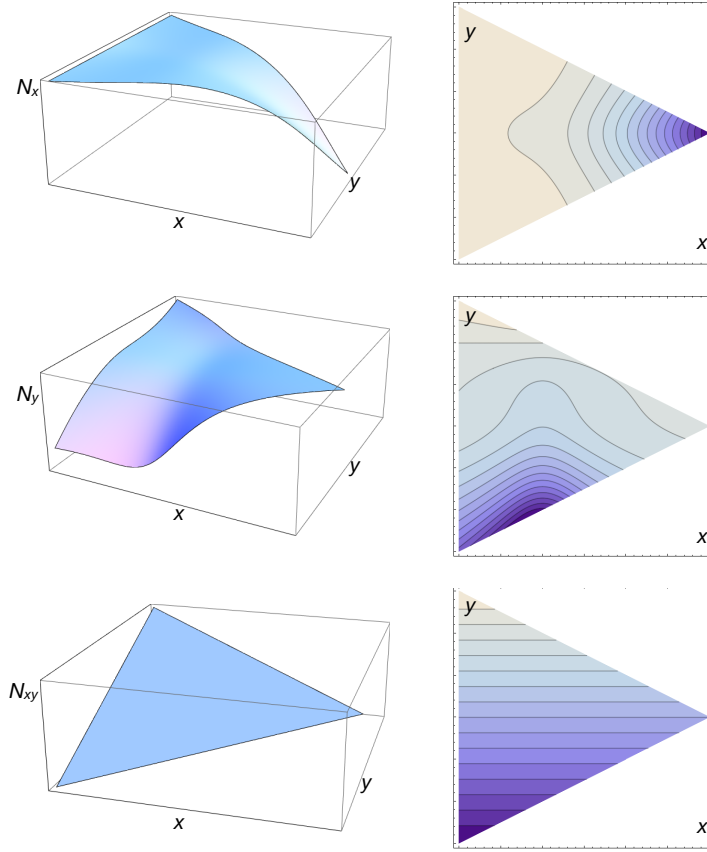


Figure 7.49: Case of a paraboloid of revolution with $a = 3, h = 1, \mathcal{P}_z = 1$: 3D plots and contourplots of N_x, N_y, N_{xy} .

7.7.3 Elliptic paraboloid

As last case, we consider an elliptic paraboloid, on the rectangle $x \in [-\frac{a}{2}, \frac{a}{2}], y \in [-\frac{b}{2}, \frac{b}{2}]$, of equation

$$z = \frac{x^2}{h_1} + \frac{y^2}{h_2}, \quad (7.255)$$

see Fig. 7.50, submitted to the vertical force, per unit of horizontal surface, $\mathcal{P}_z = \mathcal{P}$. In this case,

$$a(x, y) = \frac{\partial^2 z}{\partial y^2} = \frac{2}{h_2}, \quad b(x, y) = \frac{\partial^2 z}{\partial x \partial y} = 0, \quad c(x, y) = \frac{\partial^2 z}{\partial x^2} = \frac{2}{h_1}, \quad q(x, y) = \mathcal{P}, \quad (7.256)$$

and eq. (7.231) becomes

$$\frac{1}{h_2} \frac{\partial^2 \varphi}{\partial x^2} + \frac{1}{h_1} \frac{\partial^2 \varphi}{\partial y^2} = -\frac{\mathcal{P}}{2}. \quad (7.257)$$

As boundary conditions, we impose that

$$\begin{aligned} N_x \left(x = \pm \frac{a}{2} \right) = 0 &\rightarrow \frac{\partial^2 \varphi}{\partial y^2} \left(x = \pm \frac{a}{2} \right) = 0, \\ N_y \left(y = \pm \frac{b}{2} \right) = 0 &\rightarrow \frac{\partial^2 \varphi}{\partial x^2} \left(y = \pm \frac{b}{2} \right) = 0, \end{aligned} \quad (7.258)$$

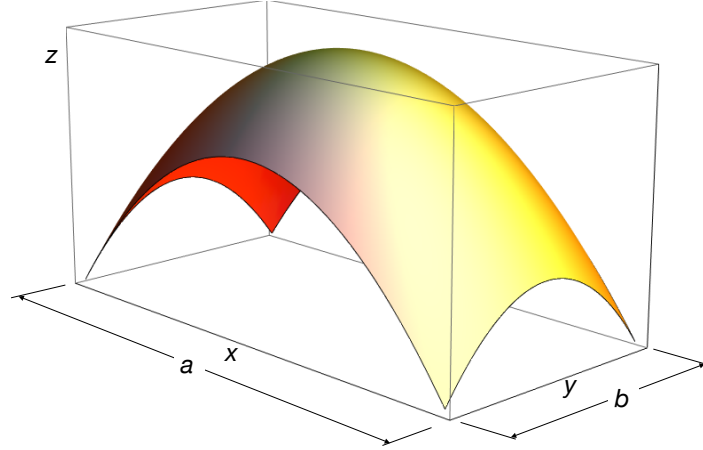


Figure 7.50: Elliptic paraboloid with $a = 2, b = 1, h_1 = 2, h_2 = 1$.

i.e., on the boundaries the normal forces are null (this is the case of free edges or of supports realized by diaphragms unable to sustain thrusts orthogonal to their plane). To satisfy these conditions, $\varphi(x, y)$ must be linear with respect to x or y along the respective edges. Because the second derivatives are proportional to the membrane forces, without affecting the generality, we can pose

$$\varphi\left(\pm\frac{a}{2}, y\right) = \varphi\left(x, \pm\frac{b}{2}\right) = 0. \quad (7.259)$$

We then construct $\varphi(x, y)$ as

$$\varphi(x, y) = \varphi_0(x, y) + \varphi_1(x, y), \quad (7.260)$$

with

$$\varphi_0(x, y) = \mathcal{P}\frac{h_1}{4}\left(\frac{b^2}{4} - y^2\right), \quad (7.261)$$

a particular solution of (7.257) and

$$\varphi_1(x, y) = \sum_{n=1}^{\infty} f_n(x) \sin\frac{n\pi}{2} \cos\frac{n\pi y}{b} \quad (7.262)$$

a form of the integral of the associated homogeneous equation. Both φ_0 and φ_1 are null for $y = \pm b/2$. If φ_1 is injected into the associated homogeneous equation

$$\frac{1}{h_2} \frac{\partial^2 \varphi}{\partial x^2} + \frac{1}{h_1} \frac{\partial^2 \varphi}{\partial y^2} = 0, \quad (7.263)$$

this is satisfied for each term if $f_n(x)$ is determined as solution of the equation

$$\frac{1}{h_2} \frac{d^2 f_n}{dx^2} - \frac{1}{h_1} \frac{n^2 \pi^2}{b^2} f_n = 0, \quad (7.264)$$

which gives

$$f_n(x) = A_n \cosh\frac{n\pi x}{c} + B_n \sinh\frac{n\pi x}{c}, \quad (7.265)$$

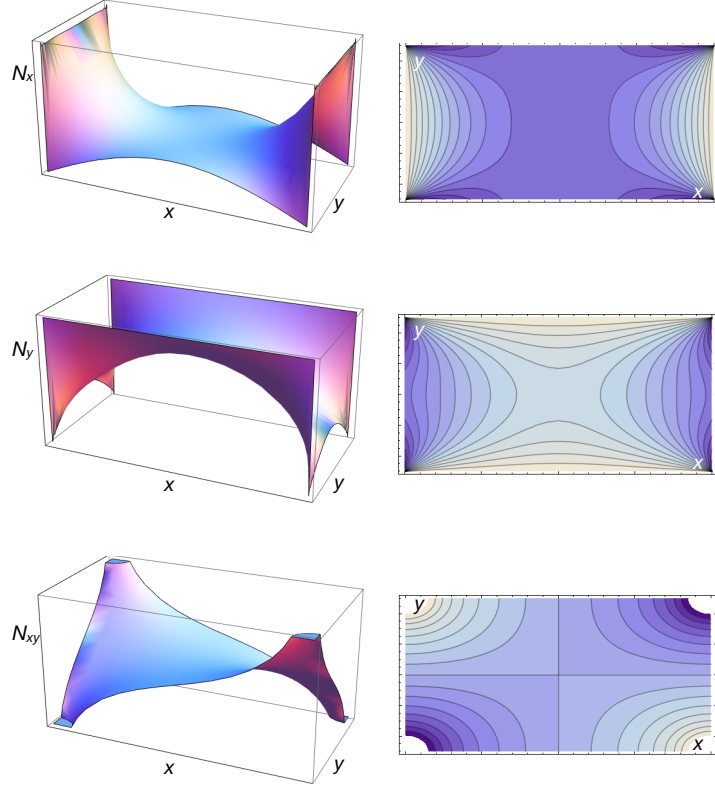


Figure 7.51: Case of an elliptic paraboloid with $a = 2, b = 1, h_1 = 2, h_2 = 1, \mathcal{P}_z = 1$: 3D plots and contourplots of N_x, N_y, N_{xy} .

with

$$c = b\sqrt{\frac{h_1}{h_2}}, \quad (7.266)$$

Because $f_n(x)$ must be symmetric with respect to $x = 0$, $B_n = 0$ and

$$\varphi_1(x, y) = \sum_{n=1}^{\infty} A_n \cosh \frac{n\pi x}{c} \sin \frac{n\pi}{2} \cos \frac{n\pi y}{b} \quad (7.267)$$

We still need to satisfy the boundary conditions on $x = \pm a/2$; to this purpose, we rewrite φ_0 in the equivalent form

$$\varphi_0(x, y) = \frac{\mathcal{P}h_1}{4} \frac{8b^2}{\pi^3} \sum_{n=1}^{\infty} \frac{1}{n^3} \sin \frac{n\pi}{2} \cos \frac{n\pi y}{b}, \quad (7.268)$$

So now imposing that $\varphi = \varphi_0 + \varphi_1 = 0$ for $x = \pm a/2$ and $\forall y \in [-b/2, b/2]$, we get the condition

$$A_n = -\frac{1}{\cosh \frac{n\pi a}{2c}} \frac{\mathcal{P}h_1}{4} \frac{8b^2}{\pi^3} \frac{1}{n^3}, \quad (7.269)$$

and finally

$$\varphi(x, y) = \frac{\mathcal{P}h_1}{4} \left(\frac{b^2}{4} - y^2 - \frac{8b^2}{\pi^3} \sum_{n=1}^{\infty} \frac{1}{n^3} \sin \frac{n\pi}{2} \cos \frac{n\pi y}{b} \frac{\cosh \frac{n\pi x}{c}}{\cosh \frac{n\pi a}{2c}} \right). \quad (7.270)$$

The membrane forces can now be calculated following the usual procedure:

$$\begin{aligned}
 N_x &= -\frac{\mathcal{P}h_2}{2} \sqrt{\frac{h_1^2 + 4x^2}{h_2^2 + 4y^2}} \left(1 - \frac{4}{\pi} \sum_{n=1}^{\infty} \frac{1}{n} \sin \frac{n\pi}{2} \cos \frac{n\pi y}{b} \frac{\cosh \frac{n\pi x}{c}}{\cosh \frac{n\pi a}{2c}} \right), \\
 N_y &= -\frac{2\mathcal{P}h_1}{\pi} \sqrt{\frac{h_2^2 + 4y^2}{h_1^2 + 4x^2}} \sum_{n=1}^{\infty} \frac{1}{n} \sin \frac{n\pi}{2} \cos \frac{n\pi y}{b} \frac{\cosh \frac{n\pi x}{c}}{\cosh \frac{n\pi a}{2c}}, \\
 N_{xy} &= -\frac{2\mathcal{P}}{\pi} \sqrt{h_1 h_2} \sum_{n=1}^{\infty} \frac{1}{n} \sin \frac{n\pi}{2} \sin \frac{n\pi y}{b} \frac{\sinh \frac{n\pi x}{c}}{\cosh \frac{n\pi a}{2c}}.
 \end{aligned} \tag{7.271}$$

The diagrams of N_x , N_y and N_{xy} are plotted in Fig. 7.51; it can be noticed that $N_{xy} \rightarrow \pm\infty$ in the corners, as a consequence of the point support.

It is interesting to remark that if the ratio $h_1/h_2 \rightarrow \infty$ or to 0, then the shell tends towards cylindrical vault with parabolic cross-section, see e.g. the case in Fig. 7.52.

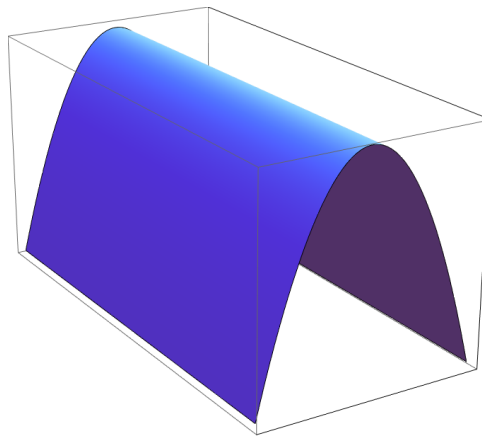


Figure 7.52: Parabolic vault obtained as a limit case of an elliptic paraboloid with $h_1/h_2 = 10^6$.

Suggested texts

1. A. E. H. Love: *A treatise on the mathematical theory of elasticity*. Fourth edition. Dover, 1944.
2. S. P. Timoshenko: *Strength of materials - Parts I & II*. Second edition. Van Nostrand, 1945.
3. I. S. Sokolnikoff: *Mathematical theory of elasticity*. McGraw-Hill, 1946.
4. S. P. Timoshenko, J. N. Goodier: *Theory of elasticity*. Second edition. McGraw-Hill, 1951.
5. S. P. Timoshenko, S. Woinowsky-Krieger: *Theory of plates and shells*. McGraw-Hill, 1959.
6. V. V. Novozhilov: *Thin shell theory*. Noordhoff, 1959.
7. H. L. Langhaar: *Energy methods in applied mechanics*. Wiley, 1962.
8. J. Heyman: *Equilibrium of shell structures*. Clarendon Press, 1977.
9. M. E. Gurtin: *An introduction to continuum mechanics*. Academic Press, 1981.
10. F. Hartmann: *The mathematical foundation of structural mechanics*. Springer, 1985.
11. J. R. Barber: *Elasticity*. Kluwer Academic Publishers, 1992.
12. P. Villaggio: *Mathematical models for elastic structures*, Cambridge University Press, 1997.
13. P. Podio-Guidugli: *A primer in elasticity*. Journal of Elasticity, v. 58: 1-104, 2000.
14. B. Audoly, Y. Pomeau: *Elasticity and geometry*, Oxford University Press, 2010.
15. J.-J. Marigo: *Mécanique des milieux continus I*. Ecole Polytechnique, 2014.
<https://cel.archives-ouvertes.fr/cel-01023392>
16. P. M. Mariano, L. Galano: *Fundamentals of the Mechanics of Solids*, Birkhäuser, 2016.